Neurophysiology and neuropharmacology of visual attention.

Jose Luis Herrero

A thesis submitted for the degree of Doctor of Philosophy

(PhD)

Institute of Neuroscience

Newcastle University

January 2011

ABSTRACT

There is ample evidence that attention to stimuli can facilitate perception under different experimental tasks. For example, human observers are faster and more accurate at detecting an object in a visual scene when they know in advance its location, motion or colour. Previous electrophysiological studies on attentional modulation have characterized the effects of attention on firing rates and oscillatory activity. They have also studied how attention can change basic neuronal integration properties, such as the size of the classical receptive field or its summation area. However, the cellular mechanisms underlying this response modulation are not clear. In this thesis, I investigate which neurotransmitters and receptors contribute to attentional modulation in the primate brain. I use pharmacological manipulations on neurons in the primary visual cortex (V1) while monkeys perform a visual spatial attention task. The contribution of two main neuromodullatory systems, the cholinergic and glutamatergic system, to visual attention is examined. Findings reveal that the amount of attentional modulation in V1 is augmented when the cholinergic system is pharmacologically enhanced. This effect is mediated by the activation of muscarinic, but not nicotinic, receptors. Glutamatergic NMDA receptor activation also leads to enhanced attentional modulation in V1, although the effects are largely restricted to improved response reliability and less to increased response gain. We note that both attention and acetylcholine can alter basic neuronal coding, namely integration properties of V1 neurons. Our findings show that acetylcholine affects contextual integration through muscarinic receptors, while nicotinic receptors affect the gain with no changes in the integration. Additional investigations of the cholinergic (and gabaergic) mechanisms in extrastriate area (area MT) are conducted, as ACh may result in improved direction selectivity computations similar to those reported in the attention literature. It appears that acetylcholine does not increase neuronal sensitivities as measured by a sharpening in the motion-direction tuning curve. Instead, it improves response reliability to optimal stimulus features. Taken together, these findings may have implications to neuromodulatory accounts of visual attention.

Acknowledgements

The work here would not have been possible without the support given by my supervisor, Alex Thiele, and by the staff at his lab including Alwin Gieselmann, Sascha Gotthardt, Mario-Joao Bartolo, Simon Bauman, Mehdi Sanayei, and Xing Chen. Also, I thank the staff working at the Centre for Behavioural Biology (CBC) for their help with the surgical facilities. Discussions held with Alwin Gieselmann and Sascha Gotthardt were very important for some of the data analysis presented in Chapter 1 and 2. The collaboration held with Pieter Roelfsema at the Department of Vision and Cognition (Netherlands Institute for Neuroscience, NIN) and some of the people at his lab (Arezoo Pooresmaeili & Matthew Self) were also of the essence for Chapter 3, particularly for publication of part of this work. The collaboration with Peter Hoofman and Claudia Distler at the Department of Zoology and Neurobiology (Ruhr University, Bochum) was essential for carrying out the experiments in Chapter 4. Other people also contributed to this work. At the Department of Engineering (University of Leicester, laboratory of Rodrigo Quian Quiroga), Juan Martinez-Gomnez advice on preprocessing of the digital signal was very useful. At the Institute of Neuroscience (Newcastle, ION), discussions with Ignacio Serrano-Pedraza were very important to the understanding of research method techniques. The academic support of Anya Hurlbert and Collin Ingram was excellent, as well as the seminars from the in-vitro group led by Miles Whittington. At the NIN, Timo Van Kerkoerle and Jasper Poort (NIN) advice on analysis of the analogue signal were very useful. Discussions with other researchers at the Society for Neuroscience meeting (SFN, 2008, 2009, and 2010), were also very inspiring. These include talks with Antonino Raffone, Michael Silver, Ariel Rokem, John Reynolds, Wolf Zinke, Michael Goldberg, Mark Roberts, and Pascal Fries. The altruistic help of my family was also very important, including the endless support of Magali Pettier, Pilar, Jose Luis, Ana, David, Fernando, Estela Herrero, Diego Rabanos, and Diego Canas.

Abbreviations

acetylcholine (ACh)

acetylcholine receptors (AChRs)

analysis of variance (ANOVA)

attention (att)

baseline power spectrum (BPSM)

cathode-ray tube (CRT)

conductance (g)

conductance of α -amino-3-hydroxy-5-methylisoxazole-4-propionate receptors (gAMPA)

conductance of N-methyl-d-aspartate receptors (gNMDA)

contrast Response Function (CRF)

contrast at half maximum saturation response (c50)

coefficient of variation (CV)

direction index (DI)

dorsolateral prefrontal cortex (DLPFC)

fano factor (F)

frontal eye field (FEF)

full width at half height (FWHH)

gabazine (Gab)

guanine nucleotide exchange factor (GEF).

inter-spike-interval (ISI)

local field potentials (LFP)

mean power spectrum (PSM)

mecamylamine (Mec)

milliseconds (ms)

multiple unit activity (MUA)

muscarinic acetylcholine receptors (mAChRs)

N-methyl-D-aspartate (NMDA)

nicotinic acetylcholine receptors (nAChRs)

non-classical receptive field (nCRF)

nucleus basalis magnocellularis (NBM)

opposed direction (OD)

peri-stimulus time histograms (PSTH)

posterior parietal cortex (PPC)

potential of Hydrogen (pH)

preferred direction (PD)

reaction times (RT)

receptive field (RF)

receiver operating characteristics (ROC)

repeated measurements (RM)

response at the saturation point (Rmax)

scopolamine (Scop)

single unit activity (SUA)

spike-field coherence (SFC)

standard deviation of baseline power spectrum (BPSSD)

standard error of the mean (s.e.m)

stimulus-induced power spectrum (Pz)

2-amino-5-phosphonovaleric acid (APV)

α-amino-3-hydroxy-5-methylisoxazole-4-propionate (AMPA)

Table of contents

GENERAL INTRODUCTION

GI.1. Attentional modulation overview

The seminal psychophysical studies investigating visual attention showed that human observers are faster and more accurate at detecting an object in a visual scene when they know in advance something about its features, such as its location, motion or colour (Colegate et al., 1973, Eriksen and Hoffman, 1973, Sperling, 1979, Posner et al., 1980). How does the implementation of attentional signals come about? The traditional view supports the idea that higher areas of the visual, parietal and frontal cortices control the selection of relevant visual information (Moran and Desimone, 1985, Spitzer et al., 1988, Motter, 1993, Desimone and Duncan, 1995). Areas such as the Frontal Eye Field (FEF) and the Intraparietal Sulcus (IPs) are argued to send a feedback signal to the earlier visual areas in order to aid the integration of incoming visual information. This view has been supported by fMRI studies which, having the ability of measuring whole brain activity, showed increased BOLD activation with attention in regions of the dorsal parietal and frontal cortex (Corbetta and Shulman, 2002, Serences and Boynton, 2007, Serences and Yantis, 2007). Importantly, the activation in these areas (FEF, anteriorIPs, posteriorIPs) is sustained after the presentation of the cue, while it is transient in occipital areas (e.g., human middle temporal area [MT+], (Shulman et al., 1999). Single-cell recordings in macaque prefrontal cortex (dorsolateral prefrontal cortex [DLPFC, FEF) and parietal cortex (lateral intraparietal area [LIP], and areas 7a and V3A) showed increases in baseline firing rate when the monkey anticipates the onset of a stimulus (Bushnell et al., 1981, Rizzolatti et al., 1987, Colby et al., 1996, Nakamura and Colby, 2000). Similar increases have been observed in more general tasks involving some degree of preparation such as in the premotor cortex before an arm movement (Wise et al., 1983) or in the FEF before a saccade (Bruce and Goldberg, 1985). These results suggest that preparatory control signals originate in high-level areas, which led the authors to assume that the signals propagate to low-level areas to influence the incoming stimulus-related activity. Against this traditional view a new perspective has recently emerged (Roelfsema, 2005, Buschman and Miller, 2007), where visual and frontal cortices work synergistically to select the relevant items in the display. Future studies need to disentangle these two competing views in order to reveal whether the brain processes visual information in a hierarchical manner or rather, a more distributed manner.

Single-unit recordings in monkeys have revealed that behaviorally relevant target objects typically evoke stronger responses than non-target objects in a range of cortical visual areas involved with visual processing and object recognition. One of the first pioneer studies (Moran and Desimone, 1985) recorded activity from cells in V4 while monkeys performed a discrimination task at one location in the visual field, ignoring simultaneously presented distracters at a second location. For a given trial, the target location was indicated to the monkey by a spatial cue at the start of that trial, i.e. top-down attentional bias. When target and distracter were both within the receptive field (RF) of the recorded cell, the neuronal response was determined primarily by the target; while responses to the distracter were greatly attenuated. The authors suggested that the cells responded as though their RFs had shrunk around the target (see also (Richmond et al., 1983)). Interestingly, when one of the two locations was placed outside the RF of the recorded cell, attention

no longer had any effect on the response because target and distracter were no longer competing for the cell's response (Luck et al., 1993). Attempts to explain the neuronal mechanisms of spatial attention in various visual areas were done by Luck and colleagues (Luck et al., 1997a, Luck et al., 1997b). They observed V2 and V4 cells showing a sustained elevation of their baseline (prestimulus) firing rates whenever the monkey directed attention towards the neuron's RF. Interestingly, when attention was shifted to different regions within the same RF, the magnitude of the baseline shift varied according to the distance between the focus of attention and the RF center, suggesting that the spatial resolution of this source was very high. The parametric manipulations of the spatial relationship between the stimulus in the RF center and the focus of attention were conducted in another study (Connor et al., 1996). Similar to Luck (Luck et al., 1997a, Luck et al., 1997b), they found evidence that the RF profile shifts toward the attentional focus; in 49% of the cells responses were greater for bars near the attended ring. Additionally, the overall response level in 84% of the cells in that study depended on the direction in which attention lay relative to the stimulus in the center of the RF (e.g., to the left, right, above, or below). The authors suggested that V4 cells are able of carrying information about the spatial relationship between visual stimuli and attention.

GI.2. Cholinergic system overview

Acetylcholine (ACh) is a key neurotransmitter acting on a wide number of functions and tissues. ACh has long been known to have an important role in the central nervous system (Bulbring and Burn, 1941). In the cortex, ACh release in the extracellular medium was found to be related to spontaneous electrical activity (MacIntosh and Oboring, 1955). An increase in ACh release from the sensorimotor and parietal cortex could be elicited by stimulation of several areas such as the forepaw (Mitchell, 1963), the mesencephalic reticular formation (Kanai and Szerb, 1965), and the nucleus basalis (Casamenti et al., 1998). Visual stimulation could also elicit ACh output in the sensorimotor and parietal cortex (Phillis, 1968), while its shortage depressed behavioural and EEG activity (Beani et al., 1968). These early experiments suggested that activation of the cholinergic neurons innervating the cerebral cortex was a component of gross behavioral changes or arousal mechanism (for further evidence see (Randic and Padjen, 1967, Szerb, 1967).

Upon release ACh can have a variety of different actions. It can: 1) Bind to presynaptic receptors: presynaptic activation or inhibition leads to automodulation of the presynaptic cholinergic neuron. 2) Be degradated by acetylcholinesterase: activity of this enzyme on ACh triggers its degradation into choline and acetyl coenzyme A, thus terminating its effect. 3) Bind to postsynaptic receptors: activation of these receptors by ACh leads to cholinergic response. There are multiple classes of ACh receptors (AChRs) which can be generally subdivided in two families: ionotropic (nicotinic) (Metherate, 2004) and metabotropic (muscarinic) (Brown et al., 1997). In structural terms, muscarinic AChRs are G-coupled protein receptors, while nicotinic AChRs are ligand-gated ion channels. When ACh binds to ligand-gated ion channels, the pore of the nicotinic AChR opens and Na+ ions flow down the concentration gradient into cells. This results in the depolarization of the effector cell. When ACh binds to G-coupled protein receptors, muscarinic AChRs undergo a conformational change which allows it to act as a guanine nucleotide exchange factor (GEF). The G-coupled protein receptor

can then activate an associated G-protein by exchanging its bound GDP for a GTP. The G-protein's α subunit, together with the bound GTP, can later affect intracellular signaling. This chain of reactions is assumed to take a relatively long time, also exact time courses of action in vivo are, to the best of my knowledge unknown. This assumed extended time course means that the kinetics (i.e. postsynaptic effects on secondary channels) of the muscarinic AChRs are slower compared to the kinetics of the nicotinic AChRs. Nicotinic receptors mediate rapid channel opening and desensitization which make them adequate for short-term neuronal signalling (Cockcroft et al., 1990) (although see (Prusky et al., 1987a) who argues for a role of nicotinic receptors in both short and long term signalling).

In macaques, the neocortex receives its cholinergic innervation from the nucleus basalis of Meynert (NBM) (Pearson et al., 1983). In V1 of the macaque, muscarinic AChRs primarily the m1 and m2 subtypes (Tigges et al., 1997)) and nicotinic AChRs (Han et al., 2000) are expressed at significant levels. Nicotinic receptors are located presynaptically on thalamic axons arriving in primary sensory areas. For example in cat area 17 (Parkinson et al., 1988), nicotinic receptors were most concentrated in layer IV, while the 17/18 and 18/19 borders showed much fewer nicotinic receptors (but see (Prusky et al., 1987a, Wonnacott, 1997). In the rat somatosensory and visual cortex, nicotinic sites were also concentrated in layer IV, while muscarinic receptors were mostly located in superficial and deep layers (Gil, 1997, Kimura and Baughman, 1997). These studies showed that ACh decreases the efficacy of lateral/feedback connections by means of presynaptic muscarinic receptors. ACh also boosts the efficacy of thalamocortical connections through presynaptic nicotinic receptors (Gil, 1997), primarily located on thalamocortical/feed-forward synapses (Prusky et al., 1987b, Sahin et al., 1992, Lavine et al., 1997). These data suggests that ACh is able to dynamically adjust the flow of feed-forward and lateral/feedback information by controlling the efficacy of specific synapses (Hasselmo and Bower, 1992, Hasselmo, 1995, Kimura et al., 1999, Kimura, 2000).

GI.3. Attentional modulation and the cholinergic system

The study of the role of ACh release on complex cognitive behaviours has often been prevented by the limitations of the techniques used to sample ACh concentration (see for example Beani et al. (1968) for limitations on the cortical cup technique). Recent work has shown that ACh output may have a more specific influence on cognitive function, particularly cortical plasticity (Juliano et al., 1991, Brocher et al., 1992), learning (Yu and Dayan, 2002, Rokem and Silver, 2010), memory (Hasselmo and Stern, 2006), and attention (Sarter et al., 2005, Hasselmo and Sarter, 2010). Recent in-vivo studies have shown that ACh reduces the spread of excitation: it reduces the classical receptive field (CRF) summation area of V1 neurons (Roberts et al., 2005), the spread of membrane voltage fluctuations (Kimura et al., 1999), and the spread of BOLD activation (Silver et al., 2008). Further evidence for the involvement of ACh in attentional modulation comes from studies that observed persistent attentional impairments when cortical areas were depleted from the normal supply of ACh. For example, McGaughy (McGaughy et al., 2002) infused the cholinergic immunotoxin 192 IgG-saporin (SAP) into the nucleus basalis magnocellularis (NBM) of rats before they performed a five-choice serial reaction time task (5CSRTT). This manipulation produced cell loss in the NBM, and reduced ACh efflux in the medial prefrontal cortex as measured by *in-vivo* microdialysis during task execution. They found that the degree of

attentional impairment was dose-dependent: decreased cortical ACh efflux in rats with more extensive lesions of the NBM showed the strongest attentional deficits, while incomplete lesions produced deficits only when attentional demands were increased. In rats with smaller PFC lesions, PPC function may be preserved (McGaughy et al., 2002). The interaction between dose and task demands was later explained by the coarseness of the ACh innervation (Nelson et al., 2005) (but see (Fournier et al., 2004) who found modality and region specific ACh release in rat neocortex). Increases in prefrontal activity can stimulate cholinergic efflux in other cortical areas such as the posterior parietal cortex (PPC) (Nelson et al., 2005). The parietal cortex controls spatial (Posner et al., 1987) as well as temporal (Coull and Nobre, 1998, Koenigs et al., 2009) orientating of attention and maintains focus in the presence of distraction (Shomstein and Yantis, 2004). Thus, the recruitment of PPC by PFC may result from increased attentional demand.

Overall these results support the idea that ACh in PFC is involved in top-down allocation of attentional resources (Sarter et al., 2005, Parikh and Sarter, 2008). However, their conclusions were confined by limitations on the temporal resolution at which ACh concentration can be measured (5-10 min fastest) in sharp contrast to the fast effects of attentional modulation. Recent advances in amperometric neurochemical recordings have been able to measure phasic ACh releases at a resolution 0.5s. The first study to apply the technique in behaving animals was (Parikh et al., 2007). *They* showed rats with a light cue that predicted reward delivery 6±2 s later at one out of two reward ports (ITI=90+/-30s). When the cue evoked orientation behaviour toward the reward ports (i.e., it was not missed), an increase in ACh concentration was registered by the enzyme-coated electrode located in the mPFC. This steep increase in cholinergic activity lagged the onset of the cue by 2-3s, and it was not observed in 1) missed trials, 2) trials with reward but no cue, and 3) before the cue-reward contingency was learned. Although neuronal signals were not recorded in this study (only chemical signals), it was later proposed (Hasselmo and Sarter, 2010) that the persistent spiking, hypothetically underlying correct detection in hit trials, could be triggered by an initial steep increase in cholinergic activity.

GI.4. Attentional modulation and the glutamatergic NMDA receptor

Theoretical models describing the function of NMDA glutamatergic receptors are largely based on studies of hippocampal slice preparations. They found that NMDA receptors are activated only under conditions of particularly intense or high-frequency synaptic drive (Collingridge and Bliss, 1987), such as that necessary to produce long-term potentiation (LTP) (Cotman et al., 1988). Slice preparations from the visual cortex in normal neural transmission found minor NMDA components on the EPSPs produced by electrical stimulation. When IPSPs were minimized, (i.e., by suppressing GABAergic mechanisms (Artola and Singer, 1987, Jones and Baughman, 1988) or using zero extracellular concentrations of Mg2+ (Thompson, 1986)), however, the contribution of NMDA receptors was much larger. In contrast to the in-vitro studies, in-vivo studies suggested that NMDA receptors are active during normal synaptic transmission in adult cat visual cortex (Hagihara et al., 1988, Miller et al., 1989), predominantly in layers II and III (Fox et al., 1989). Moreover, blocking NMDA receptors in-vivo with APV can substantially reduce spontaneous activity while having little effect on stimulus-induced activity of cells in the deeper visual layers (Fox et al., 1989). There is a strong similarity between the

gain changes seen with NMDA receptor activation in the above studies and the gain changes seen with attention in the awake-behaving monkey. Increased neuronal gain with selective attention has been reported in many cortical visual areas including MT (Treue and Maunsell, 1996), V4, V2 (Reynolds et al., 1999), V1 (Roelfsema et al., 1998). Similar gain increases have been observed in V1 when NMDA receptors are activated (Fox et al., 1990). We also note that the dynamics of their effects are very similar, with attention affecting mostly the sustained part of the responses of visual neurons (e.g.(Roelfsema et al., 1998)), and NMDA receptor activation mostly affecting the sustained part of the response of neurons in the ventrobasal thalamus (Salt, 1986). Interestingly, a variety of different NMDA receptors contribute to cortico-cortical interactions between layer 4 cells in the mouse barrel cortex (Fleidervish et al., 1998). In the macaque cortex, the specific contribution of NMDA and non-NMDA receptors to different aspects and epochs of figure-ground segregation (Self et al., 2008) and motor preparation/execution (Shima and Tanji, 1993b), has been demonstrated. These studies, together with others suggesting that NMDA receptor activation is implicated in synaptic mechanisms underlying learning, memory, and developmental plasticity (Cotman et al., 1988, Collingridge and Singer, 1990), strongly suggest that NMDA mechanisms may be involved in attentional modulation.

GI.5. Attentional modulation and neuronal oscillations

In addition to altering firing rates, attention can also modulate the degree of temporal coherence across the neural population (Fries et al., 2001). Specific temporal patterns of correlated activity have long been associated with different states of alertness (Steriade, 2001), but more recent studies have suggested their implication in sensory processing and cognition (see for review (Womelsdorf et al., 2007)). For example, neurons in area V1 display increased oscillatory activity in the gamma frequency band (20-80Hz) during the coding of visual stimuli (Gray and Singer, 1989, Berens et al., 2008, Giesselmann et al., 2008). Interestingly, spatial attention increased gamma-band activity in V4 neurons (Fries et al., 2001, Womelsdorf et al., 2007), while V1 neurons exhibited an opposite effect (i.e., spatial attention reduced gamma-band activity (Chalk et al., 2010)). These studies highlight the prevalence of periodic activity patterns, but do these synchronous patterns result from intrinsic activity in the visual cortex or from inputs from other structures? A recent study (Gregoriou et al., 2009a) addressed this question by recording simultaneously from FEF and area V4 while directing attention to a stimulus located in the overlapping receptive field of both areas. The authors found enhanced oscillatory coupling between the two areas, particularly at gamma frequencies. The coupling was initiated by FEF (although see (Khayat et al., 2009)) and was time-shifted by 8-13 ms in V4. This result is in line with 1) the idea that FEF initiates gamma frequency oscillations in V4, and 2) the fact that synaptic conduction delays between these two reciprocally and monosynaptically connected areas are ~10 ms (Nowak et al., 1997). They concluded that this time-shifted coupling at gamma frequencies optimizes the postsynaptic impact of FEF spikes onto V4 neurons. As a result, communication between areas at opposite ends of the visual hierarchy is improved with attention (Gregoriou et al., 2009b). However this conclusion is at odds with the assumed conception that gamma rhythms are used for local computations (Kopell et al., 2000), as opposed to long-range or polysynaptic communication across distant brain areas. For this, beta rhythms are more suitable (von Stein et al., 2000).

It is known that some neuronal types contribute more efficiently than others to the generation of oscillatory network activity. Although inhibitory neurons constitute only 20% of the cells in the cortex their role in synchrony and oscillations is very important (Traub et al., 2003). According to the normalization model of attention (Reynolds and Heeger, 2009), inhibitory interneurons may be responsible for both normalization and synchronization, as well as reductions in response variability (Tiesinga et al., 2004, Mitchell et al., 2009). A recent study (Mitchell et al., 2007) distinguished narrow and broad spiking neurons in behaving monkeys based on their waveform and firing rate properties. They found that the strongest attentional modulation occurred among narrow spike neurons (presumed local interneurons). In this study attention also increased the reliability of neuronal responses (Fano factor) of both cell types, but the effect was stronger among putative interneurons. This finding raises the possibility that specific cell-types and therefore specific neurotransmitters contribute to attentional modulation. Converging evidence for the role of interneurons in the amplification of cortical activity was found by simultaneous recordings from cortical-projecting GABAergic neurons in the basal forebrain (BF) and prefrontal cortex local field potentials (LFPs) (Lin et al., 2006). Transient synchronization of spike bursts in BF was accompanied by increased gamma oscillations in prefrontal cortex (i.e., BF synchronization events preceded the troughs of LFPs in prefrontal cortex). These results led the authors to conclude that synchronization of BF ensembles, which is likely mediated by cortical-projecting GABAergic neurons within BF, is responsible for fast cortical modulations to provide transient amplification of cortical activity.

GI.6. Objectives of this Thesis

The studies on attentional modulation described in the preceding sections of this thesis have characterized the effects of attention on neuronal responses. However, the cellular mechanisms underlying this response modulation are not clear. Within this thesis I investigated which neurotransmitters and receptors contribute to attentional modulation in the primate brain, focussing mostly on the cholinergic system (Chapter 1) and the glutamatergic NMDA receptor (Chapter 2). We used local pharmacological manipulations of these systems as opposed to more global pharmacological approaches (e.g. systemic application of drugs) and not yet well established/implemented techniques (e.g., amperometry). We used the relatively old technique of iontophoresis, although in its revised form (Thiele et al., 2006), to probe directly in the cortex the contribution of cholinergic and glutamatergic function to attentional modulation. Of course this technique has limitations, as it is not capable of applying drugs in a realistic way as the brain would do (i.e., with high spatiotemporal resolution). However, it is a good compromise if one wants to study animal models and task settings capable of disentangling fine aspects of attentional modulation, as those described above. Therefore, this thesis is the first attempt to my knowledge to bridge the gap between neuropharmacology and spatial attention in the awake-behaving macaque monkey.

Chapter 1 demonstrates that cholinergic mechanisms contribute to attentional modulation in V1 of the macaque monkey (Herrero et al., 2008), suggesting an involvement of cholinergic inputs from the basal forebrain (Szerb, 1967). Intracortical sources cannot be excluded though, as the existence of intracortical cholinergic neurons has recently been reported (von Engelhardt et al., 2007). It also reveals the receptor

specificity of the cholinergic contribution. In Chapter 2 we examine the glutamatergic NMDA receptor contribution to attentional modulation. This was done because of the apparent coarseness of the ACh innervation may be incompatible with the highly localized and fast effects of spatial attention. This raises the question of whether non-cholinergic mechanisms are more directly contributing to attentional modulation. Under this scenario, ACh release from presynaptic cholinergic terminals increases the level of glutamate which activates NMDA receptors. And it is the activation of these receptors that allows the demands of attentional performance. There is a strong similarity between the gain changes that are seen with NMDA receptor activation (Fox et al., 1989) and the gain changes seen with attention in the awake-behaving monkey (Roelfsema et al., 1998, Roberts et al., 2007).

In this chapter, I examine whether NMDA receptor activation contributes to attentional modulation in the awake-behaving monkey. The attentional modulation in visual cortex could be mediated by higher cortical areas (e.g. FEF, PPC) through glutamatergic feedback inputs. Although V1 does not receive direct feedback projections from FEF, it should also be affected through indirect projections from prestriate areas V4 and V2 (Ungerleider et al., 1989). One possibility is that increased amounts of ACh alter the strength of the synapses among V1 neurons (and their biophysical state) which may then allow spatially specific glutamatergic feedback to enhance specific incoming information. To investigate this hypothesis, iontophoretic pharmacological analysis of glutamatergic NMDA receptors was combined with single cell recordings in V1 while macaque monkeys performed a task that demanded top-down spatial attention.

In Chapter 3, I also probed how the cholinergic system might influence neuronal integration properties. This was done to better understand the effects of acetylcholine in relation to basic sensory processing, namely spatial integration properties. The study of integration properties may shed light on the mechanisms of attentional modulation, as recent work in the macaque has found that spatial attention modulated centre-surround interactions (Zenger-Landolt and Koch, 2001, Roberts et al., 2007, Sundberg et al., 2009) possibly through cholinergic mechanisms (Roberts et al., 2005). In line with this, we further explored neuronal integration properties in this chapter by determining how ACh's actions can aid integration properties.

The preceding chapters reported experiments performed in primary visual cortex of the awake macaque. To also determine the effects of cholinergic mechanisms to neuronal coding in extrastriate areas, I performed additional investigations in motion selective area MT of the anesthetized macaque (Chapter 4). Here I asked whether ACh can sharpen tuning curves in MT, which has previously, although in a somewhat qualitative manner, been suggested for V1. Given a variety of attention studies on MT activity, which has found wide ranging effects, it seemed sensible to ask whether ACh sharpens tuning curves in a manner similar to attention (Martinez-Trujillo and Treue, 2004a) or instead scales all responses equally regardless of feature preference? For example, (Sillito and Kemp, 1983) found that V1 neurons of anesthetized cats increased their response to optimal stimuli but not to non-optimal stimuli. In sharp contrast with this facilitatory effect, application of bicuculline methiodide (BMI, a GABAa antagonist) produced general disinhibition which led to increased responses to both optimal and non-optimal stimuli (Sillito and Kemp, 1983). For similar effects see (Sato et al., 1987a, Murphy and Sillito, 1991, Sato et al., 1996). Other studies found that ACh did not sharpen

orientation/direction tuning curves of V1 neurons. Instead, it improved their response variability (Sato et al., 1987b, Zinke et al., 2006) and signal-to-noise ratios (Sato et al., 1987b).

Chapter 1. Contribution of cholinergic receptors to attentional modulation in macaque V1

1.1. Introduction

There is ample evidence that attention to visual stimuli can facilitate its perception (Colegate et al., 1973, Eriksen and Hoffman, 1973, Sperling, 1979, Posner et al., 1980). A large sample of rodent studies have demonstrated that ACh contributes to attention (McGaughy et al., 2002, Fournier et al., 2004, Nelson et al., 2005, Sarter et al., 2005), and that the deficit in cognitive control including attentional deficits in humans also points to an important role of ACh in attention (Robbins, 2005, Furey et al., 2008). Previous work from Thiele's lab showed that attention reduced spatial integration of V1 neurons (Roberts et al., 2007), while a separate study showed that ACh had a similar effect (Roberts et al., 2005). However, a direct link between acetylcholine function and attentional modulation at the cellular level has not yet been established. The current study aimed to establish this link. Here, we investigate which neurotransmitters and receptors contribute to attentional modulation in the primate brain.

Single-unit recordings in primates have revealed that attended stimuli typically evoke stronger responses than distracter stimuli in a range of cortical visual areas (Richmond et al., 1983, Moran and Desimone, 1985, Luck et al., 1993). For example, Luck and collaborators (Luck et al., 1997a, Luck et al., 1997b) observed V2 and V4 cells showing a sustained elevation of their spontaneous and stimulus-induced firing rates whenever the monkey directed attention towards the neuron's RF. Studies in the primary visual cortex (V1) were able to replicate the effects, although the degree of response facilitation was reduced (Roelfsema et al., 1998, Roberts et al., 2007, Thiele et al., 2009). This attentional modulation is believed to be mediated by feedback connections from higher cortical areas (Moran and Desimone, 1985, Spitzer et al., 1988, Motter, 1993, Desimone and Duncan, 1995). However, these higher cortical areas (e.g., DLPFC) can also influence sensory areas indirectly, through connections to cholinergic neurons in the basal forebrain (BF) that have ascending projections to sensory areas (Russchen et al., 1985, Sarter et al., 2005), but see (Preuss, 1995). In this chapter, I propose that this alternative route (Frontal cortex –> BF –> Visual cortex) is not only mediating general arousal states but also selection of visual information.

The precise nature of the contribution of ACh to attentional modulation in the cortex is at present unclear. Thus, we recorded the strength of attentional modulation in neurons from V1 of three macaque monkeys, while simultaneously performing pharmacological analysis of cholinergic receptor contributions (Thiele et al., 2006). Subjects performed a task demanding voluntary allocation of attention under control conditions and when ACh, or muscarinic or nicotinic receptor antagonists, were iontophoretically applied in the vicinity of the neurons under study. Increased amounts of ACh may strengthen synaptic efficacy and the biophysical state of the neurons (i.e. spatial and temporal integration properties of the neuron's membrane). The aim of this chapter is to explore whether these effects interact with attentional modulation (and stimulus parameters) or are an independent phenomena only contributing to general arousal states. Parts of the results (firing rate based and psychophysics) presented here have been published (Herrero et al., 2008), while the data relating to local field potential analysis have not yet been published.

1.2. Methods

General

All experiments were carried out in accordance with the European Communities Council Directive 1986 (86/609/EEC), the US National Institutes of Health Guidelines for the Care and Use of Animals for Experimental Procedures, and the UK Animals Scientific Procedures Act.

Paradigm and behavioural control

While fixating a central fixation spot and retaining the position of the fovea within a small window (<0.7°, see Data Collection), the monkey's task was to detect a small change in luminance contrast that occurred at a cued (attended) location, while ignoring a change at a non-cued location (Figure 1.1). A trial was initiated by holding a touch bar and fixating a red fixation point (FP, 0.1° diameter) presented centrally on a 20" analogue CRT monitor (75 Hz or 110 Hz, 1,600 * 1,200 pixels, 57 cm from the animal) on a grey background (21 cd/m2). A cue (blue annulus, 0.24° outer diameter, 0.18° inner diameter) was presented for 400 ms on one side of the fixation spot. The location of the cue indicated the location to which the monkey had to covertly attend. The cue was presented displaced along the axis connecting the FP and the receptive field location by one quarter of the eccentricity of the neuron's RF. The cue was displaced either towards or away from the RF to indicate whether attention should be directed towards or away from the stimulus presented in the RF. After cue offset, a 900 ms blank (250 ms in monkey B) period occurred with just the FP present. Thereafter, two identical stimuli were presented (test stimuli), one centered on the RF, the other at the same eccentricity in the opposite hemi-field. Spatial and temporal separation of the cue from the test stimuli ensured that it had no direct effect on the neuronal response to the test stimulus. Test stimuli were dark bars of preferred orientation at a medium luminance contrast of 20-40% (Michelson contrast). After 500-800 ms (randomized in 1 ms steps) a brighter patch (0.1° square) appeared at the centre of one of the bars. If presented in the cued location it is referred to as 'target', if presented in the un-cued location it is referred to as 'distracter'. The target or distracter was brighter than the test stimuli by 7.3 cd/m² (±2 cd/m²) depending on the contrast of the test stimulus and on the training of the monkey. After the presentation of a target, the monkey had to release the touch bar within 500 ms to receive a juice reward. If a distracter was presented first the monkey had to continue to hold the touch bar and maintain fixation until target appearance. This occurred 1000-1300 ms (randomized in 1 ms steps) after the distracter appeared. If the monkey made no response, the trial was terminated 500 ms after presentation of the target or distracter, whichever appeared last. Premature (or incorrect) releases of the touch bar or failure to maintain fixation resulted in immediate trial termination. Correct touch bar releases also resulted in trial termination such that the monkey could have his reward and get ready to perform the next trial. Eye movements were recorded by scleral search coils in monkeys B and HU (temporal resolution 250 Hz, spatial resolution of 1.5'), and by an infra-red based system in monkey HO (Thomas Recording, temporal resolution 220 Hz, spatial resolution 2.5'). Eye position during all trials was restricted to be within ±0.3-0.5 of the fixation point in monkeys B and HU, and to be within ±0.5-0.7 in monkey HO. We have previously demonstrated that tiny residual eye movements were not responsible for the attentional modulation of the data set reported here (Herrero et al., 2008); see also (Roberts et al., 2007).

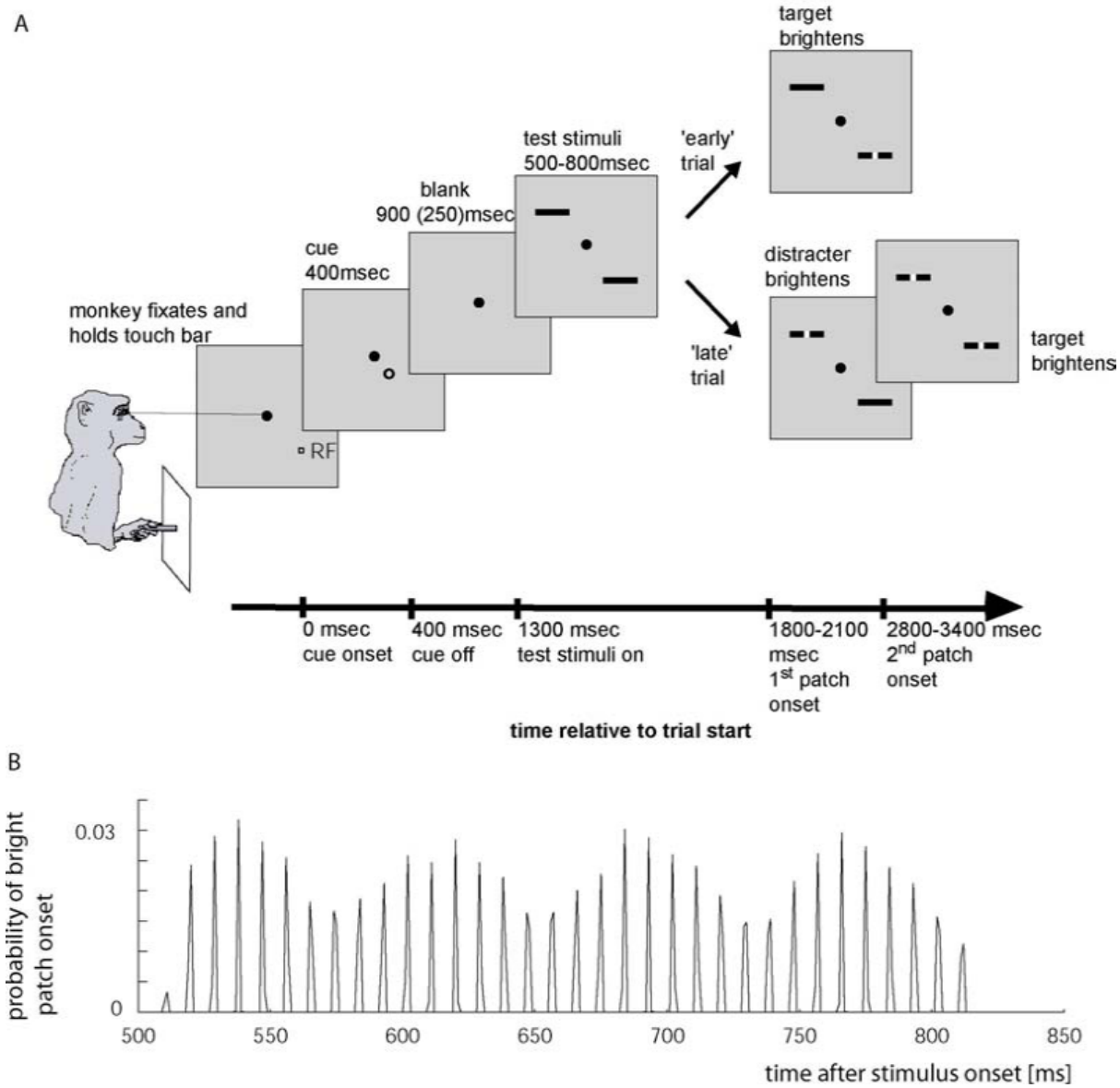

Figure 1.1: A) Behavioural paradigm: Monkeys had to fixate and hold a touch bar. If they did so a cue appeared which indicated where to attend (in the example the animal would have to attend to the stimulus within the receptive field). Following a gap period two stimuli were presented, one in the receptive field of the neuron under study another in the opposite hemifield. In early trials, the animal had to detect a bright patch (target) in the cued location. In late trials, it had to also detect a target in the cued location but only after ignoring the appearance of another bright patch (distracter) in the un-cued location. B) Probability distribution of onset time for the bright patch after bar onset obtained from an experiment where the refresh rate of the monitor was 110 Hz. Onsets were spaced by 9 ms (or by 13.3 ms when the refresh was 75 Hz). Additionally, it resulted in a sinusoidal modulation of the probability at a periodicity of 81 ms.

Electrophysiological recordings and drug application

Recordings were performed with tungsten-in-glass electrodes flanked by two pipettes (Thiele et al., 2006). Drugs were applied iontophoretically through these pipettes (NeuroPhore BH-2, Digitimer, Welwyn Garden City, Hertfordshire, England). Pipette opening diameter varied between 1-4 µm. Pipette resistance varied

between 10-150 MΩ, with most recordings (>90%) at 20-80 MΩ. Hold currents for acetylcholine, scopolamine and mecamylamine were usually -10 nA, on rare occasions (when the pipette resistance was 10-20 MΩ) it was -40 nA. Pipette-electrode combinations were inserted into V1 through the dura mater on a daily basis without the use of guidetubes. The integrity of the electrode and the pipettes were checked under the microscope before and after the recording sessions, in addition to measurements of the pipette impedance made before and after the recording at each recording site. The details regarding drug concentration, pH and application current were: Acetylcholine (0.1M, pH 4.5, application current varied between 5-50 nA, with most recordings at 5-20 nA; median current strength: 15nA, 25percentile: 10nA, 75 percentile: 20 nA), scopolamine (0.1M, pH 4.5, median current strength: 40nA, 25percentile: 30nA, 75 percentile: 50 nA), and mecamylamine (0.1M, pH 4.5, median current strength: 10nA, 25percentile: 5nA, 75 percentile: 10 nA). Drug application was continuous during blocks of 'drug applied'. The duration of each block could vary depending on the number of bar lengths used, depending on the number of repetitions for each condition that we aimed for, and depending on the speed/accuracy of the animal. On average drug application for each block was ~5-15 minutes. For the data analysis we removed the first 2 trials for each condition (condition 1, bar lengths; condition 2, attend RF/away) from the data set, as drug effects and recovery usually occur with a slight delay of ~0.5-3 minutes. We regularly compensated for the change in current during the ejection condition by increasing the hold current of one of the two pipettes, thereby keeping the overall current identical between the 'hold' and 'eject' conditions.

Data collection and surgical procedures

We recorded neurons in three male macaques (Macaca mulatta; monkeys B, HU, and HO). After initial training, monkeys were implanted with a head holder and recording chambers above V1 under general anaesthesia and sterile conditions (for details of surgical procedures, see Thiele et al., 2006). Stimulus presentation and behavioral control were managed by Remote Cortex 5.95 (Laboratory of Neuropsychology, National Institute for Mental Health, Bethesda, MD). Neuronal data was collected by Cheetah data acquisition (Neuralynx) interlinked with Remote Cortex. The waveforms of all spikes that exceeded a threshold set by the experimenter were sampled at 30 kHz. Offline sorting of these MU spike samples was carried out based on waveform features (Neuralynx spike sorting software, Version 2.10).

Receptive field characterization and visual stimulation

For each recording site we initially determined the location of the receptive field as well as the optimal orientation, spatial frequency and phase using reverse correlation techniques (DeAngelis et al., 1994, Gieselmann and Thiele, 2008). The RF location was estimated by mapping the classical receptive field with briefly presented dark and light squares (0.1º width, 100% contrast) at pseudo-random locations on a 10x10 grid (a 1x1° area). The RF centre was taken as the location of the peak of a 2-dimensional Gaussian fitted to the response distribution (Roberts et al., 2007). RFs centres were located in the lower quadrant, at an eccentricity of 2.5° to 7°. Tuning properties were estimated using static sinusoidal gratings (1° diameter) centred on the RF. These gratings varied in orientation (12 orientations, 0–165°), spatial frequency (1, 3, 5, 7, 8, 9 or 10 cycles / °)

and phase (0, 0.5π, π, 1.5π) every 60 ms in a pseudo-randomized order. The stimulus that yielded the peak response was taken to represent the preferred orientation, spatial frequency, and phase of the neuron under study. The obtained parameters were used to determine the orientation of the test stimuli that was used in the main experiments.

Visual stimulation

Test stimuli were dark bars of preferred orientation at a medium luminance contrast of 20-40% (Michelson contrast). We used either 3, 4, 6 or 7 bar lengths to determine the effect of drug application on attentional modulation. Initially we always used 6 or 7 bar lengths, as we wanted to allow for the possibility that the effect of the drug on attentional modulation depends on the stimulus (bar length). This was indeed sometimes the case, but we found that reducing the number of bar stimuli to 4 (or 3) still covered that eventuality. Therefore we reduced the number of stimuli initially to 4 and then 3, as it still allowed us to determine possible interactions between drug, attention and the stimulus, while simultaneously allowing us to maximize the number of trials. The size of the bars used was 0.2, 0.4, 0.6, 0.8, 1.2, 1.6, 2.4, and 3.2° centered on the neuron's RF. During acetylcholine application we used 7 different bar lengths while recording from 101 cells, 6 bar lengths while recording from 12 cells, 4 bar lengths while recording from 28 cells and 3 bars while recording from the remaining 15 cells. During scopolamine application we used 7 bars while recording from 98 cells, and 4 bars for the remaining 20 cells. During mecamylamine application we used 7 bars while recording from 108 cells and 3 bars while recording from the remaining 43 cells.

Analysis of spiking activity

Spike data from the recording electrode were obtained by band-pass filtering the raw signal from 600–9000 Hz. Offline sorting of these filtered data (MU spike samples) was carried out based on waveform features (Neuralynx spike sorting software, Version 2.10). In some occasions two or three clusters of single unit activity could be segregated, while in others only one. Single-unit activity from the window of interest (200-500 ms after stimulus onset) was subjected to ANOVA; 3 factors (attention, drug application and stimulus length). Only neurons with a significant main effect of attention and a significant main effect of drug application, or a significant interaction between these two factors were included for further analysis ($p<0.05$).

Analysis of spiking activity; neuronal sensitivity

Neuronal sensitivity to the different attention, drug and stimulus conditions was calculated by deriving a modulation index [MI = (activity attend away - activity attend RF) / (activity attend away + activity attend RF)]. A non-parametric measure of neuronal thresholds was calculated for the different attention, drug, and bar length conditions. This was done by calculating the area under the receiver operating characteristic (ROC) curve on the basis of single-trial responses (200-500 ms after stimulus onset) (Swets, 1988). ROC values of 0.5 indicate that an ideal observer can only perform at chance level in detecting where the animal attends to. Higher ROC values indicate greater separation of response distributions, whereby an ideal observer performs at better than chance levels. Thus, if the presence of ACh (or attention) increased firing rates, ROC values

should be increased in ACh-applied (or attend-RF) condition relative to control condition (or attend-away). Conversely, if scopolamine/mecamylamine decreased firing rates, ROC values should be decrease in the presence of drug compared to its absence.

Analysis of local field potentials (LFPs)

While the higher-frequency components of the neuronal signals (>300 Hz) are likely dominated by the currents associated with action potentials, the LFP is defined as the low-frequency (< 250 Hz) components of the raw field potential. These low-frequency fluctuations are thought to be dominated by current flow due to synaptic activity (Destexhe 1998; Freeman 2000; Logothetis 2002; Nicholson and Freeman 1975; Mitzdorf, 1985). The LFP-recording electrode samples the activity of a population containing thousands of neurons, as the sources of the LFP are thought to be located within 500 µm (Kruse and Eckhorn, 1996). In this study, the LFP signal was band-pass filtered between 1–200 Hz (using a 6th order Butterworth filter) to remove low-frequency direct current fluctuations and reduce high-frequency noise. Then 50 Hz power line noise was removed by applying a band pass-filter (49–51 Hz, 3rd order Butterworth filter) to the original data, and subtracting the resulting filtered signal from the original data. Because we were mainly interested in the sustained LFP response after stimulus presentation, we focused on a time window ranging from 256 to 512 ms following stimulus onset for the LFP analysis. The time period of 256–512 ms was chosen because it is the period wherein attentional modulation of firing rates was most profound (Roberts et al., 2007, Herrero et al., 2008). For each trial, the raw power spectral density of the LFP response (RPS) over the time period of 256–512 ms after stimulus onset was estimated using a multitaper technique (Percival and Walden, 1993), under the Chronux toolbox with a time-bandwidth product of TW = 3 with K = 5 tapers. For each recording site the mean power spectrum (PSM) was then calculated from the single-trial RPS data.

In order to provide a quantitative understanding of how attention modulated the LFP signal, we divided the power spectrum into four different frequency bands (alpha: 7–13 Hz, beta: 13–30 Hz, gamma: 30–60 Hz, and high gamma: 60-100 Hz), and analyzed the effects of attention on the LFP response power separately for each frequency band. Before pooling recording sites from no-drug periods (i.e., baseline, recovery_1, recovery_2), we checked that the effects were consistent. This was done by visually inspecting the effect of attention on the MUA as well as on the raw power (gamma band), and making sure that a similar trend was observed. For example, a recording site was excluded from the analysis if attention reduced the MUA/raw gamma power during the baseline condition but increased it during the recovery condition. For the analysis reported here, all periods were pooled together in two conditions; control condition where activity from all no-drug periods was included, and drug condition with activity from all drug periods.

In addition to the stimulus driven raw LFP and the associated spectra (PSM), we obtained the single-trial baseline LFP and spectra from the time period 256–0 ms before stimulus onset for each recording site and the attend-RF versus attend-away condition. This was done for both control and drug-applied conditions. From these single-trial spectra the mean baseline power spectrum (BPSM) and the standard deviation of the baseline power spectrum (BPSSD) averaged over all trials (i.e., not separated according to where the animal

attended to) was calculated. Using this baseline power allows us to determine the stimulus-induced (Pz) power spectrum which was calculated as follows:

$$Pz = (PSM - BPSM) / BPSSD$$

These were obtained for each attentional, drug and stimulus condition. It provides a measure of spectral power that is induced by the stimulus. Additionally, the spike-field coherence (SFC) was calculated to determine the synchrony between the neuronal spiking activity and the local network (LFP) oscillations. To calculate SFC we binned the single trial multiunit spike data in 1 ms bins. We then calculated the power spectra for the binned spike and the LFP data, as well as their cross spectra, using multitaper analysis. (Chronux toolbox under Matlab 7.5 (Mathworks), time-bandwidth product of TW = 3 with K = 5 tapers). These spectra and cross-spectra were averaged over trials before calculating coherence. Coherence was obtained by taking the absolute value of the coherency data. All multitaper analyses were performed using the Chronux toolbox (www.chronux.org) under Matlab 7.5 (Mathworks), using a time-bandwidth product of TW = 3 with K = 5 tapers. SFC data were subjected to population analysis and statistical tests.

Analysis of behavioural responses

Animals speed and accuracy was monitored across different attention, drug and stimulus conditions. They had to release a manual lever as soon as they detected a small contrast luminance change in the target bar, while ignoring luminance changes in the distracter bar. Lever releases faster than 50 ms were considered as incorrect responses, as well as releases slower than 500 ms. Accuracy (% correct) and RTs (time to release the lever from target onset) were subjected to repeated measures ANOVA.

1.3. Results

1.3.1. Behavioural performance

On a trial by trial basis the cue indicated to the animal the location where to attend to. This location, however, did not change randomly from one trial to the next but could only change after a block of trials (2* the number of bar lengths tested) was correctly performed by the animal. Thus, in principle the animal did not need to heed the cue, but could engage in a win-stay/lose-switch strategy, i.e. attend to the opposite location in the next trial if a decision failed to yield a reward in the current trial. To test whether the animals heeded the cues, or engaged in the lose-switch strategy it is possible to analyse the animal's performance on trials when the cue direction changed from one location to the opposite location. If the animals did not heed the cue, but engaged in the lose-switch strategy the performance on these trials should be close to 0% correct. If they heeded the cue the performance should be above chance level. Figure 1.2 shows the animals' performance for the conditions when the cue (and attention) location did not switch and for those trials immediately after a switch. Monkey B seemed to heed the cue almost perfectly, as there was no difference between cue-change and cue-stay trials (P=0.949, RM-ANOVA) and he performed at >98% correct on all trials. Monkeys HU and HO showed significant differences between cue-stay and cue switch trials ($p<0.001$, RM ANOVA), however, performance

on cue-switch trials was still close to or above 80%, i.e. in ~4 out of 5 trials the animals correctly switched immediately when the cue location changed. This demonstrates that the animals heeded the cue at least to some extent. Overall performance of the animals was >95% for all conditions (note that cue-switch was rare, i.e. the performance on cue switch trials only contributes little to the overall performance).

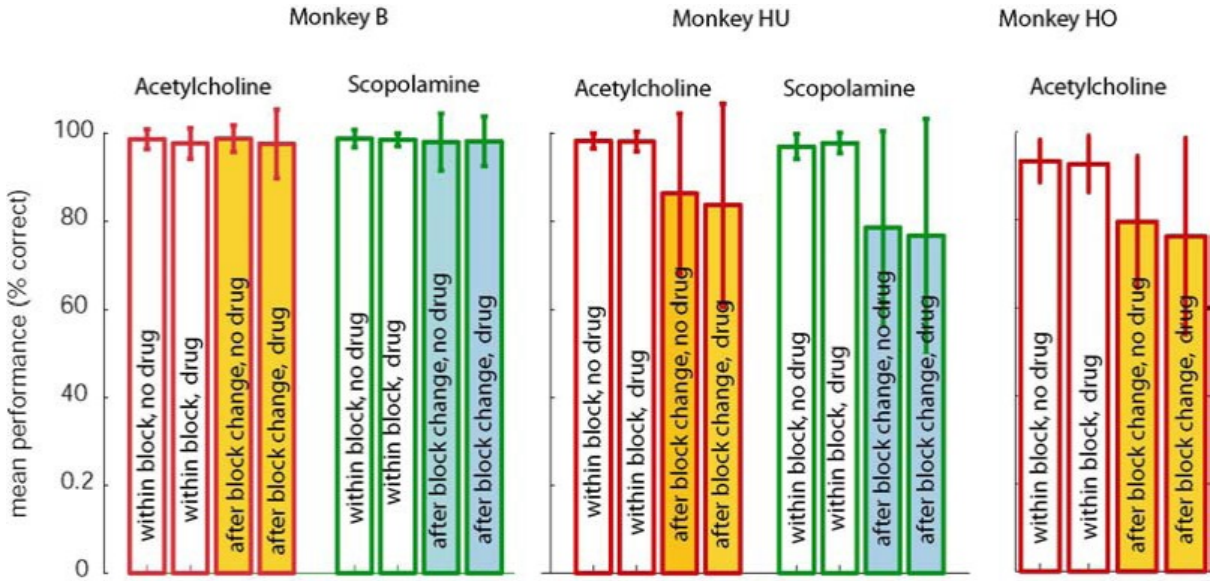

Figure 1.2: Mean performance as a function of experimental trials (error bars, SD). Within block performance indicates the performance (% correct decisions) when the cued location on the current trial was the same as the cued location on the previous trial. The performance after a block change is indicated by the 'after block change' insets. It refers to trials where the cue on the current trial was different from the cue on the previous trial. If the animals did not heed the cue, but switched the location of attention when they were not rewarded for their choice (win-stay/ lose-switch strategy) they should have performed close to 0% correct on 'after block change' trials. This was not the case for any of the monkeys. All performed >75-80% correct on block change trials, indicating that they heeded the cue at least to some extent. The extent of this differed between monkeys. Monkey B performed at the same rate on cue-stay as on cue (block) change trials, and there was no effect of either drug on his performance (RM-ANOVA, $p=0.949$). In monkey HU performance on block-change trials was significantly lower than on within block trials (RM-ANOVA, $p<0.001$ for all comparisons of within- vs. after block trials).There was no significant effect of drug application for either within or after block performance comparisons (RM ANOVA, $p>0.05$). The same was true for the performance data from monkey HO.

1.3.2. Effect of Acetylcholine on reaction times

Application of acetylcholine had a significant effect on reaction times (Fig 1.3). It somewhat speeded reaction times (RTs) when the animals attended to the stimulus within the receptive field of the neuron under study, i.e. when they attended to the location that was represented by the neurons that were influenced by ACh, however the effect itself was not significant ($F=1.48$, $p=0.223$). More interestingly, when the animals attended away, low dosage ACh application slowed RTs ($F=12.93$, $p=0.0003$). We found a significant interaction of ACh application and where the animals attended (drug*attentional locus interaction: $F=11.06$, $p=0.0009$, 3 way ANOVA). Slower RTs in the attend-away condition could be due to improved neuronal processing at the injection site which then prevented efficient disengagement from the irrelevant location. These effects depended on the strength of ACh application in a manner reminiscent of the effects on neuronal attentional

modulation (see next section). While at low dosage of ACh application (current <=15 nA) slower RTs were observed in the attend-away condition, when ACh currents were higher (>=20nA), these effects were not present anymore (drug attention interaction: F=0.01, p=0.943, 3 Factor ANOVA).

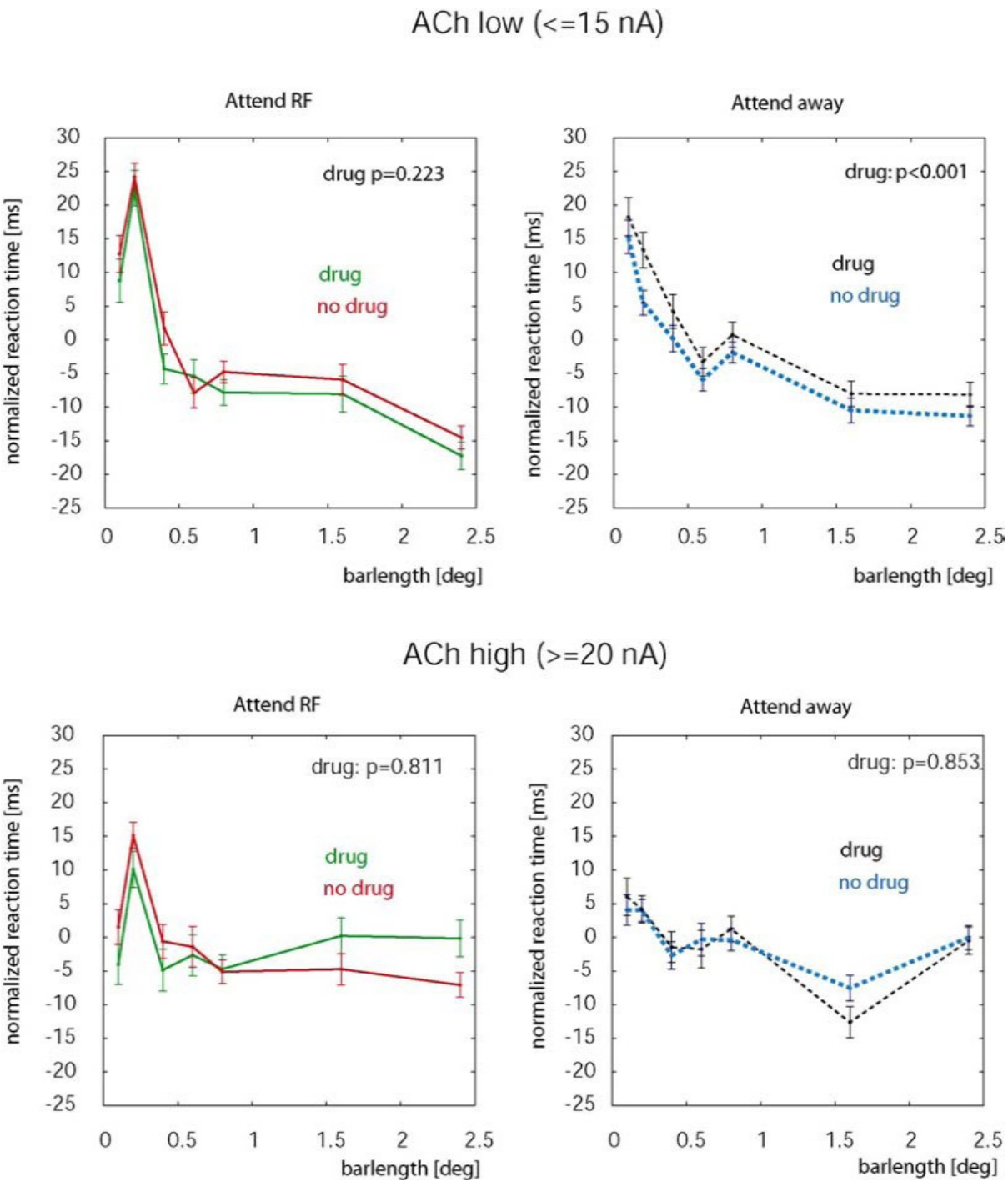

Figure 1.3: Effect of ACh application depending on attentional locus and application strengths. Experiments were subdivided into those where relatively small application currents were applied, and those where application currents were larger. When low application currents were applied, ACh significantly affected RTs, and the effect depended on where the animal attended (drug* attention interaction:

p=0.0009). At higher application currents these effects disappeared, suggesting that ACh only benefits attention within a relatively small range (see also the dependence of neuronal attentional modulation on application strength, next section).

1.3.3. Effect of ACh on single cell responses

An example cell is shown in Fig. 1.4. ACh increased the response of the neuron to a bar of different lengths, as evident from the raster plots and peri-stimulus time histograms (Fig.1.4a) as well as from the averaged response (Fig.1.4b). The neuron showed a significant main effect of attention (3 factor ANOVA, p=0.0058), a significant main effect of drug (p=0.0096), and a significant main effect of bar length (p<0.001). The effect of the interaction between attention and drug was also significant (p=0.034). ROC values for this neuron showed that attentional modulation was increased on ACh application. For the 0.2° bar length ROC (-ACH) =0.62, ROC (+ACH) = 0.68; for the medium bar length, ROC (-ACH) = 0.56, ROC (+ACH) = 0.56; for the largest bar length, ROC (-ACH) = 0.73, ROC (+ACH) = 0.75. Similarly, the modulation indices (MIs) in the presence of ACH were systematically increased. For bar length 0.2°, MI (-ACH) = 0.12, MI (+ACH) = 0.26; bar length 0.8°, MI (-ACH) = 0.06, MI (+ACH) = 0.13; bar length 2.4°, MI (-ACH) = 0.16, MI (+ACH) = 0.24.

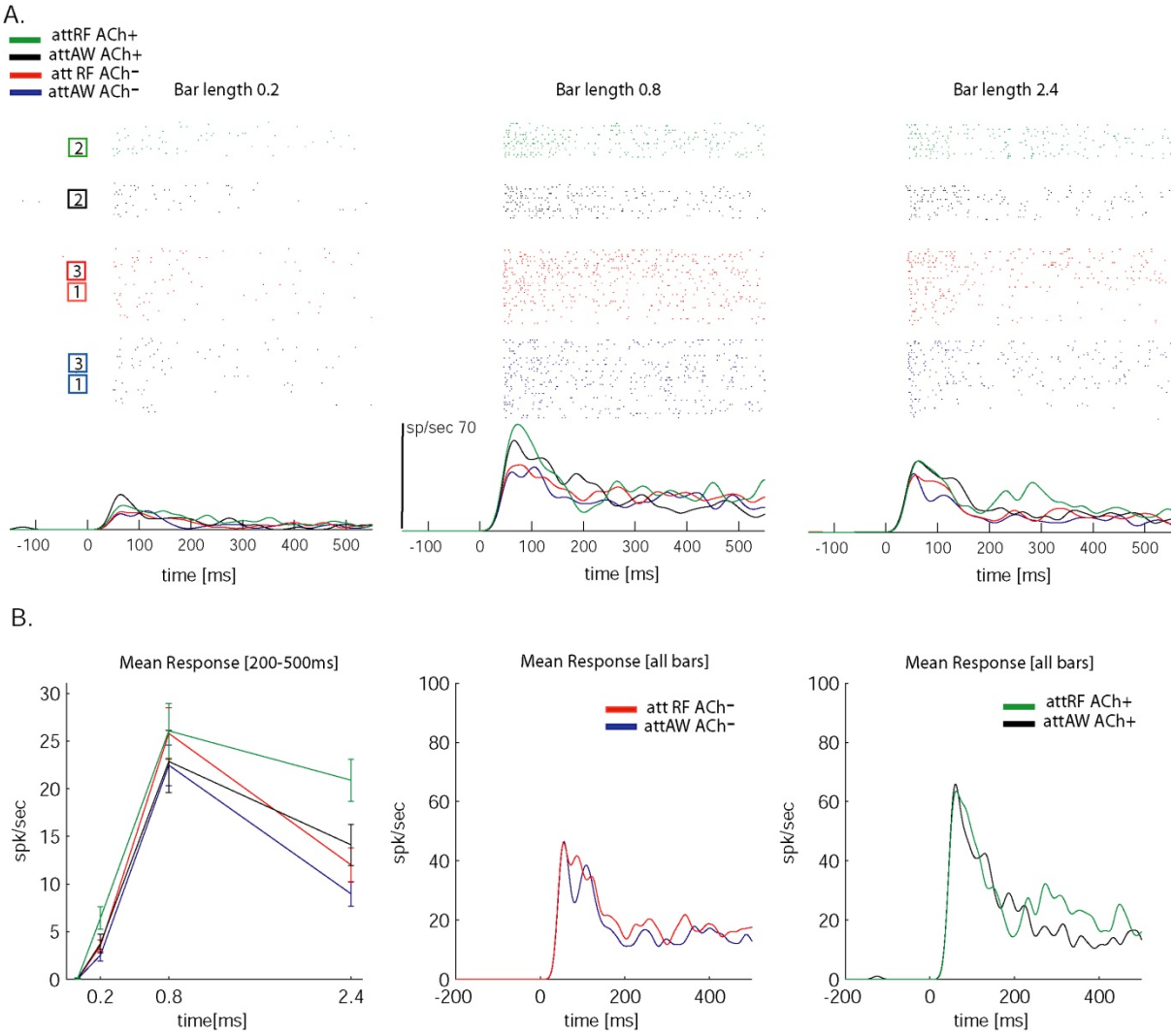

Fig. 1.4. Drug effects on attentional modulation. A) Attentional enhancement by application of ACh. We recorded the effect of attention on firing rates when no ACh was applied for three bar lengths in the attend-inside RF versus attend-outside (away) condition (box 1, 16 trials). Thereafter we recorded the effect of attention when ACh was applied (16 trials; box 2) followed by recovery (16 trials; box 3). B) Left, average activity (from 200 ms to 500 ms after stimulus onset) for the different stimulus, attention and drug conditions. Middle, averaged activity pooled across the 3 bar lengths in the absence of ACh. Right, same as middle plot except that in the presence of ACh. ACh increased attentional modulation. Error bars represent s.e.m.

Figure 1.5 shows the population data for the neurons tested with ACh. In 86/156 neurons we found a significant main effect of attention and a significant main effect of drug application, or a significant interaction between these two ($p<0.05$, 3 factor ANOVA, factors: attention; drug; stimulus). A significant interaction was found in 23/86 neurons (27%). In 21/23 cells acetylcholine increased the attentional modulation, while in the remaining 2 it decreased attentional modulation.

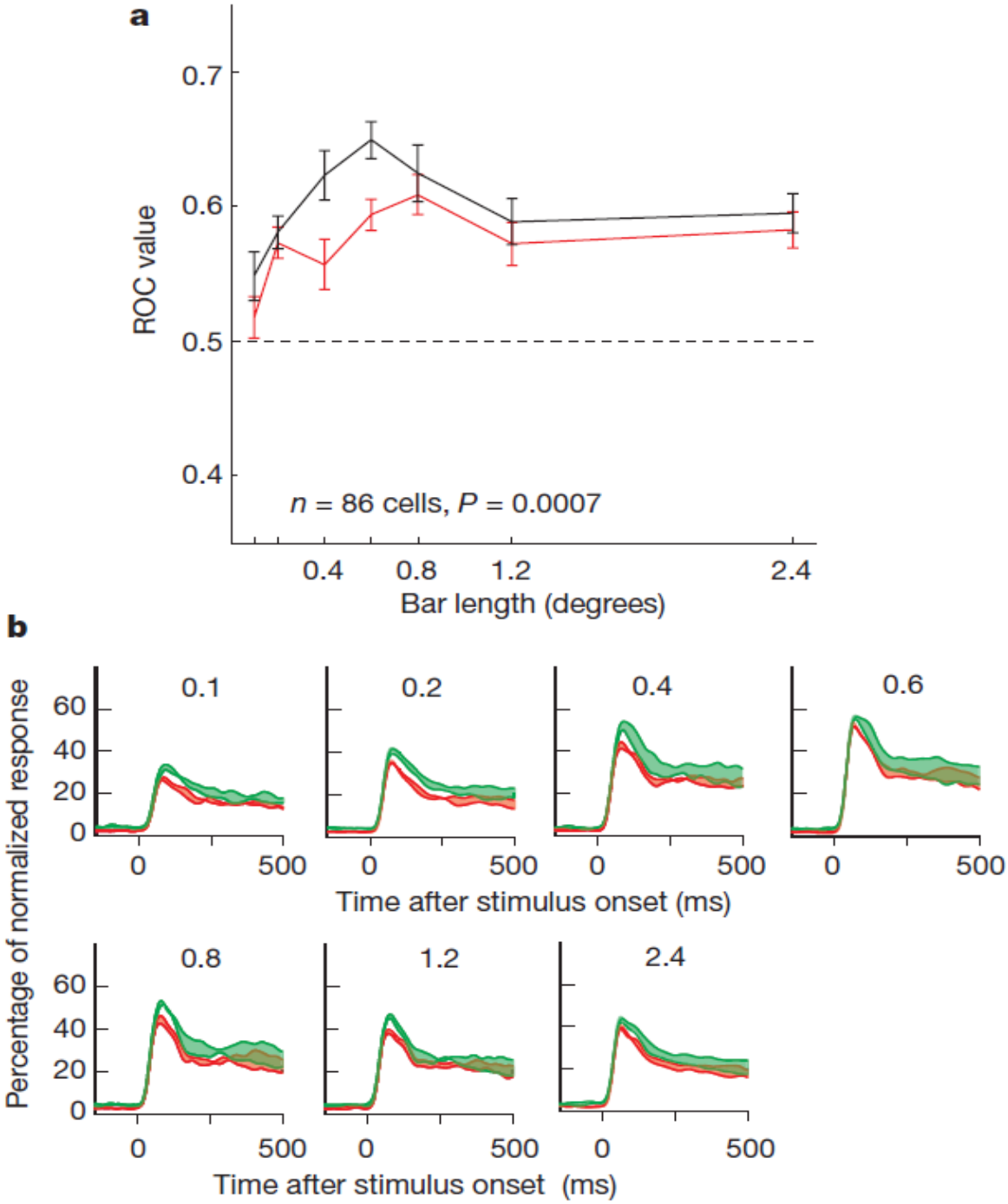

Figure 1.5. Acetylcholine effects on attentional modulation. a, Quantification of attentional modulation by mean population ROC for different bar length with (black line) or without (red line) ACh application (86 cells; error bars denote s.e.m.). b, Normalized population response depending on ACh application, stimulus (bar length; indicated at the top of each subplot) and attention condition. Activity levels were normalized relative to the peak activity of each neuron and averaged across the population. The red lines indicate activity without ACh application; green lines represent activity with ACh application. The upper line of each colour plot shows the normalized activity when attention was directed to the neuron's receptive field, the lower line when it was directed away from the receptive field. Widths of the coloured areas show strength of attentional modulation. ACh increased attentional modulation.

1.3.4. Effect of muscarinic blockade on single cell responses

An example cell is shown in Fig. 1.6. Scopolamine decreased the response of the neuron to a bar of different lengths. The neuron showed a significant main effect of attention ($p=0.004$), a significant main effect of drug ($p<0.001$), and a significant main effect of bar length ($p<0.001$). The effect of the interaction between attention and drug was significant ($p=0.025$). ROC values showed that attentional modulation was reduced on Scopolamine application. For the 0.2˚ bar length ROC (-SCOP) = 0.61, ROC (+SCOP) = 0.57; for the medium bar length, ROC (-SCOP) = 0.81, ROC (+SCOP) = 0.55; for the largest bar length, ROC (-SCOP) = 0.71, ROC (+SCOP) = 0.52. Similarly, the modulation indices (MIs) in the presence of SCOP were systematically reduced for all bar lengths.

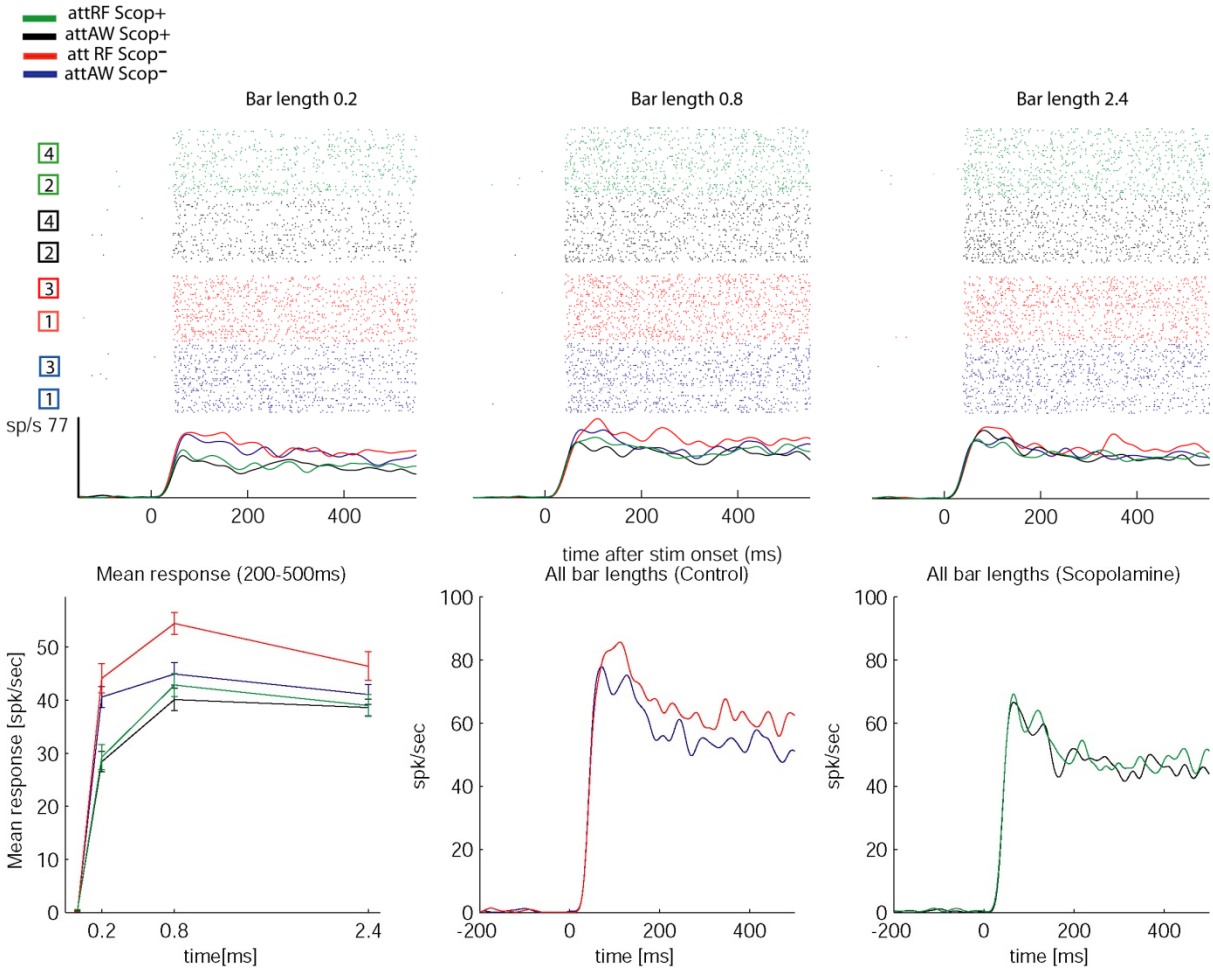

Fig. 1.6. Attentional reduction by application of Scopolamine. Same conventions as in figure 1.5 Top; note that an additional drug block (box 4) was recorded after recovery. Bottom; **(left)** average activity (200-500 ms after stimulus onset) for the different stimulus, attention and drug conditions. Middle, averaged PSTH pooled across the 3 bar lengths in the absence of Scopolamine. Right, same as middle except that in the presence of Scopolamine. Scopolamine reduced attentional modulation. Error bars represent s.e.m.

The effects of scopolamine for the population are shown in Figure 1.7. In 41/118 neurons we found a significant main effect of attention and a significant main effect of scopolamine application or a significant interaction between these two ($p<0.05$, 3 factor ANOVA, factors: attention; drug; stimulus). A significant

interaction was found in 18 of these 41 neurons (44%). In 16 of these 18 cells scopolamine reduced the attentional modulation, while in the remaining 2 it increased attentional modulation.

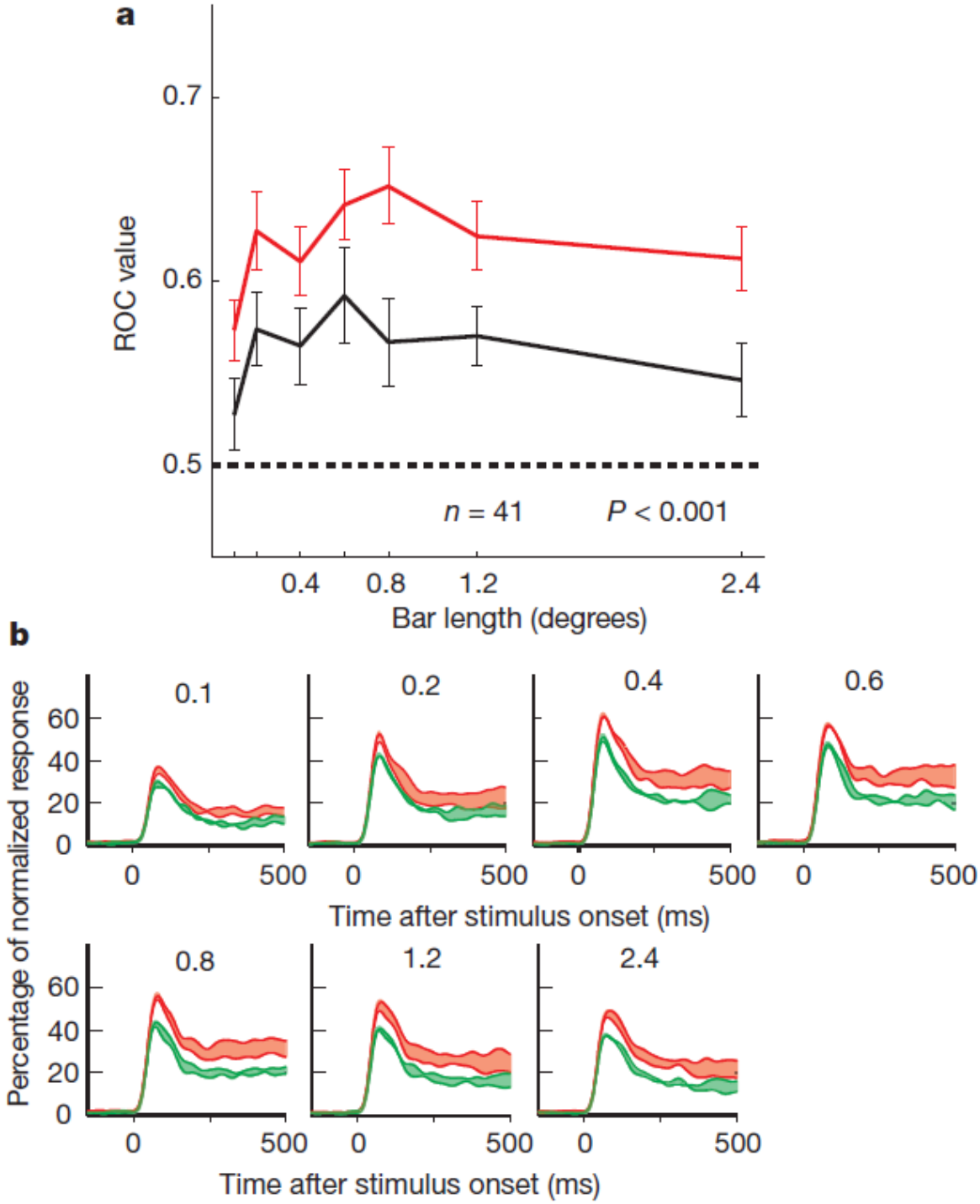

Figure 1.7. Scopolamine effects on attentional modulation. a, Quantification of attentional modulation by mean population ROC for different bar length with (black line) or without (red line) Scop application (41 cells; error bars denote s.e.m.). b, Normalized population response depending on Scop application, stimulus (bar length; indicated at the top of each subplot) and attention condition. Activity levels were normalized relative to the peak activity of each neuron and averaged across the population. The red lines indicate activity without

Scop application; green lines represent activity with Scop application. Same conventions as in figure 1.6. Scop reduced attentional modulation as shown by reduced widths of the green coloured area.

1.3.5. Effect of nicotinic blockade on single cell responses

In 65/151 neurons tested with mecamylamine we found a significant main effect of attention and a significant main effect of drug application or a significant interaction between these two ($p<0.05$, 3 factor ANOVA, factors: attention; drug; stimulus). A significant interaction was found in 15 of these 65 neurons (23%). In 9/15 cells mecamylamine reduced the attentional modulation, while in the remaining 6 it increased attentional modulation. Figure 1.8 shows the average ROC values for the population data. Application of Mecamylamine did not change these values significantly ($p=0.465$).

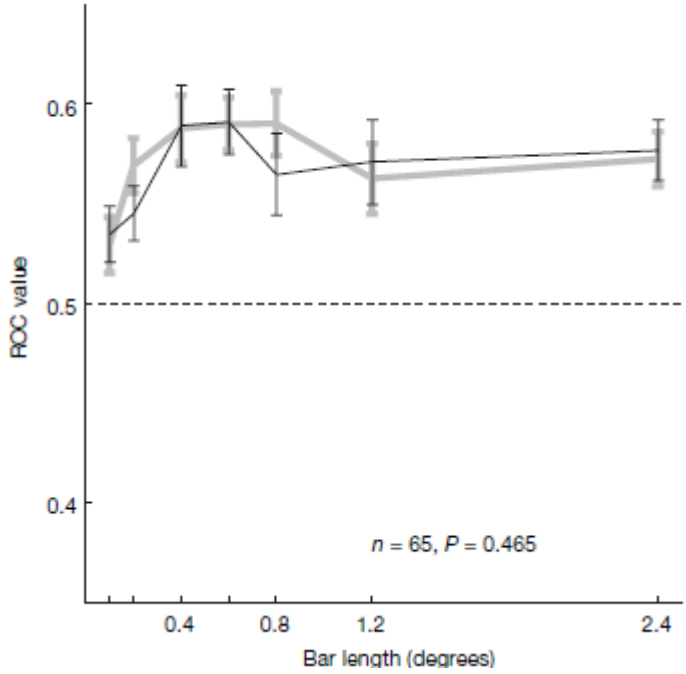

Figure 1.8. Mecamylamine effects on attentional modulation. Quantification of attentional modulation by mean population ROC (65 cells; error bars denote s.e.m). Control (grey line) and Mecamylamine-applied (black line) conditions. Mecamylamine did not have an effect on attentional modulation.

1.3.6. Control experiments: pH application

In further control experiments we used saline in one of the pipettes (0.9%, pH 4.5), and compared its effect to the effects of the drug of interest (n=11 cells). In these control experiments we never saw specific effects of saline application on firing rate or attentional modulation. For additional controls of pH effects we filled both pipettes with 0.9% saline (pH 4.5), and recorded a total of 31 cells, with and without saline (pH 4.5) applied (application current was 5-10nA, to match the most effective ACh current conditions). In this sample we found significant effects of saline application on 5 cells (Fig 1.9b). However, the effect did not result in any systematic

changes of attentional modulation or significant effects on overall firing rates, i.e. in some cells firing rates increased, while in others it decreased. Similarly, when averaging over all the cells from this sample that showed significant effects of attention (n=20, irrespective of significant saline/pH effects), there was no systematic effect of saline (pH) application on the strengths of attentional modulation (figure 1.9a). The fact that currents for the three drugs and the pH were identical during hold and application conditions, while the effects on neuronal activity and attentional modulation differed significantly between the three drugs, further argues against the possibility that application current or pH could have contributed our findings.

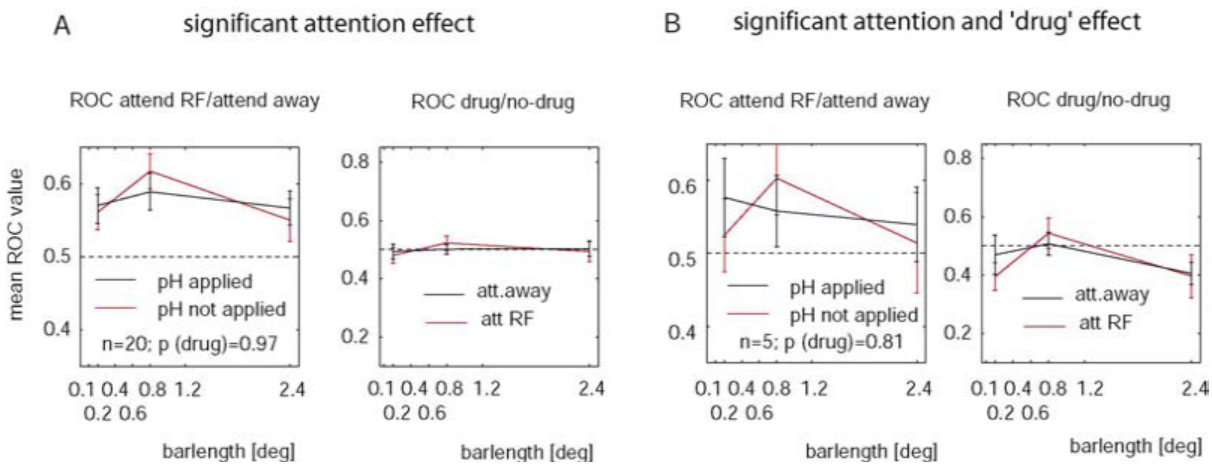

Figure 1.9: ROC values for saline/pH control recordings. A) Average ROC values for the different bar length across all cells that showed a significant effect of attention (irrespective of whether saline application had a significant effect or not). The left subplot shows the ROC values for the attend-away vs. attend-RF conditions separately for 'saline/pH not applied' and 'saline/pH applied'. Application of saline/pH did not change the attentional modulation. The right subplot shows the ROC values for the 'saline/pH not applied' and 'saline/pH applied' in the two attention conditions, i.e. it reveals the effect of 'saline/pH' on the distribution of firing rates (it determines whether saline/pH increased or decreased firing rates). The fact that ROC values were close to 0.5 shows that no systematic increase or reduction occurred. B) Average ROC for the different bar length across all cells that showed a significant effect of attention and of saline/pH application. All other conventions are as in A.

1.3.7. Effect of muscarinic blockade on the LFP

The mean population-evoked LFP response for 57 recording sites (48 in monkey HU, 6 in monkey BL and 3 in monkey HO) is shown in Fig 1.10. It shows the response from the different bar lengths and attentional conditions when scopolamine was not applied (top) and when it was applied (bottom). The onset of the stimulus onset resulted in a stereotypical deflection of the LFP which lasted for about 200–250 ms. After this period, the evoked LFP response remained reasonably stationary, a prerequisite for performing the spectral analyses reported below. The evoked potentials in the scopolamine-applied and control condition appeared virtually identical during the late response period.

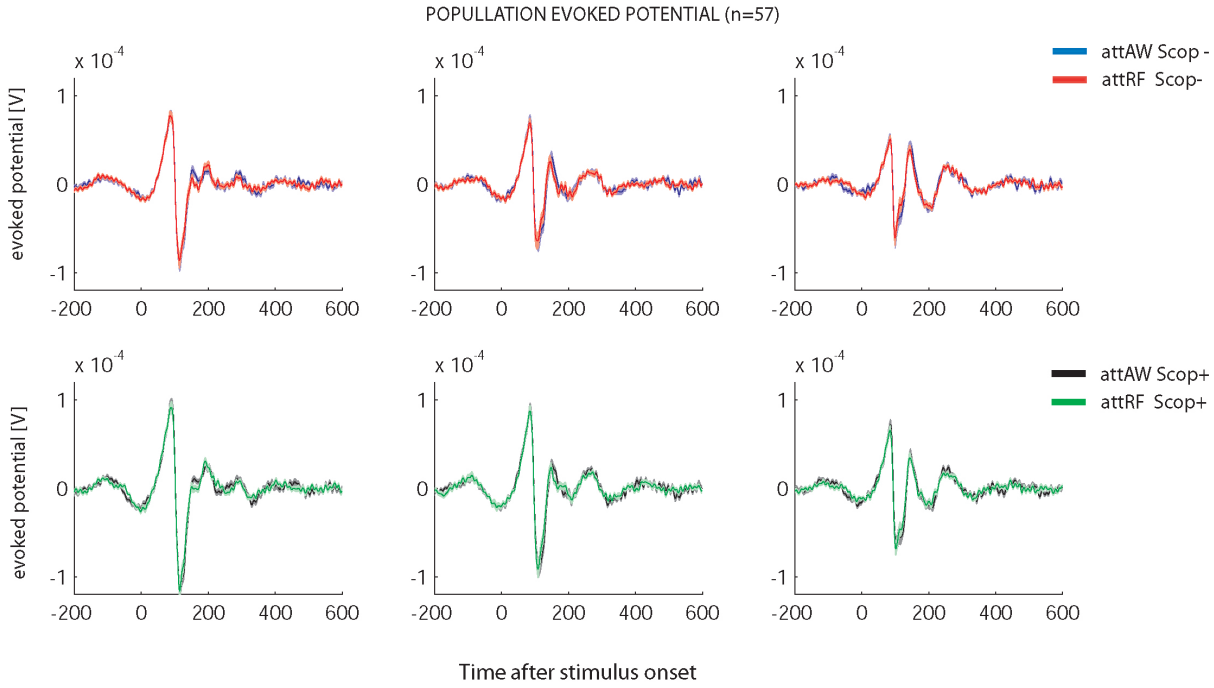

Fig 1.10. Population-evoked potential of the LFP for the different bar lengths, attention, and drug conditions (57 recording sites). [Top] SCOP not applied. Red curve shows the activity in the attend-RF condition and blue curve, the activity in the attend-away condition. [Bottom] SCOP-applied; green curve shows the activity in the attend-RF condition and black curve, the activity in the attend-away condition. The evoked potentials in the SCOP-applied and control condition were virtually identical.

To investigate the effects of attention and drug application on the sustained LFP response, we calculated the LFP response power spectrum averaged over the time interval of 256–512 ms after stimulus presentation using a multitaper technique (Percival and Walden, 1993). The time period of 256–512 ms was chosen because it is the period where attentional modulation of firing rates was most profound (Roberts et al., 2007, Herrero et al., 2008). This effect on the MUA for the population data is shown in Fig 1.11 (n=57). Attending towards the RF location increased the firing rate of the neurons compared with the rate achieved in the attend-away condition ($p < 0.001$, signed rank test). This was true for all bar lengths tested in the recorded population and for the control and scopolamine-applied conditions ($p < 0.001$, signed rank test). The population data shown here included all sites, except those that showed drifts on the neuronal activity during the course of the recording (i.e., baseline, drug_1, recovery_1, drug_2, recovery_2). That is, 5/67 recording sites showed clear drifts in the MUA following drug application and were discarded from further analysis (i.e., activity never recovered). An additional 5/67 sites were discarded because the effects during the course of the recording were not consistent. This means that e.g. we encountered facilitatory effects of attention on MUA during the baseline period but inhibitory effects of attention during the recovery period (or vice versa). Additionally, the consistency of the effects in the LFP during the course of the recording was also visually inspected. All recording sites included here (n=57) showed consistent effects of attention in the MUA and/or raw LFP gamma power during the baseline and subsequent recovery periods. For the analysis reported here, all periods were pooled together in two conditions; control condition where activity from all no-drug periods was included, and drug condition with activity from all drug periods. We included all recording sites but also

conducted an additional analysis where only recording sites with a main effect of drug and attention (or an interaction between drug*attention) on the MUA were included. The effects were virtually identical, except that the drug*attention interaction effect did not reach significance (p=0.145) possibly due to the low number of sites.

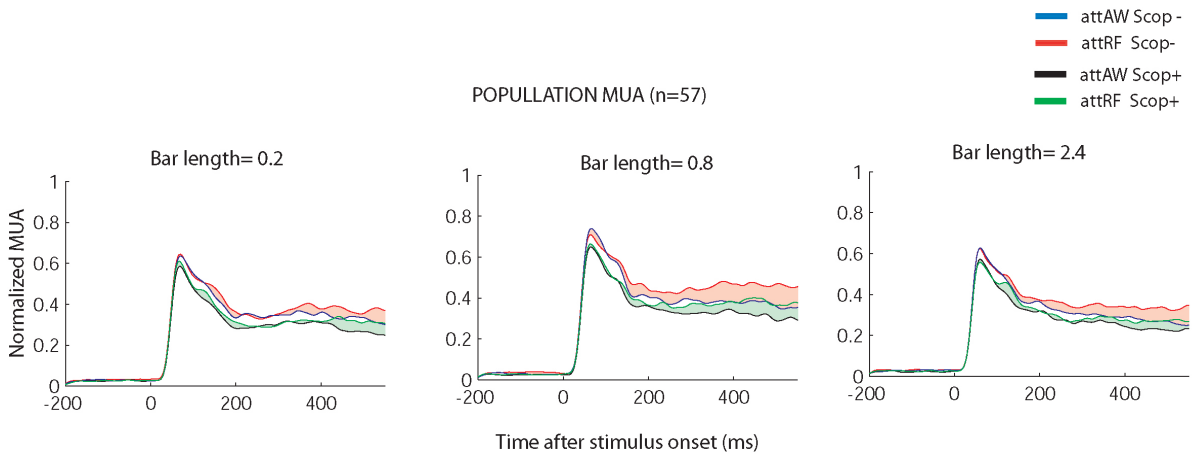

Fig 1.11. Normalized population PSTHs from the recording sites included in the LFP analysis (n=57). Response to different bar lengths, attention, and drug conditions. The shaded areas show the strength of the attentional modulation in no-drug (red) and scopolamine-applied (green) condition. In the no-drug condition, red lines show the activity in the attend-RF and blue lines the activity in the attend-away condition. In the scopolamine-applied condition, green lines show the activity in the attend-RF and black lines the activity in the attend-away condition.

Figure 1.12a shows the average LFP power spectrum for the recordings when scopolamine was not applied, pooled across the three monkeys (n=57). The attend-away condition is shown in blue, and the attend-RF condition is shown in red. Power spectra exhibited their maximum at low frequency, dropping off with increasing frequency and showing a peak in the gamma band (30–60 Hz) provided the stimulus was large enough. Gamma oscillations were usually larger for the attend-away, compared with the attend-RF, condition.

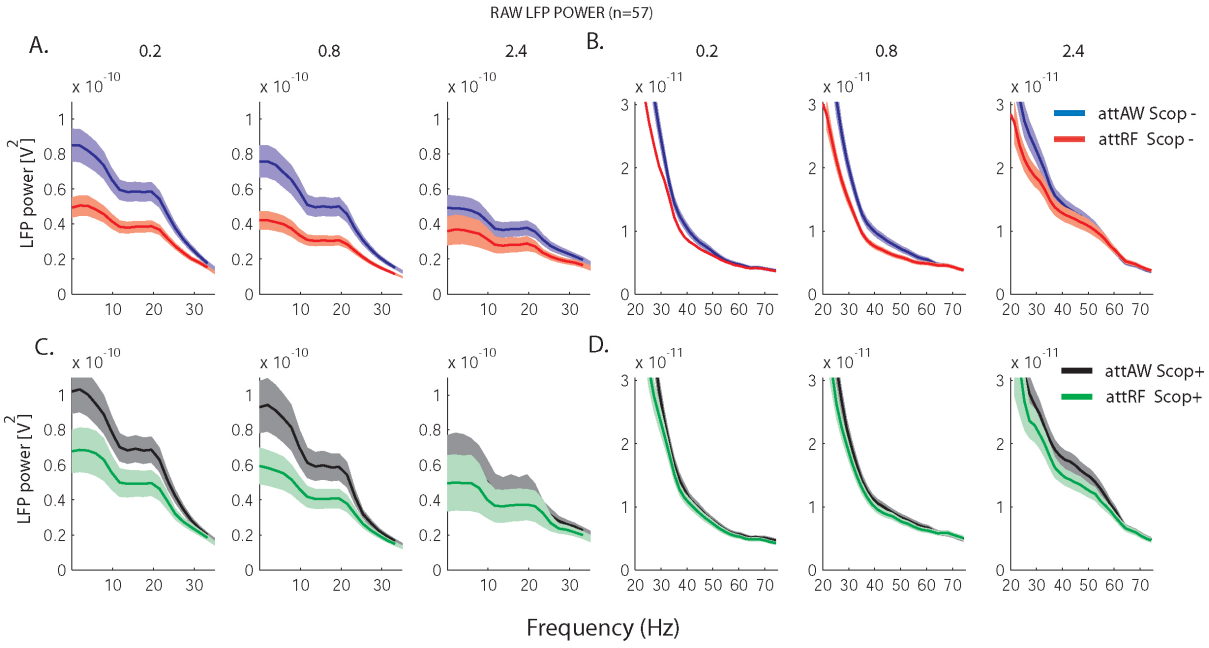

Figure 1.12. Average LFP responses (57 recording sites) showing the raw power spectrum in the different attention, bar length and drug conditions. Lower frequencies (1-30Hz) are shown in the left (A and C) and higher frequencies (20-70 Hz) in the right (B and C). Top. Scopolamine not applied. Red curves show the activity in the attend-RF condition; blue curves, the activity in the attend-away condition. Bottom. Scopolamine applied; green curves show the activity in the attend-RF condition and black curves, the activity in the attend-away condition. Shaded areas show SEM.

The peak in the gamma band (30–60 Hz) can be seen more clearly in the next figure (Fig 1.13) that shows the stimulus-induced power spectrum, that is, the spectrum normalized relative to baseline. It shows the data across the three animals over the time interval of 256–512 ms after stimulus presentation (spontaneous activity was taken from 256–0 ms before stimulus presentation). The amplitude of the gamma peak was stronger when the stimulus induced a V1 network state that favoured gamma oscillations (i.e., a large stimulus encroached on the suppressive surround (Gieselmann and Thiele, 2008)). In addition to the dependence on stimulus type, the attend-away condition resulted in more stimulus-induced power in the gamma range than the attend-RF condition. Scopolamine application (Fig 1.13b) appeared to increase overall stimulus induced power and to reduce the influence of attention on LFP gamma power for the smaller bar lengths.

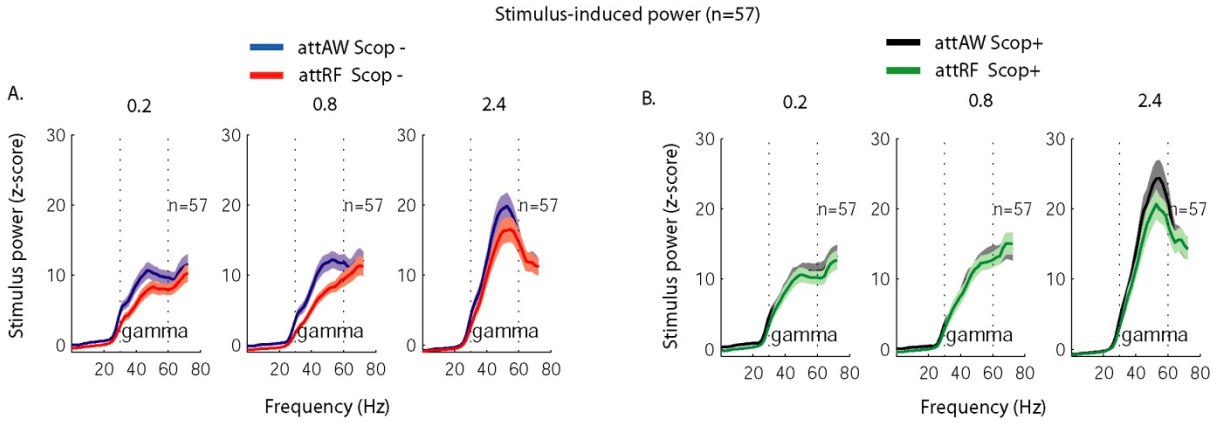

Figure 1.13. Stimulus-induced power for the different drug, attention, and bar length conditions (57 recording sites in three monkeys). A. Control condition. Red lines show attend RF while blue lines attend-away. B. Scop-applied condition, green curves show the activity in the attend-RF condition and black curves. Shaded areas show SEM, and vertical dotted lines demarcate the boundaries of the gamma band used in this study (30-60Hz).

In order to provide a quantitative understanding of how attention modulated the LFP signal, the power spectrum was divided into four different frequency bands (alpha: 7–13 Hz, beta: 13–30 Hz, gamma: 30–60 Hz, and high gamma: 60–100 Hz). The effects of attention on the LFP response power were analysed separately for each frequency band. Figure 1.14a shows the raw LFP power for the different frequency bands (n = 57 recording sites from three monkeys), and table 1.1 in the appendix summarizes the effects. Bar length had a significant effect on all frequency bands ($p < 0.05$, three-factor RM ANOVA). Increasing the stimulus size significantly reduced the overall power in the alpha and beta bands ($p < 0.001$). LFP power significantly increased with bar length in the gamma ($p < 0.001$) and high gamma bands ($p < 0.05$). Attending to the RF of the recording sites significantly reduced the power in the alpha, beta, and gamma bands, ($p < 0.001$), while this effect was not significant in the high gamma ($p>0.1$). The attention-induced power changes in the gamma and high gamma bands were not different across bar lengths (ANOVA interaction term: len*att, $p>0.05$). In the alpha and beta band, the largest attention-induced power changes occurred for the shorter and medium bar lengths (ANOVA interaction term: len*att, $p<0.001$). Applying scopolamine (green and black lines) increased the power in all frequency bands, although it only reached significance in the gamma and high gamma bands (drug, $p<0.001$). Additionally, only the gamma band showed an interaction between drug and bar length (ANOVA interaction term: drug*len, $p<0.05$), with the stronger drug-related power increments at the longest bar length. The interaction between drug and attention was not significant for any of the frequency bands ($p > .1$).

The population stimulus-induced power (n = 57) for the different frequency bands and drug conditions is shown in Fig 1.14b. Bar length had a significant effect on all frequency bands ($p < 0.001$, three-factor RM ANOVA). Increasing the stimulus size significantly reduced the stimulus-induced power in the alpha and beta bands ($p < 0.001$, three-factor RM ANOVA), while increasing it in the gamma and high gamma bands ($p < 0.001$). Attending to the RF of the recording sites significantly reduced the power in the alpha, beta, and gamma bands (att, $p < 0.01$). Applying scopolamine increased the power in all frequency bands (drug, $p<0.02$). The interaction between length and drug only reached significance in the gamma band (len*drug, $p<0.05$), with larger power increments at the longest stimulus size. The interaction between drug and attention was

only significant for the gamma band (dr*att, p<0.05), with smaller attention-induced changes in the drug compared to the control condition.

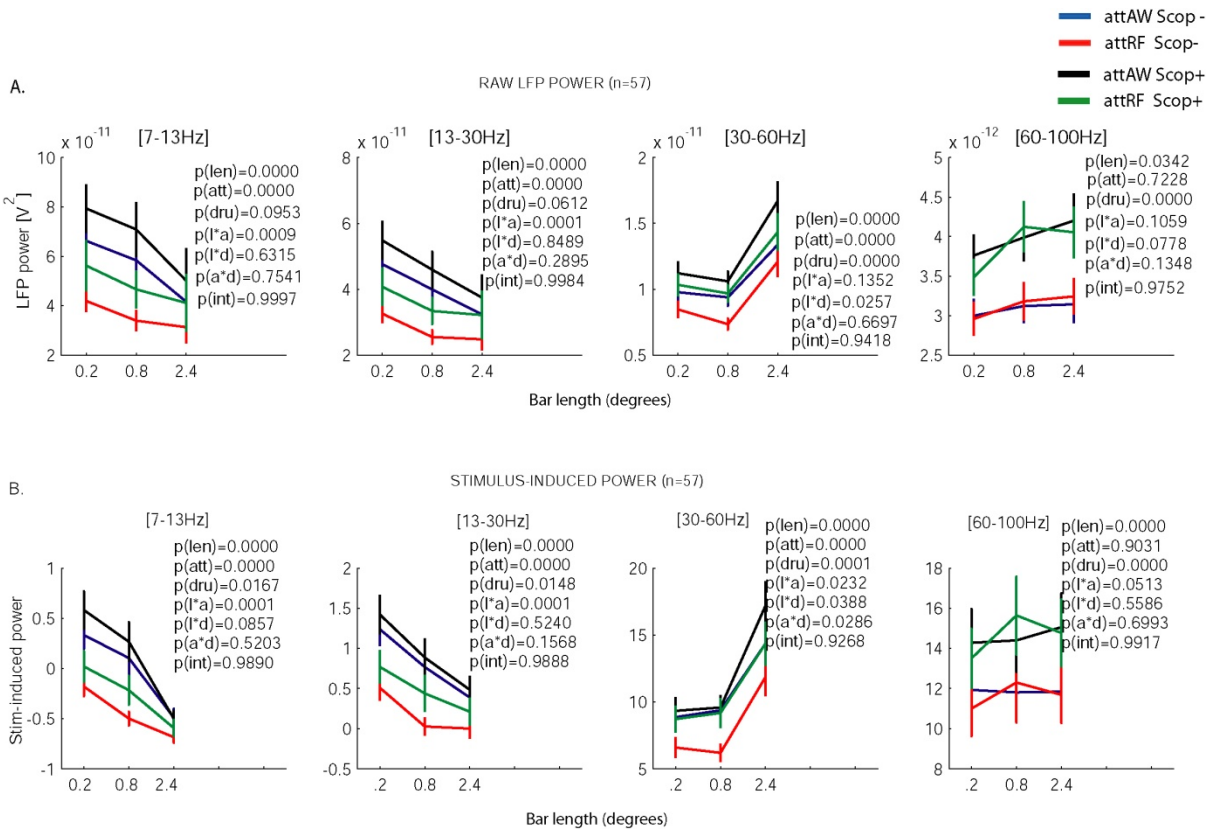

Figure 1.14. Population LFP power for the different frequency bands and experimental conditions (n = 57 recording sites from three monkeys). A) Raw LFP power in control (red and blue lines) and scopolamine-applied (green and black) conditions. B. Stimulus-induced power in control (red and blue lines) and scopolamine-applied (green and black) conditions. Conventions for att-RF and att-away as shown before. Error bars show SEM.

Additionally, the spike-field coherence (SFC) was calculated to determine the synchrony between the neuronal spiking activity and the local network oscillations. Figure 1.15 shows the population SFC for the different frequency bands and drug conditions (n = 57 recording sites from three monkeys). Bar length had a significant effect on the alpha and gamma bands ($p < 0.001$, three-factor RM ANOVA). Increasing the stimulus size significantly reduced the SFC in the alpha band while increasing it in the gamma band. Attending to the RF of the recording sites reduced the SFC on the alpha and beta frequency bands (att, $p<0.001$). Applying scopolamine (black and green lines) did not change the SFC on any of the frequency bands (drug, $p>0.05$). The only interaction effect that was significant was restricted to the alpha and beta bands. The interaction between attention and stimulus size (len*att, $p<0.05$) revealed less attention-induced effects on the longest stimulus size compared to the shorter ones.

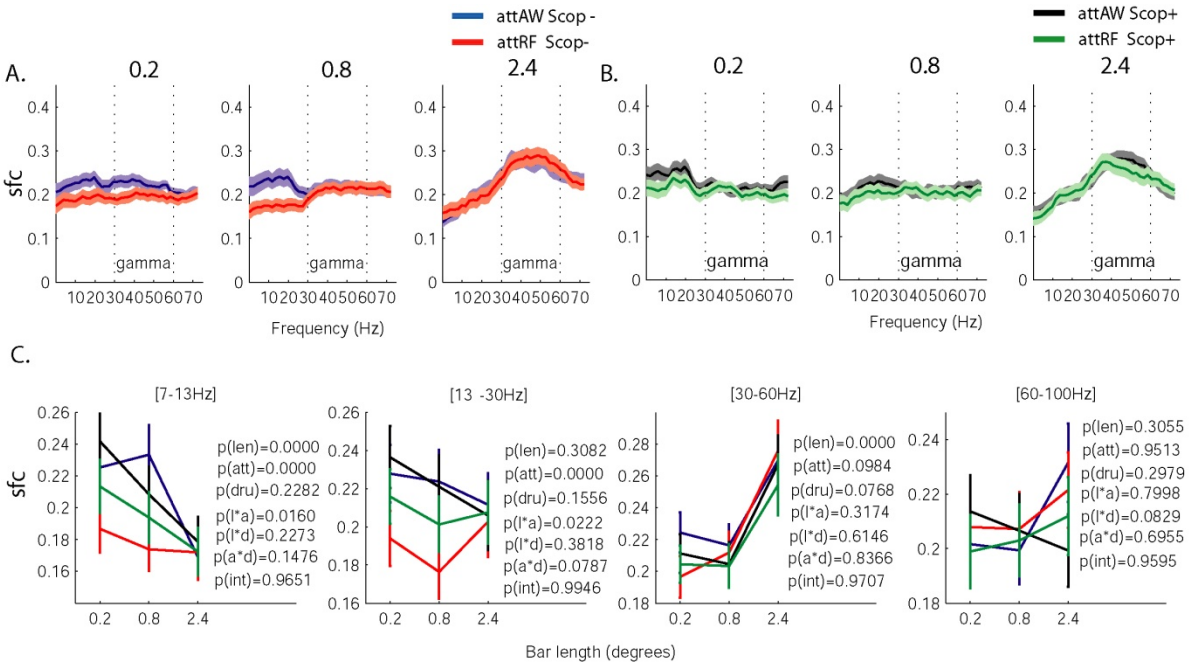

Figure 1.15. Population SFC in the different drug, attention, and stimulus sizes (57 recording sites in three monkeys). **A.** Control condition; red and blue lines show SFC values in the attend-RF and att-away condition. **B.** Scopolamine-applied condition; green and black lines show SFC values in the attend-RF and att-away condition. **C.** Quantification of SFC values across different frequency bands. Bars show SEM.

1.3.8. Effects of nicotinic blockade on the LFP

Figure 1.16 shows the LFP data for the gamma band (n = 61 recording sites from two monkeys; see Appendix figure 1.4 for all frequency bands). Similar to the above results, the overall and stimulus-induced power decreased with bar length in the lower frequency bands (factor 1: length, $p < 0.001$) and increased in the gamma bands ($p < 0.001$). Attending to the RF of the recording sites significantly reduced the overall and stimulus-induced power in all bands (factor 2: attention, $p < 0.001$), except the high gamma. Applying the nicotinic antagonist mecamylamine increased the overall and stimulus-induced power in the gamma bands (factor 3: drug, $p<0.05$). It shows that the interaction between attention and drug was not significant for any measurements (attention*drug, $p<.1$). This result suggests that nicotinic receptors do not affect attentional modulation: while gamma power per se was affected, it did not systematically interfere with its modulation by attention. Additionally, the attention-induced power changes in the gamma band were different across stimulus sizes: shorter bar lengths showed larger attentional modulation than longer bars did (length*attention, $p>0.01$).

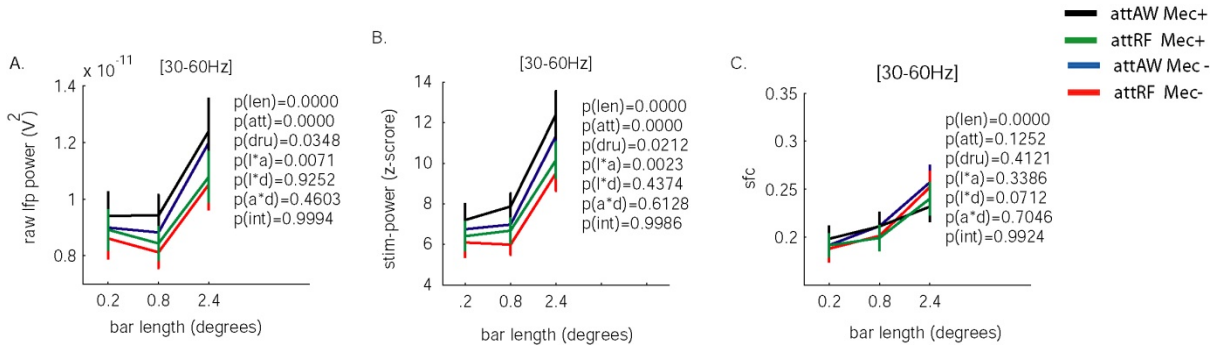

Figure 1.16. Population LFP gamma power for the different drug, attention and stimulus conditions (n = 61 recording sites, 2 monkeys). A) Raw LFP power in control (red and blue lines) and mecamylamine-applied (green and black) conditions. B. Stimulus-induced power. C. Spike-field coherence. Other conventions as before. Error bars show SEM.

1.3.9. The effect of Acetylcholine on the LFP

The effects of stimulus size and attentional modulation on the LFP power and coherence were very similar as those reported above. However, the application of Acetylcholine did not have a systematic effect on the LFP power for any of the frequency bands. Figure 1.17 shows the results for the gamma band (n = 47 recording sites from two monkeys; see Appendix figure 1.5 for results on all frequency bands). ACh did not change the raw power, stimulus-induced power or SFC (factor drug, p>0.1). Additionally, the attentional modulation was very similar in the absence and presence of acetylcholine (drug* attention, p>.1).

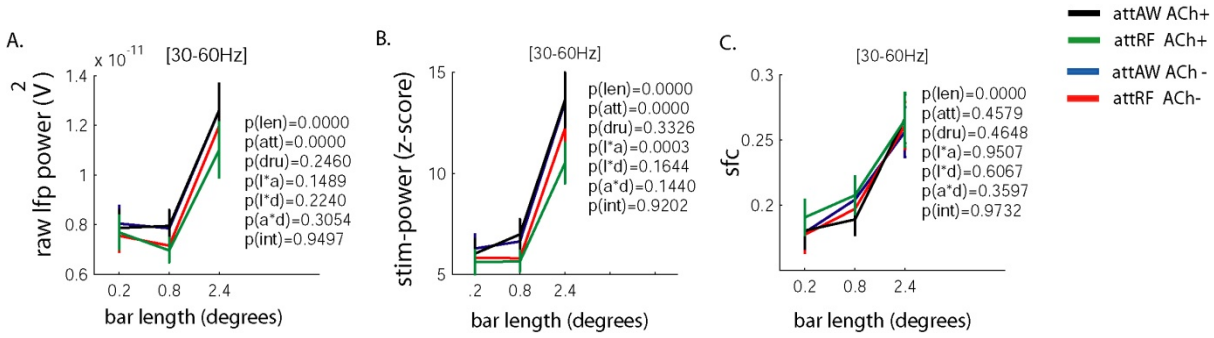

Figure 1.17. Population LFP gamma power for the different drug, attention and stimulus conditions (n = 47 recording sites, 2 monkeys). **A)** Raw LFP power in control (red and blue lines) and ACh-applied (green and black) conditions. **B.** Stimulus-induced power. **C.** Spike-field coherence. Other conventions as before. Error bars show SEM.

1.4. Discussion

The results reported here are in line with previous studies that found that directing attention to a stimulus inside the receptive field (RF) of a V1 neuron results in increased firing rates (Roelfsema et al., 1998, Roberts et al., 2007), and decreased LFP power and spike-field coherence in the gamma frequency range (Chalk et al., 2010). Attention is transferred by top-down inputs, presumably coming from higher areas of the visual,

parietal and frontal cortices (Moran and Desimone, 1985, Spitzer et al., 1988, Motter, 1993, Desimone and Duncan, 1995, Moore and Fallah, 2004). These top-down inputs are mostly excitatory and drive pyramidal neurons through glutamatergic receptors (Johnson and Burkhalter, 1996, Shao and Burkhalter, 1996). An alternative possibility is that this drive is mainly cholinergic, as cortical cholinergic inputs originating from the basal forebrain system have been demonstrated to mediate important aspects of attentional processing (Sarter et al., 2005). For example, studies in the rat showed persistent attentional impairments when cortical areas (e.g. mPFC) were depleted from the normal supply of ACh (McGaughy et al., 2002, Nelson et al., 2005), while cue-evoked orientation behaviour increased ACh concentration in the mPFC (Parikh et al., 2007). We found that ACh contributes to attentional modulation in V1 of the macaque monkey through muscarinic, but not nicotinic, receptor mechanisms. This was evident from the spiking activity of single neurons and from the oscillatory activity of neuronal ensembles (LFP analyses). Blocking muscarinic receptors reduced both the attentional modulation of firing rates and the reduction of stimulus-induced LFP power. This latter result is in line with a previous study in the cat visual cortex (Rodriguez et al., 2004) that demonstrated the involvement of cholinergic mechanisms in gamma oscillations and response synchronization. However, the authors found that application of scopolamine decreased LFP gamma power, while we found the opposite. This systematic increase in power with muscarinic blockade is in line with other studies that found ACh to reduce the spread of membrane voltage fluctuations (Kimura et al., 1999) and the spread of BOLD activation (Silver et al., 2008). This means that blockade of muscarinic receptors could increase the spread of excitation, leading to an increase in LFP power as in our study. We also found systematic increases in gamma power with mecamylamine, which is in line with a recent in-vitro study (Lucas-Meunier et al., 2009) that found complex interactions between different types of nicotinic receptors (and between deep and superficial layers) in V1. One such finding was that endogenous ACh could also enhance inhibition by acting directly on GABAergic interneurons presynaptic to the recorded cell. Under such a scenario, mecamylamine would release the recorded cell from a bath of inhibition, possibly leading to increased oscillatory activity as in our study. Mecamylamine application increased overall gamma frequency oscillations while reducing the gain in the spiking response. A similar effect (increased gamma oscillations and decreased gain) was observed by (Gieselmann and Thiele, 2008) when stimulating the surround of V1 neurons in the intact brain. One possibility to explain the finding in our study is that blockade of nAChRs at thalamocortical terminals shifts the cortical circuitry in favour of lateral connections. However, we did not find a nicotinic receptor contribution in attentional modulation in V1.

The ACh diffusion diameter in cortical tissue during prolonged iontophoresis was estimated to be in the 300 µm range (Haidarliu and Ahissar, reported as unpublished observations in (Ego-Stengel et al., 2001)). Due to this relatively local spread, we did not expect strong changes in behaviour with drug application. However, we did find modest changes: when the animals attended away from the neurons being recorded, low dosage ACh (<15nA) applied to these neurons slowed significantly RTs. We suggest that improved neuronal processing at the 'wrong' injection site makes it harder to disengage attention from this location, thus slowing RTs. When ACh currents were higher (>=20nA) these effects were not present anymore, in line with studies that found only optimal doses of dopamine to improve cognitive performance (Goldman-Rakic et

al., 2000). Surprisingly, ACh did not increase LFP gamma power as it would have been expected based on previous studies. For example, Metherate and colleagues (Metherate et al., 1992) showed EEG activation in the auditory cortex and concomitant changes in cellular membrane potential fluctuations (from high amplitude and low-frequency oscillations to small-amplitude and gamma frequency) after stimulation of the nucleus basalis. See (Munk et al., 1996) for similar findings after stimulation of the mesencephalic reticular formation, and (Lucas-Meunier et al., 2009) for increased endogenous ACh release after electrical stimulation in V1 (layer 1) . Our finding, however, could be due to the efficacy of acetylcholine-esterase in breaking down acetylcholine quickly and efficiently, preventing it from affecting larger parts of the network. A previous study (Rodriguez et al., 2004) also failed to find increase gamma power directly with ACh, although it affected gamma synchronization at longer timescales.

Taken together, these results demonstrate that muscarinic cholinergic mechanisms play a central part in mediating the effects of attention in V1. There is some concerns, however, as the coarseness of the ACh innervation (Nelson et al., 2005) may be incompatible with the highly localized and fast effects of spatial attention. This raises the question of whether non-cholinergic mechanisms are more directly contributing to attentional modulation. Under this scenario, ACh release from presynaptic cholinergic terminals increases the level of glutamate which activates NMDA receptors. And it is the activation of these receptors that allows the demands of attentional performance (Hasselmo and Sarter, 2010). The possibility that NMDA receptor activation contributes to attentional modulation in the awake-behaving monkey will be examine in chapter 2.

Chapter 2. Contribution of NMDA receptors to attentional modulation in macaque V1

2.1. Introduction

In the previous chapter, the involvement of cholinergic mechanisms in attentional modulation was studied. It was demonstrated that cholinergic mechanisms contribute to attentional modulation in V1 (Herrero et al., 2008), suggesting an involvement of cholinergic inputs from the basal forebrain (Szerb, 1967). Intracortical sources cannot be excluded though, as the existence of intracortical cholinergic neurons has recently been reported (von Engelhardt et al., 2007). Another concern is the apparent coarseness of the ACh innervation, which is in sharp contrast with the highly localized and fast effects of spatial attention. This raises the question of whether non-cholinergic mechanisms are more directly contributing to attentional modulation. Under this scenario, ACh release from presynaptic cholinergic terminals might increase the level of glutamate in NMDA receptor rich synapses (the argument is based on reasons outlined further down). And it is the activation of these receptors that allows the demands of attentional performance.

Theoretical models describing the function of NMDA glutamatergic receptors are largely based on studies of hippocampal slice preparations (Collingridge and Bliss, 1987, Cotman et al., 1988). Slice preparations from the visual cortex found minor NMDA components on the EPSPs produced by electrical stimulation unless IPSPs were minimized (Artola and Singer 1987; Jones and Baughman 1988). Later in-vivo studies in cat visual cortex found that NMDA receptors were also active during normal synaptic transmission (Hagihara et al. 1988; Miller et al. 1989), predominantly in layers II and III (Fox et al., 1989, 1990). Modelling work suggested that NMDA receptor activation could enable synaptic reverberations in recurrent circuits, such as those necessary for persistent mnemonic activity (Wang, 2001). This persistent activity which may underlie working memory processes can be conceptually related to spatial attention, as top-down spatial attention has often been regarded as a spatial working memory signal (Downing, 2000, Deco and Thiele, 2009). Increased neuronal gain with selective attention has been reported in many cortical visual areas including MT (Treue and Maunsell, 1996), V4 , V2 (Reynolds et al., 1999), V1 (Roelfsema et al., 1998), and subcortical areas such as the LGN (McAlonan et al., 2008), TRN (Crick, 1984) and SC (Robinson and Kertzman, 1995).

There is a strong similarity between gain changes that are seen with attention in the awake-behaving monkey (e.g., (Roelfsema et al., 1998)) and the gain changes seen with NMDA receptor activation in the above studies ((Fox et al., 1989, 1990); see also (Salt, 1986, Shima and Tanji, 1993b, a, Fleidervish et al., 1998)). Gain increases have been observed in the visual cortex when NMDA receptors are activated (Fox et al., 1990). The authors found that iontophoretic application of NMDA in V1 of anesthetized monkeys increased the slope of the linear portion of the CRF (i.e., they found an amplification of responses). This effect strikingly resembles the effect of attention on CRFs, at least that observed by some models (compare Figure 1 in (Thiele et al., 2009) and Figure 6a in the Fox's study (Fox et al., 1990)). Activation of non-NMDA receptors in that study, in contrast, resulted in a constant component being added to visual responses of all magnitudes (i.e., simple linear summation). Additionally evidence for the similarity between attention and NMDA gain changes comes from their time course. Attention affects mostly the sustained part of responses in V1 (e.g. Roelfsema et al., 1998),

similar to the selective contribution of NMDA receptors to the sustained part of the response in the ventrobasal thalamus (Salt, 1986).

In this chapter, I examine whether NMDA receptor activation contributes to attentional modulation in the awake-behaving monkey. The attentional modulation in visual cortex could be mediated by higher cortical areas (e.g. FEF, PPC) through glutamatergic feedback inputs. Although V1 does not receive direct feedback projections from FEF, it should also be affected through indirect projections from prestriate areas V4 and V2 (Ungerleider et al., 1989). One possibility is that increased amounts of ACh alter the strength of connections among V1 neurons (and their biophysical state) which may then allow spatially specific glutamatergic feedback to enhance specific incoming information. To investigate this hypothesis, iontophoretic pharmacological analysis of glutamatergic NMDA receptors was combined with single cell and LFP recordings in V1 while macaque monkeys performed a task that demanded top-down spatial attention.

2.2. Methods

General

All experiments were carried out in accordance with the European Communities Council Directive 1986 (86/609/EEC), the US National Institutes of Health Guidelines for the Care and Use of Animals for Experimental Procedures, and the UK Animals Scientific Procedures Act.

Paradigm

The paradigm used in these experiments was basically identical to that in chapter 1, except that the stimuli presented could also vary in luminance contrast (contrast experiments) as well as length (bar experiments). For that reason I do not reiterate the details here, and simply refer to chapter 1. Although this equally applies to some aspects of the data analysis, I repeat the details, as some details are similar to those used in chapter 1, while others differ, and I assume that a full account may aid the clarity.

Electrophysiological recordings and drug application

A tungsten-in-glass electrode flanked by two pipettes was used for the recordings (Thiele et al., 2006). Drugs were applied iontophoretically through these pipettes (NeuroPhore BH-2, Digitimer, Welwyn Garden City, Hertfordshire, England). Pipette opening diameter varied between 1-4 μm. Pipette resistance varied between 12-120 MΩ, with most recordings at 20-75 MΩ. Hold currents for NMDA and APV were usually -10 nA, in rare occasions (when the pipette resistance was 10-20 MΩ) it was -40 nA. Pipette-electrode combinations were inserted into V1 through the dura on a daily basis without the use of guide tubes. The integrity of the electrode and the pipettes were checked under the microscope before and after the recording sessions, in addition to measurements of the pipette impedance made before and after the recording at each recording site. Drug application was continuous during blocks of 'drug applied'. The duration of each block could vary depending on the number of bar lengths used, depending on the number of repetitions for each condition that we aimed for, and depending on the speed/accuracy of the animal. On average drug application for each block was ~5-15 minutes. For the data analysis we removed the first 2 trials for each condition (condition 1, bar lengths; condition 2, attend RF/away) from the data set, as drug effects and recovery usually occur with a slight delay

of ~0.5-3 minutes. We regularly compensated for the change in current during the ejection condition by increasing the hold current of one of the two pipettes, thereby keeping the overall current identical between the 'hold' and 'eject' conditions.

Data collection and surgical procedures

Two male macaques (monkeys HU and HO) were used for the recordings. After initial training, monkeys were implanted with a head holder and recording chambers above V1 under general anaesthesia and sterile conditions (for details of surgical procedures, see Thiele et al., 2006). Stimulus presentation and behavioral control were managed by Remote Cortex 5.95 (Laboratory of Neuropsychology, National Institute for Mental Health, Bethesda, MD). Neuronal data was collected by Cheetah data acquisition (Neuralynx) interlinked with Remote Cortex. The waveforms of all spikes that exceeded a threshold set by the experimenter were sampled at 30 kHz. Offline sorting of these MU spike samples was carried out based on waveform features (Neuralynx spike sorting software, Version 2.10). Eye movements were recorded by scleral search coils in monkey HU (temporal resolution 250 Hz, spatial resolution of 1.5'), and by an infra-red based system in monkey HO (Thomas Recording, temporal resolution 220 Hz, spatial resolution 2.5'). Eye position during all trials was restricted to be within ±0.3-0.5 of the fixation point in monkey HU, and to be within ±0.5-0.7 in monkey HO.

Receptive field characterization and visual stimulation

We initially determined the location of the receptive field for each recording site as well as the optimal orientation, spatial frequency and phase using reverse correlation techniques (DeAngelis et al., 1994, Gieselmann and Thiele, 2008). The RF location was estimated by mapping the classical receptive field with briefly presented dark and light squares (0.1º width, 100% contrast) at pseudo-random locations on a 10x10 grid (a 1x1° area). The RF centre was taken as the location of the peak of the Gaussian fitted to the response distribution (Roberts et al., 2007). RFs centres were located in the lower quadrant, at an eccentricity of 2.5° to 6°. Thereafter, the tuning properties were estimated using static sinusoidal gratings (1° diameter) centred on the RF. These gratings varied in orientation (12 orientations, 0–165°), spatial frequency (1, 3, 5, 7, 8, 9 or 10 cycles ⁄ °) and phase (0, 0.5π, π, 1.5π) every 60 ms in a pseudo-randomized order. The stimulus that yielded the peak response was taken to represent the preferred orientation, spatial frequency, and phase of the neuron under study. The obtained parameters were used to determine the orientation of the test stimuli that was used in the main experiments.

Visual stimulation

In the bar experiments the visual stimuli was identical to those in Chapter 1, except that only 3 bar lengths were used (0.2°, 0.8°, and 2.8°). They were centered on the neuron's RF. In the contrast experiments the bar length used was fixed to 0.5°, while the luminance contrast varied: 5%, 10%, 15%, 20%, 25%, and 50% (Michelson contrast).

Analysis of spiking activity

Spike data from the recording electrode were obtained by band-pass filtering the raw signal from 600–9000 Hz. Offline sorting of these filtered data (MU spike samples) was carried out based on waveform features (Neuralynx spike sorting software, Version 2.10). In some occasions two or three clusters of single unit activity could be segregated, while in others only one. Single-unit activity from the window of interest (200-500 ms after stimulus onset) was subjected to ANOVA; 3 factors (attention, drug application and stimulus length/contrast). Only neurons with a significant main effect of attention and a significant main effect of drug application, or a significant interaction between these two factors were included for further analysis ($p<0.05$).

Neuronal sensitivity

Strengths of attentional modulation were quantified in two ways. First, by calculating a modulation index (MI) which normalizes explicitly for firing rates. The MI for each cell, drug condition and bar length/contrast was calculated as follows: MI = (activity attend receptive field – activity attend away) / (activity attend receptive field + activity attend away). By activity we mean the averaged response across all trials of a given condition. Second, the strength of attentional modulation was calculated by the area under the receiver operating characteristic (ROC) curve on the basis of single trial responses given knowledge of the bar length/contrast (Swets, 1988, Roberts et al., 2007) . Unlike MIs, ROC analysis takes into account the variance of the response. ROC values of 0.5 indicate that an ideal observer can only perform at chance level in deciding the locus of attention. Higher ROC values indicate greater attentional response enhancement, thus if NMDA increased attentional modulation, ROC values should be increased in NMDA-applied conditions relative to control conditions.

Trial-to-trial response reliability

Given that attentional modulation can be encoded in terms of variance changes rather than spike rate changes (Mitchell et al., 2007), the Fano factor (F) was calculated. The Fano factor is the ratio of spike count variance to mean spike count (variance/mean), and it was calculated for the different attention, drug and bar-length conditions. To examine the time course of the effects, a time-resolved fano factor was calculated in 100ms time windows starting from stimulus onset (window 1, 0-100ms; window 2, 100-200ms, window 3, 200-300ms, window 4, 300-400ms, window 5, 400-500ms). Additionally, we determined the degree at which the response variance scales with the mean response by fitting the power function to the mean vs. the variance data (variance$= aR^b$) (Gur et al., 1997). This function corresponds to a straight line, with intercept a and slope b. Following transformation of the mean and variance of the firing rate into logarithmic values, we used a robust linear regression (Matlab 13, Mathworks) to obtain the coefficients a and b for each cell when NMDA (or APV) was not applied and when it was applied, and when attention was directed to the RF or away.

Contrast Response Functions

For each neuron, we measured the mean activity during the 200-500ms time interval to 6 different stimulus contrasts. To determine the effect of attention on contrast tuning in the presence and absence of drug, contrast response functions were obtained for each neuron in the condition when no drug was applied, and

then when drug applied. Each contrast response function was based on the responses to 10-20 repetitions of each contrast. Contrast response functions were fitted with a hyperbolic ratio function of the following form:

$$R(c) = R_{max} * (c^n / [c^n + c50^n]) + M$$

where R_{max} is the saturated response, *c50* is the contrast at which the half maximal response is reached, *n* determines the slope of the contrast response function, and *M* corresponds to the spontaneous activity. This model provides a good approximation of contrast response functions in monkey visual cortex (Albrecht and Hamilton, 1982, Thiele et al., 2004b, Williford and Maunsell, 2006), and we used multidimensional unconstrained nonlinear minimization (Nelder-Mead) to minimize the summed squared difference between data and model (Matlab 7.1, Mathworks). To determine whether R_{max} or *c50* differed significantly with attention/drug, we fitted each data set independently with the hyperbolic ratio function and determined the chi-square error of the individual fits, and also when fits were forced to obtain the same R_{target_max} (*c50*). In the rare cases where a contrast response function upon drug application became so flat (i.e. almost complete response suppression) that the position of c50 became unreliable, the neuron was excluded from the analysis.

Additional analysis

All the methods regarding behavioural and LFP data analysis were completely identical as those described in chapter and we ask the reader to refer to them if necessary.

2.3. Results

For the experiments where bar length was varied, I recorded 146 neurons from 2 monkeys (112 in monkey HU and 34 in monkey HO) in the absence and presence of APV application. For the experiments where luminance contrast was varied, I recorded 61 neurons (monkey HU) in the absence and presence of APV application. Another 130 neurons (80 in monkey HU and 50 in monkey HO) were recorded in the absence and presence of NMDA application.

2.3.1. Bar-length experiments: effect of NMDA receptor blockade on single unit activity (APV)

A total of 84 out of 146 neurons (58/112 from monkey HU and 26/34 from monkey HO) passed the basic statistical test (i.e. significant effect of attention and drug on firing rates, or n interaction between the two factors, three factor ANOVA) on application of APV. An example cell is shown in Fig. 2.1. APV decreased the response of the neuron to a bar of different lengths, as evident from the raster plots and peri-stimulus time histograms (Fig2.1a) as well as from the averaged response during the 200-500ms window (Fig2.1b). The neuron showed a significant main effect of attention ($p<0.001$), a significant main effect of drug ($p<0.001$), and a significant main effect of bar length ($p<0.001$). There was no significant interaction between attention and drug ($p=0.858$), suggesting that the attentional modulation in the absence of APV did not differ from that in its presence. ROC values showed that attentional modulation was not reduced on APV application. For the smallest bar length ROC (-APV) = 0.7393, ROC (+APV) = 0.8438; for the medium bar length, ROC (-APV) =

0.7109, ROC (+APV) = 0.6875; for the largest bar length, ROC (-APV) = 0.6187, ROC (+APV) = 0.6211. Similarly, the modulation indices (MIs) in the absence of APV were not systematically reduced; MI (-APV) = 0.1809, MI (+APV) = 0.3087 for the 0.2° bar length, MI (-APV) = 0.1378, MI (+APV) = 0.1520 for the 0.8° bar length, and MI (-APV) = 0.1520, MI (+APV) = 0.1019 for the 2.4° bar length.

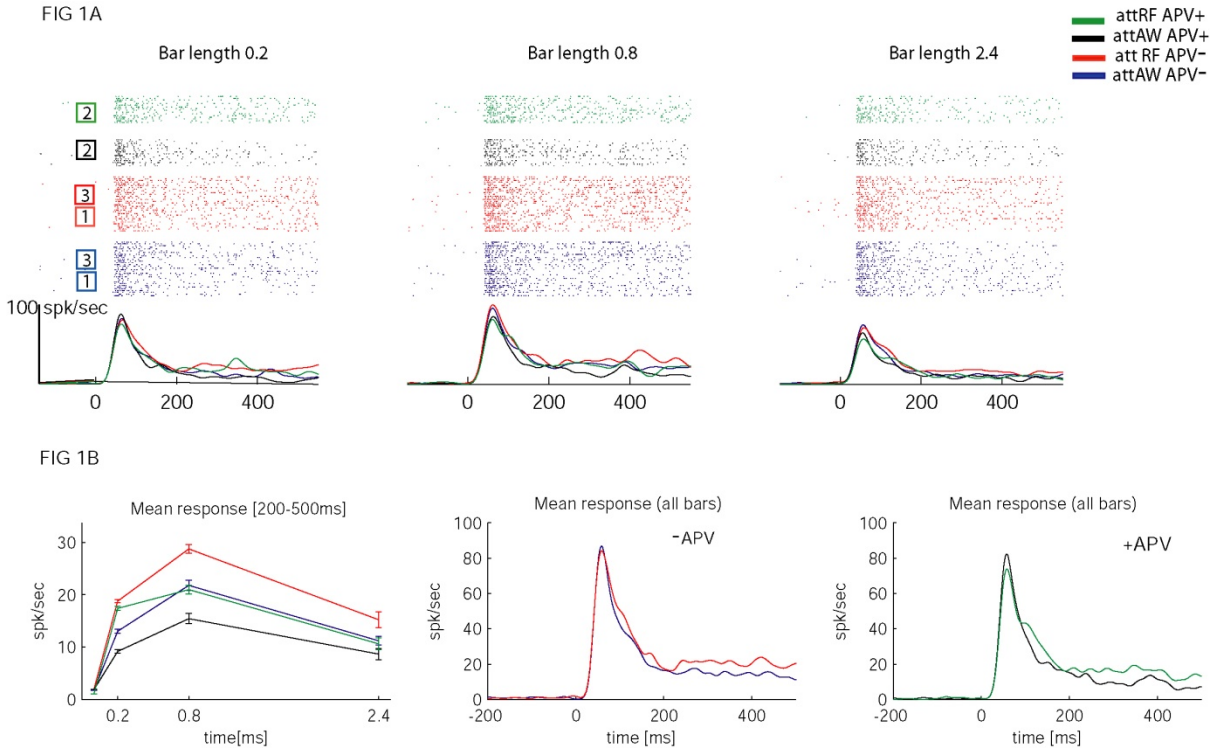

Fig. 2.1. Drug effects on attentional modulation. A) Application of APV has no effect on the attentional modulation. We recorded the effect of attention on firing rates when no APV was applied for three bar lengths in the attend-inside RF versus attend-outside (away) condition (box 1, 20 trials). Thereafter we recorded the effect of attention when APV was applied (20 trials; box 2) followed by recovery (20 trials; box 3). B) Left, average activity (from 200 ms to 500 ms after stimulus onset) for the different stimulus, attention and drug conditions. Middle, averaged activity pooled across the 3 bar lengths in the absence of APV. Right, same as middle plot except that in the presence of APV. APV had no effect on the attentional modulation. Error bars represent s.e.m.

A second example cell is shown in Fig 2.2. Here APV reduced not only the response rate but also the attentional modulation, as indicated by an interaction between drug and attention ($p<0.01$), and an overall reduction in ROC values. Bar length 0.2˚, ROC (-APV) = 0.6027, ROC (+APV) = 0.6024; bar length 0.8˚, ROC (-APV) = 0.7819, ROC (+APV) = 0.6559, bar length 2.4˚, ROC (-APV) = 0.665, ROC (+APV) = 0.591. The MIs were also reduced with APV (data not shown).

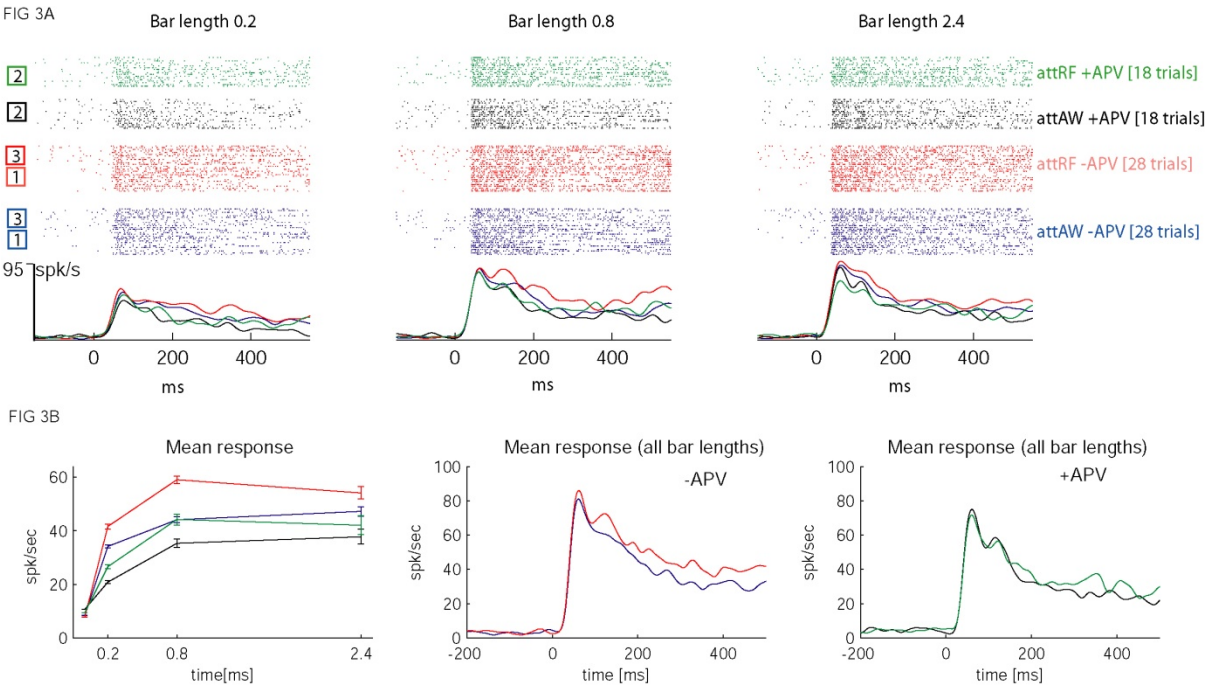

Fig. 2.2. Drug effects on attentional modulation. All conventions as before. A) APV application reduced attentional modulation. B) Left, average activity (200-500 ms after stimulus onset) for the different stimulus, attention and drug conditions. Middle, averaged activity pooled across the 3 bar lengths in the absence of APV. Right, same as middle plot except that in the presence of APV. APV reduced both the gain and the attentional modulation. Error bars represent s.e.m.

The population response (84 neurons) is shown in Fig. 2.3a. Activity levels were normalized relative to the peak activity of each neuron and averaged across the population. The red lines indicate activity without APV application, and the black lines represent activity with APV application. The upper line of each colour plot shows the activity when attention was directed to the neuron's receptive field, the lower line when it was directed away from the receptive field. Widths of the coloured areas show strength of attentional modulation. APV reduced firing rates but its effect on the attentional modulation was not clear (i.e., attentional modulation may be relatively preserved in the presence of APV). The population ROC values for the drug and control condition are shown in Fig. 2.3a. In the presence of APV, ROC values were decreased. A two factor ANOVA showed that the effect was significant for the population of cells and did not depend on bar length: Factor 1, drug application ($p=0.0048$), factor 2, bar length ($p<0.001$), drug*bar lengths interaction ($p=0.153$). Individually, the effect of APV application on attentional modulation was significant in monkey HO (26 cells, $p=0.02$) and near to significant in monkey HU (58 cells, $p=0.063$).In contrast to the ROC analysis, the modulation index (MI) analysis found that APV application did not significantly increase the population modulation index. Factor 1, drug application ($p=0.69$), factor 2, bar length ($p=0.94$). This was independent of bar length; drug*bar lengths interaction ($p=0.22$).

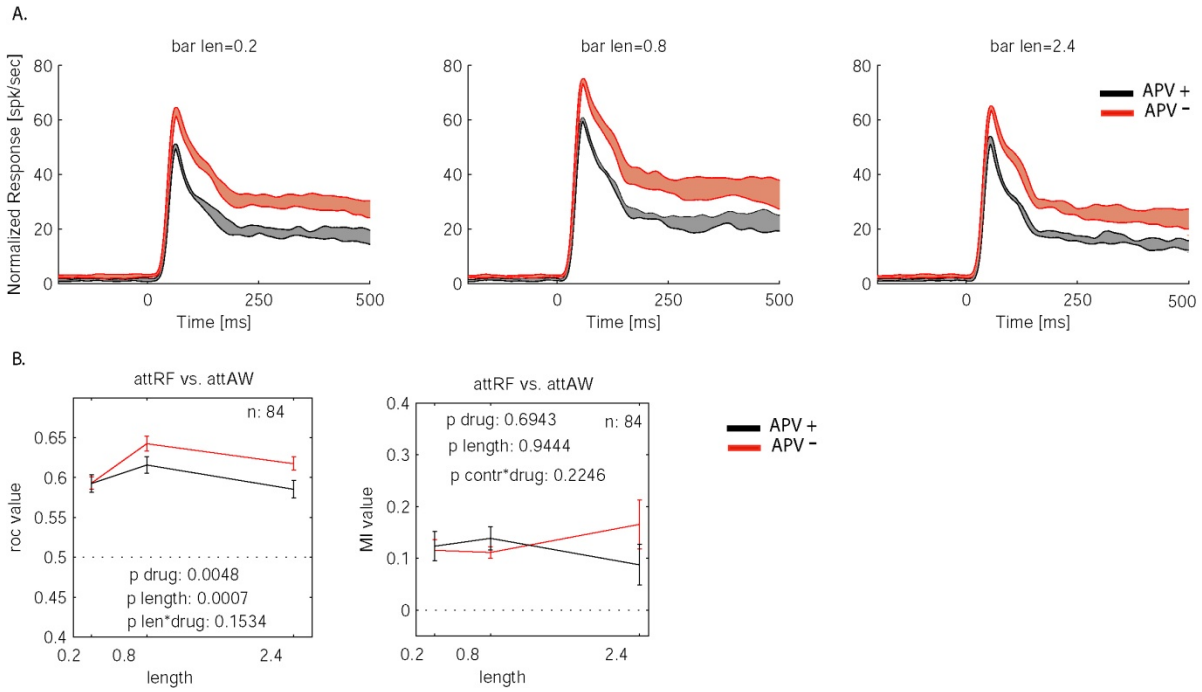

Figure 2.3. **A.** Normalized population response (n=82) depending on APV application, stimulus (bar length; indicated at the top of each subplot) and attention condition. Activity levels were normalized relative to the peak activity of each neuron and averaged across the population. Red lines show activity without APV application; black lines represent activity with APV application. Strength of attentional modulation is represented by the width of the coloured areas. The upper line of each colour plot shows the normalized activity when attention was directed to the neuron's receptive field, the lower line when it was directed away from the receptive field. **B.** APV reduced attentional modulation as measured by ROCs analysis (left) but not when measured by MIs analysis.

To understand the discrepancy between ROC and MI results, we analysed the trial-to-trial reliability of neuronal responses using the fano factor. We aimed to model the effects of fano factor changes on ROC values in the presence of unchanged proportional changes (MIs). The prediction is that if MIs (i.e. mean responses) do not change, but variance of responses is increased, then ROCs have to decrease. Figure 2.4 shows the fano values in the absence (fig 2.4a) and presence (fig 2.4b) of APV for the different attention, bar-length, and time-response windows. Fano scores were subjected to a four-way ANOVA: Factor 1, attention, factor 2, drug application, factor 3, time window, factor 4, bar-length). Similar to previous reports in area V4 (Mitchell et al., 2007) , directing attention to the RF of V1 neurons reduced the fano factor. A main effect of time window was also found ($p<0.001$), with larger fano factors at the later time windows (attention * time, $p<0.05$). Application of APV reduced the fano factor ($p<0.001$). This latter result was unexpected: we expected increased fano factor in the APV condition, in line with the decrease in ROCs. We noticed however that previous studies reported a positive correlation between response amplitude and variance (Tolhurst et al., 1981). Given that APV reduced response amplitude in most of the cells, the variance should also be reduced. This means that the important result here may not be the effect of APV itself, but the interaction between attention and APV. A trend towards significance (attention * drug, $p=0.0885$) was observed. Figure 2.4c shows this trend after fano scores were averaged across all bar lengths (i.e., scores were first calculated and then pooled across bar

lengths). Attention reduced the variance more effectively in the absence of APV compared to its presence. This result supports the previous finding that APV reduced ROC values.

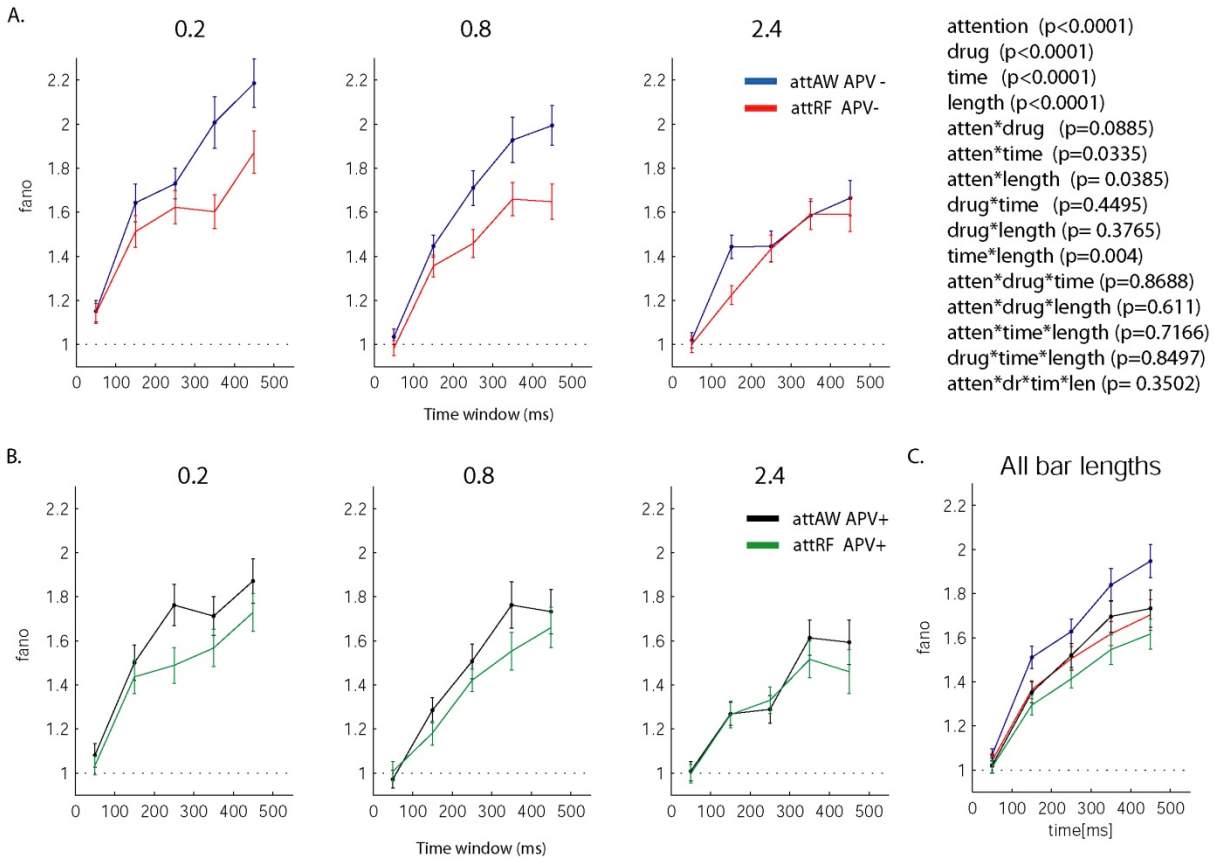

Figure 2.4. Time-resolved fano factor for the population data across the different drug, attention, and stimulus size conditions (n=83). Five time windows of 100 ms each were considered (other conventions as before). A. Control condition. B. APV-applied condition. C. Data were pooled across bar lengths after calculation. Attention reduced the fano factor more effectively in the absence of APV (i.e., the interaction between attention and APV application showed a trend towards significance).

The relationship between neuronal response and trial-to-trial variance was explored further. We tried to determine whether the decrease in variance with APV could fully be accounted for by the reduced firing rate, or whether APV on its own was a contributing factor. To this end we fitted a power function (variance= aR^b) to the four data sets (Gur et al., 1997). Figure 2.5 shows the results across the different drug and attention conditions (the factor of bar-length was not considered for this analysis, thus all lengths contributed to this data). We found that APV had different effects on the relationship between mean and variance in the attend-RF compared to attend-away condition. In the absence of APV, attention reduced the strength in which the variance scaled with the response as shown by a reduced slope (no-APV att-away=1.05; no-APV att-RF=0.83; difference of 0.22). In the presence of APV, the difference was only 0.08 (APV att-away=0.957; APV att-RF=0.869), suggesting that attention did not efficiently reduce the strength in which the variance scales with the response. For this interpretation to be true, the intercepts should be similar across conditions.

However, we found that the intercepts also changed (no-APV: att-away=6.12 and att-RF=11.83; APV: att-away=7.98 and att-RF=11.86), precluding us from making claims on these analysis.

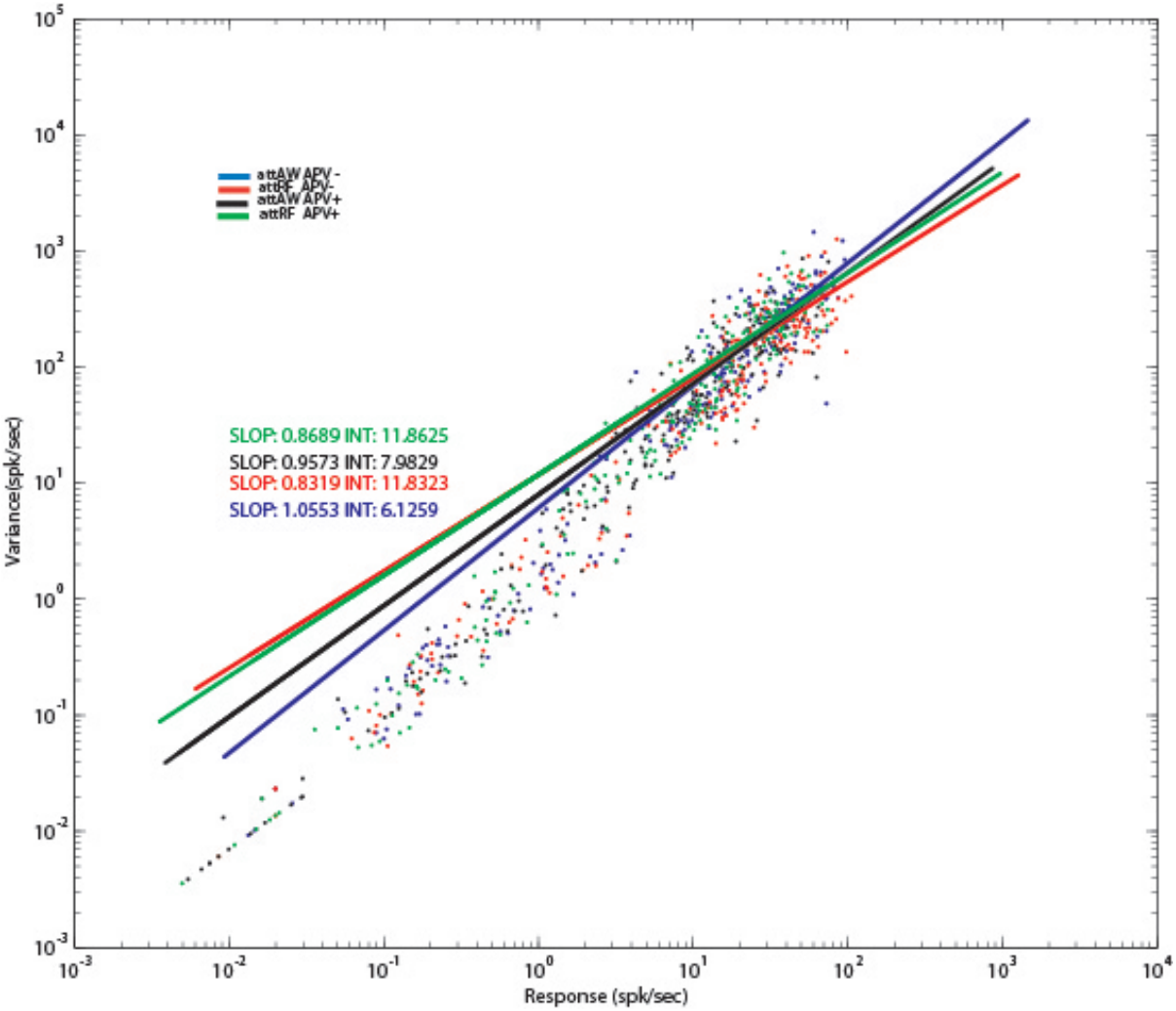

Figure 2.5: Relationship between response amplitude and trial-to-trial variance across the different drug and attention conditions (population data, n=83). A function (variance= aR^b) was fitted to the data and y-intercepts and slopes were calculated. Each neuron contributes 4 data points to the analysis (one data point for each bar length used, and an additional data point for the corresponding spontaneous activity; the results excluding the spontaneous activity were virtually identical). Attention reduced the slope of the fitted function in the absence of the drug but not in its presence, however, concomitant changes in intercepts precluded us from making claims about this result.

2.3.2. Contrast experiments: effect of NMDA receptor blockade on single unit activity (APV)

For the experiments where bar contrast was varied, a total of 21 out of 61 neurons (all from monkey HU) passed the basic statistical test (three factor ANOVA) on application of APV. An example cell is shown in Fig 2.6. APV decreased the response of the neuron to a bar of different contrasts. The neuron showed a significant main effect of attention ($p=0.013$), a significant main effect of drug ($p<0.001$), and a significant main effect of bar contrast ($p<0.001$). The effect of the interaction between attention and drug was not significant ($p=0.99$). ROC values showed that attentional modulation was not systematically reduced on APV application. It was

reduced for some contrasts, while it was increased for others. Similar results were seen on the modulation indices (MIs).

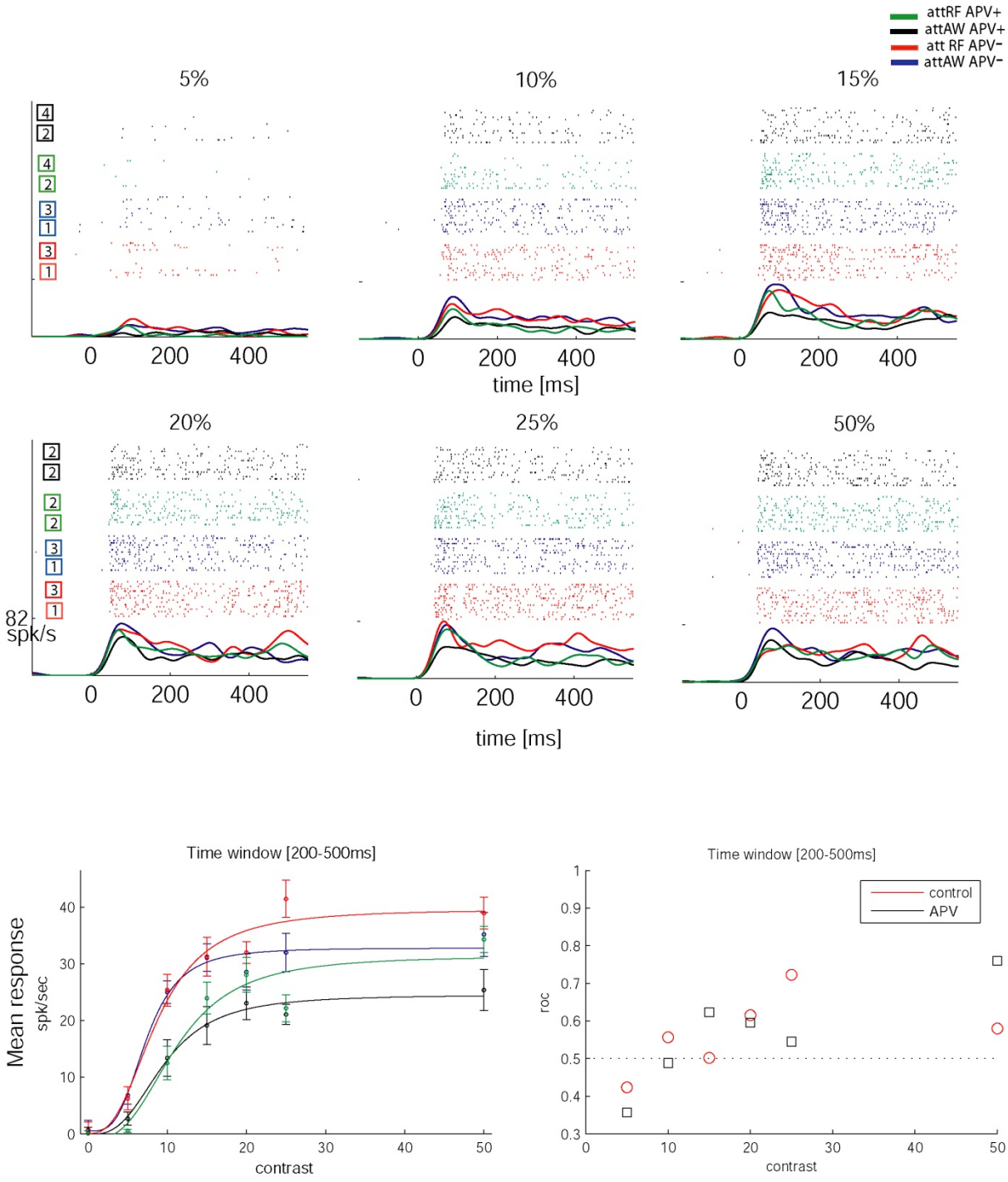

Fig. 2.6. Application of APV has no effects on the attentional modulation on an example neuron. (Top) Raster plots to bar segments of 6 different contrasts. Spikes were recorded when no APV was applied in the attend-inside RF versus attend-outside (away) condition (box 1, 20 trials). Thereafter we recorded the effect of attention when APV was applied (20 trials; box 2) followed by recovery (20 trials; box 3). B) Left, average activity (from 200 ms to 500 ms after stimulus onset) for the different stimulus, attention and drug conditions. Data points were fitted with and Nakarushton function. Right, mean roc values in the absence (red) or presence (black) of APV. APV did not systematically reduced roc values. Error bars represent s.e.m.

The population response (21 neurons) is shown in Fig. 2.7 (top). The red lines indicate activity without APV application, and the black lines represent activity with APV application. As in the bar length experiments, widths of the coloured areas represent strength of attentional modulation. APV reduced firing rates but the attentional modulation was preserved. This is also clear from Fig. 2.7 (bottom left), which plots the population contrast response functions (CRF) for the different drug and attention conditions. The activity levels were normalized relative to the peak activity of each neuron and averaged across the population. The population ROC values for the drug and control condition are shown in Fig. 2.7 (bottom right). In the absence of APV, ROC values were not significantly different from those in its presence. A two factor ANOVA showed that the effect of drug was not significant for the population of cells and did not depend on bar contrast. The main effect of bar contrast was significant. Factor 1, drug application ($p=0.6795$), factor 2, bar contrast ($p<0.001$), drug*bar contrast interaction ($p=0.7957$). The MIs showed similar results; APV application did not significantly increase the population indexes. Factor 1, drug application ($p=0.827$), factor 2, bar contrast ($p<0.001$); drug*bar contrast interaction ($p=0.7459$).

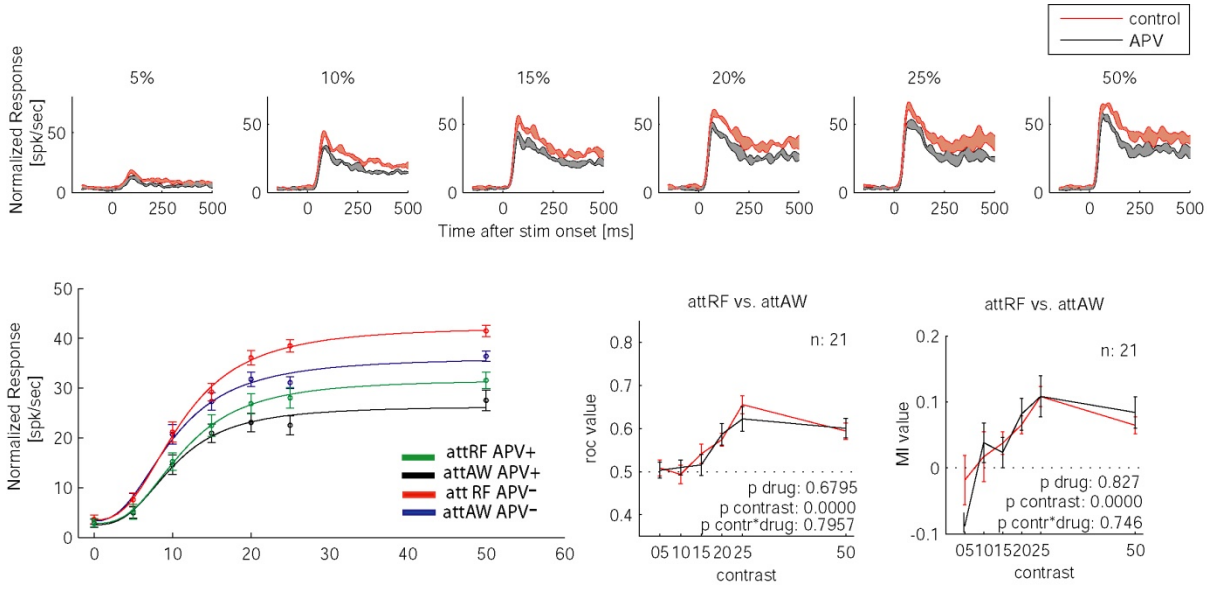

Figure 2.7. (Top) Normalized population response (n=21) depending on APV application, stimulus (bar contrast; indicated at the top of each subplot) and attention condition. Activity levels were normalized relative to the peak activity of each neuron and averaged across the population. Red lines show activity without APV application; black lines represent activity with APV application. Strength of attentional modulation is represented by the width of the coloured areas. (Bottom) Contrast response functions for the population data. APV had no effect on the attentional modulation as measured by ROCs (left) or MIs (right) analysis .

The time-resolved fano factor for the population data is shown in figure 2.8. Fano scores were subjected to a four-way ANOVA: Factor 1, attention, factor 2, drug application, factor 3, time window, factor 4, bar contrast. Although attention generally decreased the Fano factor for most bar contrasts the effect did not reach significance ($p=0.108$). The fano factor was reduced upon APV application ($p=0.0042$), and was increased at the late time windows and high bar contrasts ($p<0.001$). Most importantly, the interaction between attention and drug was not significant (att*dru, $p=0.287$), suggesting that APV did not systematically reduce

attentional modulation. No other effects reached significance. We wondered whether the reduced fano factor with APV was due to the fact that for many neurons we only recorded spikes during 2 control periods (baseline and recovery) and 1 drug-applied period. When baseline and recovery were pooled together, it may have led to an increased fano factor, as the activity may have varied. We tested baseline vs. drug and the results were virtually identical.

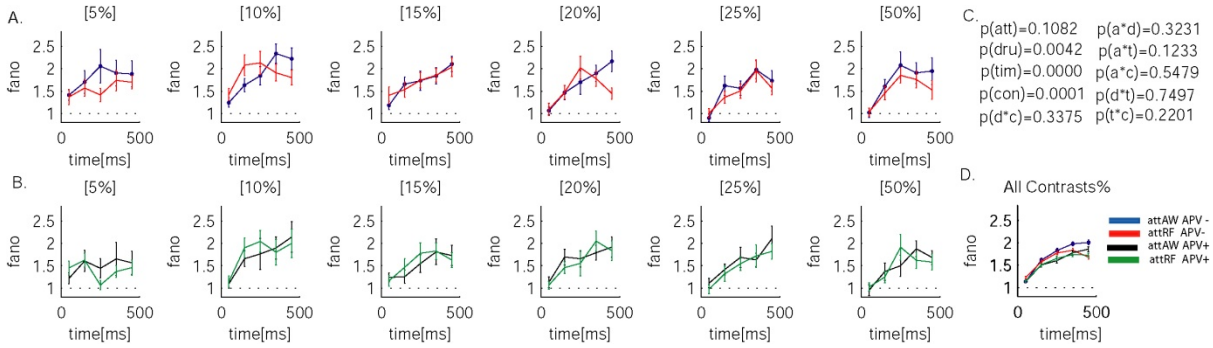

Figure 2.8. Time-resolved fano factor across different drug, attention, and contrast conditions (population data, n=21). A. Absence of APV. B. Presence of APV. C. Statistics for main and simple interaction effects. Double and triple interaction effects were not significant. D. Summary of the results when the data were pooled across bar contrasts (after calculation). APV application reduced the fano factor but the interaction between attention and APV application did not reach significance.

Additionally, we used the CRFs to calculate Rmax (saturation point) and c50s (contrast at half-saturation point). Only well fitted neurons were included in this analysis; 18/21 fittings could account for >75% of the variance. Rmax values were increased in the attention condition ($p<0.001$, 2 factor ANOVA), and reduced when APV was applied ($p<0.001$). There was no interaction between attention and drug condition ($p>.1$), suggesting that the APV-induced reduction did not depend on attentional state. Additionally, attention did not change significantly c50s ($p>.1$), nor did the application of APV ($p>.1$). C50s have been considered as an index of neuronal sensitivity, with lower values indicating improved sensitivity to detect a specific stimulus contrast. However, we did not find reduced c50s with attention, nor increased c50s with APV. This means that even if NMDA receptors contribute to attentional modulation, c50s would not be able to pick up the effect.

2.3.3. Contrast experiments: effect of NMDA receptor activation on single unit responses (NMDA)

A total of 43 out of 130 neurons (22/80 from monkey HO; 21/50 from monkey HO) passed the basic statistical test (three-factor ANOVA) on application of NMDA. The population response (43 neurons) is shown in Fig. 2.9 (top). The red lines indicate activity without NMDA application, and the black lines represent activity with NMDA application. Widths of the coloured areas represent strength of attentional modulation. NMDA increased firing rates as well as the attentional modulation for most stimulus contrast. This is illustrated in figure 2.9 (bottom left) which plots the population CRF, and quantified in figure 2.9 (bottom right) which plots the population ROC values for the drug and control condition. In the presence of NMDA, ROC values were significantly increased compared to those in its absence. A two factor ANOVA showed that the effect of drug was significant for the population of cells (Factor 1, drug; $p=0.0079$) and did not depend on bar contrast

(drug*contrast; p=0.43). The main effect of bar contrast was significant (p=0.0009). The effect of the drug in the MIs showed a similar trend of results but did not reach significance (Factor 1, drug application, p=0.1089). The effect of the bar contrast was not significant either (p=0.88). However, the interaction between drug and contrast was significant (drug*bar contrast, p=0.0352).

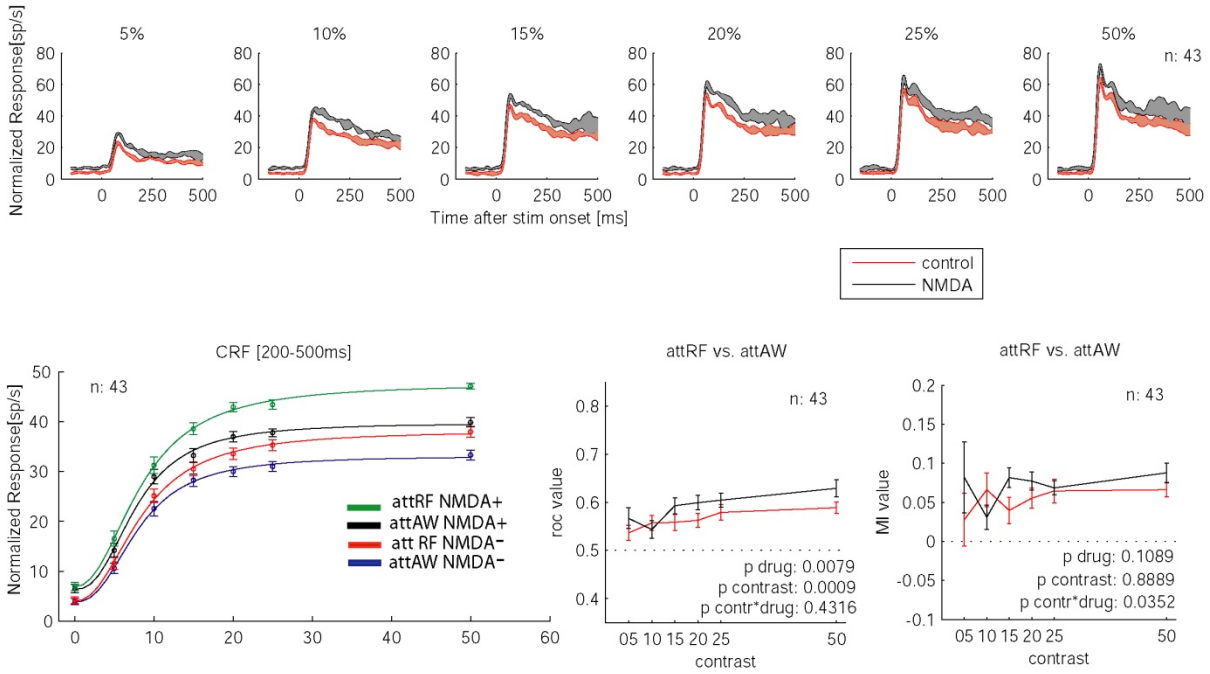

Figure 2.9. [Top] Normalized population response (n=43) depending on NMDA application, stimulus (bar contrast; indicated at the top of each subplot) and attention condition. Activity levels were normalized relative to the peak activity of each neuron and averaged across the population. Red lines show activity without NMDA application; black lines represent activity with NMDA application. Strength of attentional modulation is represented by the width of the coloured areas. [Bottom] Contrast response functions for the population data during the 200-500 ms response window (left). NMDA application increased the attentional modulation as measured by ROCs analysis (centre) but not as measured by MIs analysis (right).

The time-resolved fano factor for the population data is shown in figure 2.10 (n=43). Fano scores were subjected to a four-way ANOVA: Factor 1, attention, factor 2, drug application, factor 3, time window, factor 4, stimulus contrast. The Fano factor was reduced upon NMDA application (drug factor, p=0.039), and increased for the late time windows and high contrast stimulus (p<0.001). Although the main effect of attention did not reach significance (attention, p=0.1241), there was a significant interaction between attention and time window (att* time, p=0.025), suggesting that the effect of attention on the fano factor occurred at the late time windows. The interaction between attention, drug and time window was not significant (att * drug * time, p=0.19), nor it was the interaction between attention and drug (att * drug, p=0.723). These effects somehow suggest that NMDA activation did not systematically play a role in attentional modulation of response variance. This seems at odds with the ROC analysis reported above, where ROC values increased with NMDA. However, we did observe a significant interaction between drug and stimulus contrast (dru*contr, p=0.0024): in the absence of NMDA response variance increased with stimulus

contrast, while in its presence the opposite effect is observed (i.e., response variance decreases with contrast). No other interaction effects were found significant.

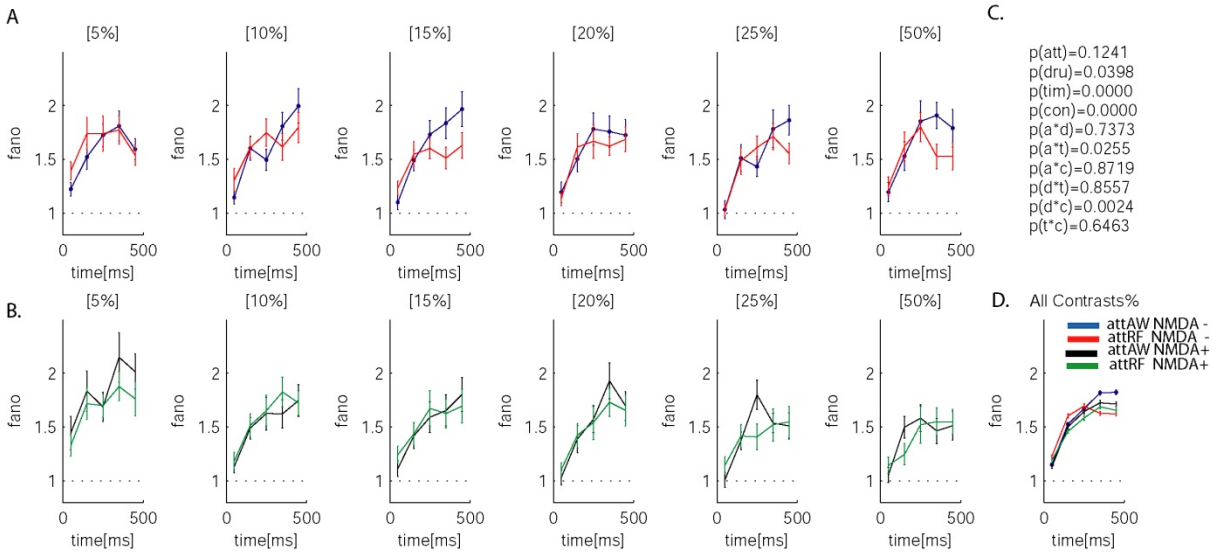

Figure 2.10. Time-resolved fano factor across different drug, attention, and contrast conditions (population data, n=21). A. Absence of NMDA. B. Presence of NMDA. C. Statistics for main and simple interaction effects. Double and triple interaction effects were not significant. D. Summary of the results when the data were pooled across bar contrasts (after calculation). NMDA application reduced the fano factor but the interaction between attention and APV application did not reach significance.

We used the CRFs to calculate Rmax (saturation point) and c50s (contrast at half-saturation point). Only well fitted neurons were included in this analysis; 33/43 fittings could account for >75% of the variance. Attention and NMDA application increased the neuronal gain, as measured by an increased in Rmax ($p<0.05$). There was no interaction between attention and drug application ($p>.1$). Attention did not reduce significantly the c50s, nor did the application of NMDA. C50s have previously been considered as an index of neuronal sensitivity. However, we did not find reduced c50s with attention. This means that even if NMDA receptors had an influence on attentional modulation, c50s would remain unchanged.

2.3.4. Effect of NMDA receptors on behavioural performance

At the behavioural level, intra-basalis administration of the NMDA receptor antagonist APV was found to impair the ability of rats to detect signals in sustained attention tasks (Turchi and Sarter, 2001a, b). We tested whether blockade of NMDA receptors in the cortex had a significant effect on reaction times. In the bar-length experiment (Fig 2.11, left), APV slowed RTs when the animal attended to the stimulus within the RF of the neuron under study, i.e. when they attended to the location represented by the neurons influenced by APV (drug*att, p=0.007). This effect shows that APV slows the monkey down particularly when attending, and is line with the rat studies (Turchi and Sarter, 2001a, b) and with the ROC analysis shown before (i.e., decreased ROCs with APV). Activation of NMDA receptors in the bar-contrast experiment resulted in less clear effects (Fig 2.11, right), as there was no systematic effect of NMDA on RT. Nevertheless, a significant interaction between

NMDA and stimulus contrast was found (drug*contrast, p=0.02). This effect shows that the monkey is speeded up for the highest contrast, and is in line with the results of the MI analysis which showed increased MIs with NMDA at the highest contrasts tested. It is also supported by the slice studies showing that NMDA receptors are activated under conditions of particularly intense or high-frequency synaptic drive (Collingridge and Bliss, 1987).

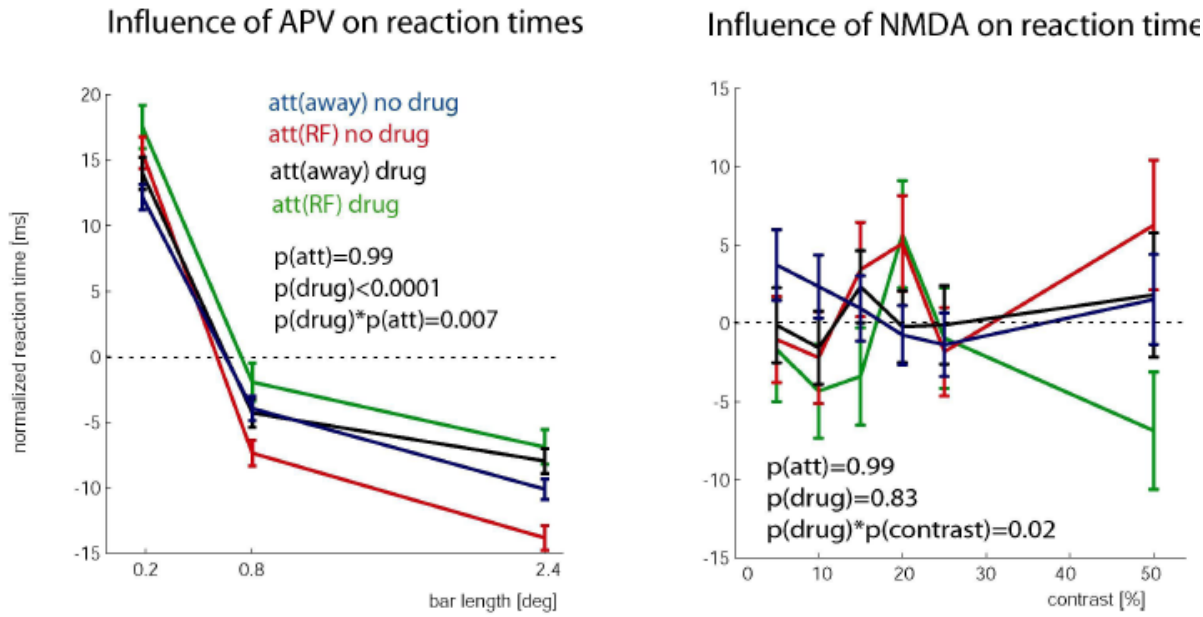

Figure 2.11: Effect of NMDA activation/blockade depending on attentional locus and stimuli used. (Left) NMDA blockade significantly affected RTs, and the effect depended on where the animal attended. (Right) NMDA activation did not significantly affected RTs, although there was some facilitation for the high contrast which depended on where the animal attended.

2.3.5. Bar length experiments: effect of NMDA receptor blockade on the LFP (APV)

Figure 2.12 shows the population-evoked LFP response (47 recording sites) from the different bar lengths and attentional conditions when APV was not applied (top) and when it was applied (bottom). It shows that stimulus onset resulted in a stereotypical deflection of the LFP which lasted for about 200–250 ms. After this period, the evoked LFP response remained reasonably stationary, a prerequisite for performing the spectral analyses reported below.

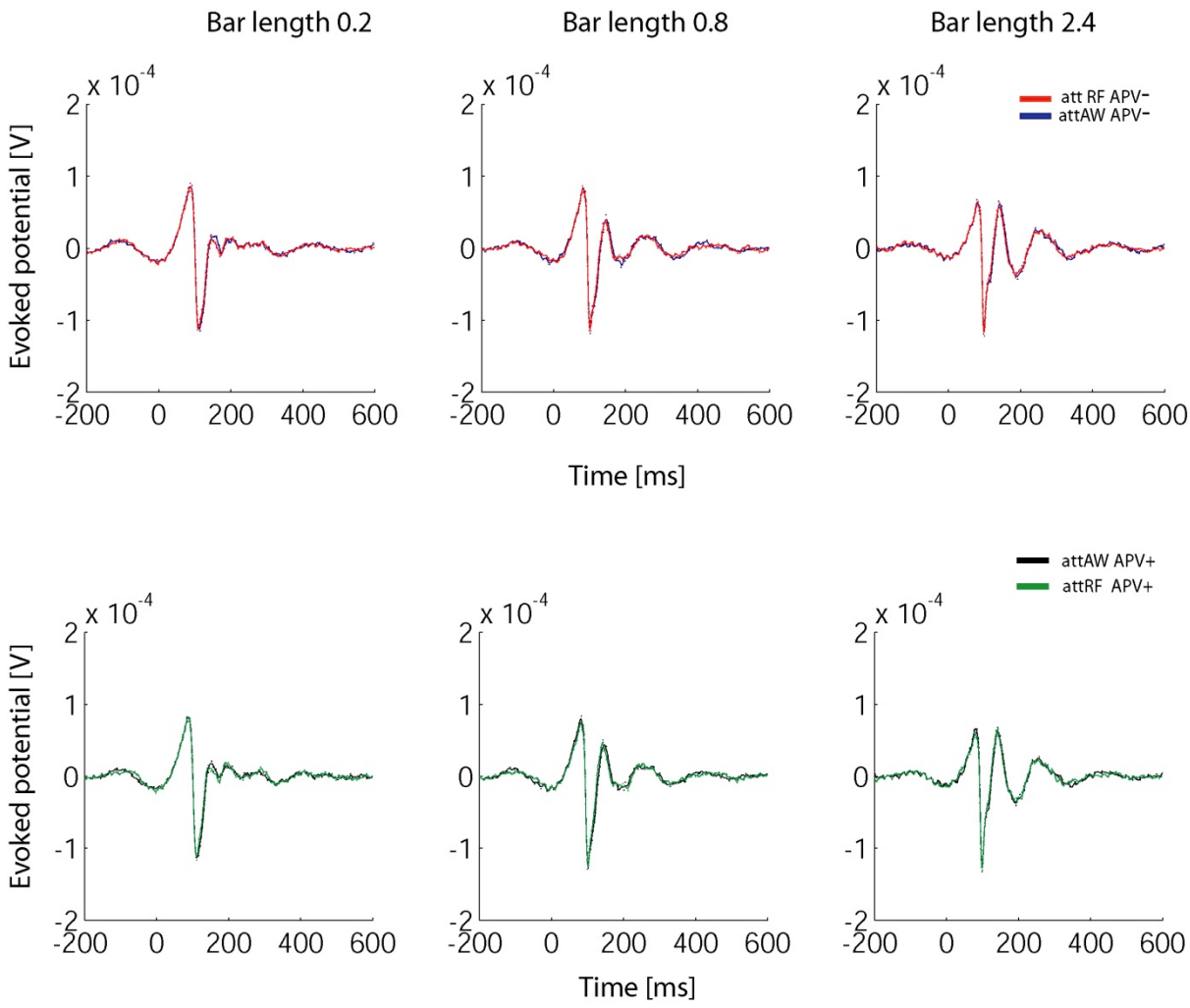

Fig 2.12. Population-evoked potential of the LFP for the different bar lengths, attention, and drug conditions (47 recording sites). [Top] APV not applied. Red curve shows the activity in the attend-RF condition and blue curve, the activity in the attend-away condition. [Bottom] APV-applied during attend-RF condition (green curve) and attend-away condition (black curve). The initial deflections in the evoked potentials and the stationary thereafter were virtually identical in the APV-applied and APV-not applied conditions.

To investigate the effects of attention, drug application, and stimulus type on the sustained LFP response, we calculated the LFP response power spectrum averaged over the time interval of 256–512 ms after stimulus presentation. The time period of 256–512 ms was chosen because it is the period wherein attentional modulation of firing rates was most profound (Roberts et al., 2007, Herrero et al., 2008). Figure 2.13 (top) shows the average LFP power spectrum for the recordings when APV was not applied (top), pooled across the two monkeys. The attend-away condition is shown in blue, and the attend-RF condition is shown in red. Power spectra exhibited their maximum at low frequency, dropping off with increasing frequency and showing a peak in the gamma band (30–60Hz) when the stimulus was large enough (i.e., 2.4 degrees). Gamma oscillations were usually larger for the attend-away, compared with the attend-RF condition.

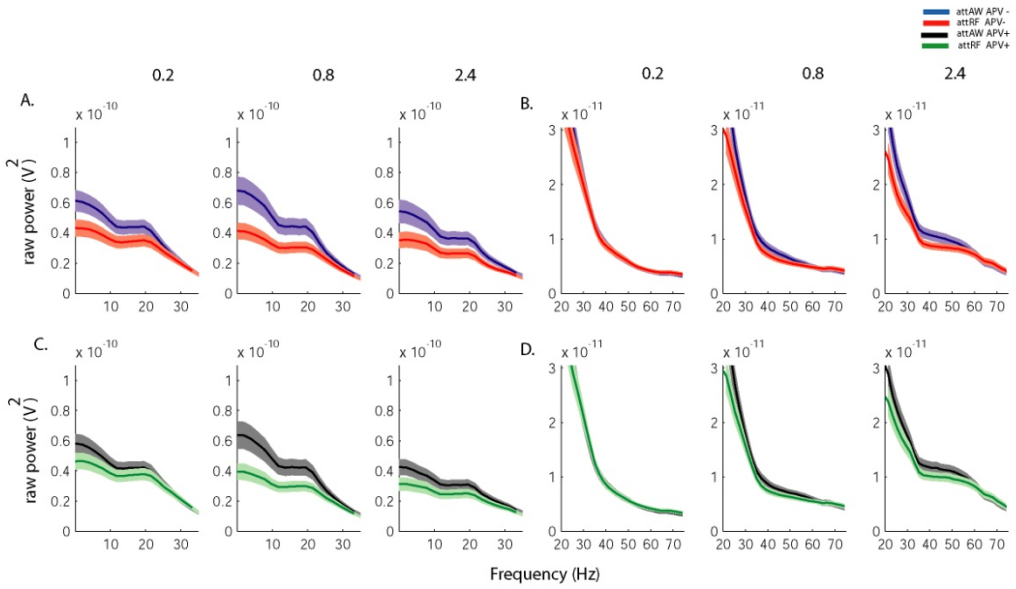

Figure 2.13. Average LFP Responses (47 recording sites). Spectrum during the period from 256 to 512 ms after stimulus presentation. Plots are separated according to frequency range: A and C show the data for the 0-30 Hz, while B and D show the frequency for the 20-80 Hz. [Top] APV not applied. Red curves show the activity in the attend-RF condition; blue curves, the activity in the attend-away condition. [Bottom] APV applied. Green curves show the activity in the attend-RF condition; black curves, the activity in the attend-away condition. Dotted lines show SEM.

The peak in the gamma band (30–60 Hz) can be seen more clearly in the stimulus-induced power spectrum (Fig 2.14). It shows the stimulus-induced power spectrum averaged for the two animals (47 recording sites) over the time interval of 256–512 ms after stimulus presentation. The amplitude of the gamma peak was stronger when the stimulus induced a V1 network state that favoured gamma oscillations (i.e., a large stimulus encroached on the suppressive surround (Gieselmann and Thiele, 2008)). In addition to the dependence on stimulus type, the attend-away condition resulted in more stimulus induced power in the gamma range than the attend-RF condition.

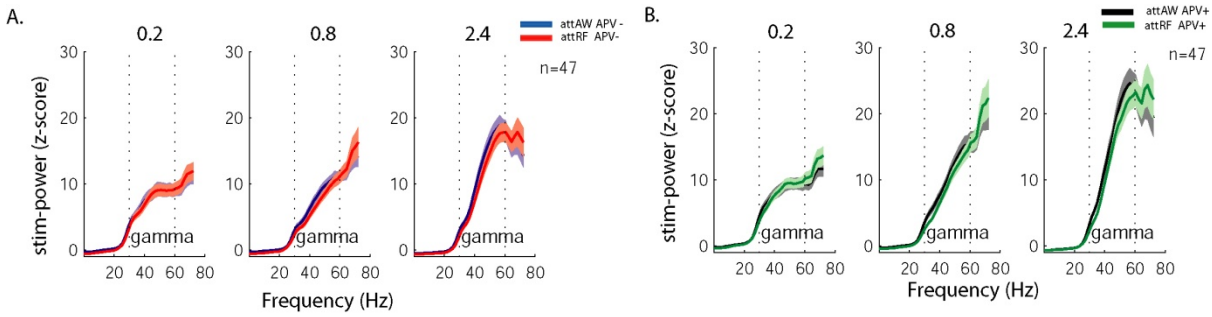

Figure 2.14. Power spectrum normalized for stimulus induced effects (47 recording sites). It was normalized by the power spectrum prior to stimulus presentation separately for the control (A) and APV-applied condition (B). Dotted areas show SEM.

In order to provide a quantitative understanding of how attention modulated the LFP signal, the power spectrum was divided into four different frequency bands (alpha: 7–13 Hz, beta: 13–30 Hz, gamma: 30–60 Hz, and high gamma: 60–100 Hz). The effects of attention on the LFP response power were analysed separately for each frequency band. Figure 2.15 shows the raw LFP power for the different frequency bands (n = 47 recording sites from two monkeys). Applying APV increased the power in the gamma (p=0.0129) and high gamma (P=0.009) bands, and had no effect in the lower bands (alpha, p=0.0549; beta, p=0.307, three-factor repeated measurement (RM) ANOVA). Attending to the RF of the recording sites significantly reduced the power in the alpha, beta, and gamma bands, ($p < 0.01$, three-factor RMANOVA), while it had the opposite effect in the high gamma ($p<0.05$). Bar length had a significant effect on all frequency bands ($p < 0.01$, three-factor RM ANOVA). Increasing the stimulus size significantly reduced the overall power in the alpha and beta bands ($p < 0.001$, three-factor RM ANOVA). LFP power significantly increased with bar length in the gamma and high gamma bands ($p < 0.001$, three-factor RM ANOVA). The interaction between drug and attention was significant only in the alpha and beta bands ($p<0.01$), but not in the gamma and high gamma bands. There was an interaction between bar-length and attention in the gamma band ($p < 0.001$, three-factor RM ANOVA): the largest attention-induced power changes occurred for long bars. In the alpha and beta band, the largest attention-induced power changes occurred for medium bar stimuli (0.8 degrees). The interaction between drug and bar-length was also significant in all frequency bands ($p<0.05$).

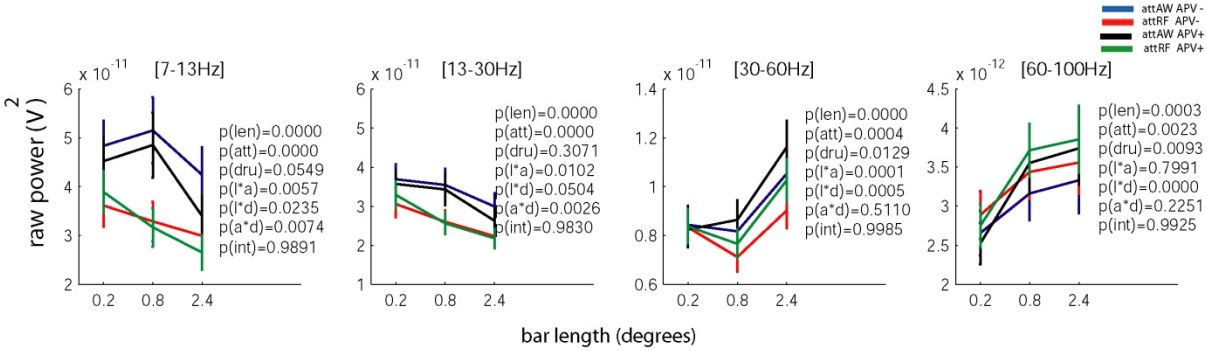

Figure 2.15. Raw LFP power for the different frequency bands and drug conditions (n = 47 recording sites from two monkeys). [Top] Control condition where APV was not applied. [Middle] APV-applied condition. [Bottom] Comparison of control (solid lines) and APV-applied (dashed lines) conditions.

Figure 2.16 shows the population stimulus-induced power for the different frequency bands and drug conditions (n = 47 recording sites from two monkeys). Applying APV increased the power in most frequency bands: alpha (p=0.0821), beta (p=0.0035), gamma (p<0.001), and high gamma (p<0.001, three-factor RM ANOVA). Attending to the RF of the recording sites significantly reduced the power in all bands ($p < 0.01$, three-factor RM ANOVA), while it increased it in the high gamma ($p<0.05$). Bar length had a significant effect on all frequency bands ($p < 0.001$, three-factor RM ANOVA). Increasing the stimulus size significantly reduced the stimulus-induced power in the alpha and beta bands ($p < 0.001$, three-factor RM ANOVA). Stimulus-induced power significantly increased with bar length in the gamma and high gamma bands ($p < 0.001$, three-

factor RM ANOVA). The interaction between drug and attention was only significant in the alpha band ($p<0.001$). There was an interaction between bar-length and drug ($p<0.001$, all bands). In the gamma band the largest APV-induced changes occurred for the longest bar. The interaction between bar-length and attention was significant only in the gamma band ($p<0.001$), with larger attention-induced changes at the long bars.

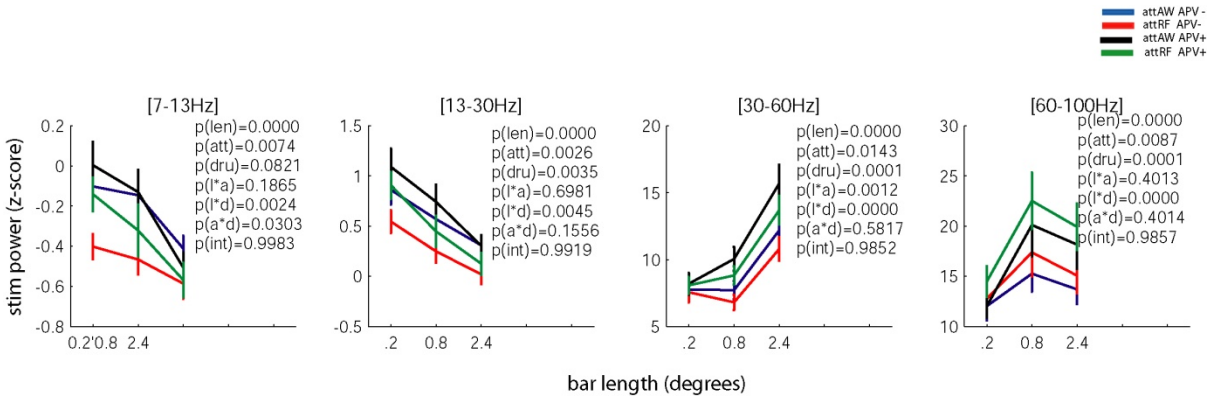

Figure 2.16. Stimulus-induced power in the different frequency bands, attention, and drug conditions (n = 47 recording sites from two monkeys). Control condition where APV was not applied (red and blue lines). APV-applied condition (green and black lines). Attend receptive field (red and green lines), attend-away (blue and black lines).

Additionally, the spike-field coherence (SFC) was calculated to determine the synchrony between neuronal spiking activity and local network oscillations. Figure 2.17 shows the population SFC for the different frequency bands and drug conditions (n = 47 recording sites from two monkeys). Applying APV had no effect on the SFC ($p>.1$, three-factor RM ANOVA). Attending to the RF of the recording sites increased the SFC in the high gamma ($p <0.01$), but had no effect on the other bands. Bar length had a significant effect on most frequency bands (alpha and beta, $p < 0.001$, gamma, $p=0.053$). Increasing the stimulus size significantly reduced the SFC in the lower bands (alpha and beta, $p < 0.001$), and increased in the gamma band ($p=0.053$). The only significant interaction in the gamma band was between length and drug ($p<0.001$), with larger bars being more affected by APV.

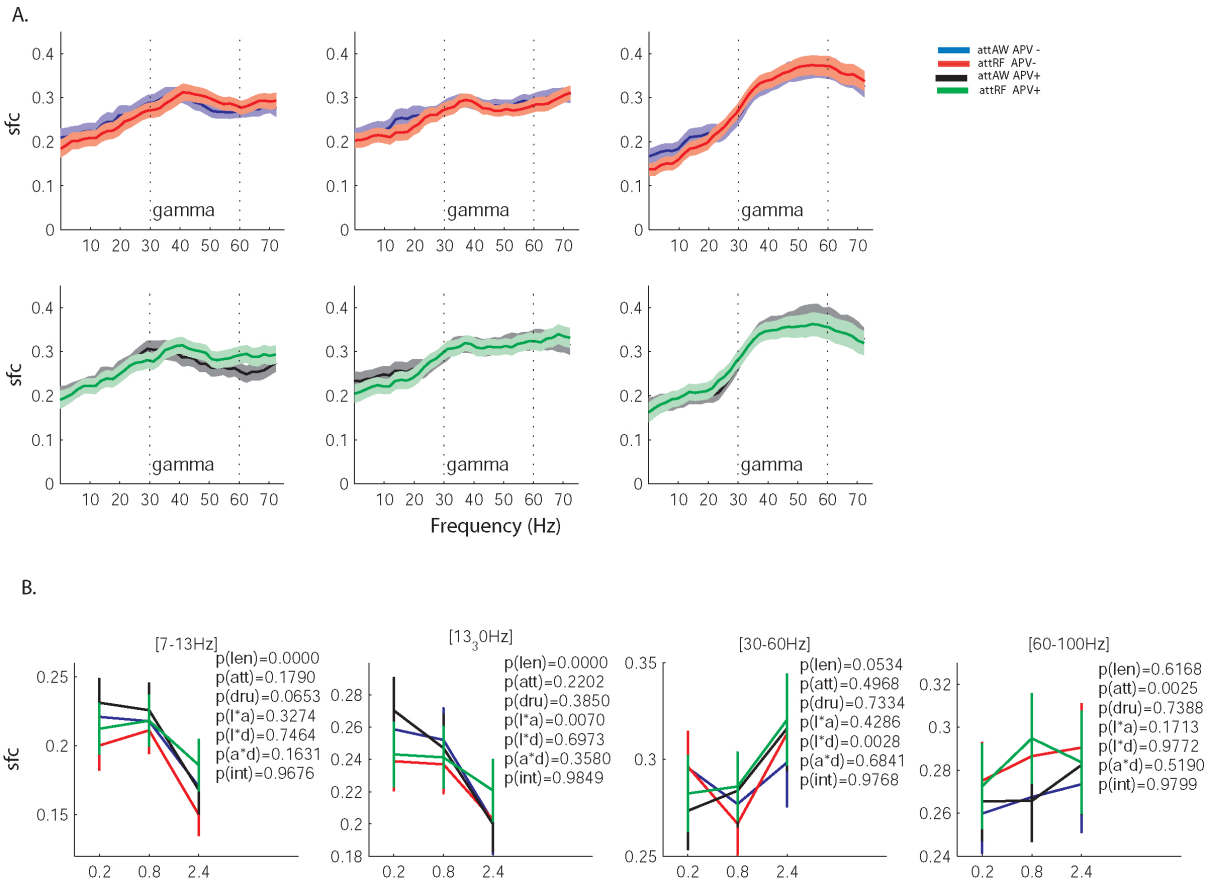

Figure 2.17. SFC across the different drug, attention, and stimulus size conditions (n = 47 recording sites from two monkeys). A. Control condition where APV was not applied (top), and APV-applied condition (Bottom). B. Quantification of SFC across the different frequency bands.

2.3.6. Contrast experiments: effect of NMDA receptor blockade on the LFP (APV)

Figure 2.18 shows the population stimulus-induced LFP power (n = 21 recording sites from monkey HU). Increasing the contrast of the stimulus appears to increase the stimulus-induced power. Directing spatial attention to the stimulus insight the RF of the V1 neurons appears to decrease the stimulus-induced power (fig 2.18a). The attention-induced effect appears stronger for high contrast stimuli and seems to not depend on the presence of the drug.

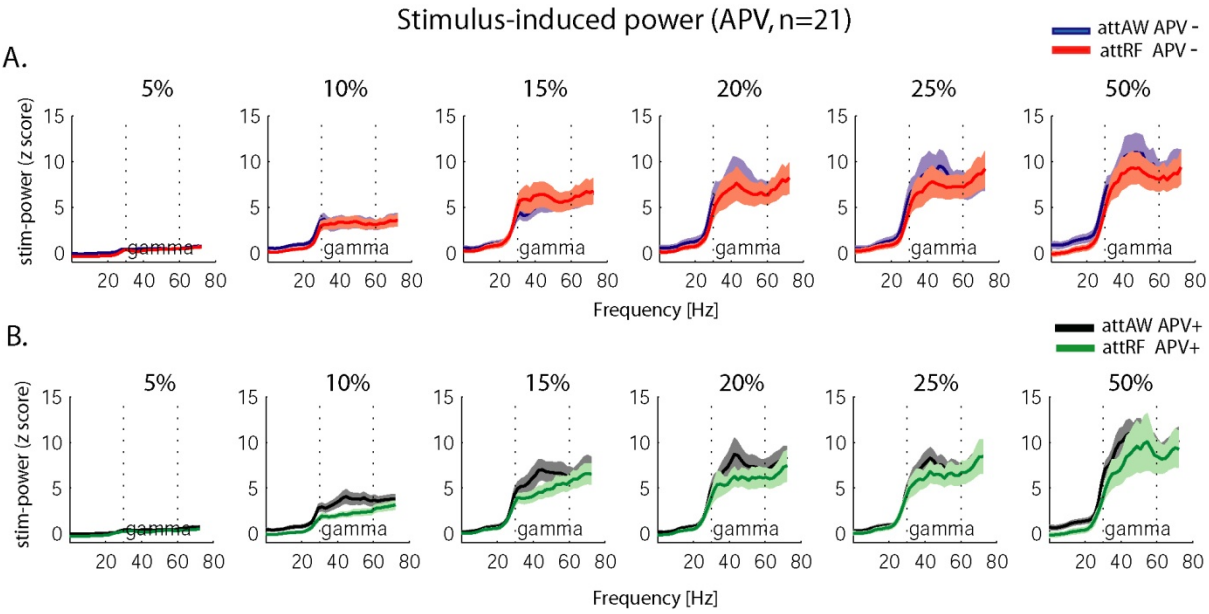

Figure 2.18. Stimulus-induced LFP power for the different drug and attention conditions (n = 21). A. Control condition where APV was not applied. B. APV-applied condition. Shaded areas SEM .

Similar to the analyses performed in the bar length experiments, the power spectrum obtained from the contrast experiments was divided into four different frequency bands (alpha: 7–13 Hz, beta: 13–30 Hz, gamma: 30–60 Hz, and high gamma: 60–100 Hz). The effects of attention, drug, and contrast on the LFP response power were analysed separately for each frequency band. Figure 2.19 shows the stimulus-induced LFP power for the different frequency bands. Applying APV did not significantly change the stimulus-induced power in most frequency bands (alpha, $p=0.0978$; beta, $p=0.044$; gamma, $p=0.25$; and high gamma, $p=0.4369$, three-factor RMANOVA). Attending to the RF of the recording sites significantly reduced the power in all frequency bands ($p < 0.01$, three-factor RMANOVA), except the high gamma ($p<.1$). Increasing the contrast of the stimulus significantly increased its induced power in all frequency bands ($p < 0.001$). The interaction between drug and attention was not significant ($p>.1$, all bands). There was an interaction between contrast and attention ($p<0.01$, all bands except high gamma), with larger attention-induced changes at the highest contrast.

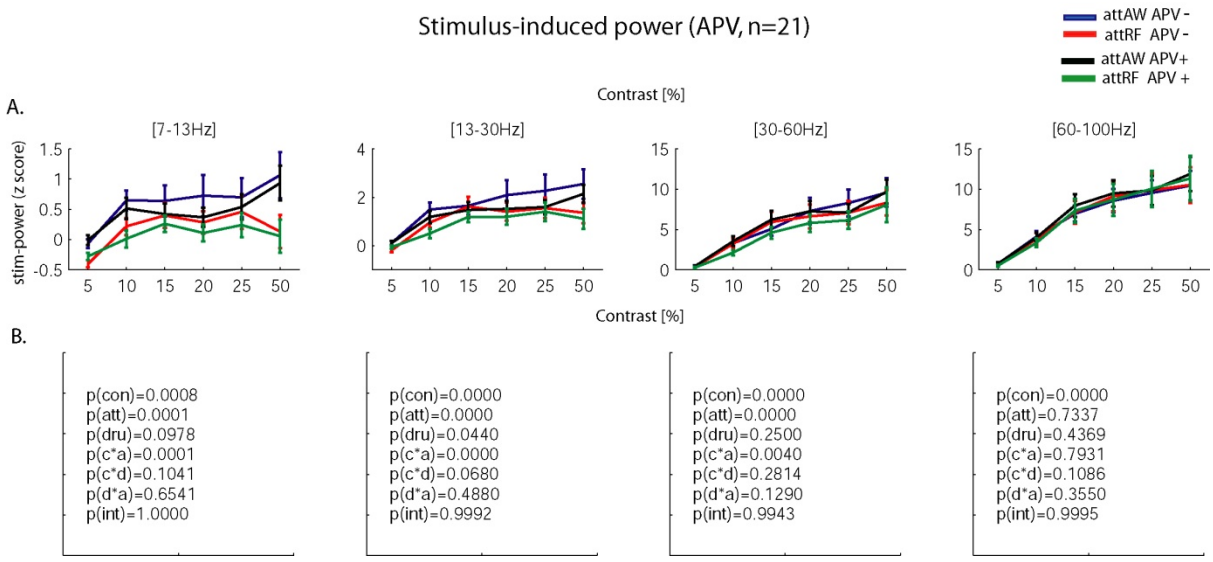

Figure 2.19. Stimulus-induced LFP power for the different frequency bands (n = 21). A. Mean stimulus power (z-score) across different drug, attention, and contrast conditions. B. Statistical values for the different frequency bands and conditions. Shaded areas SEM .

The raw LFP power is shown in Figure 2.20. Applying APV did not significantly change the raw power (p>.1, all bands). Attending to the RF of the recording sites significantly reduced the power in all bands ($p < 0.01$), except the high gamma. Increasing the contrast of the stimulus increased its raw power ($p < 0.001$, all bands). There was no significant interaction between drug and attention (p>.05, all bands). The only significant interaction was between attention and bar-contrast (gamma, $p<0.001$), with larger attention-induced increases for high contrast stimuli.

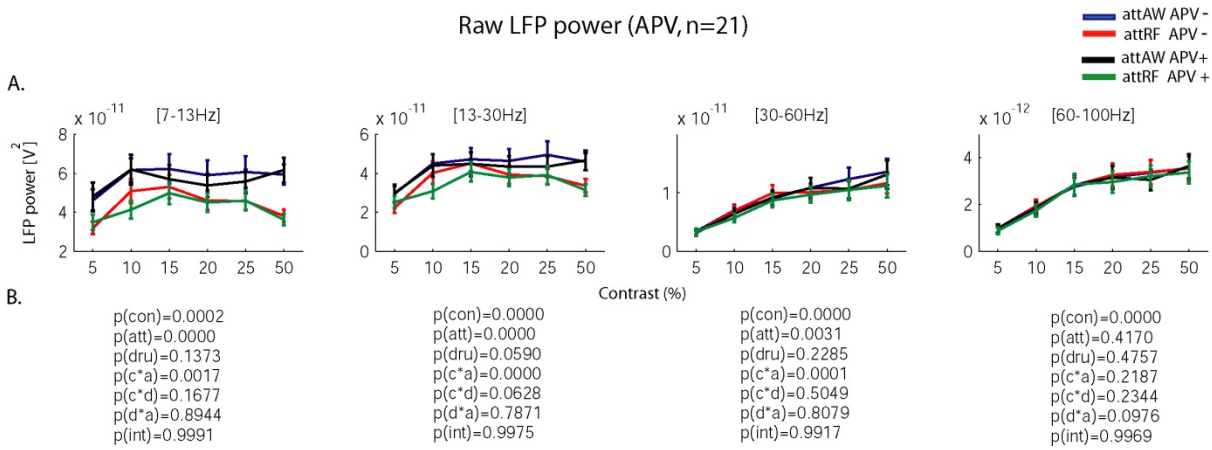

Figure 2.20. Raw LFP power for the different frequency bands (n = 21). A. Mean raw power across different drug, attention, and contrast conditions. B. Statistical values for the different frequency bands and conditions.

The results of the SFC are shown in Figure 2.21. Applying APV did not change the SFC (p>.1, all bands). Attending to the RF of the recording sites significantly reduced the SFC in the gamma band ($p < 0.05$). Increasing the contrast of the stimulus increased SFC ($p < 0.001$, all bands). There was no significant interaction

in the gamma band between drug and attention (p>.1), although the lower bands showed this interaction (p<0.05). No other interaction effects were significant.

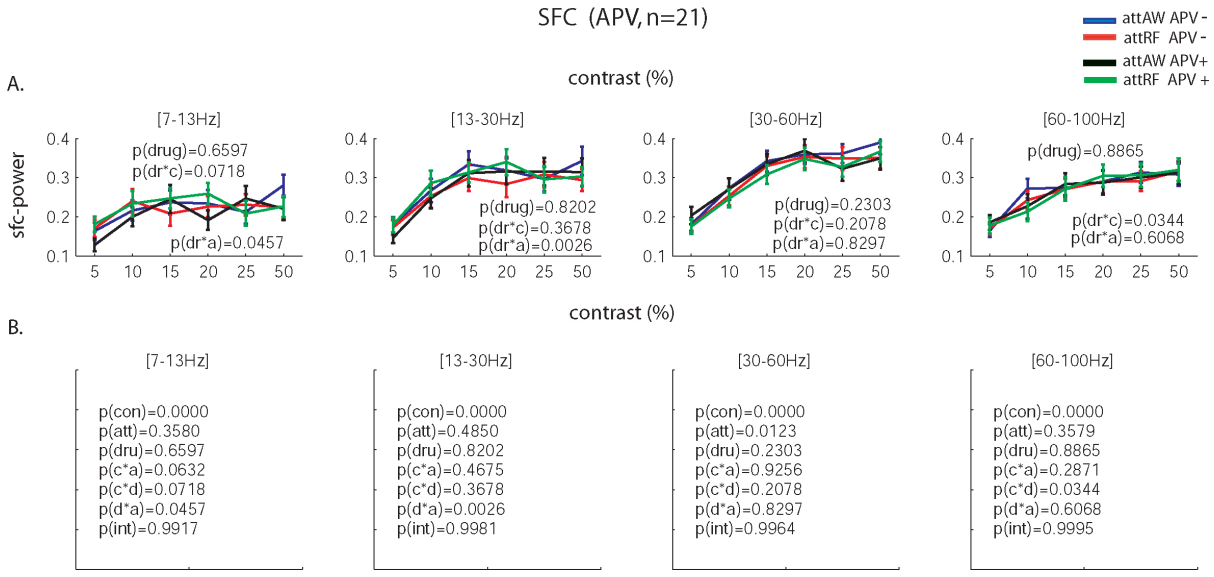

Figure 2.21. Spike-LFP coherence for the different frequency bands (n = 21). A. Mean sfc across different drug, attention, and contrast conditions. B. Statistical values for the different frequency bands and conditions.

2.3.7. Contrast experiments: effect of NMDA receptor activation on the LFP

Figure 2.22 shows the population stimulus-induced LFP power (n = 35 recording sites from monkey HU and HO) in the absence and presence of NMDA. It appears that NMDA does not change the overall stimulus-induced power, nor the attention-induced effects (i.e., stimulus-induced power seems reduced by attention regardless of NMDA application). Increasing the contrast of the stimulus seems to increase the stimulus-induced power, especially for high contrast stimuli, as shown above.

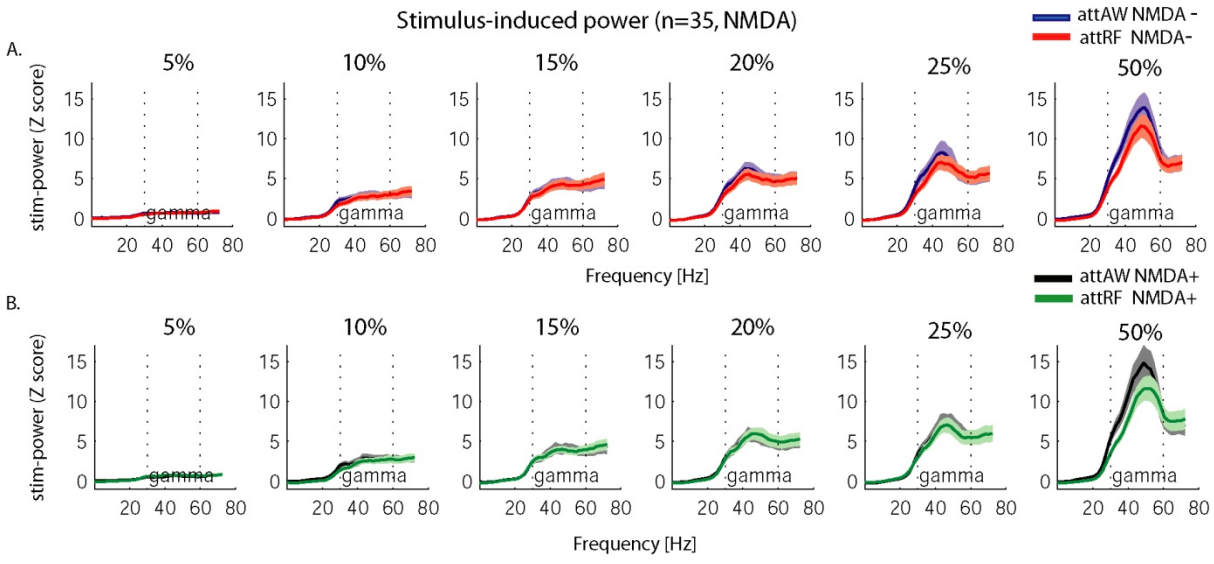

Figure 2.22. Stimulus-induced LFP power for the different drug and attention conditions (n = 35). A. Control condition where NMDA was not applied. B. NMDA-applied condition. Shaded areas SEM .

The power spectrum obtained from these 35 recording sites was divided into four different frequency bands (alpha: 7–13 Hz, beta: 13–30 Hz, gamma: 30–60 Hz, and high gamma: 60–100 Hz). Figure 2.23 shows the stimulus-induced LFP power for the different frequency bands. Applying NMDA did not significantly change the stimulus-induced power in any frequency band (p.>1, three-factor RMANOVA). Attending to the RF of the recording sites significantly reduced the power in the beta and gamma bands ($p < 0.05$). Increasing the contrast of the stimulus significantly increased its induced power in all frequency bands ($p < 0.001$), except in the alpha band (p>.1). There was no interaction between drug and attention (p>.1, all bands). The only significant interaction in the gamma band was between attention and contrast (p<0.001), with larger effects at high contrast.

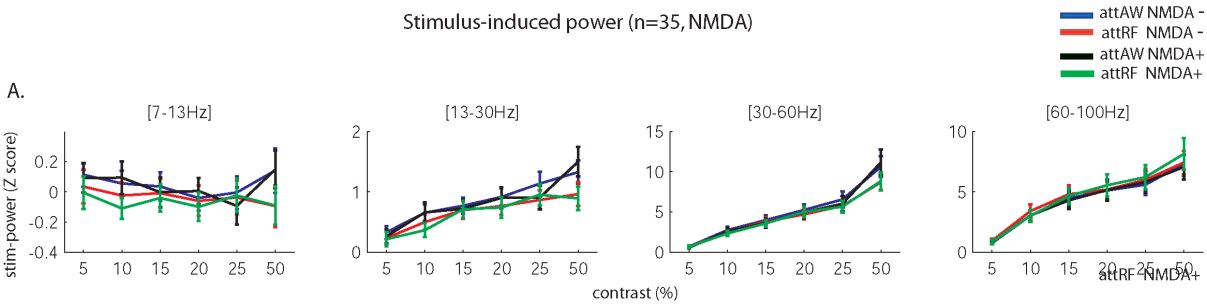

B.

[7-13Hz]	[13-30Hz]	[30-60Hz]	[60-100Hz]
p(con)=0.7875	p(con)=0.0000	p(con)=0.0000	p(con)=0.0000
p(att)=0.0553	p(att)=0.0006	p(att)=0.0166	p(att)=0.0556
p(dru)=0.5213	p(dru)=0.5364	p(dru)=0.6149	p(dru)=0.7706
p(c*a)=0.0654	p(c*a)=0.0004	p(c*a)=0.0000	p(c*a)=0.2617
p(c*d)=0.9879	p(c*d)=0.8688	p(c*d)=0.2852	p(c*d)=0.1665
p(d*a)=0.7782	p(d*a)=0.9513	p(d*a)=0.5346	p(d*a)=0.6462
p(int)=0.9999	p(int)=0.9968	p(int)=0.9993	p(int)=0.9939

Figure 2.23. Stimulus-induced LFP power for the different frequency bands (n = 35). A. Mean stimulus power (z-score) across different drug, attention, and contrast conditions. B. Statistical values for the different frequency bands and conditions. Shaded areas SEM .

Very similar results were observed in the raw LFP power (Figure 2.24). Applying NMDA did not significantly change the stimulus-induced power in any frequency band (p.>1, three-factor RMANOVA). Attending to the RF of the recording sites significantly reduced the power ($p < 0.05$, all bands). Increasing the contrast of the stimulus significantly increased its induced power in all frequency bands ($p < 0.001$), except in the alpha band (p>.1). There was no interaction between drug and attention for any band (p>.1, all bands), except the high gamma. The only significant interaction in the gamma band was between attention and contrast (p<0.001), with larger effects at high contrast.

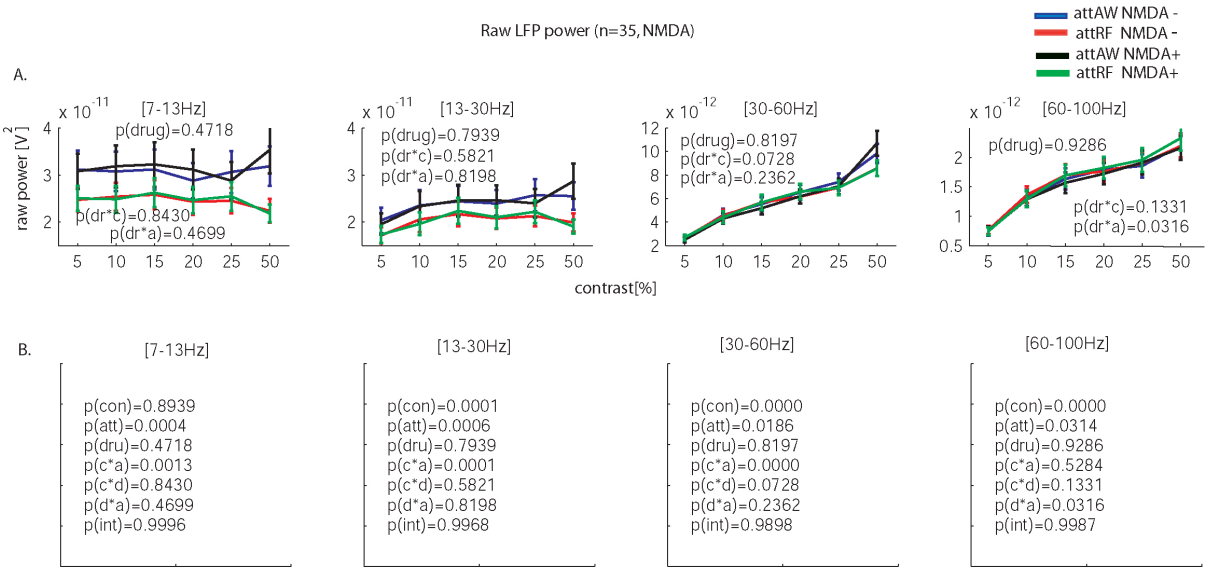

Figure 2.24. Raw LFP power for the different frequency bands (n = 35). A. Mean raw power across different drug, attention, and contrast conditions. B. Statistical values for the different frequency bands and conditions. Shaded areas SEM.

NMDA application did not change the SFC (p>0.05, all bands). Attending to the RF of the recording sites did not change systematically SFC power (p>0.05, all bands). Increasing the contrast of the stimulus significantly increased SFC power in all frequency bands (p < 0.001, three-factor RM ANOVA), except the alpha band (p=0.1635). The interaction between drug and attention in the gamma band was not significant (p=0.082), nor were any other interactions.

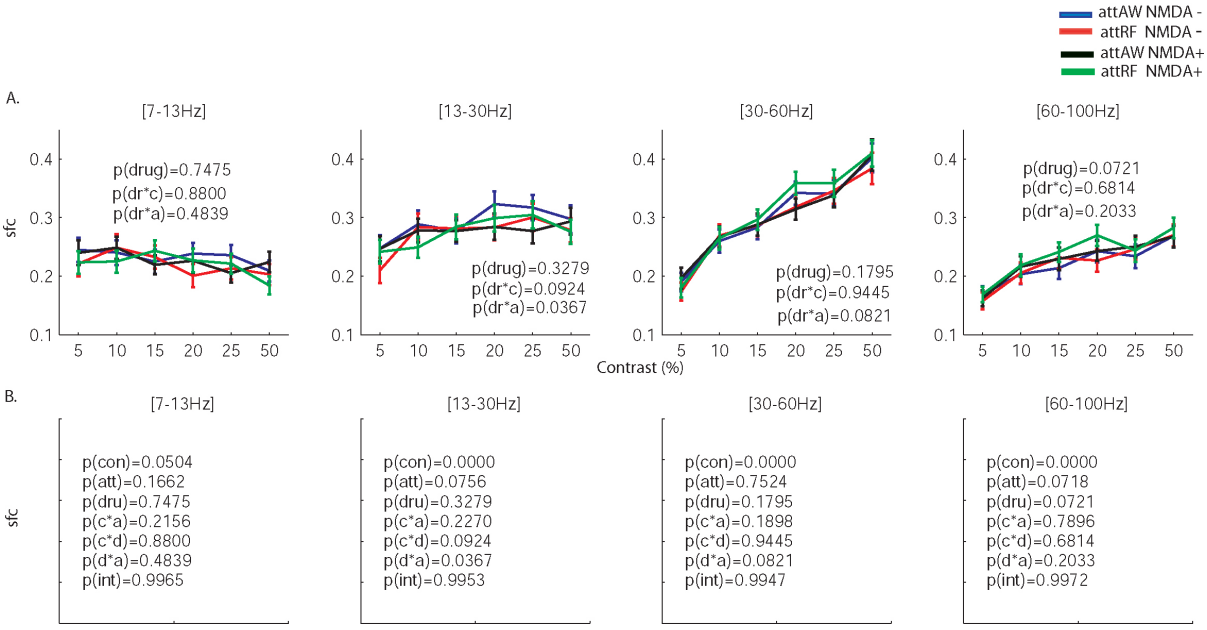

Figure 2.25. Spike-LFP coherence for the different frequency bands (n = 35). A. Mean sfc across different drug, attention, and contrast conditions. B. Statistical values for the different frequency bands and conditions.

2.4. Discussion

Similar to previous results in V1 of the anesthetized monkey (Fox et al., 1990), we found that NMDA receptor activation increased the response gain in the awake-behaving monkey (e.g. increased Rmax). Conversely, NMDA receptor blockade reduced the response gain as measured by decreased Rmax. Given the different results between in-vitro and in-vivo studies on NMDA receptor function, confirmatory evidence from the awake animal was necessary. When the levels of the excitatory drive were varied, we also found that the degree of NMDA receptor activation is proportionally the same for small and large responses. This means that, rather than resulting in an all or none activation threshold, the voltage sensitivity of the NMDA-activated channel produced a continuous range of proportional response amplification from threshold to saturation. Blocking NMDA receptors reduced the gain of the CRF but did not change its half maximum response point (c50). This result was also found by (Fox et al., 1990) for neurons in layers II and III, where we assume that most of our recordings were done (we usually recorded the activity of the first isolated neurons we encountered, which will likely have been in superficial layers). When the authors recorded from the deep layers, they found reduced spontaneous activity but no changes in the stimulus-induced activity (i.e., similar gains of CRFs). A tonic background level of receptor activation not related to the visual response was held responsible for the observed effect. However, in our recordings we also found reduced spontaneous activity with APV, which may be explained by differences in tonic receptor activation between anesthesized and awake states in the superficial layers. NMDA activation in our study also increased the spontaneous activity, which again differed from the Fox et al.'s (i.e., their spontaneous activity was only marginally increased). Other studies, however, suggested that glutamate increases tonic background and stimulus-induced activity, while ACh mainly increases stimulus-induced activity (Sillito and Kemp, 1983, Murphy and Sillito, 1987, Sato et al., 1987b, Sato et al., 1996); but see (Zinke et al., 2006).

As for the role of NMDA receptors in attentional modulation, we found that activation of these channels in V1 of the macaque improved the attentional modulation especially when the visual stimulus elicited a strong input drive (high contrast, 50%). This was demonstrated by an interaction between attention and drug in the spiking activity (MIs analysis), and is in line with slice studies showing that NMDA receptors are activated under conditions of particularly intense or high-frequency synaptic drive (Collingridge and Bliss, 1987). This effect was also observed in our behavioural data, where NMDA speeded up reaction times to attended high contrast stimuli. In light of these similarities between gain changes with NMDA receptor activation (Salt, 1986, Fox et al., 1989, 1990, Shima and Tanji, 1993a, Fleidervish et al., 1998) and gain changes with attention (Roelfsema et al., 1998, Roberts et al., 2007), it is tempting to conclude that NMDA receptor-rich synapses are selectively recruited during attention. Recent work has suggested that feedback projections recruit synapses with NMDA/AMPA receptor ratios different from those of feedforward projections (Self et al., 2008), although the latter authors investigated figure-ground segregation and detection, not spatial attention mechanisms. Our study provides some support for this notion, even though some parts of the data set were somewhat inconsistent. Blocking NMDA receptors reduced the neuronal gain, but it did not systematically reduce the attentional modulation for any of the contrast stimulus tested. However, in the length experiment we found a significant reduction of ROC values when NMDA receptors were blocked. While this was not obvious from the analysis of mean firing rates (MI analysis) technique, we were able to show that this was

likely due to a differential effect on response variance. Blockade of NMDA receptors affected the reliability of neuronal responses rather than its strength, similar to what has been shown for attention in V4 (Mitchell et al., 2007). We found that an attention-induced reduction of the response variability was diminished by APV application. This effect was demonstrated by means of the fano factor and by a differential scaling of the response with the variance. As for the interaction between stimulus type and NMDA receptor function, available evidence in the LGN (Kwon et al., 1992) observed weaker NMDA-related effects on spiking activity when inhibitory mechanisms were at play. This was not observed in our SU data, where drug-induced effects on the spiking activity did not differ across bar lengths. However, differences in RF sizes between LGN and V1 may account for the observed discrepancies. Additionally, it remains to be tested whether larger contrast values than the ones used in this study (>50%) yield different results in the visual cortex of the macaque.

Recent modelling work predicts that NMDA receptor manipulations should mostly affect the strengths of attention-induced gamma oscillations, with minor implications to attention-induced rate modulations (Buehlmann and Deco, 2008). Analysis of the oscillatory activity in our experiment showed the following results: 1) Directing attention reduced the raw and stimulus-induced gamma. 2) The attention-induced effects were stronger when inhibitory mechanisms were engaged (larger stimuli in the length experiments) or when the input drive was high (high contrast stimuli in the contrast experiments) setting in contrast normalization mechanisms. 3) Blocking NMDA receptors with APV increased the raw and stimulus-induced gamma power. 4) The APV-induced effect did not depend on attentional condition. 5) The APV-induced effect depended on the size of the stimuli: it was stronger for larger size stimuli (length experiments). Indeed, in the contrast experiments where the size of the stimuli was smaller, APV failed to increase the raw and stimulus-induced gamma power. 6) NMDA receptor activation had no systematic effect on the raw and stimulus-induced LFP power, 7) nor did it have an effect on the attentional modulation. 8) NMDA receptor activation did not depend on the contrast of the stimuli. 9) These results were found in the raw and stimulus-induced LFP gamma power, but less so in the SFC.

Taken together, the analysis of the oscillatory activity provides converging evidence to the conclusion that NMDA receptors are not specifically involved in the attention-induced gamma oscillations, as proposed by recent modelling work in V4 (Buehlmann and Deco, 2008). However, it should be noted, that we found a consistent reduction of gamma oscillations with attention, while the opposite was found for V4 (Fries et al., 2001), the result that was modelled by Buehlmann and Deco (2008). According to the authors, attention-induced increases of gamma synchrony depend on a finely tuned balance of NMDA and AMPA receptors activation. A change of the ratio of gAMPA/gNMDA, as that achieved with application of APV, will abolish attention-induced changes in gamma power. We did not find evidence to support such claims and note that other receptors, namely AMPA and non-NMDA receptors, have been found to play a dominant role in the generation of gamma oscillations of hippocampal and cortical slices (Buhl et al., 1998, Fisahn et al., 1998, LeBeau et al., 2002). Future studies of attentional modulation should also take these receptors types into account, as well as their interactions with stimulus type.

2.5. Conclusions

We found that NMDA receptors contribute to attentional modulation at the single neuron spiking level in primary visual cortex, although the effects mostly affected response variance. Attention per se reduced response variance in V1, and this reduction was diminished by blockade of NMDA receptors, while mean firing rate differences were not systematically affected. Although the results were significant for large parts of the data set, they were overall less consistent than the results reported in chapter 1, where acetylcholine's effects were probed.

Chapter 3. Effects of muscarinic and nicotinic receptors on contextual modulation in macaque area V1.

3.1. Introduction

The previous two chapters have been dedicated to the study of the neuromodullatory mechanisms of spatial attention in area V1 of the primate brain. The contribution of two main neuromodullatory/transmitter systems, the cholinergic and glutamatergic system, to visual attention was examined. It was found that muscarinic receptors are important during attention. NMDA receptor-rich synapses were also recruited but the effects were somewhat less consistent. We also probed how the cholinergic and glutamatergic systems influenced basic response and neuronal integration properties. This was done by manipulating the size of the visual stimuli in the length experiments, with the objective of better understanding the effects of ACh and NMDA in relation to integration properties. The study of integration properties may shed light on the mechanisms of attentional modulation, as recent work in the macaque has found that spatial attention modulated centre-surround interactions (Zenger-Landolt and Koch, 2001, Roberts et al., 2007, Sundberg et al., 2009) possibly through cholinergic mechanisms (Roberts et al., 2005). In line with this, we further explored neuronal integration properties in this chapter by determining how ACh's actions can aid integration properties, and we did this in the absence of a cognitive task, as it reduces the number of conditions involved.

Literature on integration has shown that the spatial context embedding an image element has a strong influence on the perception of the image element itself (Gilbert et al., 1990, Albright and Stoner, 2002, Paradiso et al., 2006). This influence can be facilitatory under certain conditions, and suppressive under others. Psychophysical studies have observed contextual facilitation when a foveally presented low contrast Gabor target is flanked by collinear Gabor elements (Shani and Sagi, 2005; Williams and Hess, 1998), particularly if they are located at 2-4 times the wavelength (λ) of the Gabor element (Morgan and Dresp, 1995; Polat and Sagi, 1993; Polat and Sagi, 1994). Suppressive influence of the spatial context occurs for flankers located closer to the target (<2λ), especially if they are not collinear, and/or the target stimulus has a high-contrast (Adini and Sagi, 2001; Chen and Tyler, 2002). At the neuronal level, these contextual effects have often been attributed to lateral interactions between neurons in the primary visual cortex, as well as feedback connections from V2 (Kapadia et al., 1995). Neurons representing the relevant image element and the adjacent flanking elements interact with each other in order to facilitate or suppress the detection of the relevant image element (reviewed in Series et al., 2003). Neurophysiological studies have shown that collinear flankers increase V1 neuronal responses to a central target (Crook et al., 2002; Mizobe et al., 2001), especially if the target contrast is low (Polat et al., 1998, Kapadia et al., 2000). Orthogonal flankers however, exert a weaker facilitatory effect or even suppress the neuronal activity (Kapadia et al., 1995, Das and Gilbert, 1999); but see (Zenger-Landolt and Koch, 2001).

Given that these contextual effects are proposed to occur through intracortical lateral and/or feedback connections they should, according to the ACh literature, be altered with altered cholinergic drive. In-vitro studies showed that ACh decreases the efficacy of lateral/feedback connections by means of presynaptic

muscarinic receptors (Gil, 1997, Kimura and Baughman, 1997). ACh also boosts the efficacy of thalamocortical connections through presynaptic nicotinic receptors (Gil, 1997), primarily located on thalamocortical/feed-forward synapses (Lavine et al. 1997; Prusky et al. 1987; Sahin et al. 1992). These data suggests that ACh is able to dynamically adjust the flow of feed-forward and lateral/feedback information by controlling the efficacy of specific synapses (Hasselmo 1995; Hasselmo and Bower 1992, 1993; Kimura 2000; Kimura et al. 1999; Linster and Hasselmo 2001). This dynamic shifting of information could have implications for contextual interactions. ACh should thus result in reduced impact of stimuli presented in the non-classical receptive field (nCRF) while increasing the effect of stimuli placed within the CRF. Recent in-vivo studies have shown that ACh reduces the spread of excitation: it reduces the classical receptive field (CRF) summation area of V1 neurons (Roberts et al., 2005), the spread of membrane voltage fluctuations (Kimura et al., 1999), and the spread of BOLD activation (Silver et al., 2008).

If the spread of excitation is reduced by ACh it is likely that the contextual influences are also changed. The present study tests this proposal (i.e. whether ACh alters the effect of surround modulation). If the effect of the surround is inhibitory, ACh should reduce this inhibition by reducing the efficacy of feedback/lateral connections through activation of presynaptic muscarinic receptors. In contrast if the surround modulation is facilitatory, as that previously seen in the spiking response of V1 neurons (Polat et al., 1998), then equally this facilitation should be reduced by acetylcholine application through presynaptic muscarinic receptors, while simultaneously boosting classical receptive field responses through nicotinic receptor activation. To test this, we combined iontophoretic pharmacological analysis of muscarinic and nicotinic receptors (mAChRs & nAChRs) with single-cell recordings while stimulating the RF surround of V1 neurons in the alert fixating macaque monkey. We found that collinear flanker-induced facilitation occurred in a small fraction of the cells recorded, whereby flanker-induced suppression was the most common effect ((Pooresmaeili et al., 2010); for similar findings see (Macknik and Haglund, 1999, Li et al., 2000). Nevertheless, in those cells that showed flanker-induced facilitation, blockade of muscarinic receptors reduced the facilitation whereas blockade of nicotinic receptors did not. Additionally, in the many cells that showed flanker-induced suppression we saw that blockade of muscarinic receptors reduced the suppressive effect, while nicotinic blockade had no effect. These results suggest an important role of ACh via muscarinic receptors to contextual modulation in the primary visual cortex, by affecting surround facilitation and suppression.

3.2. Materials and methods

The experiments and surgeries were performed in accordance with the European Communities Council Directive 1986 (86 / 609 / EEC), the National Institutes of Health (Guidelines for Care and Use of Animals for Experimental Procedures), the Society for Neurosciences Policies on the Use of Animals and Humans in Neuroscience Research, and the UK Animals Scientific Procedures Act.

Electrophysiological recordings and behavioural procedures

We recorded neurons in three male macaque monkeys (Macacca mulatta). After initial training, monkeys were implanted with a head holder and recording chambers above V1 under general anaesthesia and sterile

conditions (for details of surgical procedures, see Thiele et al., 2006). Single-cell discharges were recorded extracellularly using a tungsten-in-glass electrode flanked by two pipettes (Thiele et al., 2006, Herrero et al., 2008). Drugs were applied iontophoretically through these pipettes using the NeuroPhore BH-2 System (Digitimer). Stimulus presentation and behavioral control were managed by Remote Cortex 5.95 (Laboratory of Neuropsychology, National Institute for Mental Health, Bethesda, MD). Neuronal data was collected by Cheetah data acquisition (Neuralynx) interlinked with Remote Cortex. The waveforms of all spikes that exceeded a threshold set by the experimenter were sampled at 30 kHz. Offline sorting of these MU spike samples was carried out based on waveform features (Neuralynx spike sorting software, Version 2.10).

Monkeys were trained to keep fixation (eye window 1.2° in diameter) while a small oriented Gabor was presented in parafoveally, with or without two collinear flankers (Figure 3A). The fixation point (FP, 0.1° diameter) was presented centrally against a grey background (21 cd/m²) on a 20" analogue cathode ray tube monitor (100 Hz, 1,600 x 1,200 pixels, 57 cm from the animal). Eye position was recorded with an infrared based camera system (Thomas Recording GmBH) and sampled at a rate of 250Hz.

A trial started as soon as the monkey's eye position was within a fixation window centred on the fixation point. After 500 ms a sequence of 4 oriented Gabor stimuli was presented for 700 ms each with 300 ms gaps between presentations of each Gabor. At the end of the four presentations, the fixation point disappeared and monkeys were rewarded if their eye position had been within the fixation window for the trial duration. If the monkey broke fixation before the FP disappeared the condition was repeated later in the block. Twenty trials per stimulus, contrast, and drug application conditions were recorded in most recordings. Cells were excluded if fewer than 10 trials per stimulus, contrast, and drug application conditions were available.

Drug application procedures

The opening diameter of the pipettes varied between 1-4 µm and their resistance was higher than 20 MΩ in most recordings. Hold currents for scopolamine and mecamylamine were usually -10 nA, in rare occasions (when the pipette resistance was 10-20 MΩ) it was -40 nA. Pipette electrode combinations were inserted into V1 through the dura on a daily basis without the use of guide tubes. The integrity of the electrode and the pipettes were checked under the microscope before and after the recording sessions, in addition to measurements of the pipette impedance made before and after the recording at each recording site. The details regarding drug concentration, pH and application current were: scopolamine (0.1M, pH 4.5, median current strength: 30nA, 25 percentile: 15nA, 75 percentile: 45 nA), and mecamylamine (0.1M, pH 4.5, median current strength: 10nA, 25 percentile: 15nA, 75 percentile: 5 nA).

Drug application was continuous during blocks of 'drug applied'. The duration of each block could vary depending on the number of repetitions for each condition that we aimed for, and depending on the number of eye fixation errors that the monkey made. On average drug application for each block was ~7-12 minutes. For the data analysis we removed the first 2 trials of each condition from the data set, as drug effects and recovery usually occur with a slight delay of ~30 seconds. We regularly compensated for the change in current during the ejection condition by increasing the hold current of one of the two pipettes, thereby keeping the overall current identical between the 'hold' and 'eject' conditions.

Stimuli

Stimuli consisted of either central Gabor elements presented in isolation or flanked by two iso-oriented flankers. The orientation and spatial frequency of the Gabors matched the neuron's preference (see below). Each Gabor moved within a Gaussian aperture at 4Hz temporal frequency. The motion was perpendicular to the Gabor's orientation, and reversed direction at a frequency of 4Hz. Within the sequence of 4 presentations per trial the order of stimulus presentation within a trial and between trials was randomised.

Central and flanker Gabors were identical in all respects except for their contrasts. The contrast of the central Gabor was varied between 0, 4, 8, 12, 16, 24, 32, and 64% (Michelson contrast), while the contrast of the flanking Gabors was fixed at 48%. The distance between the central and flanking Gabors could be 1, 2 or 3-4 times the Gabor wavelength (λ). The exact wavelength varied slightly with the spatial frequency preference. High spatial frequencies of for example 6 cyc/° would result in centre flanker distances of 0.166° at a distance of 1λ, whereby the receptive field centre would be filled by flankers. To account for this we used distances of 1.5, 2.8, and 4λ for spatial frequencies of >=6 cyc/°, and distances of 1, 2, and 3λ for spatial frequencies of <6 cyc/°. The large majority of our neurons preferred spatial frequencies of <=4 cyc/° and only 8 neurons were measured with >=6 cyc/°. We included them in our overall sample and treated them as if the wavelengths had been 1, 2, and 3λ, respectively. We also scaled the size of our stimuli, whereby the half width at half height of the Gaussian envelope was 0.3 times the spatial frequency for spatial frequencies of <2 cyc/°, it was 0.4 times the spatial frequency for spatial frequencies between 2 cyc/° and 4 cyc/°, 0.5 times the spatial frequency for spatial frequencies between 4 cyc/°, and 6 cyc/°, and 0.6 times the spatial frequency for spatial frequencies of >=6 cyc/°.

Receptive field characterization

For each recording site we initially determined the location of the receptive field as well as the optimal orientation, spatial frequency and phase using reverse correlation techniques (DeAngelis et al., 1994, Gieselmann and Thiele, 2008). Briefly, the location of the RF was estimated by mapping the classical receptive field with briefly presented dark and light squares (0.1º width, 100% contrast) at pseudo-random locations on a 10x10 grid (a 1x1° area). The RF centre was taken as the location of the peak of the Gaussian fitted to the response distribution (Roberts et al., 2007). The mean RF eccentricity was 3.25°, 5.6°, and 5.7° in monkeys DO, HU, and HO, respectively. Thereafter, the tuning properties were estimated using static sinusoidal gratings (1° diameter) centred on the RF. These gratings varied in orientation (12 orientations, 0–165°), spatial frequency (1, 3, 5, 7, 8, 9 or 10 cycles / °) and phase (0, 0.5π, π, 1.5π) every 60 ms in a pseudo-randomized order. The stimulus that yielded the peak response was taken to represent the preferred orientation, spatial frequency, and phase of the neuron under study. The obtained parameters were used to determine the spatial frequency and orientation of the central and the flanking Gabor elements, which had identical properties. These reverse correlation procedures were conducted while monkeys fixated centrally on the CRT monitor.

Analysis of the physiological data

First, we looked at trials before any drug was applied (i.e., trials during the baseline period). In a total of 124 cells from three monkeys we tested whether the contrast of the central Gabor or the presence of flankers significantly affected neuronal activity, and whether there was a significant interaction between these factors (ANOVA, $p<0.05$). We used the response period from 200 to 700 ms after stimulus onset for our analysis because of our interest in the steady-state response. Neurons were analysed further if contrast and flanker presence, significantly affected firing rates, or if a significant interaction between contrast and flanker occurred (ANOVA, $p<0.05$). A total of 119 out of 124 cells (48, 19, and 52 from monkey DO, HU, and HO, respectively) passed the basic statistical test (two-factor ANOVA: factor 1, contrast; factor 2, flanker presence). For the initial recordings we used two target-flankers spatial distances (1 and 3λ) instead of three (31 cells out of 67 cells, all recorded in monkey DO), but in our later recordings we used three flanker distances to increase the flanker-distance sampling density.

The cells that passed the basic statistical test (119/124) were tested for drug effects (three-factor ANOVA: factor 1, contrast; factor 2, flanker presence, factor 3, drug application). Neurons were analysed further if drug application significantly affected firing rates, or if a significant interaction between drug and contrast/flanker occurred (ANOVA, $p<0.05$). A total of 108 cells passed the drug test (ANOVA, $p<0.05$). Some neurons were stable for a long period of time, allowing us to test the effect of two different drugs subsequently (after recovery). Other recordings showed apparent drift of recording quality, shortly after the initial recovery was completed, in which case only one drug was tested. A third group of neuronal recording sites showed drift even before the initial recovery was completed, and they were discarded because of this. A total of 93 out of 108 neurons exhibited a good recovery after drug application and were subjected to further analysis. From these, 48 were tested with scopolamine and 45 with mecamylamine.

We quantified the target-evoked response R_{Target} for each contrast level c at three target-flanker separation distances under control and drug-applied conditions. This was done by subtracting neuronal responses elicited (in a period 200-700 ms after stimulus onset) by the presence of flankers alone ($R_{Flankers}$) from the responses when the flankers were presented in conjunction with the target, $R_{Target}(c) = R_{Target+Flankers}(c) - R_{Flankers}$. To determine the effect of the flankers on contrast tuning in the presence and absence of drug, contrast response functions were obtained for each neuron in the condition when no drug was applied, and then when drug was applied. Each contrast response function was based on the $R_{Target}(c)$ to 10-30 repetitions of each contrast, flanker, and drug condition. Contrast response functions were fitted for each flanker condition with a hyperbolic ratio function of the following form:

$$R_{\text{target}}(c) = R_{\text{target\_max}} * (c^n / [c^n + c50^n]) + M$$

where R_{target_max} is the saturated response, $c50$ is the contrast at which the half maximal response is reached, n determines the slope of the contrast response function, and M corresponds to the spontaneous activity. This model provides a good approximation of contrast response functions in monkey visual cortex (Albrecht and

Hamilton, 1982, Thiele et al., 2004b, Williford and Maunsell, 2006), and we used multidimensional unconstrained nonlinear minimization (Nelder-Mead) to minimize the summed squared difference between data and model (Matlab 7.1, Mathworks). To determine whether R_{target_max} or *c50* differed significantly when the flankers were introduced (in both control and drug conditions), we fitted each data set independently with the hyperbolic ratio function and determined the chi-square error of the individual fits, and also when fits were forced to obtain the same R_{target_max} (*c50*). In the rare cases where a contrast response function became so flat that the position of c50 became unreliable, the neuron was excluded from the analysis. This explains the different number of neurons tested at each wavelength. Notice also that fewer neurons were tested at the wavelength of 2, as this condition was implemented later on in the experiment.

ROC analysis of neuronal activity

Neuronal thresholds as a function of flanker and drug influences were quantified by calculating the area under the receiver operating characteristic (ROC) curve on the basis of single-trial responses (Swets, 1988). ROC values of 0.5 indicate that an ideal observer can only perform at chance level in detecting the target Gabor. Higher ROC values indicate greater contrast response enhancement, whereby an ideal observer performs at better than chance levels. Thus, if the presence of flankers increased contrast detection, ROC values should be increased in flanker condition relative to no-flanker condition. Likewise, if scopolamine or mecamylamine decreased contrast detection, ROC values should be decrease in the presence of drug compared to its absence. After calculating ROC values for each contrast level (in each flanker condition under the presence or absence of drug), we fitted a Weibull function (Weibull, 1981) to each set of eight ROC values for each flanker and drug condition. This function has the form:

$$Pu = 1-(0.5 * \exp[-(C_u/\alpha_u)^{\beta}])$$

where C_u is the contrast of the target Gabor; α_u is the contrast threshold yielding 82% correct ideal observer performance, and β is the slope of the function. The contrast where the fitted function reached 82% of its maximum was defined as neuronal threshold. In rare cases this value was never reached and was excluded from the analysis (see Figure 3.7 for details of numbers across the different flanker conditions). We tested whether thresholds from no-flanker conditions were significantly different to thresholds from flanker conditions. This was done by statistically comparing the chi-square errors of the ROC fitted curves (Watson, 1979). Neurons with significantly smaller thresholds in flanker compared to no-flanker condition were considered to be facilitated by the flankers ($Threshold_{without\_flankers} > Threshold_{with\_flankers}$), while neurons with smaller thresholds in no-flanker conditions ($Threshold_{without\_flankers} > Threshold_{with\_flankers}$) where considered to be suppressed. This was usually taken as criterion of facilitation vs. suppression, and was used to test whether the parameter of interest significantly changed when a drug was applied. To quantify differences in neuronal thresholds across the population, a modulation index (MI) was calculated: Modulation index =

($Theshold_{without\_flankers} - Threshold_{with\_flankers}$) / ($Theshold_{without\_flankers} + Threshold_{with\_flankers}$) for the neurons that showed flanker-induced facilitation or flanker-induced suppression.

3.3. Results

We will first describe the results before any drug was applied (control recordings similar to Polat et al. (Polat et al., 1998). This part of the chapter has been published previously (Pooresmaeili et al., 2010). In that publication we pooled our data with data from the Roelfsema group as they had performed a very similar experiment without either us or them knowing about it. Upon mutual discovery we realized that our data had the strengths of single unit recordings, while their data had the strengths of recordings with behavioural judgements. We decided that the combined data set would have a greater impact. I will however only describe the data set recorded in Newcastle here. After having described these basic effects of flankers on contextual integration I will continue by comparing these results with those obtained in the presence of the different drugs.

3.3.1. Effect of collinear flankers in control (no-drug) conditions

During the experiment, monkeys were engaged in a fixation task while passively viewing a sequence of Gabor elements that were centred in the RF of each V1 neuron (Figure 3.1a). The first 10-30 trials per contrast and flanker condition performed in this task were recorded under control (no-drug) condition, and these are the data presented here. We measured the R_{target} as the difference between the response of the target plus flankers were present and the flankers only condition (averaged in a time window from 200-700 ms after the stimulus onset) to construct the population contrast response functions (Figure 3.1b). We then fitted a hyperbolic ratio function (see Materials and Methods) to these population data. We anticipated two possible neuronal correlates of the flankers effect. Firstly, the flankers might increase or decrease the maximal response maximum (R_{target_max}). Secondly, the flankers could increase or decrease the contrast at which the half maximal response is obtained (*c50*). An increase in R_{target_max} or a decrease in *c50* would indicate flanker facilitation and the reverse would indicate flanker suppression. Contrary to our expectation, the main effect of the collinear flankers in our population of 119 neurons was a suppression of the response induced by the centre target, which was observed at all contrast levels and at every target-flanker separation (compare black curve with other coloured curves in Figure 3.1b). The suppressive effect of the flankers was strongest for smaller flanker distances.

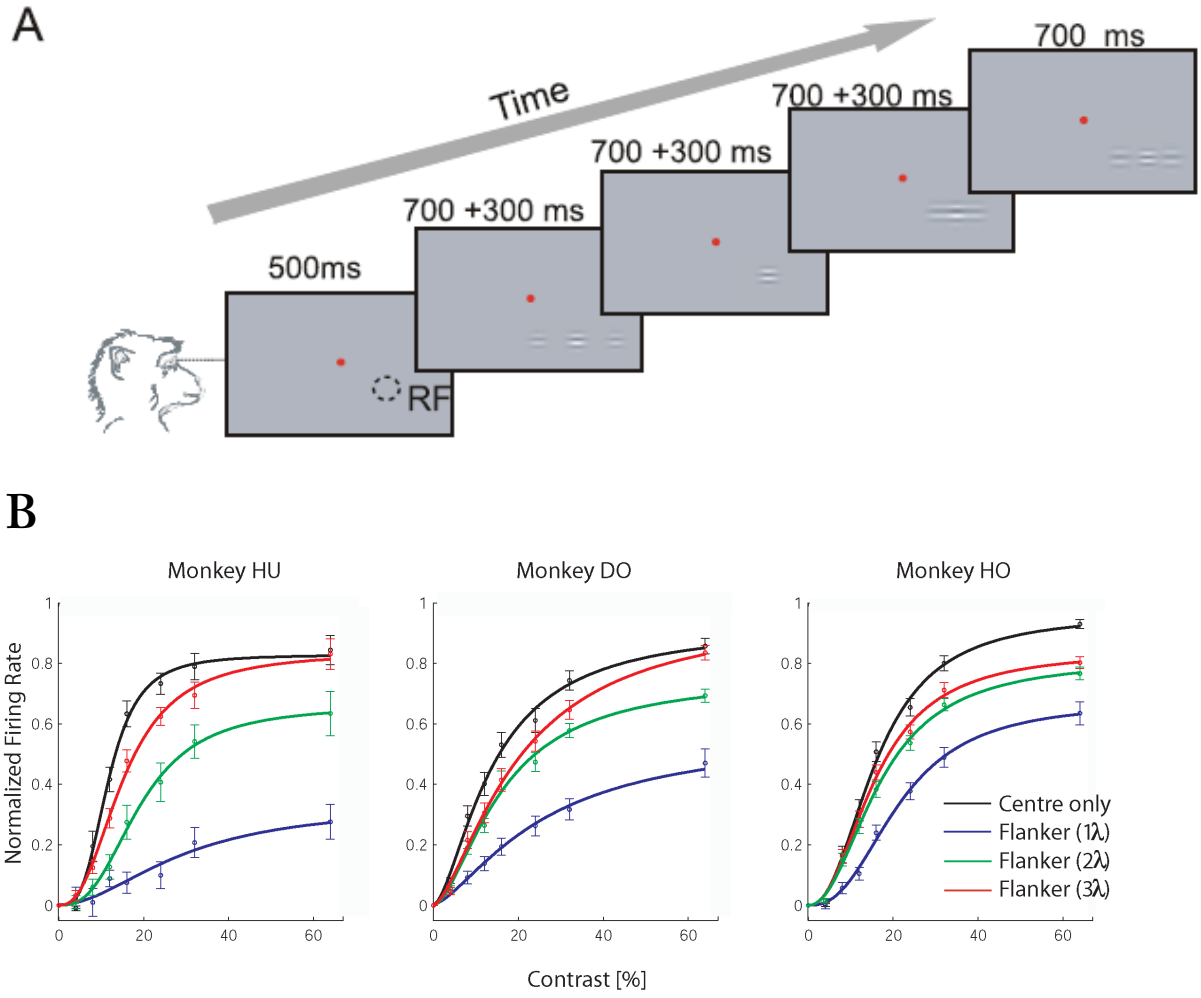

Figure 3.1. Experimental paradigm and popullation analysis of the effects of collinear flankers. **A)** The fixation task. Monkeys fixated a central point (red) and passively viewed a sequence of 4 stimuli displays. Each display consisted of a central target Gabor presented in the RF (dashed circle) of the neuron under study, either in isolation or together with two collinear flankers. Each display lasted 700 ms, with a 300 ms blank interval. **B)** Population contrast response functions in area V1 for the three monkeys (n=119). The error-bars denote the s.e.m. across the neurons. The curves are hyperbolic ratio functions.

Next we quantified these flanker effects. Figure 3.2 shows the distribution of flanker effects on the R_{target_max} and *c50* across all the recorded neurons. It compares the responses in the absence (abscissa) and presence (ordinate) of collinear flankers. At all flanker distances (1, 2 and 3λ), flankers induced a strong suppression indicated by a significant decrease in R_{target_max} and a significant increase in *c50* compared to the no-flanker condition (paired *t*-test, all $P < 0.02$). In the rare cases where a contrast response function became so flattened that the position of c50 became unreliable, the neuron was excluded from the analysis. This explains the different number of neurons tested at each wavelength. Notice also that fewer neurons were tested at the wavelength of 2, as this condition was only implemented later on in the experiment.

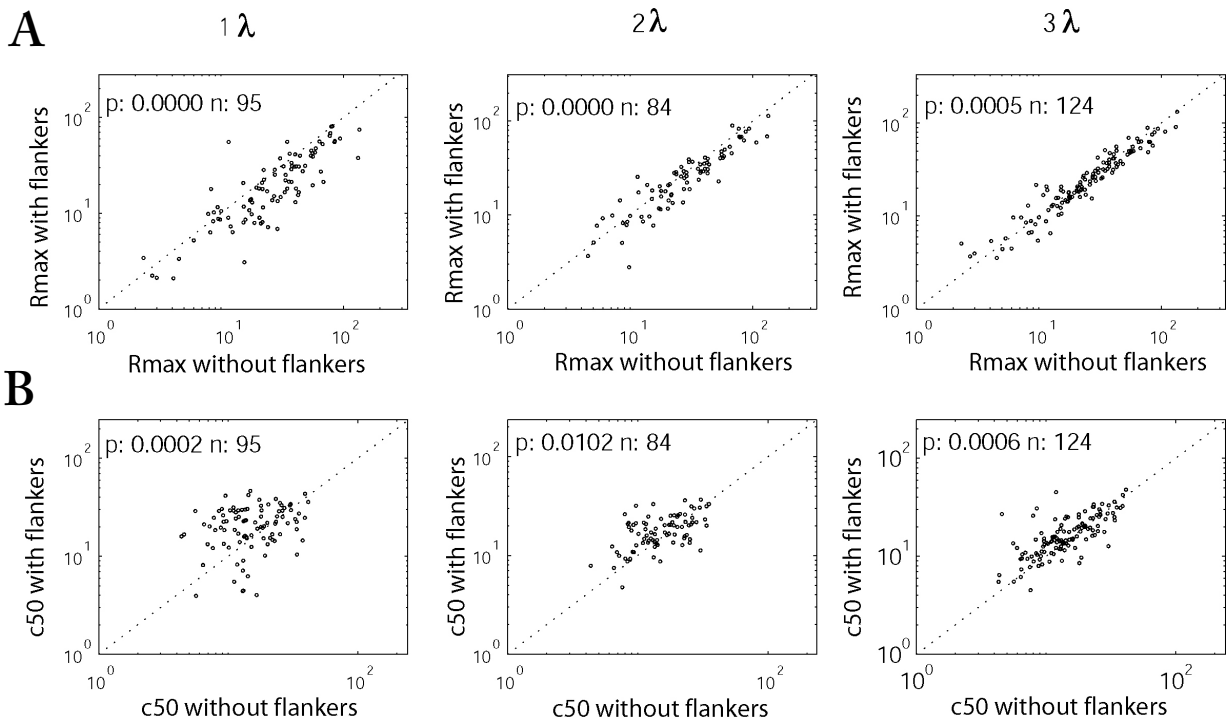

Figure 3.2. Population analysis of the effects of collinear flankers. **A)** Distribution of R_{target_max} values derived from the fits to the responses of all V1 units. Each point represents R_{target_max} of a single cell in the presence (ordinate) or absence (abscissa) of flankers. **B)** Distribution of *c50* values derived from the fits. *P* values are derived from a paired *t*-test.

3.3.2. Effect of collinear flankers in drug conditions

Figure 3.3 illustrates the response of an example neuron to different contrasts during control (blue) and scopolamine-applied (red) conditions. We recorded the effect of flankers on firing rates when scopolamine was not applied (12 trials, box 1). Thereafter we recorded the effect of the flankers when scopolamine was applied (12 trials; box 2), followed by recovery (12 trials; box 3). In the absence of the flankers and without central stimulation of the receptive field (0% contrast stimulus), the neuron's firing rate remained at the level of the spontaneous activity. As expected, the appearance of a central Gabor elicited a response that increased with the contrast of the stimulus ($p<0.001$, 3 Factor ANOVA: contrast, drug, flankers). Scopolamine decreased the response (drug, $p<0.001$). The presence of the flankers also had a main effect on the response of this neuron (flankers, $p<0.001$). Furthermore, there was a significant interaction between contrast and drug (contrast*drug, $p<0.001$), with stronger drug effects at higher contrasts. The interaction between contrast and flankers was also significant (contrast*flankers, $p<0.05$), with weaker contrast effects at the shorter wavelengths. When two collinear flankers were presented without the central target ($R_{Flankers}$), the neuron's responses often increased above the spontaneous activity level. This response was significant for close flankers (1λ and 2λ) ($P<0.001$ and $P<0.05$ respectively, pairwise comparisons). The responses to the far flankers (3λ) were not significantly different from the neuron's spontaneous activity ($P>0.05$, pairwise comparison). These flanker effects did not depend on whether scopolamine was applied, as no interaction between drug and flanker condition was found (flanker*drug, $P>0.05$,). $R_{Flankers}$ was increased at the shorter wavelengths because

we mimicked the psychophysical experimental settings where flanker distance was measured in wavelength λ, the inverse of spatial frequency. This example cell was tested with 2 cyc/° spatial frequency Gabor stimuli, which means that flankers located at 1λ corresponds to an absolute distance of 0.5° (centre of the target to centre of the flanker), and the flankers therefore likely infringe on the neurons' classical RF. Other neurons were tested with spatial frequency stimuli of 4cyc/°, where 1λ corresponds to an absolute distance of 0.25°, while one wavelength corresponds to a distance of 1° for a spatial frequency of 1cyc/°, which may not infringe on the CRF if it is small (e.g. 0.5° diameter).

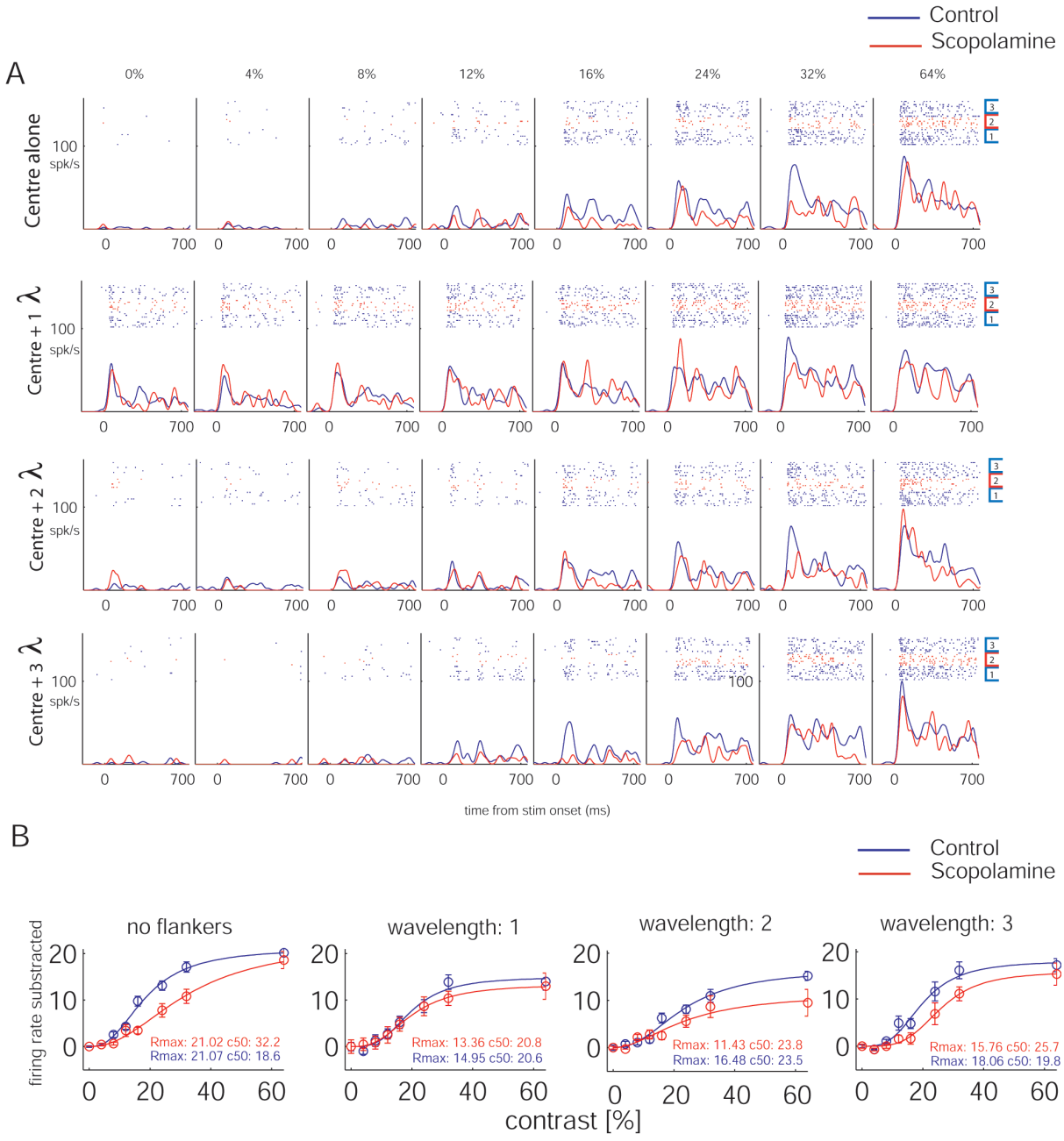

Figure 3.3. Effects of scopolamine and collinear flankers on a representative sample neuron. **A**. Single trial responses (raster plots) and peri-stimulus time histograms (PSTHs) of an example neuron during control (blue) and drug-applied (red) conditions. Each column shows a different contrast of the central Gabor (flankers contrast was fixed to 48%), and each row a different flanker condition. First we recorded

responses when scopolamine was not applied (12 trials, Box 1), followed by responses when scopolamine was applied (12 trials, Box 2) and a recovery period (12 trials, Box 3). The first 2 trials from each block are not shown as they were excluded from the analysis. The appearance of a central Gabor elicited a response that increased with the contrast of the stimulus. Scopolamine decreased the response particularly at high contrasts and some flanker conditions more than others. In the absence of a central Gabor (0% contrast), flankers at closer distances increased responses to a greater extent than flankers at longer distances due to intrusion in the receptive field. **B**. Contrast R_{target} functions of the cell shown above in the absence (blue) or presence (red) of scopolamine for the different flanker conditions (time window: 200-700ms after stimulus onset). c50s and R_{target_max} are shown below. The lowest c50 was registered in the absence of flankers and in the absence of scopolamine. c50s increased when flankers were presented and/or scopolamine was applied. Scopolamine mostly increased c50s in the absence of flankers and when the intrusive effect of the flankers on the classical RF was not too large (i.e., in the largest flanker distance). R_{target_max} were also reduced when flankers were presented. Scopolamine also reduced R_{target_max} in all flanker conditions.

Figure 3.3b shows the contrast response functions of the same neuron during control (blue) and drug-applied (red) conditions. During control condition (blue), flankers suppressed the response of the neuron as indicated by a reduction in the R_{target_max} in flankers-present relative to flankers-absent condition. Fitted R_{target_max} (blue lines) in the absence of flankers was 21.07 spikes/s, and decreased to 14.95 (1λ), 16.48 (2λ), and 18.06 (3λ) when flankers were presented. Flankers also increased *c50s* for all three flanker distances; c50s increased from 18.6% in the absence of flankers to 20.6% (1λ), 23.5% (2λ), and 19.8% (3λ) in the presence of flankers. Application of scopolamine had a very similar effect as presenting flankers; it decreased R_{target_max} and increased c50s. Compared to the no-drug condition, Scopolamine reduced R_{target_max} for all flanker conditions; no-flankers (from 21.07% to 21.02%), flankers-1λ (from 14.95% to 13.36%), flankers-2λ (from 16.48% to 11.43%), and flankers-3λ (from 18.06% to 15.76%) condition. Moreover, scopolamine increased c50s in all flanker conditions; c50s increased from 18.6% to 32.2% (no-flanker), 20.6% to 20.8% (1λ), 23.5% to 23.8% (2λ), and 19.8% to 25.7% (3λ). Please not the stronger effect in the no-flanker and flanker-3λ condition.

The contrast response functions of the cell in Figure 3.3b are representative of the effects observed at the population level. However, we did find cells with flanker facilitation such as the example neuron shown in Figure 3.4. Flankers presented at 2λ and 3λ strongly increased the response of this neuron to a central target stimulus. The facilitatory effect of the flankers was reflected by a decrease in c50 from 18.8% in the absence of flankers to 14.7% and 15.7% for flankers at 2 and 3*λ*, respectively. Flanker facilitation did not occur for distances lower than 2λ. For flankers at 1*λ* suppression was observed, as reflected by an increase in c50 from 18.8% to 29.4%, and a decreased in R_{target_max} from 60.37 to 21.2. Scopolamine decreased R_{target_max} and increased c50s for this cell. Scopolamine reduced R_{target_max} from 60.37 to 51.7 in the absence of flankers, from 55.97 to 52.64 for flankers at 2λ, and from 52.03 to 51.08 for flankers at 3λ. Moreover scopolamine increased c50s from 18.9% to 19.2% in the absence of flankers, from 15.9% to 18.4% for flankers at 2λ, and from 15.7% to 16.3% for flankers at 3λ. For flankers at 1λ, R_{target_max} was increased and *C50* was decreased with scopolamine.

To find out whether flanker facilitation improves contrast detection at the lowest contrasts, we calculated neuronal thresholds based on ROC analysis (see Materials and Methods). Figure 3.4b (3^{rd} and 4^{th} plots) shows the ROC values for the example neuron. There was a threshold reduction from a value of 9.37% in the absence of flankers to a value of 6.95% for flankers at 3λ (P<0.001, chi-square fitting). There was a trend

towards flanker facilitation for flankers at 2λ as reflected by a reduction in thresholds from 9.37% to 9.2%, but this effect did not reach significance (*P*=0.145, chi-square fitting). More importantly, scopolamine reduced the facilitation observed for flankers at 3λ: while thresholds were significantly reduced from 9.37% to 6.95% in the control condition, they were only marginally reduced from 8.95% to 8.27% in the drug condition (P=0.198, chi-square fitting).

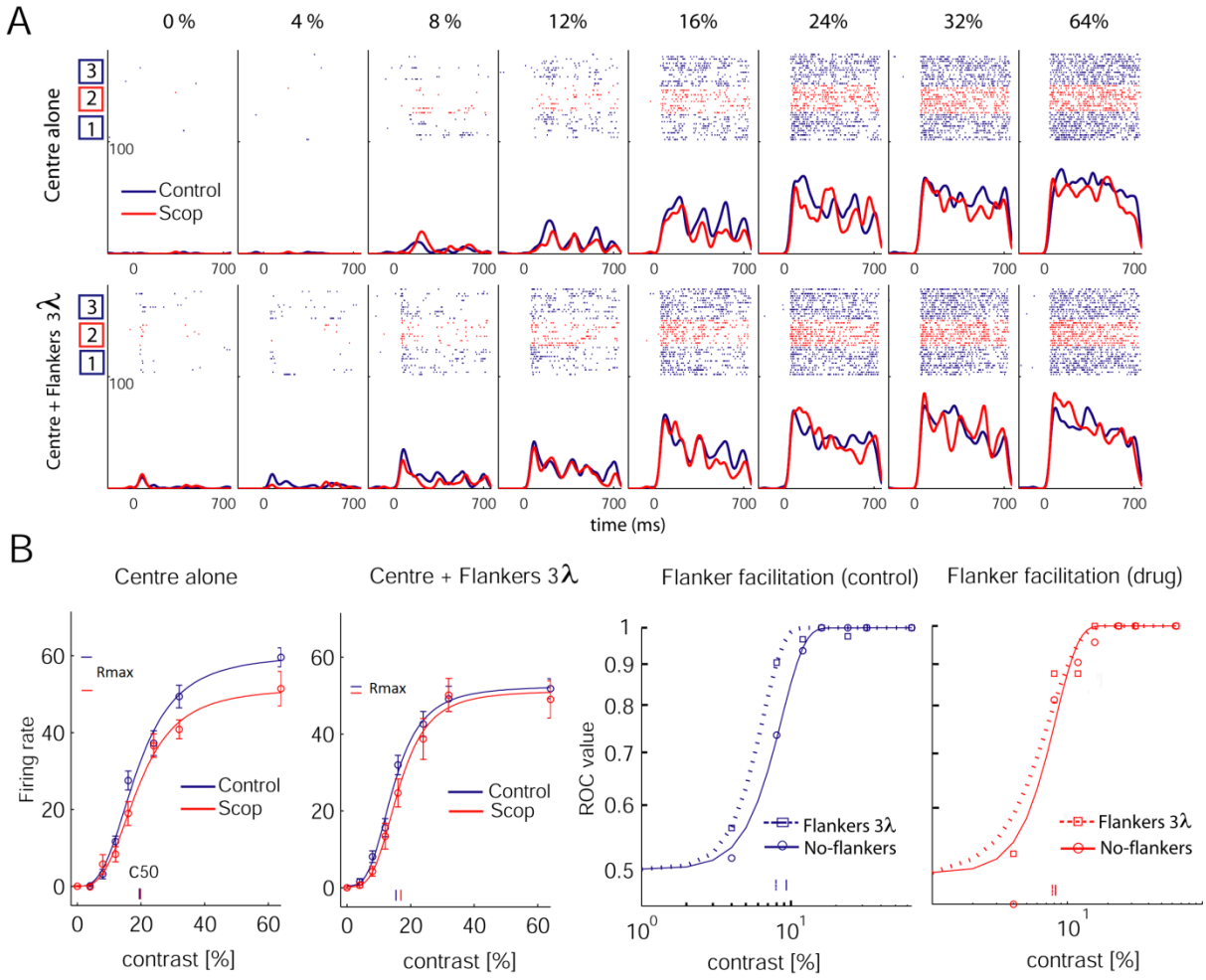

Figure 3.4. Effect of scopolamine on an example neuron which displayed flanker facilitation in the no drug condition. **A)** All conventions as in Figure 3.3, except that only two flanker conditions (centre alone and flankers 3λ) are shown. The appearance of a central Gabor elicited a response that increased with the contrast of the stimulus, but this increase was stronger for flankers at 3λ at least at low and medium contrasts, relative to centre-alone (i.e., flanker-induced facilitation). **B)** Contrast R_{target} functions of the cell shown above. When the central Gabor was presented with flankers at 3λ the c50 was reduced compared to when it was presented alone (compare blue lines in x-axis of both plots and see text for values). Scopolamine reduced the facilitation as shown by a larger difference between c50s in the flankers than in the centre-alone condition (see text for values). The facilitatory effect of the flankers was not reflected on the R_{target_max} (centre-alone=60.37%, 2λ=55.97%, 3λ=52.03%), as it was mostly present for low and medium contrast stimuli. **C.** ROC values showing the strength of flanker facilitation under control (blue) and scopolamine-applied (red) conditions. Flanker facilitation (ROCs) was larger in the control compared to the drug condition. The point where the fitted function reached 82% of its maximum was taken to be the neuronal threshold. The difference between thresholds was much larger in the control than in the drug condition, which demonstrates that scopolamine reduces flanker facilitation in this cell.

3.3.3. Effect of collinear flankers in drug conditions (population data)

A total of 93 cells out of 108 passed the basic statistical test and displayed a good recovery (see Materials and Methods). From these, 48 cells were tested with scopolamine and 45 with mecamylamine. Most cells were tested at three flanker distances, except for a few cells tested at two distances (see methods). Figure 3.5A shows the effect of both drugs on the mean R_{target_max} across all the cells. Both drugs reduced R_{target_max} (scopolamine, p=0.002; mecamylamine, p<0.001, ANOVA). We compared the R_{target_max} in the absence (abscissa) or presence (ordinate) of the drugs (Figure 3.5B). At all flanker distances, the majority of R_{target_max} data points lie below the line of unity, in line with the predominantly suppressive effect of the drugs (signed rank test, all p<0.03).

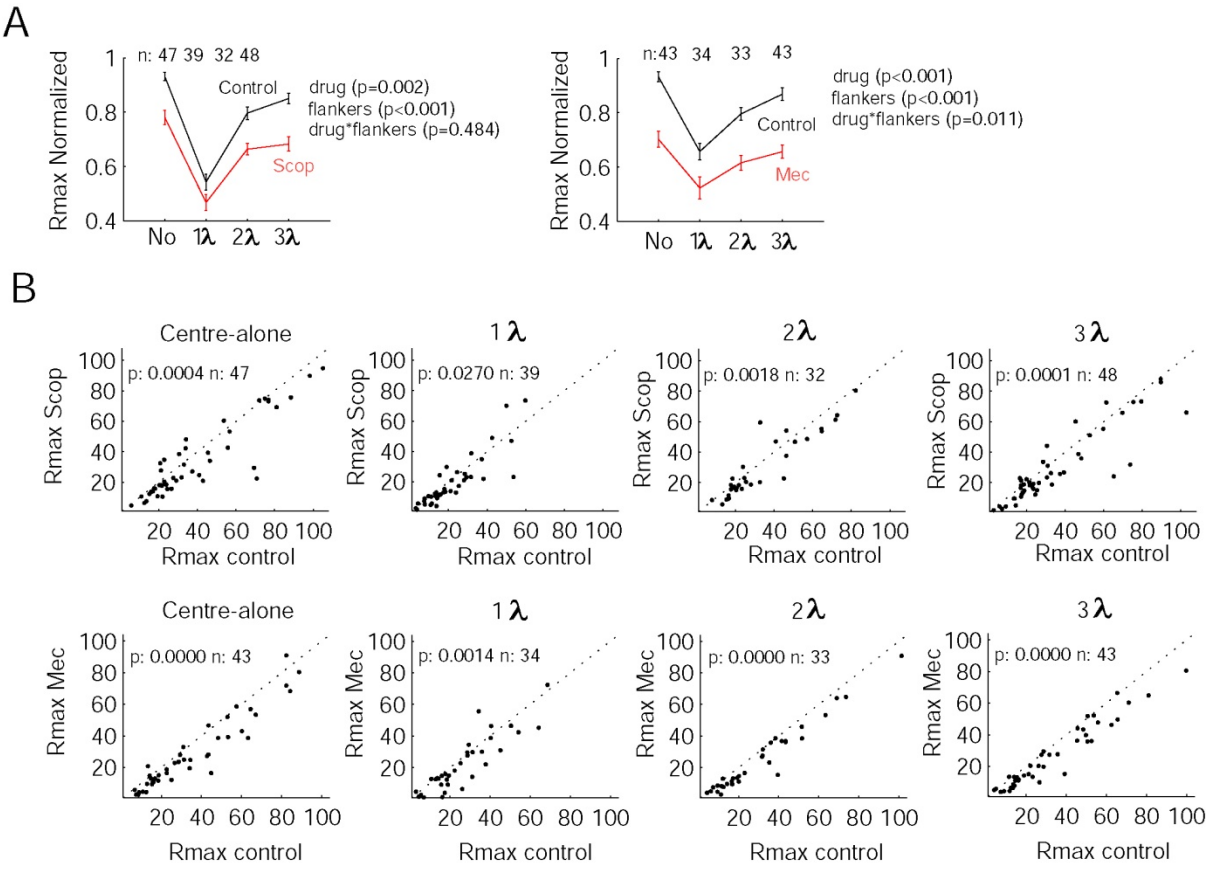

Figure 3.5. Effects of muscarinic/nicotinic blockade on contextual modulation as measured by Rmax (population data). **A.** Mean Rmax normalized values in the absence and presence of scopolamine (left) and mecamylamine (right). Both, flankers and drug application reduced Rmax values. **B.** Distribution of Rmax for all neurons tested with scopolamine (top) and mecamylamine (bottom).

The drug-induced suppression was also evident in the c50s, as shown in Figure 3.6a where both drugs showed a trend to increase the c50 (scopolamine, p=0.081; mecamylamine, p<0.033, ANOVA). More detailed comparison of the c50 at each flanker distance (Figure 3.6b) revealed that the effect of the drugs occurred at specific distances. For no-flankers and flankers at 3λ most *c50* data points lie above the line of unity, in line with the suppressive effect of the drugs (scopolamine; no-flankers, p=0.0149, 3λ-flankers, p=0.0664; mecamylamine; no-flankers, p=0.0073, 3λ-flankers, p=0.00225; signed rank test). This was not the case for

closer flankers at 1 and 2λ (signed rank test, all *P*> 0.05). In these flanker conditions the effect of the flankers itself was too strong (see figure XA), likely overriding the relatively smaller effect of the drug on the c50.

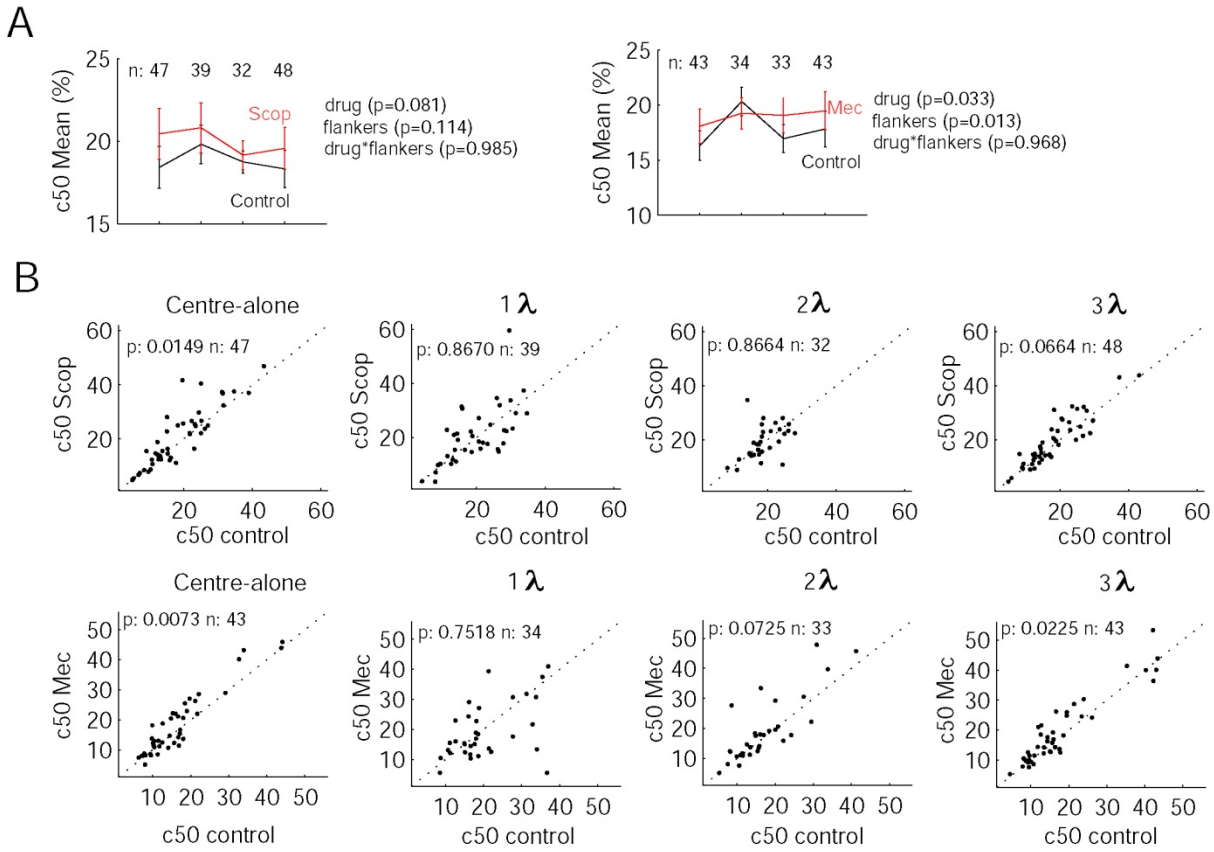

Figure 3.6. Effects of muscarinic/nicotinic blockade on contextual modulation as measured by c50s (population data). **A.** Mean C50s normalized values in the absence and presence of scopolamine (left) and mecamylamine (right). Both, flankers and drug application increased c50 values. **B.** Distribution of c50s for all neurons tested with scopolamine (top) and mecamylamine (bottom).

However, c50s are not an appropriate measure of neuronal sensitivity, as they just provide a measure of when neurons reach their half maximal firing rate, which has no real relation to discriminability. Conversely, neuronal thresholds calculated through ROC analysis reflect how well neurons detect the presence of a stimulus. Figure 3.7 shows the neuronal thresholds obtained from fitting ROC values with a Weibull function for the population of cells. In line with the c50 analysis, both drugs increased thresholds in the absence of flankers (scopolamine, p=0.0054; mecamylamine, p=0.0137, signed rank test). At a flanker distance of 3λ scopolamine significantly reduced neuronal thresholds (p<0.0002), and there was a trend for reduced thresholds when mecamylamine was applied, although it did not reach significance (p=0.0812, signed rank test). Neither of the drugs had a significant effect on neuronal thresholds for flankers at 2λ (Scopolamine; *p*=0.516; Mecamylamine; p=0.4887, signed rank test) or flankers at 1λ (Scopolamine; *p*=0.162; Mecamylamine; p=0.92, signed rank test).

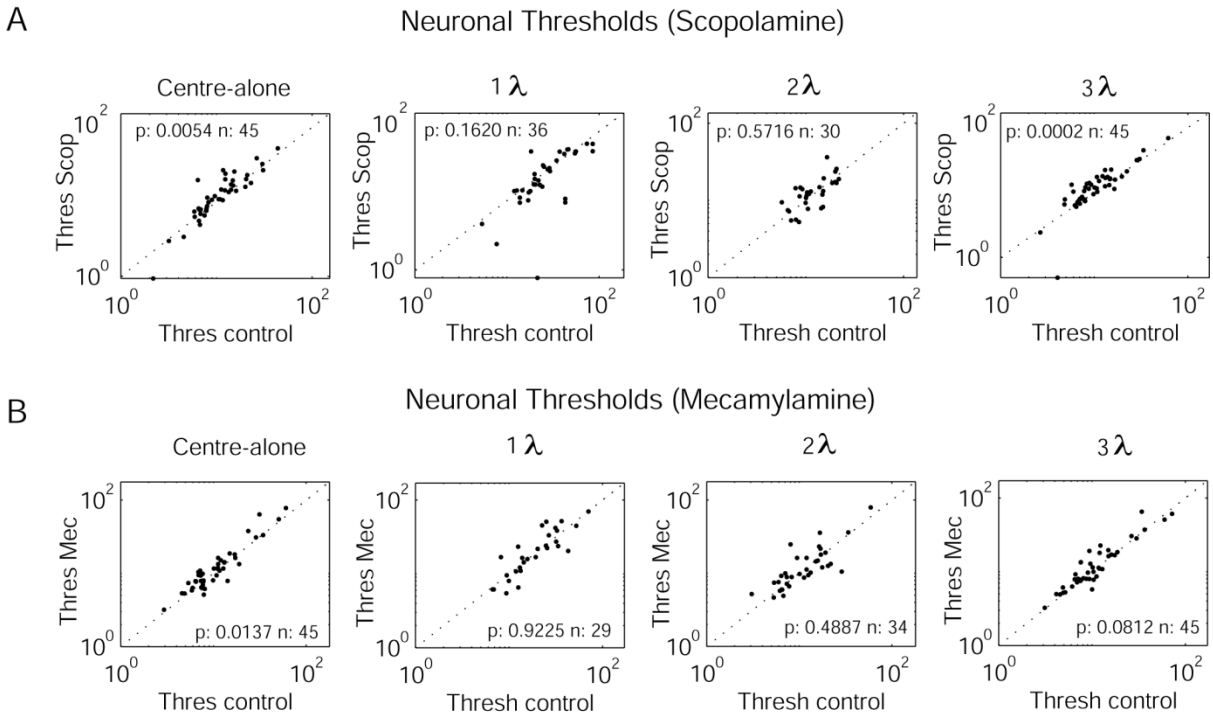

Figure 3.7. Effects of muscarinic/nicotinic blockade on contextual modulation (population data). **A.** Neuronal thresholds were increased in the presence of Scopolamine (y-axis) compared to its absence (x-axis). This effect was significant when the activity of the flankers did not override the relatively smaller effect caused by the drug. **B.** Mecamylamine reduced neuronal thresholds in the centre-alone condition and showed a similar trend in the 3λ condition.

3.3.4. Differential contribution of scopolamine and mecamylamine

The analysis performed so far on the neuronal population showed that both scopolamine and mecamylamine seem to suppress neuronal thresholds in a similar way. This strikingly similar effect could however be the result of pooling across flanker-facilitated and flanker-inhibited neurons. To account for this possibility, we now analyse the effect of the drug separately for cells that showed significant signs of flanker facilitation at some wavelengths, and for cells that showed flanker induced suppression at all wavelengths. Only the significantly facilitated flanker wavelengths were selected for this analysis ($p<0.05$, see methods). 36 wavelengths conditions showed significant facilitation in the scopolamine data set, and 24 wavelengths conditions in the mecamylamine data set. They included mostly wavelength 3, which constituted 60% of the data reported below ($Threshold_{without\_flankers} > Threshold_{with\_flankers\_wavelengh3}$, $p<0.05$), with the other 30% of data recruited from wavelength 2, and the remaining 10% from wavelength 1. This facilitation was assessed in the control condition, and later compared to the effect when scopolamine/mecamylamine was applied. A modulation index was calculated for each flanker-facilitated data point in the two drug conditions: modulation index = $(Threshold_{without\_flankers} - Threshold_{with\_flankers}) / (Theshold_{without\_flankers} + Threshold_{with\_flankers}$. Figure 3.8 (left) shows the effect of the drugs on the mean modulation index and their respective distributions. Scopolamine significantly decreased the modulation index ($p=0.047$, signed rank test), while mecamylamine did not ($p=0.241$, signed rank test). These results show that the flanker-induced facilitation was greatly reduced when

scopolamine was applied. The negative data points in the ordinate axis (Figure 3.8B) represent extreme cases of this reduction; neurons that were facilitated by the flankers in the absence of scopolamine, but suppressed in its presence. In contrast, mecamylamine did not significantly reduce the flanker-induced facilitation in those cells that were originally facilitated. However, this effect could be due to fewer data points in the mecamylamine (n=24) compared to the scopolamine (n=30) data set, as a tendency towards reduce MIs was observed with both drugs. To measure whether this effect was significantly different we calculated an index (I = MIcontrol – MIdrug) for the 24 neurons tested with mecamylamine, and a similar index for the 30 neurons tested with scopolamine (I = MIcontrol – MIdrug). We compared these two indices statistically (signed rank test), and found no significant difference between mecamylamine and scopolamine (p=0.62). This suggests that both drugs reduce flanker facilitation.

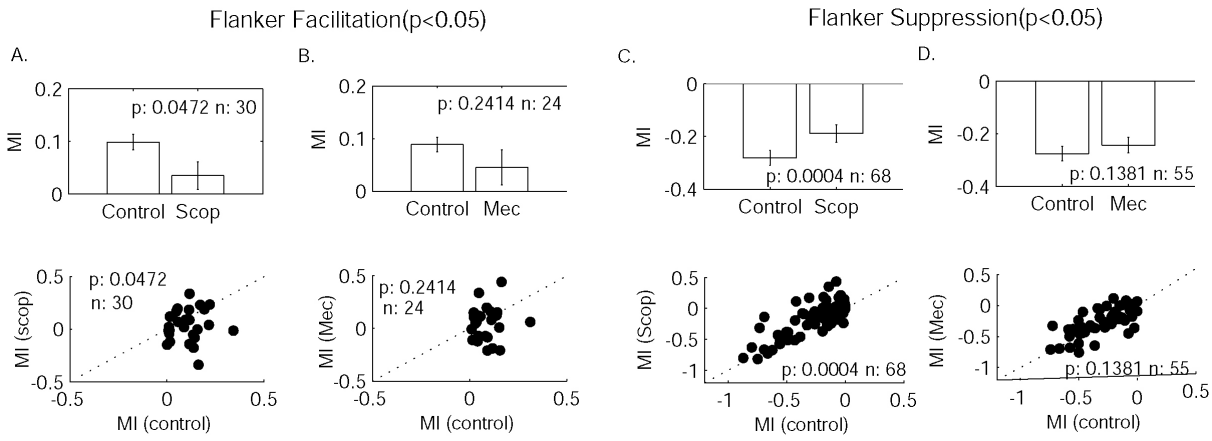

Figure 3.8. Differential contribution of scopolamine and mecamylamine to contextual modulation. **Left.** Flanker-facilitated neurons modulation indexes (MI) in the control and drug conditions. A, Scopolamine (mean MI and distribution). B. Mecamylamine. The flanker-induced facilitation was reduced by Scopolamine but not by Mecamylamine. **Right.** Flanker-suppressed neurons modulation indexes (MI) in the control and drug conditions. **C.** Scopolamine. D. Mecamylamine. The flanker-induced suppression was also reduced by scopolamine but not by mecamylamine.

Next, we selected wavelengths that were significantly suppressed by the presence of flankers (threshold without flankers < threshold with flankers, p<0.05). Because suppression was the most common effect we found many more data points here compared to the facilitation analysis: 68 wavelengths showed significant suppression in the scopolamine data set and 55, in the mecamylamine data set. They included all wavelengths although the most common were wavelength 1 and 2. This suppression assessed in the control condition was compared to the effect when scopolamine/mecamylamine was applied. We calculated modulation indexes for each drug condition with the same formula ($Threshold_{without\_flankers} - Threshold_{with\_flankers}$) / ($Theshold_{without\_flankers} + Threshold_{with\_flankers}$). Initially, we expected these neurons to undergo a smaller reduction when scopolamine was applied. Scopolamine significantly reduced the flanker-induced suppression (p=0.0004, signed rank test), with most data points lying above the line of unity (Fig 3.8c). In contrast, mecamylamine did not change significantly the flanker-induced suppression (Fig 3.8d, p=0.138, signed rank test). Similar to above, we tested if the differential effect across drugs was significant by calculating an index (I = MIcontrol – MIdrug) for mecamylamine and scopolamine, separately, and comparing them statistically (signed rank test). We found a

trend (p=0.09), with scopolamine reducing the flanker-induced suppression slightly more strongly than mecamylamine.We note that scopolamine/mecamylamine application itself tended to increase thresholds in the target-alone condition (e.g. from a threshold of 10% contrast in no-scopolamine condition to a threshold of 18% in scopolamine condition), posing limitations to the calculation of the MIs. For example, if the activity is already very reduced by the drug in the no-flanker condition, the efficacy of the flankers to promote a further reduction may be dampened. We found that both drugs reduced neuronal activity in the majority of cells, but mecamylamine did so more strongly (see Figure 3.5a). To test whether scopolamine truly reduced the flanker-induced suppression more than mecamylamine, we selected neurons with similar thresholds in drug-applied and control condition when stimulated by the target-alone, but different thresholds when stimulated by the target-plus-flankers (flanker*drug interaction, see Materials and Methods). This allowed us to test the effect of the drug on the amount of flanker-induced suppression without being confounded by the factor mentioned above. Figure 3.9 shows the data points that matched this criterion (scopolamine, n=19; mecamylamine, n=23). A similar trend as before was observed, with scopolamine reducing the amount of flanker-induced suppression but this trend did not reach significance (p=0.093, signed rank test), probably due to the low number of neurons. Importantly, mecamylamine did not have an effect, not even a trend (p=0.69, signed rank test). To compare if the differential effect across drugs was significant, we calculated the same index as previously described (I = MIcontrol – MIdrug), and compare them across the different drugs. We found a trend towards significance (p=0.133), with scopolamine reducing the flanker-induced suppression slightly more strongly than mecamylamine.

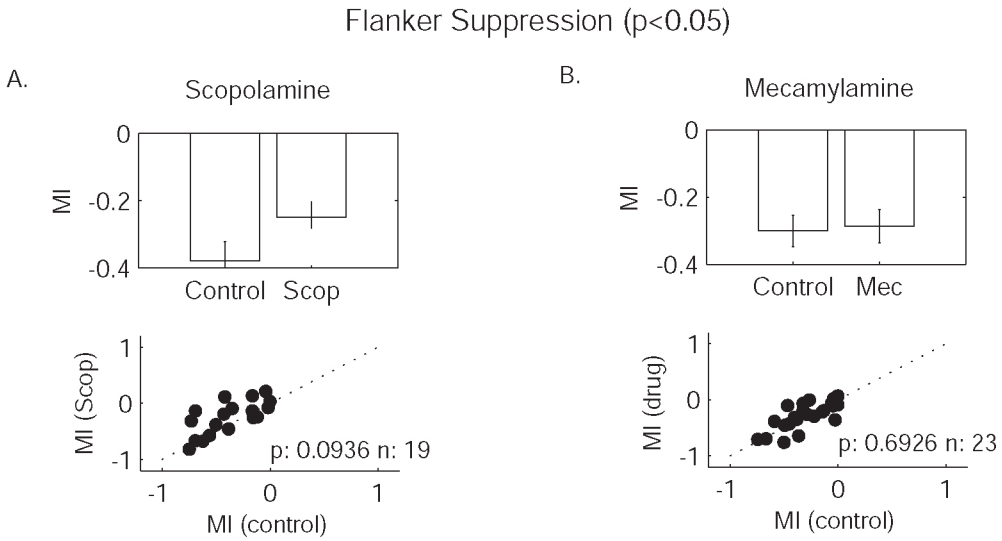

Figure3.9. Effect of scopolamine/mecamylamine on flanker-induced suppression. **A.** Mean MI across neurons (left) and their distribution are shown for the control and scopolamine-applied conditions. Scopolamine tend to increase the amount of flanker-induced suppression (MI=0, green line; MI median, red line). **B.** Mecamylamine showed an opposite trend. Error bars are 1SEM. Data points (n=17 and n=19) refer to flanker conditions that matched the criterion, i.e., two data points can belong to the same neuron.

3.4. Discussion

Our experimental set up and stimuli matched the conditions under which flanker-induced facilitation was observed in previous studies in the primary visual cortex (e.g. (Polat et al., 1998, Kapadia et al., 2000). However, the most common effect of the flankers in the present study was to suppress the response of the cell to a central Gabor stimulus. Cells, where flanker facilitation occurred, like the one shown in figure 3.4, were very rare among the population data: only 13% of neurons showed any signs of flanker-induced facilitation. This finding was surprising, but given the masking experiments by Macknik and some very other studies (Macknik and Haglund, 1999, Zenger-Landolt and Koch, 2001, Meirovithz et al., 2010), the results certainly have their precedent in the literature. Additionally, close inspection of previous studies reveals that the percentage of neurons exhibiting flanker-induced facilitation was also relatively small in those studies that focussed on flanker induced facilitation. For example, Chen et al. (2001) found that only 38% of the neurons recorded showed facilitation at low contrast and suppression at high contrast, while the majority of the neurons showed either suppression for low and high contrast or opposite effects, i.e. suppression for low and facilitation for high contrast. Even lower percentages were observed by others (14% facilitation, Ito and Gilbert, 1999; 34%, Polat et al., 1998). Controversially, the stimuli in these studies were located at more eccentric representations, where the perceptual effects of flankers are largely suppressive. In addition, interpretation of flanker related effects from anesthetized or awake-non-behaving animals is not easy, as anesthetics (Lamme et al., 1998) and attentional states (Freeman et al., 2001; Roberts et al., 2007) have been shown to influence the strength of contextual effects.

Given the low number of flanker-induced facilitated cells in our study, it was only possible to test the original hypothesis about contextual neuromodulation on a very small set of neurons. We expected, in line with the previous studies reporting collinear facilitation in the anesthetized animal, to also find facilitation in the awake monkey, and if this was mediated by lateral intracortical interactions, then this facilitation should be increase by scopolamine application, as this should increase the efficacy of intracortical lateral synapses. In contrast, blockade of nicotinic receptors which are mainly located presynaptically at thalamo-cortical terminals would mainly reduce the gain with no changes in the facilitation. However, we found that blockade of muscarinic receptors in flanker-facilitated neurons reduced the facilitation, while blocking nicotinic receptors reduced the overall gain but did not have an effect in the facilitation (fig 3.8a). Thus, the second part of our finding is in line with the simple minded straight forward proposal, while the first is not. However, it needs to be kept in mind that the effect of actylcholine on the network is rather complex, affecting not only the strength of lateral connections, but equally the excitatory connections within a column. It also affects the inhibitory drive within macaque V1, as most somatic muscarinic receptors are located on inhibitory interneurons (Disney et al., 2006b). Acetylcholine can also affect the M-current, and thus the membrane's spatial and temporal integration constant (for a review see (Lucas-Meunier et al., 2003)). Thus, even if scopolamine increases synaptic efficacy of lateral interactions, it may well be the case that it results in a reduced ability of neurons to integrate these inputs, due to increased membrane leakage, which then results in an overall reduction of flanker-induced facilitation. It would suggest that the scopolamine application effects in terms of integration ability override the effects in terms of input gain increase.

How can that be reconciled with a recent in-vivo study which has shown that ACh reduces the impact of stimuli presented in the non-classical receptive field, while increasing the effect of stimuli placed within the classical receptive field (Roberts et al., 2005)? The authors argued that this is testament for a reduced efficacy of lateral inputs, and increased efficacy of feedforward inputs. In line with the argument proposed above, it may actually show what the authors proposed, but also show a non-linear balance of integration properties vs. input efficacy.

While our results of reduced flanker-induced facilitation effects with scopolamine is not in line with our original hypothesis, our finding of modulation of flanker-induced suppression can be explained by the effects of muscarinic blockade in V1. Recent anatomical studies in V1 have shown that mAChRs are mainly expressed by inhibitory neurons, while excitatory neurons express them much more rarely (Disney et al., 2006a, Disney and Aoki, 2008). This means that blocking mAChRs as in our study, would reduce the excitability of the inhibitory neurons, such that contextual surround suppression would be less effective.

When nAChRs were blocked by mecamylamine the amount of flanker-induced facilitation remained unchanged. This was expected because reducing the efficacy of thalamic connections via nicotinic receptor blockade should not affect the flanker-induced facilitation which is either generated by intra-cortical mechanisms, likely involving local intra-areal interactions (Ichida et al., 2007), or feedback from higher areas as argued by Bair (Bair et al., 2003). This is in line with studies that found feedforward connections to not contribute to far-surround modulation (Dragoi and Sur, 2000). The amount of flanker-induced suppression was also unchanged when nicotinic receptors were blocked, contrary to muscarinic blockade that also reduced the flanker-induced suppression. We suggest that neurons that are suppressed by the flankers undergo less suppression if muscarinic receptors are blocked. This differential effect of muscarinic and nicotinic blockade could not be accounted by general drug effects (i.e., overall gain changes with scopolamine are smaller than with mecamylamine), as when this factor was factored out (figure 3.9) the effect still prevailed.

3.4.1. Differences with previous studies in the intact brain

Previous electrophysiological studies observing flanker-induced facilitation did not systematically test different wavelengths (as we did), but placed the flankers differently for each neuron depending on the extent of its summation area (Kapadia et al., 1995, Polat et al., 1998). Neurons with large summation areas were tested with flankers at long distances such that flankers did not elicit neuronal responses. In our study, flankers at the shorter distances (1 and 2λ) elicited responses while flankers at the longest distance (3λ) did generally not. This was done to replicate the psychophysical conditions where maximal perceptual facilitation was observed at the 3λ distance while suppression was observed at distances <3λ (Polat and Sagi, 1994). It could be argued that this distance is too small to find substantial facilitation, but that would contradict the psychophysical results (Polat and Sagi, 1992, 1993), and we also did not find any evidence for facilitation in the data set from the Amsterdam group in our recent publication (Pooresmaeili et al., 2010), where flankers were located at 3.5 and 4.2λ.

A second difference with previous studies is the range of contrast tested. The seminal studies which found flanker facilitation reported that the effect was restricted to low contrast target stimuli (Polat et al., 1998, Ichida et al., 2007). One may argue that we did not include enough sample points below the cell's contrast threshold. The contrasts tested in our study were 0%, 4%, 8%, 12%, 16%, 24%, 32% and 64%. This difference cannot account for the different results because of two reasons. 1) Most neurons in our population data showed no facilitation even at the lowest contrast levels tested. 2). The data set provided by our Amsterdam colleagues (Pooresmaeili et al., 2010) was obtained with lower contrast levels (0%, 3%, 6%, 4%, 6%, 9%, 14% and 20%) and again facilitation was very rare.

A third difference with previous studies is the location of the stimuli in the visual field. Although the electrophysiological studies (Polat et al., 1998, Kapadia et al., 2000) found flanker facilitation when the stimuli were at the periphery (2°-6°), the psychophysical studies reported weaker and more variable facilitation in the periphery compared to the fovea (Polat and Sagi, 1994). Our stimuli was also placed in the periphery (mean RF eccentricity was 3.25°, 5.6°, and 5.7° across monkeys). Another point is the level of cognitive involvement while performing the task. It is possible that flanker facilitation manifests only when subjects direct their attention to the target stimuli, as it is often the case in the psychophysical studies. In the present study, monkeys were passively fixating at a central spot while stimuli were placed at the periphery. However, this cannot account for the different results in the data set from the Amsterdam group (Pooresmaeili et al., 2010) monkeys had to make a saccade to the central target if it was present or to remain centrally fixating, it was absent.

3.4.2. Future directions

Iontophoretic application of cholinergic drugs could alter the RF size. For example, if scopolamine application increases the size of the RF, flankers placed at 3λ would no longer remain silent and would elicit neuronal responses. This was not directly tested in the present study because it requires mapping the RF size before, during and after drug application. This is too long a procedure which risks neuronal stability. Instead, we excluded neurons that changed their pattern of response to the flankers presented alone after drug application (see first column in fig 3.3 and 3.4). More recent studies have started to use annuli, rather than discrete flanking stimuli, to more uniformly stimulate the surround field (Ichida et al., 2007, Gieselmann and Thiele, 2008). Although these stimuli may be more appropriate to investigate centre-surround interactions, it is important to note that 1) the seminal studies used discrete Gabor patches and found facilitation (Polat et al., 1998) and 2) the perceptual facilitation has been reported before with both, discrete (Polat and Sagi, 1994) and whole field stimuli (Xing and Heeger, 2001). In addition to the type of stimuli used is its eccentricity in the visual field. Future electrophysiological studies could present the stimuli at the fovea (rather than at the periphery as we and others did), as this location could be more efficient in finding centre-surround facilitation.

Chapter 4. Contribution of cholinergic and GABAergic mechanisms to direction selectivity in macaque middle temporal area.

4.1. Introduction

In the previous 3 chapters, we have reported recordings from the primary visual cortex (area V1) of the awake macaque. To also determine the effects of cholinergic mechanisms to neuronal coding in extrastriate areas, I performed in this chapter additional investigations in motion selective area MT. The middle temporal area (MT) is the main hub for the analysis of direction of motion (Albright, 1984), and it is where all recordings reported in this chapter were made. We choose the anesthesized macaque because some aspects of neuronal coding can be equally well studied in passively viewing or anesthetized animals, as more trials can be obtained during a much shorter period of time. These aspects may still be of relevance to attentional processes. For example, previous reports have found that attention improves motion direction selectivity in MT by increasing responses to the optimal stimulus direction (Treue and Maunsell, 1996); i.e., attention changes the ratio of responses to preferred and anti-preferred directions of motion (see also (Motter, 1994)). More recent studies have argued that it proportionally scales all responses, provided only a single stimulus in the receptive field, and spatial (Martinez-Trujillo and Treue, 2004b) or feature-based (Treue and Martinez Trujillo, 1999) attention is employed. Moreover, others have demonstrated that response reliability is enhanced when attention is directed to the receptive field of V4 neurons (Mitchell et al., 2007). Thus, it is important to determine possible neuropharmacological bases of this attentional modulation. The aim here is to explore the cholinergic and GABAergic mechanisms underlying direction of motion tuning in MT.

GABA is an inhibitory neurotransmitter released from sources intrinsic to a local circuit within the cortex, while ACh is an excitatory neurotransmitter or a neuromodulator derived from extrinsic sources ((Katz and Frost, 1996) but see (von Engelhardt et al., 2007)). Previous work found that local inhibition is crucial to establish orientation/direction tuning in V1 neurons (Crook et al., 1997). In line with this finding, one study (Thiele et al., 2004b) tested the role of local inhibition in direction of motion tuning in MT by reducing intra-area inhibition through iontophoretic application of the GABAa antagonist bicuculline. In addition to being a potent GABAa receptor antagonist, bicuculline can be used to block Ca2+- activated potassium channels, which confounded the interpretation of the study by Thiele et al. (2004b) somewhat. Irrespective, their manipulation impaired the tuning of the neurons during the early response period, offering evidence of the important role of inhibitory mechanisms to establish direction selectivity in MT. An alternative to impair motion-direction selectivity computations is to try to boost them. This could be done through neuromodulators that are derived from extrinsic sources. One such neuromodulator is ACh that is synthesized in the NBM and released in the cortex (Pearson et al., 1983). The major effect of ACh on the response properties of neurons in the visual cortex is an increase in the response to receptive field stimulation without any decrement in selectivity (e.g. orientation tuning). In fact, in some V1 neurons iontophoretic application of ACh actually enhances stimulus response selectivity (Sato et al., 1987a, Murphy and Sillito, 1991, Sato et al., 1996), and spatial selectivity (Roberts et al., 2005), while reducing variability of spike occurrences within spike trains (Zinke et al., 2006).

These effects often occur without any significant change in the spontaneous activity of the cells (but see (Zinke et al., 2006)), which suggests that ACh increases the response specificity of neurons and does not simply act through disinhibition.

In this chapter I report experiments from area MT, while iontophoretically applying Gabazine (a GABAa antagonist more selective than the previously used bicuculline) and later ACh (or vice versa) in the same set of neurons. This manipulation allows direct comparison between cholinergic and GABAergic mechanisms, which may provide a better understanding of the cellular computations underlying motion-direction selectivity in MT. High levels of ACh in the extracellular space of MT neurons could alter the relative weight of feedforward and lateral synaptic input, and also alter the biophysical state of the neurons, possibly resulting in improved motion selectivity of single-cell responses. For this to happen ACh should be able to sharpen tuning curves by selectively increasing responses to optimal motion directions, similar to the effects of feature-based attention (Treue and Maunsell, 1999, Martinez-Trujillo and Treue, 2004a). The authors proposed a feature-similarity gain model, where attention increases responses to motion directions close to the neuron's preferred direction, while not modulating them to intermediate motion directions and suppressing them to antipreferred directions. Alternatively, ACh could scale all responses equally regardless of feature preference by simply adding a fixed factor (Thiele et al., 2009) or a multiplicative factor (Lee and Maunsell, 2010) in line with theories of general response elevation. If the first were true, we expect improved direction selectivity of MT neurons in our data set (i.e., a narrowing of the tuning curve). In contrast, if the latter were true, we expect a simple response scaling across all motion directions similar to that caused by general desinhibition (as it may be the case during Gabazine application).

4.2. Methods

General

All procedures were carried out in Bochum (Germany) in accordance with the Deutsche Tierschutzgesetz of 12 April 2001, the European Communities Council Directive 1986 (86/609/EEC), the US National Institutes of Health Guidelines for the Care and Use of Animals for Experimental Procedures, and the UK Animals Scientific Procedures Act. In the present investigation two adult macaques (*Macaca mulatta)* were used. One of them had previously been used for chronic recording in the awake state in unrelated investigations in the superior colliculus (SC). The animals were initially anaesthetized with ketamine hydrochloride (10 mg/kg i.m.). An intravenous. catheter was placed in the saphenous vein, the animals were intubated through the mouth and, after additional local anaesthesia with bupivacainhydrochloride 0.5% (Bupivacain^{R}), placed into a stereotaxic apparatus. During surgery they received additional doses of pentobarbital as needed. During the whole session the animals were artificially ventilated with nitrous oxide: oxygen at a 3:1 ratio containing 0.3–1% halothane. Heart rate, SPO_2, blood pressure, body temperature and endtidal CO_2 were monitored and kept at physiological levels. A craniotomy was performed according to stereotaxic coordinates to allow access to cortical area MT. Area MT was then localized electrophysiologically according to its stereotactic position and characteristic preference to stimulus movement. After all surgical procedures were completed the animals were paralyzed with 0.1mg/kg/h of vecuroniumbromide (Norcuron®). For details about histological procedures

at the end of the experiments see (Distler and Hoffmann, 2001). All histological verification of recording sites was done by Dr. Distler in Bochum, and I thus will not include the details here, as it is none of my work.

Visual Stimulation

Initially, the receptive field (RF) of each neuron was mapped by moving a bar across the screen and determining the borders beyond which no response could be elicited. Thereafter, direction selectivity was determined by presenting sine wave gratings (4 Hz, 0.5 cycles per degree, on a cathode ray tube at 1600*1200 pixels at 110 Hz) moving along twelve different directions within a circular aperture of a size that ensured strong responses were elicited when a preferred direction was presented. For the first 300 ms of each trial, the screen was homogenously gray (21 cd/m^2); thereafter, the moving stimulus was presented for 760 ms. Stimulus presentation and data acquisition were under the control of Remote Cortex 5.95 (Laboratory of Neuropsychology, National Institute for Mental Health, Bethesda) interlinked with Cheetah (Neuralynx). Spike waveforms were sampled at 30 kHz.

Recordings and drug application

Recordings were performed with tungsten-in-glass electrodes flanked by two pipettes (Thiele et al., 2006). One pipette was filled with acetylcholine and the other with gabazine which were iontophoretically applied (NeuroPhore BH-2, Digitimer, Welwyn Garden City, Hertfordshire, England). Pipette opening diameter varied between 1-4 µm. Pipette resistance varied between 10 -150 MΩ, with most recordings (>90%) at 20-80 MΩ. Hold currents during control and recovery were usually -10 nA, in rare occasions (when the pipette resistance was 10-20 MΩ) it was -40 nA. Pipette-electrode combinations were inserted into MT without the use of guide tubes. The integrity of the electrode and the pipettes were checked under the microscope before and after the recording sessions, in addition to measurements of the pipette impedance made before and after the recording at each recording site. All drugs were obtained from Sigma. The details regarding drug concentration, pH and application current were: Acetylcholine -- 0.1M, pH 4.5, application current 5-50 nA, with most recordings at 5-20 nA; Gabazine-- 3mM, pH 3, application current 5-40 nA, with most recordings at 5-20 nA. We initially recorded the neuronal activity in the absence of ACh (~5min), followed by one recording in the presence of ACh (~5min), followed by one to two recordings after a 5min waiting period (as recovery usually occurs with a slight delay). If the activity was still stable, we continued recording in the presence of gabazine and later on in its absence. We randomly alternated the order of the drug that was applied first. We regularly compensated for the change in current during the ejection condition by increasing the hold current of one of the two pipettes, thereby keeping the overall current identical between the 'hold' and 'eject' conditions.

Data Analysis

We tested whether drug application (drug vs. no-drug), motion direction (12 directions), and contrast (25% vs. 13%) significantly affected neuronal activity (three-factor ANOVA, $p<0.05$). Neurons were analysed further if drug application and motion direction significantly affected firing rates. Activity drifts were examined by comparing single trial spike counts between the initial control and the recovery measurement separately for

each stimulus condition, as well as for the spontaneous activity. If cells did not show recovery from drug application they were excluded from further analysis. We tested for drug effects by comparing spike counts during recordings when ACh/Gabazine was applied with combined data from control recordings. We determined the preferred direction (PD) of motion for each neuron within a time period of 50–760 ms after stimulus onset, and the activity for motion in the antipreferred direction (the direction of motion opposite to the PD), and calculated the direction index [DI = 1 - (activity in antipreferred direction) / (activity in preferred direction), baseline activity subtracted]. Only neurons with a DI > 0.5 were included for further analysis. To see the evolution of the DI with time, we calculated DI across 3 time windows (0-50ms, 50-200ms and 200-760 ms from response onset). Additionally, a time-resolved DI was calculated as follows: for each neuron we calculated its averaged activity to the preferred direction (PD) and opposed direction (OD) across different drug and contrast conditions, smoothed this activity with a Gaussian to obtain (8) PSTHs, and normalized these PSTHs by the maximum of all of them (often maximum was at 25% contrast and drug-applied condition). Then we calculated the neuron's DI as [DI = 1 - (PSTH in anti-preferred direction)/ (PSTH in preferred direction)].

We calculated the tuning width by fitting a wrapped Gaussian function (Swindale, 1998) to the mean response of each motion direction (least-square fitting; (Press and Teukolsky, 1997):

$$G(\theta) = B + A \sum_{n=-5}^{n=5} exp \sum \left(\frac{-(\theta - \rho + 180n)^2}{2\sigma^2} \right)$$

where $G(\theta)$ is the predicted response given the motion direction (θ), A is the tuning amplitude, σ the bandwidth, ρ the centre location (the predicted preferred motion direction), and B the offset. Bandwidth was reported as full width at half-height (FWHH). Only neurons with >50% of variance accounted for between actual and fitted values were considered for further analysis. A signed rank-test was used to determine whether any of these tuning parameters were significantly influenced by drug application.

Neuronal response latency was calculated at a resolution of 5 ms for motion in PD in the presence and absence of drugs (for details of latency analysis see (Maunsell and Gibson, 1992). To assess the regularity of spike timing within individual trials the coefficient of variation (CV) for the interspike-intervals (ISI) distribution was calculated as the standard deviation of the ISI-distribution divided by its mean (Softky & Koch, 1993; Liu & Wang, 2001). A very regular firing pattern results in a sharp peak of the ISI-distribution and a CV towards 0, whereas irregular firing pattern result in a broader ISI distribution and large CVs. To test whether the application of ACh/Gabazine showed a systematic effect on the trial-to-trial response reliability we calculated the Fano factor (F), the ratio of spike count variance to mean spike count. We computed the Fano factor when ACh/Gabazine was applied and when it was not applied over the whole (0–760 ms after response onset), the early (0–200 ms), and the late (200–760 ms) response time windows. We also tested whether the drugs affected F and CV more in some directions than others; responses to the 7 opposed non-preferred directions were pooled and compared to responses against the PD. This manipulation naturally increases the

variance for the pooled responses, but the comparison across drugs is still possible (i.e., ACh may increase spiking regularity for the PD more than Gabazine).

4.3. Results

We recorded MT responses to sine-wave gratings (25% and 13% luminance contrast) moving in twelve different motion directions when ACh or Gabazine was iontophoretically applied near the recorded neuron and when it was not applied. A total of 188 neurons were recorded (108 with Gabazine and 80 with ACh). The latencies (median value) in the absence of drugs were 93 ms (25% contrast) and 114 ms (13% contrast). In the presence of ACh latencies were very similar to those in control condition (88.7 ms at 25% contrast, and 113 ms at 13% contrast, $p>0.4$ both, signed rank test), as well as in the presence of Gabazine (89.7ms for 25% contrast, and 115 ms for 13% contrast, $p>0.4$ both, signed rank test). Analysis windows were aligned to response latency, rather than stimulus onset. From the Gabazine population 73/108 showed a significant effect of the drug on the firing rate (three-factor ANOVA, drug factor, $p<0.05$). From the ACh population 51/80 showed a significant effect of ACh ($p<0.05$). For all 123 (73+51) cells, we found a significant effect of Gabazine/ACh application on spontaneous and or stimulus-induced firing rate (3-way ANOVA), which returned to baseline after recovery. All 123 cells showed a significant effect of motion direction (three-factor ANOVA, motion direction factor, $p<0.05$), however we discarded 8 cells (4 tested with Gabazine and 4 with ACh) that did not show a DI>0.5 (see methods) given that the focus of this paper is on direction selective cells.

4.3.1. Effect of acetylcholine and gabazine on tuning curves

Of the 69 cells that were significantly affected by Gabazine application and showed a DI>0.5, 64 (92.75%) exhibited an increase of their response, while for 5 (7.2%) cells the response was reduced. Very similar effects were seen upon ACh application with 42 cells (89.4%) showing increase and 5 (10.6%), decrease. We focused on the neurons that showed enhanced response as this was the main effect observed across the population. As seen in Fig. 4.1a, Gabazine increased the stimulus-driven (and spontaneous) activity of an example neuron that preferred motion to the lower right. This effect was reflected in the amplitude of the tuning curve (see central plots) and in its baseline. Importantly, the effect of Gabazine was not confined to the preferred direction (PD). Rather, it affected several directions near the PD resulting in decreased direction selectivity, as reflected in the broadening of the tuning curve ($FWHH_{Gabazine}=42.9$, $FWHH_{noGab}=31.7$). Application of ACh in another example cell (Fig 4.1b) also increased the stimulus-driven (and spontaneous) activity but this increase did not result on impaired direction selectivity; the FWHH of the tuning curve was reduced upon ACh-applied compared to the control condition ($FWHH_{ACh}=62.6$, $FWHH_{noACh}= 67.9$).

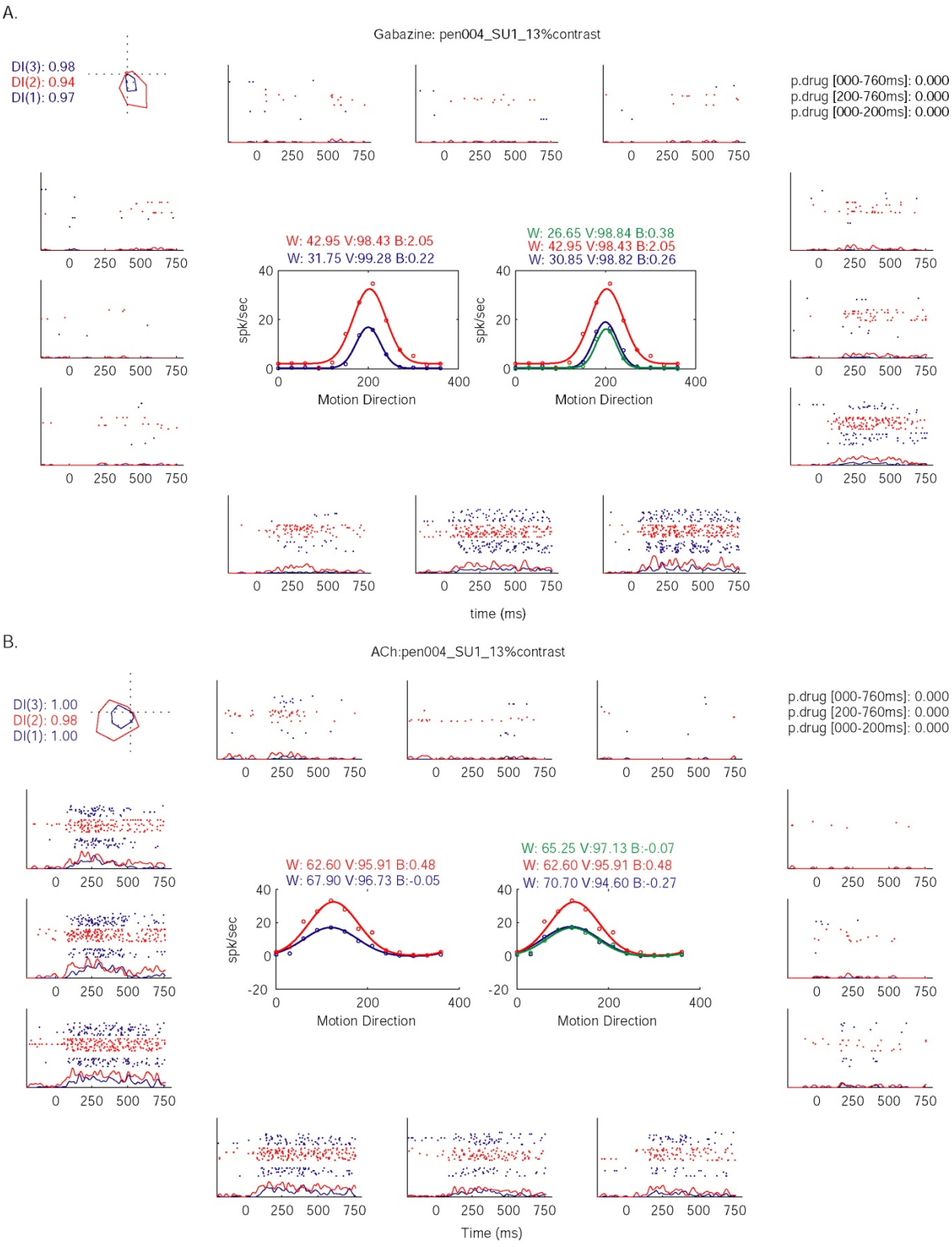

Figure 4.1. Effects of Gabazine and ACh in motion direction tuning in two example neurons. (A) Single-cell raster plots and histograms showing neuronal activity before application of Gabazine (blue), during application (red), and during recovery (blue top). Central plots show the tuning curves to the 12 motion directions during these three drug states (right), and when the baseline and recovery periods are averaged (left). Gabazine increased the response of the neuron and the FWHH of the tuning curve. Polar plot (top left) shows the directionality preference of the neuron during drug and control conditions. (*B*) Neuronal activity during application of acetylcholine. ACh

increased the response of the neuron but the FWHH of the tuning curve was reduced. Polar plot (top left) shows the directionality preference of the neuron during drug and control conditions.

Figure 4.2 shows these population activities measured in the absence and presence of Gabazine (n=64) and ACh (n=42). Gabazine application (fig 4.2a) increased the three parameters of the tuning curve, resulting in larger width ($FWHH_{gab}$ = 58.2, $FWHH_{no\_gab}$ = 52.4; p<0.01, signed rank test), larger amplitude (Amp_{gab}= 30.7; Amp_{no_gab}= 19.3; p<0.001, signed rank test), and larger baseline (Bas_{gab}=6.2 ; Bas_{no_gab} =2; p<0.001, signed rank test). In contrast, ACh did not significantly increase the width of the tuning function ($FWHH_{ach}$=49.3, W_{no_ach} = 48.2, p=0.314, signed rank test), although it increased its amplitude (A_{ach}=27.9, A_{no_ach} = 20.9, p<0.001, signed rank test) and its baseline (B_{ach}=5.2, B_{no_ach} = 1.7, p<0.001, signed rank test). These effects correspond to the 25 % stimulus contrast, but similar effects were observed for the 13 % stimulus contrast (fig2a right and Table 1). The population results for these 3 parameters are shown in the scatter plots of figure 2b (gabazine) and figure 2c (ACh).

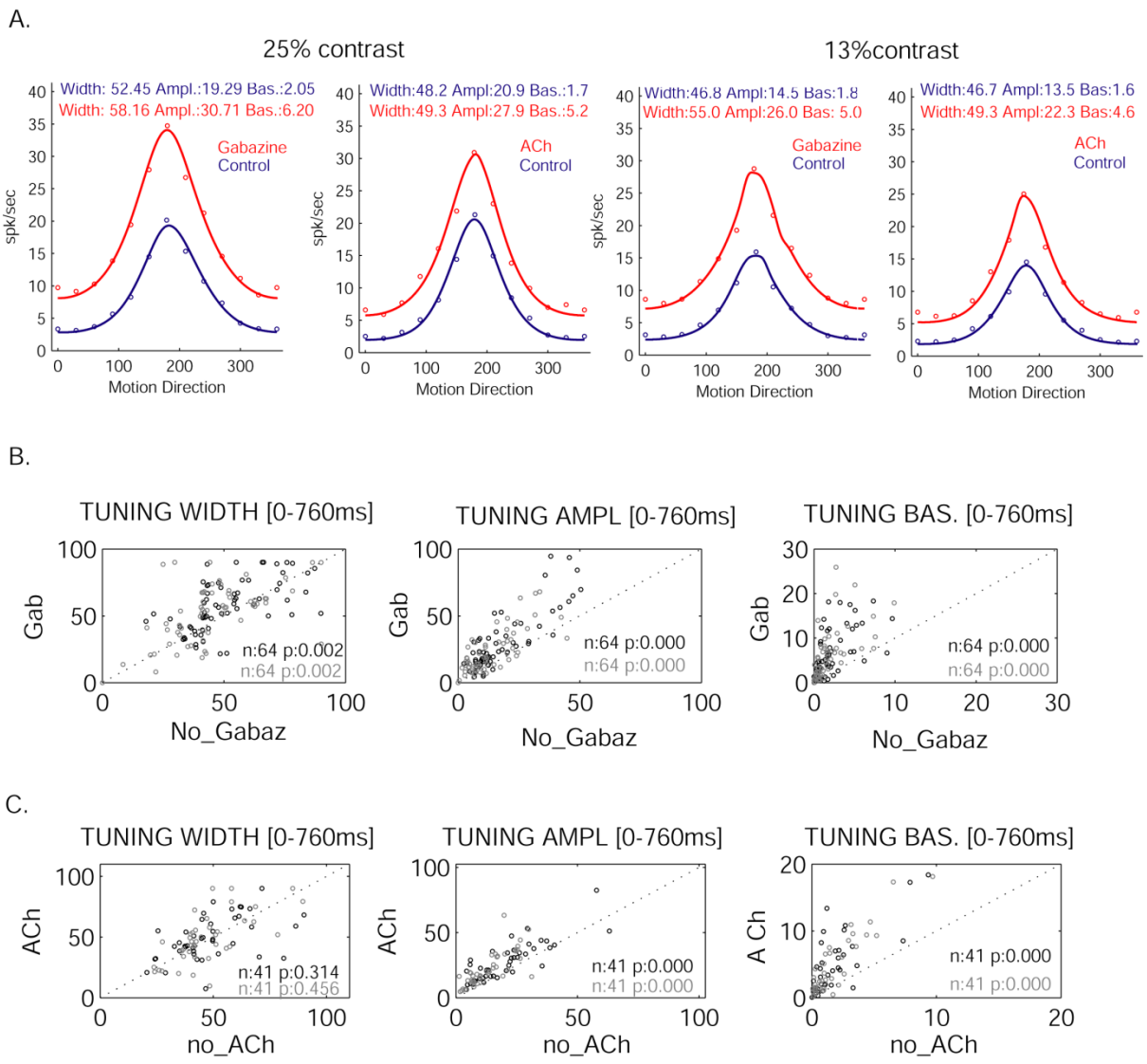

Figure 4.2. Effects of Gabazine and ACh on motion direction tuning at the population level. (A) Motion direction tuning curves (averaged across the population data) during control and drug conditions for Gabors of different contrast levels. Gabazine application increased the three tuning parameters (FWHH, amplitude, and baseline), while ACh did not significantly increase the width. B) Population tuning parameters during Gabazine and control conditions (black dots, 25% contrast; grey dots, 13% contrast). C) Population tuning parameters during ACh and control conditions.

Table4.1: Summary of Gabazine and ACh effects on motion direction tuning across different stimulus contrasts (population data).

Condition	Contrast	FWHH	Amplitude	Baseline
Gabazine vs. Control	25%	58.16 vs. 52.45; p<0.001	30.71 vs. 19.29; p<0.001	6.20 vs. 2.05; p<0.001
	13%	55.00 vs. 46.80, p<0.001	26.00 vs. 14.50; p<0.001	5.00 vs. 1.80; p<0.001
ACh vs. Control	25%	49.30 vs. 48.20, p>.1	27.90 vs. 20.90; p<0.001	5.20 vs. 1.70; p<0.001
	13%	49.30 vs. 46.70; p>.1	22.30 vs. 13.50; p<0.001	4.60 vs. 1.60; p<0.001

4.3.2. Effect of acetylcholine and gabazine on spiking regularity

These findings reported above imply that, in a subset of neurons tested with Gabazine, directional tuning is substantially shaped by inhibition mediated through $GABA_A$ from within MT. However we did not see a consistent effect of ACh (i.e., improved direction selectivity) across the population; some neurons showed smaller tuning width (see fig 4.1b), while others larger. However, ACh effects could result on improve spiking regularity rather than tuning width modulation. Previous studies have shown that ACh improves the spiking regularity within a trial (CV). This effect, if present in the spikes to the PD and not in the spikes to the other non optimal directions, could be interpreted as improved selectivity. Figure 4.3a shows that the ISI distribution became sharper upon ACh application (mean 25% contrast: CV_{Ach}=1.25, CV_{no_Ach}=1.34, p=0.006, signed rank test; mean 13% contrast: CV_{Ach}=1.29, CV_{no_Ach}=1.34, p<0.056, signed rank test) and that this effect only occurred in the PD; responses to the 7 opposed non-preferred directions did not show increased spiking reliability (both p>0.1, signed rank test). In contrast, the ISI distribution upon Gabazine application became less sharp (mean 25% contrast: CV_{Gab}=1.48, $CV_{no\_Gabazine}$=1.27, p<0.001, signed rank test; mean 13% contrast: CV_{Gab}=1.57, $CV_{no\_Gabazine}$=1.29, p<0.001, signed rank test), an effect that was not limited to the PD (figure 3b). This result implies that the spiking regularity within a trial is modulated differentially by ACh and Gabazine. The GABAergic modulator has a detrimental effect, not specific to the preferred direction, while the cholinergic modulator has a beneficial effect whereby the spiking reliability of the responses in the PD is increased.

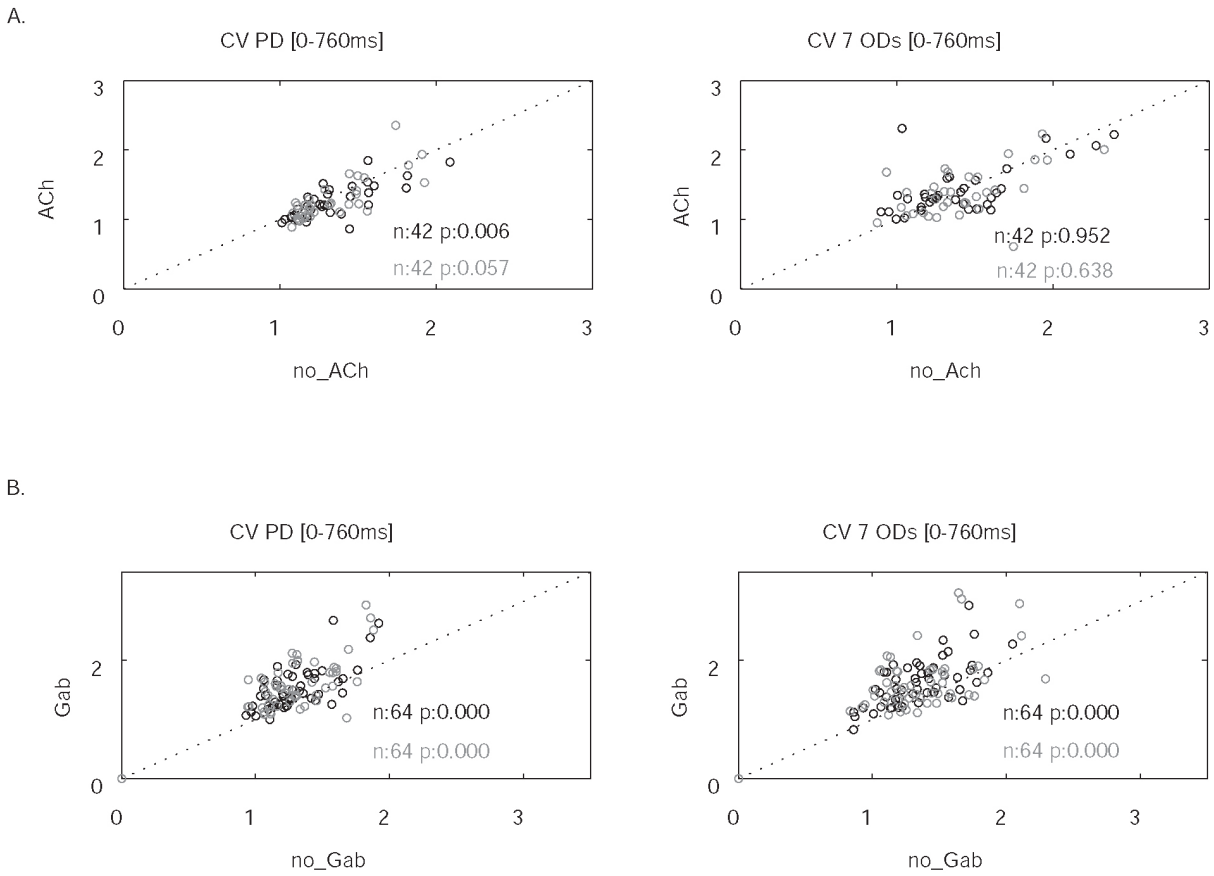

Figure 4.3. ACh and Gabazine application affect differently the coefficient of variation (CV). (A) CV under control and ACh-applied conditions for the preferred direction of motion (left) and the seven opposed directions. ACh reduced the CV only for responses to the preferred direction. (C) Same as B except that for Gabazine. Note the larger CVs when Gabazine is applied for responses to both preferred and non-preferred directions.

Figure 4.4 shows the Fano factor, i.e. the trial-to-trial response reliability. Similar to the inter-trial reliability shown in figure 4.3, ACh reduced the Fano factor among the PD trials but not among the OD trials (fig 4.4a). This effect was significant in the late response period (200-760ms after the response onset) for the 25% contrast stimulus (p=0.033, signed-rank test) and nearly significant for the 13% contrast (p=0.078). In the early period (0-200ms), the effect was not significant for any stimulus (p=0.347 and p=0.183 for 25% and 13% stimulus contrasts, signed-rank test). This means that ACh only reduced the Fano factor among trials of PD during the late response period. Gabazine, in contrast, did not affect the Fano factor among PD trials, but increased it among trials of ODs (fig 4.4b).

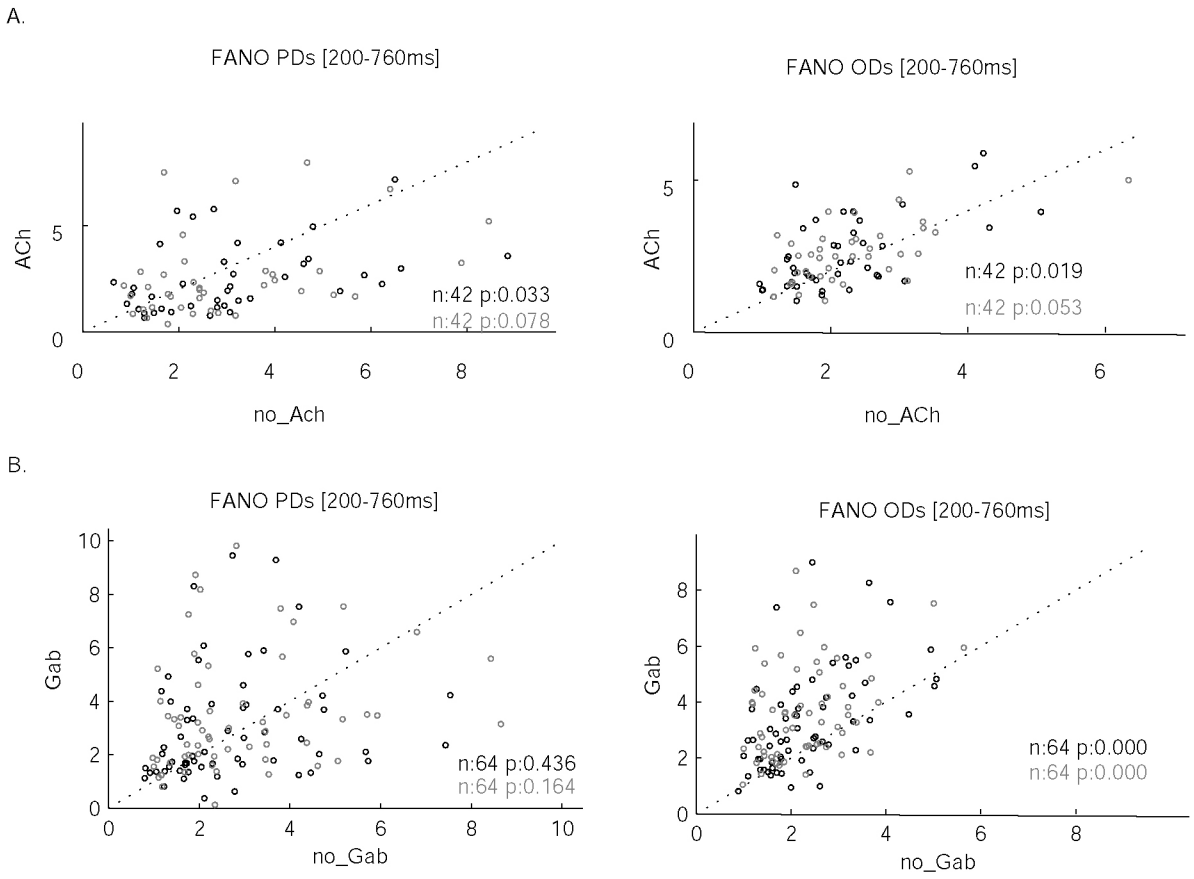

Figure 4.4. ACh and Gabazine application have different effects on the FANO factor. (A) Fano factor under control and ACh-applied conditions for the preferred direction of motion (left) and the seven opposed directions (right). Preferred direction responses showed reduced fano factor when ACh was applied, while an opposite trend is observed in the responses to the opposed directions. (B) Same as A except that Gabazine was applied. Even though Gabazine had no effect on the fano factor for preferred direction responses (left), it caused a strong increased for ODs responses.

4.3.3. Effect of acetylcholine and gabazine on preferred and opposed motion directions

To compare our results with a previous study (Thiele et al., 2004c), we also calculated motion direction selectivity indexes (DIs) based on the response ratio between PD and OD. Figure 4.5 shows the average PSTH for the population of neurons tested in the presence and absence of Gabazine (top) and ACh (bottom). While Gabazine (top) increased the response to both PD and OD, ACh (bottom) mostly increased the response to PD. A time-resolved analysis, showing the evolution of the selectivity (DIs), showed that these effects applied to the whole response period.

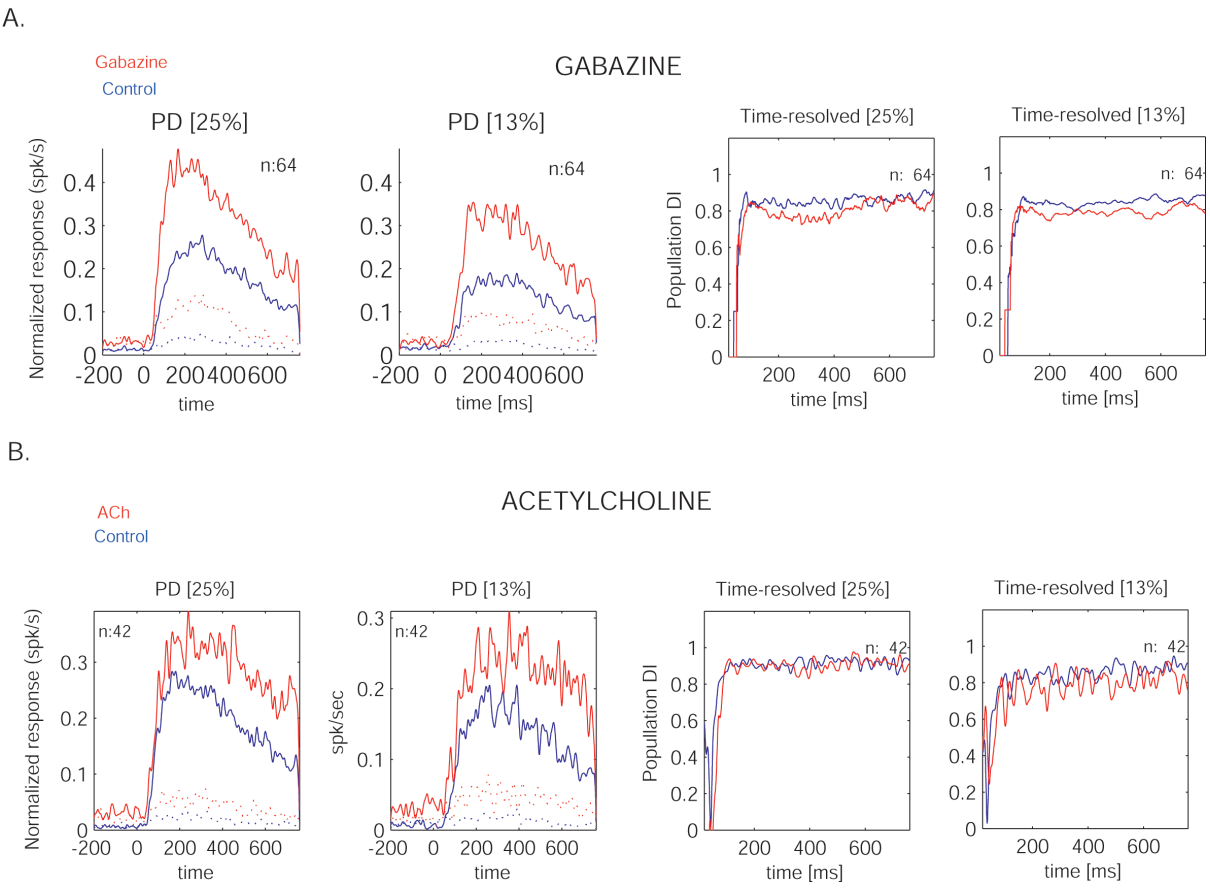

Figure 4.5. Effect of Gabazine and ACh on neuronal responses to preferred and opposed direction of motion. A. (Left) Averaged PSTH (n=64) for neurons recorded in the absence (blue) and presence (red) of Gabazine at 25% and 13% luminance contrast. Responses to the PD are shown in full lines, responses to the OD in dotted lines. (Right) Time resolved analysis of DIs (mean values). Gabazine increased the gain to PD and OD, and reduced the DIs slightly along most of the response period. B. (Left) Average psth (n=42) in the absence (blue) and presence (red) of ACh at 25% and 13% luminance contrast. (Right) Time resolved analysis of DIs. ACh mostly increased the gain to PD, and did not change the DIs at any time window.

We quantified the effect of Gabazine/ACh on the DIs across three different time windows (0-50, 50-200, and 200-760ms after response onset). Figure 4.6 shows the outcome of this analysis. Gabazine reduced DIs consistently across stimuli and time windows. Only the earliest response time window (0-50ms) for the lowest contrast tested (13%) showed no reduced DI. In contrast, ACh reduced DIs only in a few instances (i.e., only for the highest contrast stimuli tested and only for the late time windows).

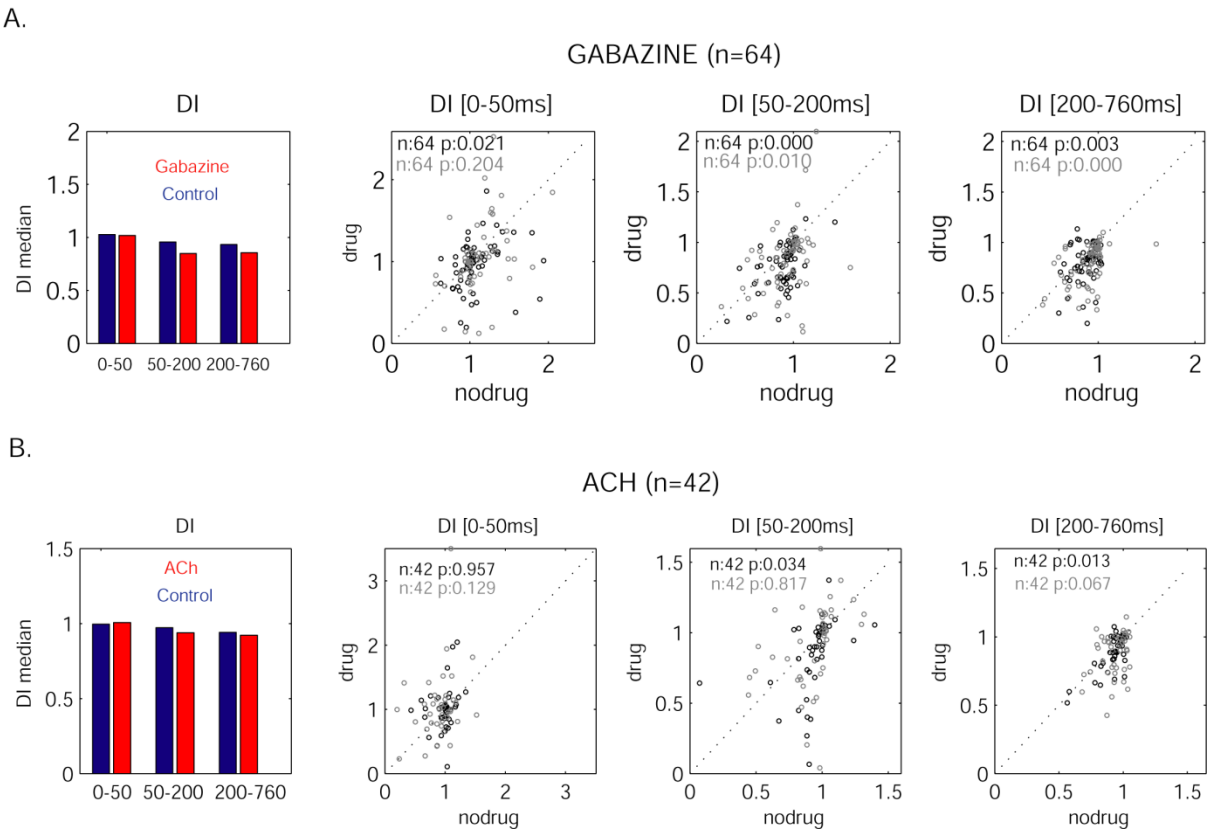

Figure 4.6. Effect of Gabazine and ACh on DIs across time. A. (Left) DIs median (n=64) for neurons recorded in the absence (blue) and presence (red) of Gabazine averaged across 25% and 13% luminance contrast stimuli. (Right) Scatter plots show the distribution of DIs for each neuron in three time windows (0-50, 50-200, and 200-760) in the absence (x axis) or presence (y axis) of Gabazine. Gabazine reduced DIs in all conditions but one. B. (Left) Same but for ACh (n=42) for neurons recorded in the absence (blue) and presence (red) of ACh at 25% and 13% luminance contrast. (Right) Time resolved analysis of DIs. ACh mostly increased the gain to PD, and did not change the DIs at any time window.

4.4. Discussion

Both ACh and Gabazine elicited increased firing rates of neurons in MT. However, ACh had no systematic effect on the width of the motion-direction tuning curve (i.e., ACh sharpened the tuning in some neurons but widened it in others). In contrast, Gabazine increased the width of the tuning function in the majority of neurons tested. This result provides evidence that neurons in MT use GABA as a local inhibitory mechanism of direction selectivity, and is in line with previous studies in areas 17/18 of the anesthetized cat that found broadening of orientation tuning and/or changes in directionality by GABA microiontophoresis (Eysel et al., 1988,1990; Crook & Eysel, 1992; Crook et al., 1991, *1992a,b,* 1996 (Crook et al., 1997). Biological models in the primary visual cortex have repeatedly demonstrated the importance of inhibitory interactions in the emergence of directional selectivity (Sillito, 1977, Sato et al., 1995, Crook et al., 1998, Murthy and Humphrey, 1999, Roerig and Kao, 1999). Based on the directionally selective input that V1 (layers 4b and 6) provides to V5/MT in the macaque, it was argued that neurons in area MT inherit their direction selectivity from neurons in areas V1, V2, and V3 (Movshon and Newsome, 1996). Contrary to this idea, Thiele and collaborators recently demonstrated that a large fraction of MT cells generate directional selectivity de novo (Thiele et al., 2004a). The authors blocked GABAa receptors by BMI iontophoresis, and found that for a large proportion of

cells only direction selectivity during the initial response period (first 100 ms) was abolished while it was preserved in later response periods. This means that a portion of MT neurons generated direction selectivity de novo (i.e., if direction selectivity would have been inherited from earlier areas it would have also been present in the early part of the response). Gabazine application in our experiments resulted in reduced direction selectivity during the whole response period, but overall the effects found here were somewhat smaller than those reported in Thiele et al.'s (2004) study. Note also that a higher contrast stimulus (100%) was used in their study, which is not ideal for testing the effect of BMI, as neuronal responses in the absence of drug may already been saturated. When the authors tested lower stimulus contrasts, they found very similar results as we did (see their Figure 4). Recently, there has been some controversy about the use of bicuculline as a neurotransmitter antagonist in in-vivo experiments, as high levels of Mg2+ in the slice have been found to 1) prolong epileptiform discharges, 2) increase the amplitude of their field potential DC shifts, and 3) augment the concomitant decreases in Ca2+ and increases in K+ that accompany the event (Avoli et al., 1995, Avoli et al., 1997). Thus, it is not a clean selective antagonist. This problem was circumvented by using Gabazine in the current study.

Contrary to previous studies (Sillito and Kemp, 1983, Sato et al., 1987a, Murphy and Sillito, 1991, Sato et al., 1996), we did not find a facilitatory effect of ACh in sharpening tuning curves (i.e., some neurons increased their directional selectivity while others reduced it). We found that ACh may contribute positively to motion-direction selectivity in MT by reducing the variability between spike times within trials. More importantly, this effect was restricted to the preferred motion direction (PD): ACh reduced the coefficient of variation (CV) only in the responses to the PD. Opposed directions (ODs) were unchanged by the drug. In contrast, Gabazine increased the CV in the responses to all directions. These effects cannot be explained by differences in firing rates because both ACh and Gabazine increased firing rates equally. A possible shortfall of the analysis presented here comes however from the definition of ODs. The 7 motion directions opposed to the PD were taken for this analysis. Because some neurons do not elicit spikes in response to the direction of motion 180° away from it (main OD), we pooled responses from several ODs. This manipulation allowed us to perform this analysis, as a certain number of interspike intervals are necessary, but it can artificially increase variability across spike times because responses to various orientations are pooled. However, we notice that this artefact should affect both drugs equally. In addition to the beneficial effect of ACh on the CV, ACh also reduced the FANO factor (i.e., the variability of firing rates across trials). Importantly, this effect was also restricted to the PD while ODs showed an opposed effect whereby ACh decreased response reliability. The effect of reduced variability in responses to the PD was restricted to the late response period (200-760ms). Importantly, Gabazine decreased response reliability across all directions of motion equally, and across early and late time periods.

The effects of ACh reported here are thus at least of some relevance to attentional processes, as previous studies in V4 (Mitchell et al., 2007, 2009) have observed increased response reliability with attention. Other studies in V1 found that ACh did not sharpen orientation/direction tuning curves. Instead, it improved their response variability (Sato et al., 1987b, Zinke et al., 2006) and signal-to-noise ratio (Sato et al., 1987b).

But the authors did not analyse whether the improved response variability was restricted to the optimal stimulus, as we did in our study, which would provide direct evidence for increased selectivity.

4.5. Conclusion

We demonstrated that directional selectivity in MT is at least somewhat sculpted by intrareal inhibitory process. Acetylcholine, by itself does not affect the directional tuning, but proportionally scales direction selective responses, reminiscent of reported multiplicative attentional effects. Moreover, it reduces variance of firing rates for the preferred direction and increases spike time regularity (reduced interspike interval variance), two factors that may equally contribute to attentional modulation in awake animals.

GENERAL DISCUSSION

As reviewed in the previous chapters, attention can aid perception and detection of visual stimuli, (Colegate et al., 1973, Eriksen and Hoffman, 1973, Sperling, 1979, Posner et al., 1980), and at the neuronal level this is reflected by increased activity of neurons representing the attended object or feature (Moran and Desimone, 1985, Spitzer et al., 1988, Motter, 1993, Desimone and Duncan, 1995), by altered basic neural integration properties, including receptive field size or location (Moran and Desimone, 1985, Connor et al., 1997, Luck et al., 1997a, Connor, 2006, Roberts et al., 2007). Additionally, attention can improve response fidelity (Mitchell et al., 2007), as well as modulate synchronous activity of neuronal assemblies (Fries et al., 2001, Chalk et al., 2010). It is generally assumed that higher areas of the visual, parietal and frontal cortices control the selection of relevant visual information (Moran and Desimone, 1985, Spitzer et al., 1988, Motter, 1993, Desimone and Duncan, 1995). By sending a feedback signal to the earlier visual areas, the higher areas (e.g., FEF, anteriorIPs, posteriorIPs) aid the integration of incoming visual information in the earlier areas (Corbetta and Shulman, 2002, Serences and Boynton, 2007, Serences and Yantis, 2007). These studies provide ample evidence that preparatory attention to stimuli can facilitate perception under different experimental tasks. However, the cellular mechanisms underlying this response modulation are not clear. This thesis investigates which neurotransmitters and receptors contribute to attentional modulation in the primate brain.

We focus on two neurotransmitter systems, the glutamatergic and the cholinergic. Many studies have demonstrated that ACh and glutamate release in the cortex contribute to general arousal states (Mitchell, 1963, Kanai and Szerb, 1965, Szerb, 1967, Phillis, 1968, Gioanni et al., 1999, Lambe et al., 2003). Only recent work, including this thesis, has shown that they can have a more specific role in cognition. ACh can particularly influence cortical plasticity (Juliano et al., 1991, Brocher et al., 1992), learning (Yu and Dayan, 2002, Rokem and Silver, 2010), memory (Hasselmo and Stern, 2006) , and attention (Voytko et al., 1994, Sarter et al., 2005, Herrero et al., 2008, Hasselmo and Sarter, 2010). For example, after depleting the medial prefrontal cortex (mPFC) from normal ACh efflux, persistent attentional impairments were found in rodents performing a five-choice serial reaction time task ((McGaughy et al., 2002); see also (Fournier et al., 2004, Nelson et al., 2005, Sarter et al., 2005)). Attentional deficits in humans also point to an important role of ACh (Robbins, 2005, Furey et al., 2008). In-vitro studies showed that ACh selectively suppresses the efficacy of intracortical synapses by activating muscarinic receptors located at their terminals (Kimura and Baughman, 1997), while boosting the efficacy of the feed-forward/thalamocortical synapses through nicotinic receptors activation (Lavine et al. 1997; Prusky et al. 1987; Sahin et al. 1992; Gil et al. 1997). This means that ACh controls the synaptic efficacy of feed-forward and intracortical synapses, shifting their balance in favour of feed-forward (Hasselmo,1995; Hasselmo and Bower 1992, 1993; Kimura 2000; Kimura et al. 1999; Linster and Hasselmo 2001).

The precise nature of the contribution of ACh to attentional modulation in the cortex is at present unclear. Chapter 1 addressed this issue using pharmacological manipulations (Thiele et al., 2006) on neurons in the primary visual cortex (V1) while monkeys perform a visual spatial attention task. In macaques, the

neocortex receives its main cholinergic innervations from the nucleus basalis of Meynert (NBM) (Pearson et al., 1983). We took advantage of the anatomical studies that quantified cholinergic receptors in visual areas. In macaque V1, muscarinic AChRs primarily the m1 and m2 subtypes (Tigges et al., 1997) and nicotinic AChRs (Han et al., 2000) are expressed at significant levels. Most muscarinic AChRs are located on the soma of inhibitory interneurons (Disney et al., 2006b). In cat area 17, nicotinic receptors were often located presynaptically on thalamic axons arriving in layer IV (Prusky et al., 1987a, Parkinson et al., 1988, Wonnacott, 1997). In the rat visual (and somatosensory) cortex, nicotinic sites were also concentrated in layer IV, while muscarinic receptors were mostly located in superficial and deep layers (Gil, 1997, Kimura and Baughman, 1997). In addition, nicotinic AChRs mediate rapid channel opening and desensitization which make them adequate for short-term neuronal signalling (Cockcroft et al., 1990) (but see (Prusky et al., 1987a), while muscarinic AChRs have slower kinetics.

In line with these studies, we note that increased amounts of ACh in V1 of the awake macaque should strengthen synaptic efficacy and the biophysical state of the neurons (i.e. spatial and temporal integration properties of the neuron's membrane). Whether these effects interact with attentional modulation (and stimulus parameters), or are independent phenomena only contributing to general arousal states, is investigated in Chapter 1. Recent in-vitro and in-vivo studies have shown that ACh reduces the spread of excitation: it reduces the spread of membrane voltage fluctuations (Kimura et al., 1999), and the spread of BOLD activation (Silver et al., 2008). Recent work from Thiele's lab showed that iontophoretic application of ACh in V1 of the anesthetized marmoset reduced the classical receptive field summation area of the neurons (Roberts et al., 2005), and a separate study resulted in a strikingly similar effect when attention rather than ACh was employed (i.e., attention reduced spatial integration of V1 neurons (Roberts et al., 2007). Chapter 1 demonstrates the direct link between ACh function and attentional modulation at the cellular level. We investigated which neurotransmitters and receptors contribute to attentional modulation in the primate brain, and found that muscarinic cholinergic mechanisms play a central part in mediating the effects of attention in V1.

However, attention is (also, if not mostly) assumed to be transferred by top-down inputs from higher areas (Moran and Desimone, 1985, Spitzer et al., 1988, Motter, 1993, Desimone and Duncan, 1995, Moore and Fallah, 2004), and these inputs are mostly excitatory driving pyramidal neurons through glutamatergic receptors (Vidal and Changeux, 1993, Johnson and Burkhalter, 1996, Shao and Burkhalter, 1996, Gioanni et al., 1999). While this is undisputed, our data in Chapter 1 showed the important role of muscarinic receptors (Herrero et al., 2008), suggesting an involvement of cholinergic inputs from the basal forebrain (Szerb, 1967). One scenario is that the higher cortical areas involved in spatial delayed-reaction tasks (e.g., PFC) influence sensory areas indirectly, through connections to cholinergic neurons in the basal forebrain (BF) that have ascending projections to sensory areas (Russchen et al., 1985, Sarter et al., 2005). We showed evidences to suggest that this alternative route (Frontal cortex –> BF –> Visual cortex) is not only mediating general arousal states but also selection of visual information. But there is a main caveat to this scenario. In rodents, the PFC (the presumed homolog of the primate DLPFC) is crucial for spatial delayed-reaction tasks similar to the one used in our paradigm. However, recent studies in primates have shown that the DLPFC does not provide input

to the BF (Preuss, 1995). Inputs to the BF are rather widespread in the frontal lobe, but are restricted to medial and orbital frontal areas, which have less of a role in delayed spatial attention tasks.

Although it is likely that in the primate medial and orbital frontal areas influence sensory areas through connections to cholinergic neurons in the basal forebrain (BF), intracortical sources cannot be excluded (Levey et al., 1984, Houser et al., 1985, von Engelhardt et al., 2007). The latter authors found intracortical bipolar cholinergic neurons in the rodent (layer 2-3). This finding needs to be replicated in the primate, however, it is interesting to note that cortical bipolar cholinergic interneurons have restricted columnar organization and may then be ideally suited to modulate locally cortical activity (von Engelhardt et al., 2007). Despite this local source of cholinergic input to cortical neurons, the main cholinergic input to the cortex has its origin in the BF, with the NBM constituting the principal source (Mesulam et al., 1983). BF neurons innervate large cortical areas (Miettinen et al., 2002), and this coarseness may be incompatible with the highly localized and fast effects of spatial attention. But this could be accounted for by a scenario, where adequate cholinergic drive enables feedback from higher cortical areas to exert its influence, and likewise mediate attentional modulation. This raises the question of which non-cholinergic mechanisms are contributing to attentional modulation.

In chapter 2 we addressed this question. We probed the possibility that NMDA receptor activation contributes to attentional modulation in V1 of the macaque monkey. Under this scenario, ACh release puts the network into a state where feedback can exert strong influences, and it may even increase the level of glutamate release by means of presynaptic cholinergic terminals on glutamatergic feedback connections which activate NMDA receptor rich synapses which then allow the demands of attentional performance (Hasselmo and Sarter, 2010). The reason to argue for NMDA rich synapses is due to the fact that there is a strong similarity between the gain changes seen with attention in the awake-behaving monkey (e.g., (Roelfsema et al., 1998)) and the gain changes seen with NMDA receptor activation (Salt, 1986, Fox et al., 1989, 1990, Shima and Tanji, 1993b, a, Fleidervish et al., 1998). For example, iontophoretic application of NMDA in V1 of anesthesized monkeys resulted in gain increases (Fox et al., 1990) similar to the amplification of responses caused by directing spatial attention to the RF of V1 neurons (Thiele et al., 2009). Both NMDA and attention increased the slope of the linear portion of the contrast response function, as predicted by multiplicative or additive gain models (Thiele et al., 2009, Lee and Maunsell, 2010). In line with these results, we found in the awake-behaving monkey that the effect of NMDA receptor activation on contrast tuning functions was a multiplicative scaling of responses. Neuronal sensitivities (e.g., c50s) were not improved with NMDA receptor activation, nor were they improved by directing attention to the RF of the neurons under study. We found that the contribution of NMDA receptors to attentional modulation was not expressed in the response amplitude, as mean firing rate differences were not systematically affected. Rather, it mostly affected response variance. Attention per se reduced response variance in V1, and this reduction was diminished by blockade of NMDA receptors. A related study in V4 found that noise correlations (i.e. correlation of rates on a trial by trial basis) between neurons was reduced with attention (Mitchell et al., 2007, Sundberg et al., 2009). This suggests that

attentional modulation in V1 in our study requires active NMDA receptors, as their blockade increased the correlation (i.e., attention no longer decorrelated activity in the presence of APV).

Although the contribution of NMDA receptors to attentional modulation was significant for large parts of the data set, it was overall less consistent than the results reported in chapter 1, where acetylcholine's effects were probed. Applying ACh systematically increased mean firing rate differences resulting in increased attentional modulation, while blockade of muscarinic but not nicotinic receptors resulted in the opposite effect. A similar effect was observed on the oscillatory activity of neuronal ensembles. We found that directing attention to the RF of the recorded neurons reduced the stimulus-induced LFP power in the gamma range (Chalk et al., 2010). This attention-induced reduction of gamma power was counteracted by blocking muscarinic but not nicotinic receptors (i.e., scopolamine reduced the influence of attention on LFP gamma power). We were not able to show that ACh application showed the opposite effect to scopolamine in terms of oscillatory activity, possibly due to the efficacy of acetylcholine-esterase in breaking down ACh quickly and efficiently, preventing it from affecting large part of the network which are necessary to appreciate changes in correlated activity (Rodriguez et al., 2004). Future studies using ACh agonists insensitive to the esterase like charbachol might be necessary to shed light on this question. Note however that none of the known exogenous agonists show an identical affinity to individual nicotinic and muscarinic receptor subtypes with that of ACh (Kimura et al., 1999). Despite this, our data demonstrate that muscarinic mechanisms contribute to attentional modulation of gamma range synchronization in V1. In contrast, activation of NMDA receptors did not systematically increase the attentional modulation of firing rates, or the attentional modulation of LFP power, although NMDA blockade strongly increased the overall oscillatory power.

The relatively moderate influence of NMDA receptors in attentional modulation (less consistent compared to ACh and largely present in altering response reliability, not strength) were somewhat surprising because NMDA receptors have been implicated in synaptic mechanisms underlying learning, memory, and developmental plasticity (Cotman et al., 1988, Collingridge and Singer, 1990). Modelling work has also suggested that NMDA receptor activation could enable synaptic reverberations in recurrent circuits necessary for persistent mnemonic activity (Wang, 2001). This activity related to working memory processes can be conceptually link to the task used in our paradigm, as top-down spatial attention has often been regarded as a spatial working memory signal (Downing, 2000, Deco and Thiele, 2009, Herrero et al., 2009). We found, however, that activation of NMDA channels in V1 improved the attentional modulation of firing rates under some conditions, particularly when the visual stimulus elicited a strong input drive (high contrast, 50%). This effect is in line with slice studies showing that NMDA receptors are activated under conditions of particularly intense or high-frequency synaptic drive (Collingridge and Bliss, 1987). This effect was also observed in our behavioural data, where NMDA speeded up reaction times to attended high contrast stimuli. In addition, NMDA receptors contributed to attentional modulation at the single neuron spiking level through changes in response reliability, rather than response strength. Attention per se reduced response variance in V1, similar to what has been shown in V4 (Mitchell et al., 2007), and this reduction was diminished by blockade of NMDA receptors.

The data in Chapter 2 provides some support for the notion that NMDA receptor-rich synapses are selectively recruited during attention, in line with a recent study (Self et al., 2008). The authors used pharmacological manipulations (pressure injection) in V1, while monkeys performed a figure-ground segregation and detection task (Lamme, 1995). Figure-ground modulation is thought to be due to feedback projections originating in extrastriate visual areas (Lamme and Roelfsema, 2000). They found that blockade of NMDA receptors reduced figure-ground modulation, while blockade of AMPA receptors reduced the overall gain (e.g., reduced peak response) but had little effect on the modulation. These results suggest that feedback projections recruit synapses with NMDA/AMPA receptor ratios different from those of feedforward projections. Recent modelling work predicts however, that NMDA receptor manipulations should mostly affect the strengths of attention-induced gamma oscillations, with minor implications to attention-induced rate modulations (Buehlmann and Deco, 2008). Analysis of the oscillatory activity in our experiment (Chapter 2) found no evidence to support such claims, as NMDA receptors were not specifically involved in the attention-induced gamma oscillations. Future studies of attentional modulation should take into account the interactions between different glutamatergic receptors, as non-NMDA receptors have been found to play a dominant role in the generation of gamma oscillations of cortical and hippocampal slices (Buhl et al., 1998, Fisahn et al., 1998, LeBeau et al., 2002). The interaction between glutamatergic and cholinergic inputs should also be properly studied, as such an interaction has been reported for the rat prefrontal cortex (Hasselmo and Sarter, 2010). Although we studied both systems, we can't comment on possible interactions, as our current experiments activated each system independently from the other.

Since both attention (Roberts et al., 2007) and acetylcholine (Roberts et al., 2005) can alter neuronal integration properties, we were interested to determine in more detail the spatial characteristics of this and the receptors that are responsible for the effect. In Chapter 3 we directly probed how the cholinergic system influenced neuronal integration properties. The integration literature has shown that the spatial context embedding an image element has a strong influence on the perception of the image element itself (Gilbert et al., 1990, Albright and Stoner, 2002, Paradiso et al., 2006), and that this influence can be facilitatory under certain conditions, and suppressive under others. At the neuronal level, these contextual effects have often been attributed to lateral interactions between neurons in the primary visual cortex (Ichida et al., 2007), as well as feedback connections from V2 (Bair et al., 2003). A number of studies in the anesthesized animal have reported that collinear flankers increase V1 neuronal responses to a central target (Crook et al., 2002; Mizobe et al., 2001), especially if the target contrast is low (Polat et al., 1998, Kapadia et al., 2000). We expected in line with these studies to also find collinear facilitation in the awake monkey, but we found that only 13% of the neurons tested showed signs of facilitation (see (Pooresmaeili et al., 2010)). We noted that we were not the only ones, and that others found similar results (Macknik and Haglund, 1999, Zenger-Landolt and Koch, 2001, Meirovithz et al., 2010). Despite this, we determined the receptors and neurotransmitters mediating the collinear facilitation on this small set of neurons. We expected that if the facilitation were mediated by lateral intracortical interactions, then the facilitation should be increased by blockade of muscarinic receptors, as this should increase the efficacy of intracortical lateral synapses. We found that blockade of muscarinic receptors

in flanker-facilitated neurons reduced the facilitation. This can possibly be explained by the complex effect of ACh on the network: ACh affects the strength of lateral connections, the excitatory connections within a column, the local inhibitory drive (Disney et al., 2006b), and the M-current (for a review see (Lucas-Meunier et al., 2003)). Thus, ACh affects the membrane's spatial and temporal integration constant. This means that even if muscarinic blockade increases synaptic efficacy of lateral interactions, it may well be the case that it results in a reduced ability of neurons to integrate these inputs, due to increased membrane leakage, which then results in an overall reduction of flanker-induced facilitation. We note that this is fairly speculative, but in light of the multitude of network effects of ACh, we currently have no better explanation.

In contrast, blockade of nicotinic receptors with mecamylamine resulted on reduced gain with no changes in the facilitation. This was in line with our expectation, as nicotinic receptors are mainly located presynaptically at thalamo-cortical terminals; i.e., reducing the efficacy of thalamic connections via nicotinic receptor blockade should not affect the flanker-induced facilitation which is likely generated by local intra-areal interactions (Ichida et al., 2007) or feedback from higher areas (Bair et al., 2003).

In a concluding chapter (Chapter 4), we studied the effects of cholinergic and GABAergic mechanisms on neuronal coding in the middle temporal area (MT), the main hub for the analysis of direction of motion (Albright, 1984). We performed these experiments in the anesthesized macaque, but the conclusions are at least somewhat relevant to attentional processes. While some studies have found that attention changes the ratio of responses to preferred and anti-preferred directions of motion (Treue and Maunsell, 1996), others have argued that it proportionally scales all responses, provided only a single stimulus is present in the RF, and spatial attention is employed (Martinez-Trujillo and Treue, 2004b). To provide a better understanding of the cellular computations underlying motion-direction selectivity in MT, we used pharmacological manipulations (Thiele et al., 2006) to compare between cholinergic and GABAergic contribution. High levels of ACh in the extracellular space of MT neurons could alter the relative weight of feedforward and lateral synaptic input, and also alter the biophysical state of the neurons, possibly resulting in improved motion selectivity of single-cell responses. For this to happen ACh should be able to sharpen tuning curves by selectively increasing responses to optimal motion directions, similar to what others have shown for feature-based attention (Treue and Maunsell, 1999, Martinez-Trujillo and Treue, 2004a). The authors proposed a feature-similarity gain model, where attention increases responses to motion directions close to the neuron's preferred direction, while not modulating them to intermediate motion directions and suppressing them to anti-preferred directions. Contrary to previous studies in MT (Treue and Maunsell, 1999, Martinez-Trujillo and Treue, 2004a) and V1 (Sillito and Kemp, 1983, Sato et al., 1987a, Murphy and Sillito, 1991, Sato et al., 1996), we did not find a facilitatory effect of ACh in sharpening tuning curves (i.e., some neurons increased their directional selectivity while others reduced it). ACh scaled all responses equally regardless of feature preference by simply employing a multiplicative factor (Lee and Maunsell, 2010) in line with theories of general response elevation. In contrast, blocking GABAa receptors with Gabazine resulted on broadening of the motion-direction tuning curve in the majority of neurons, in line with theories of response disinhibition (Thiele et al., 2004b).

Despite not having a direct effect on tuning width, we found that ACh may contribute positively to motion-direction selectivity in MT by reducing the variability between spike times within trials. A related effect was already reported in V4 when attention was directed to the RF of V4 neurons (Mitchell et al., 2007). More importantly, this effect in our data was restricted to the preferred motion direction (PD): ACh reduced the coefficient of variation (CV) only in the responses to the PD. Opposed directions (ODs) were unchanged by the drug. In contrast, Gabazine increased the CV in the responses to all directions. These effects cannot be explained by differences in firing rates because both ACh and Gabazine increased firing rates equally. In addition to the beneficial effect of ACh on the CV, ACh also reduced the FANO factor (i.e., the variability of firing rates across trials). Importantly, this effect was also restricted to the PD while ODs showed an opposed effect whereby ACh decreased response reliability. The effect of reduced variability in responses to the PD was restricted to the late response period (200-760ms). This is the period where attentional modulation is stronger (Roelfsema et al., 1998, Roberts et al., 2007). Other studies found that ACh did not sharpen orientation/direction tuning curves of V1 neurons. Instead, it improved their response variability (Sato et al., 1987b, Zinke et al., 2006) and signal-to-noise ratio (Sato et al., 1987b). But the authors did not analyse whether the improved reliability was restricted to the optimal stimulus which would provide direct evidence for increased selectivity. Importantly, Gabazine decreased response reliability across all directions of motion equally, and across early and late time periods.

Conclusions

The goal of this dissertation has been to better understand the cellular mechanisms underlying spatial attention in the primary visual cortex of the macaque monkey. The main result is that the amount of attentional modulation in the primary visual cortex is augmented when the cholinergic system is pharmacologically enhanced. This enhancement occurs through the activation of muscarinic receptors. The amount of attentional modulation is also increased when the glutamatergic NMDA receptor is enhanced although the effects seem largely restricted to improved response reliability, less to increased response gain. As for the effect of ACh on basic response properties in extrastriate area (MT), it appears that ACh does not increase neuronal sensitivities (e.g., sharpening tuning curves). Instead, it improves response reliability to optimal stimulus features.

To better understand the contribution of this thesis to current knowledge, we next provide some cartoons and diagrams that summarize the main findings. Figure GD1 shows a schematic view of the cholinergic system in the rat and monkey brain (sagittal sections). Figure GD1.A shows the basal forebrain (BF) efferent cholinergic projections to the entire cortical mantle, and the main telencephalic afferent projection systems of the BF of rat brain (adapted from (Sarter et al., 2009)). Cholinergic neurons originating from the nucleus basalis of Meynert (NBM) innervate most cortical areas and layers. The prefrontal cortex (PFC) projects back to the BF both directly and indirectly (through the nucleus accumbens (NAc)). The BF, PFC and NAc are also all innervated by dopaminergic neurons from the ventral tegmental area (vTA), and these

dopaminergic neurons in turn are contacted by PFC projections. Figure GD1.B shows the macaque monkey brain, with similar cholinergic projections (dopaminergic projections not shown). Note that the organization of the cholinergic system suggests a profound control of the BF by the PFC. Figure GD1.C shows the connections between neurons in the visual cortex (adapted from (Roelfsema, 2006)). Schematic representation of feedforward, horizontal, and feedback connections between areas of the visual cortex. In our experiments (Chapter 1), we assumed attentional modulation to be conveyed through feedback signals from the PFC. Feedback signals could modulate responses of neurons in V1 via two mechanisms. The first one is via direct connections to V4/V2, and the second one is via the BF. The PFC could send a feedback signal to the BF which in turn activates V1 neurons contributing to attentional modulation. These two mechanisms may not be exclusive, and future studies should address their interactions.

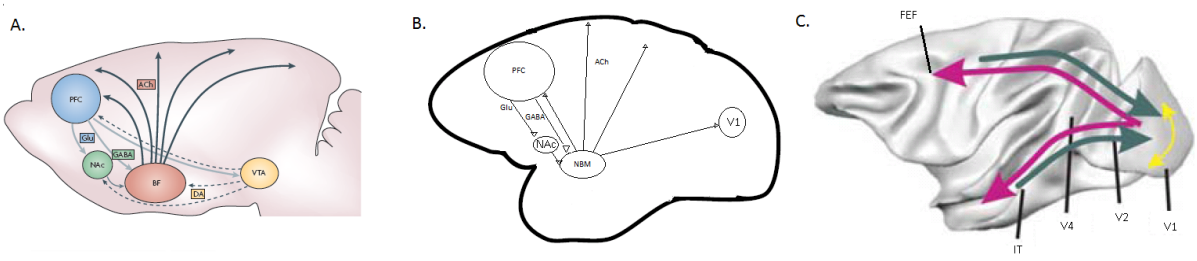

Figure GD1. Cortical cholinergic circuitry in the rat and monkey, and connections between areas of the visual cortex (sagittal views). A) Rat brain. Cholinergic and dopaminergic projections from BF and vTA (adapted from (Sarter et al., 2009)). Cholinergic neurons originating from the NBM innervate most cortical areas. This innervation can be modulated by PFC, which projects back to the BF, thus contributing to attentional modulation in visual areas. B) Similar projections could apply to the monkey brain (only cholinergic projections drawn).C) Feedforward (purple), horizontal (yellow), and feedback (green) connections between areas in the visual cortex (adapted from (Roelfsema, 2006)).

ACh acts as a neuromodulator in the visual cortex. It modulates glutamatergic transmission. Glutamate is the major excitatory neurotransmitter in the central nervous system. Upon visual stimulation excitatory neurons along the visual pathway communicate by releasing glutamate. The following cartoon (Figure GD2) shows the cholinergic modulation of glutamatergic transmission as it may happen in V1. Notice that many receptors and connections are not drawn for simplicity but that the basic sequence of steps may be as follow:

1. Depolarization of thalamocortical (TC) terminals leads to glutamate release from vesicles on the presynaptic side, activating AMPA and NMDA receptors in the postsynaptic density of the cortical neuron (Figure GD2.A).

2. ACh also contributes to glutamatergic transmission with a modulatory role. Depolarization of cholinergic neurons (from the NBM) leads to ACh release and activation of nAChRs located presynaptically at TC terminals. This results in further glutamate release (e.g., ACh increases Ca+2 influx through nAChRs and glutamate-induced depolarization), and shows that ACh modulates rather than triggers the release of glutamate.

3. When ACh levels are high due to the rapid activation of nAChRs, more glutamate is released, and the conductance through AMPA and NMDA receptors is larger. The resulting larger excitation of the postsynaptic cortical neuron can cause it to more likely fire action potentials, triggering neurotransmitter release onto downstream neurons. This could be a mechanism by which neuronal responsiveness is increased with visual stimulation as shown in Figure GD2.A. Additionally, this mechanism could underlie attention due to increase synaptic efficacy of TC connections (e.g., increased response reliability, increased SNR). The location of nAChRs, mainly in the input layer (Vidal & Changeux, 1993; Gil et al., 1997; Wonnacott, 1997), makes them ideally suited for this role (Hasselmo, 2010). However, we found that blockade of nAChRs did not reduce attentional modulation, unlike blockade of mAChRs that had a remarkable effect.

4. We suggest that ACh boosts attention only when two requirements are met (Figure GD2.B): the synaptic efficacy of TC connections is increased and at the same, the synaptic efficacy of IC connections is reduced. As it has been suggested (Hasselmo and Bower 1992, Kimura, 2000), ACh shifts the dynamics of the cortical networks into a state where afferent influence predominates over intracortical influence. IC influence could be minimized by ACh acting on presynaptic mAChRs (Metherate & Ashe, 1993; Vidal & Changeux, 1993; Murakoshi, 1995; Gil et al., 1997; Kimura & Baughman, 1997; Kimura et al., 1999; Richter et al., 1999; Hsieh et al., 2000; Kimura, 2000; Oldford and Castro-Alamancos, 2003). At least within superficial, presumably thalamo-recipient layers (2–4), ACh reduces glutamate release at IC synapses via mAChRs receptors.

5. Less glutamate release at IC synapses means less spread of excitation, possibly leading to reduce oscillatory activity. Because of the rapid degradation of ACh (due to ACHE action), we did not observe reduced gamma power in the LFP. Future studies should apply other cholinergic agonist (e.g., carbachol) to test whether gamma power is increased. However, we did observe increase gamma power when mAChRs were blocked. In addition, we also observed that the attention-induced changes in gamma power were reduced when mAChRs, but not nAChRs, were blocked. On an interesting note is that blockade of nAChRs in our study systematically increased gamma power, which is in line with recent evidence that suggests a role of nAChRs on the spread of lateral excitation (Levy et al., 2006). Future studies should examine in more detail the role of nAChRs on attentional modulation of oscillatory activity.

6. In addition to presynaptic mAChRs, there are also postsynaptic mAChRs (not drawn). Activation of these channels within supragranular layers increases neuronal excitability through blockade of several K+-currents (McCormick & Prince, 1986). This effect may contribute to the increase in firing rates observed in our study (see histograms in Figure GD2.A), as most recordings were from layer 2/3 pyramidal neurons (p2/3). Here, activation of mAChRs on p2/3 causes cell depolarization, increased excitability, and reduced spike frequency adaptation (McCormick & Prince, 1985; Mrzljak et al., 1996). This is in line with our results, as ACh increased neuronal gain in most p2/3 neurons tested. We note however that the effect of ACh can be indirect, as ACh applied to layer 1 interneurons can inhibit layer 2/3 basket cells (b2/3) which in turn would increase the excitability of pyramidal cells (p2/3) (Christophe et al., 2002). We also note that ACh can also have opposed effects. For example, activation of postsynaptic mAChRs on layer 4 cells can decrease the excitability of layer 4 neurons (Mrzljak et al., 1996), possibly reducing the excitatory feed forward drive to p2/3 cells. Additionaly, a

simultaneous activation of mAChRs located on interneurons would counteract the depolarization of the pyramidal cell, due to increased GABAergic inhibition (McCormick & Prince, 1985; but note that hyperpolarization of interneurons can also occur Xiang et al., 1998).

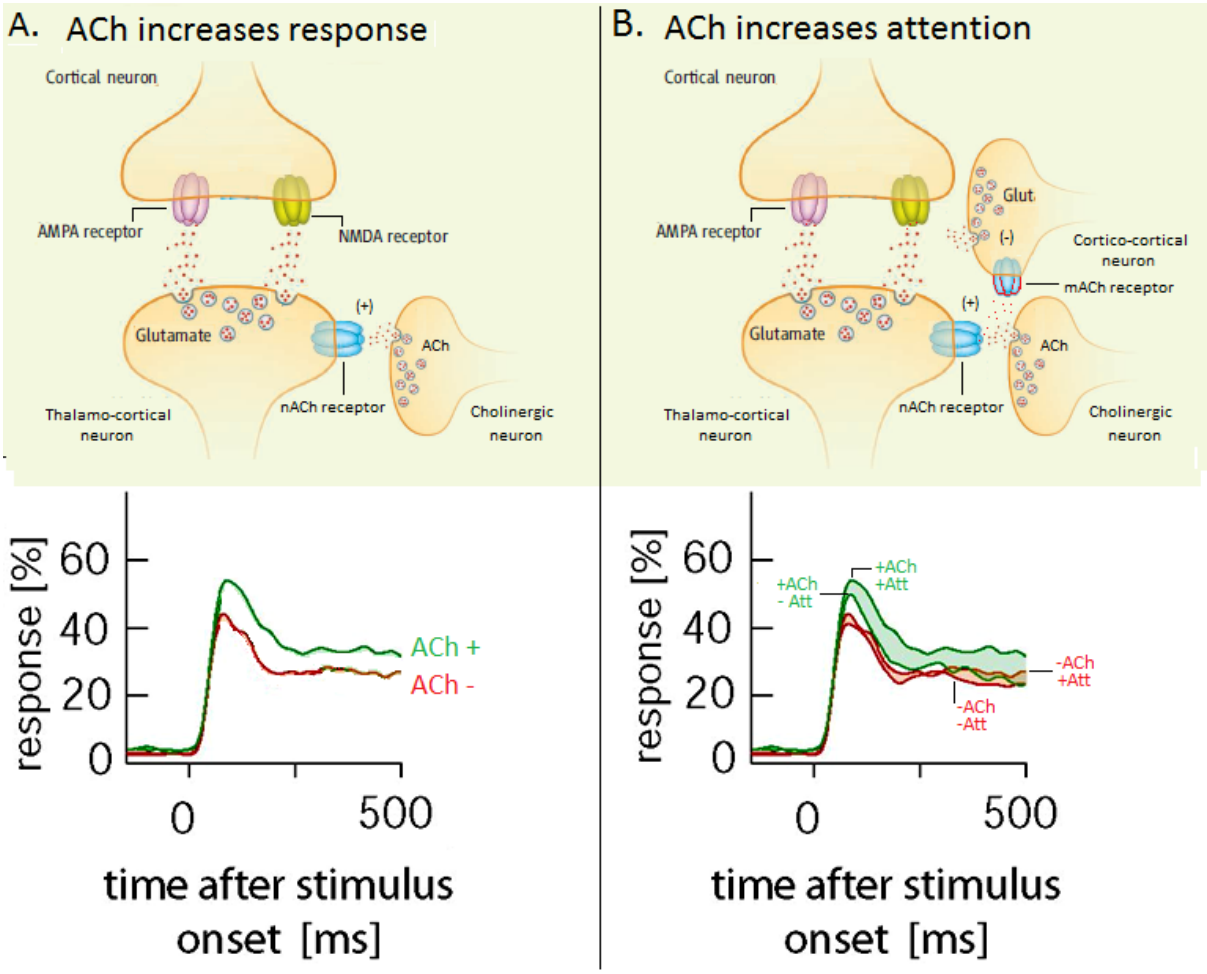

Figure GD2. Mechanisms of action of ACh on response gain and attentional modulation in V1. A) ACh increases neuronal gain. Glutamate (Glu) release from presynaptic TC terminals is modulated by ACh. ACh activates presynaptic nAChRs increasing Glu release from TC terminals (see + sign), likely contributing to larger firing rates as shown in the histograms (bottom). ACh can also activate postsynaptic mAChRs (not drawn for simplicity), likewise increasing neuronal excitability. B) ACh increases attentional modulation. In addition to activating presynaptic nAChRs at TC terminals, ACh can also activate presynaptic mAChRs at IC terminals. Activation of these receptors can in some cases (e.g., Mrzljak et al., 1996) decrease the excitability of p2/3 cells. Thus less Glu is released from IC terminals (reducing their efficacy), while more Glu is released from TC terminals (increasing their efficacy).

As shown in Figure GD1, cholinergic inputs spread to the whole cortical mantel. The coarseness of the ACh innervation may be incompatible with the highly localized and fast effects of spatial attention (see arguments from the volume transmission hypothesis, e.g. (Sarter et al., 2009)). This raises the question of whether non-cholinergic mechanisms are more directly contributing to attentional modulation. Figure GD3 shows the glutamatergic NMDA receptor contribution to response enhancement and to attentional modulation in V1. This is rather speculative proposal and further research should confirm it. Under this

proposal (Figure GD3.A), visual stimulation depolarizes TC terminals resulting in increased glutamate release and activation of postsynaptic AMPA and NMDA receptors. Application of NMDA agonists further increases glutamate release, resulting in enhanced neuronal gain as shown in the histograms (bottom). If the visual stimulus is not attended (Figure GD3.A), AMPA and NMDA receptors are active in approximately equal proportions. Attentional modulation in visual areas has long been assumed to be implemented via feedback signals from PFC. These feedback connections are mostly glutamatergic, and target excitatory neurons in extrastriate areas V2/V4 which in turn influence neurons in V1 (Ungerleider et al., 1989). This is shown in Figure GD3.B with feedback connections from higher areas possibly activating mAChRs located presynaptically at cortico-cortical terminals. This may shift the gAMPA/gNMDA ratio at TC synapses, with larger conductance through NMDA compared to AMPA receptors. The NMDA receptor bias does not result in increased amplitude of firing rates (compare shaded areas in histograms which represent the strength of the attentional modulation). Instead, response reliability is improved (see raster plot in Figure GD3.B, bottom). Because NMDA channels have slow kinetics (~100ms), further depolarization with attention does not speed up opening times (below 100ms) but it results on more reliable opening times (e.g. improved response reliability of spike times). In line with this idea, we found (Chapter 2) that blockade of NMDA receptors reduced the attention-induced changes in response reliability. Attention increased response reliability across trials (e.g., attention reduced the fano factor) when NMDA receptors were not blocked. This finding suggests that feedback connections selectively target NMDA receptor-rich synapses in V1, controlling the response reliability of V1 neurons.

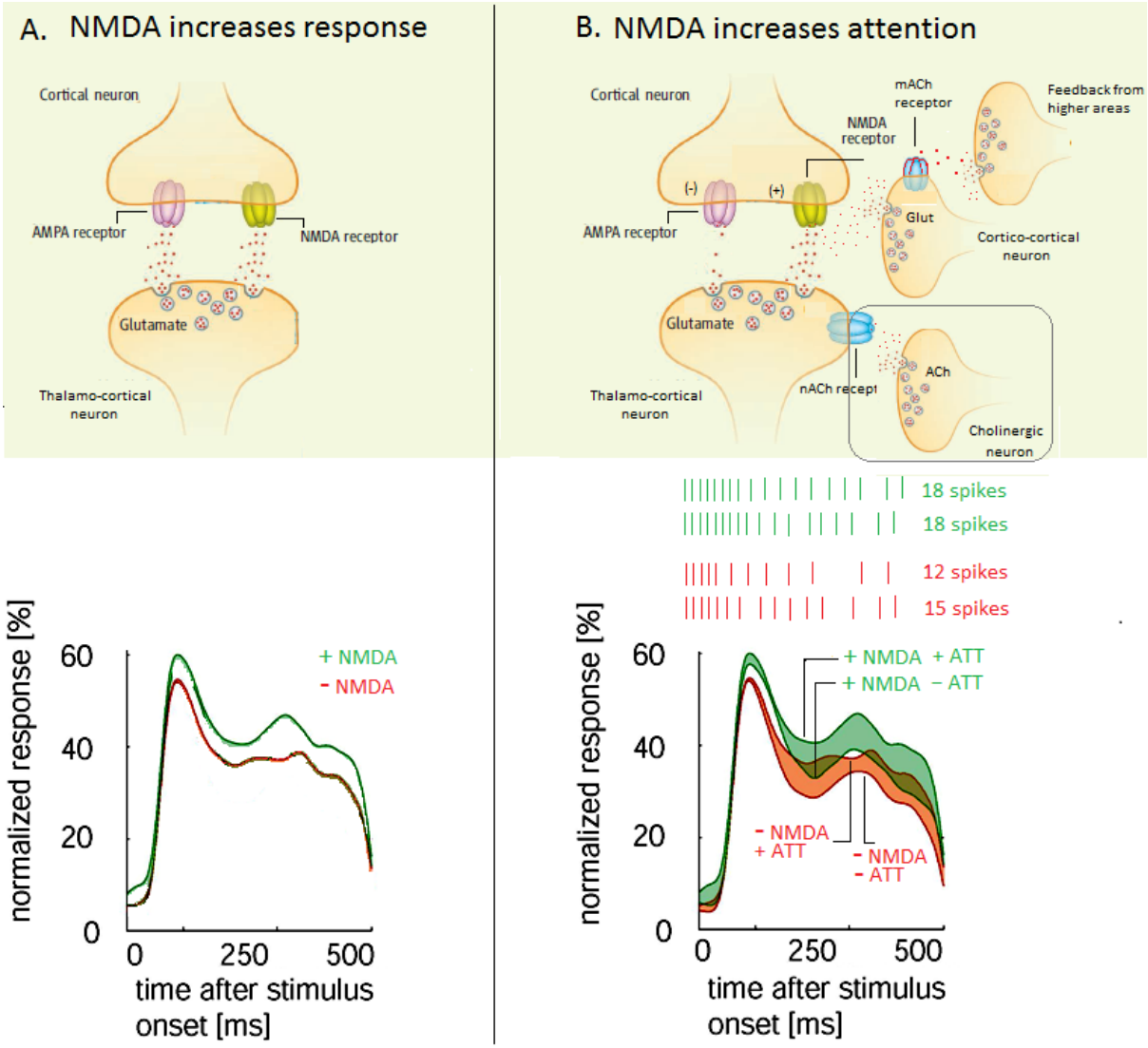

Figure GD3. Mechanisms of action of NMDA receptor activation and attentional modulation in V1. A) NMDA receptor activation increases neuronal gain. Glutamate release from TC terminals activates postsynaptic AMPA and NMDA receptors, contributing to increase firing rates (histogram, bottom). B) NMDA receptor activation boosts attention by improving response reliability. Attentional modulation of firing rates (compared red and green shaded areas) did not change upon NMDA activation. However, reliability of spike times improved upon NMDA activation. Raster plots in red show variable number of spikes across control trials (from 12 spikes in trial 1 to 15 spikes in trial 2), while raster plots in green show equal number of spikes across NMDA activated trials. Feedback from higher areas (e.g. PFC) may contribute to this effect. Feedback connections are excitatory and originally target neurons in extrastriate areas (V2/V4). They can in turn influence V1 patterns, improving their response reliability. Response amplitude does not change possibly because feedback (and lateral) connections shift the gNMDA/gAMPA ratio in favor of NMDA. Interactions between the glutamatergic and cholinergic system are also possible as shown by the inset (grey box).

The work in this thesis has examined the contribution of the cholinergic and glutamatergic system independently from each other. However, important interactions between these two neurotransmitter systems may underlie attentional processes. One possibility is that increased amounts of ACh increase the excitability of V1 neurons which may then allow spatially specific glutamatergic feedback to enhance specific incoming information (adding the grey box in Figure GD3.B depicts such scenario). Future studies should

investigate this hypothesis, by combining pharmacological analysis of cholinergic and glutamatergic NMDA receptors while macaque monkeys perform similar top-down spatial attention tasks. As mentioned above (Figure GD1), the PFC can exert a profound influence over the BF. The PFC projects back to the BF both directly and indirectly through the NAc. Activation of NBM cholinergic neurons could increase tonic levels of ACh in V1, and allow spatially specific glutamatergic feedback to enhance specific incoming information. Alternatively, phasic and spatially specific releases of ACh (on top of tonic ACh level) could also account for the rapid attention effects (Sarter et al., 2009). According to the authors, these phasic releases of ACh are controlled by the PFC: the glutamatergic input from the PFC would modulate the release of ACh in cholinergic terminals from the NBM. Future pharmacological studies of attentional modulation should further address these alternative possibilities.

Reference List

Albrecht DG, Hamilton DB (1982) Striate cortex of monkey and cat: contrast response function. J Neurophysiol 48:217-237.

Albright TD (1984) Direction and orientation selectivity of neurons in visual area MT of the macaque. J Neurophysiol 52:1106-1130.

Albright TD, Stoner GR (2002) Contextual influences on visual processing. Annu Rev Neurosci 25:339-379.

Artola A, Singer W (1987) Long-term potentiation and NMDA receptors in rat visual cortex. Nature 330:649-652.

Avoli M, Hwa G, Louvel J, Kurcewicz I, Pumain R, Lacaille JC (1997) Functional and pharmacological properties of GABA-mediated inhibition in the human neocortex. Can J Physiol Pharmacol 75:526-534.

Avoli M, Louvel J, Drapeau C, Pumain R, Kurcewicz I (1995) GABAA-mediated inhibition and in vitro epileptogenesis in the human neocortex. J Neurophysiol 73:468-484.

Bair W, Cavanaugh JR, Movshon JA (2003) Time course and time-distance relationships for surround suppression in macaque V1 neurons. J Neurosci 23:7690-7701.

Beani L, Bianchi C, Santinoceto L, Marchetti P (1968) The cerebral acetylcholine release in conscious rabbits with semi-permanently implanted epidural cups. Int J Neuropharmacol 7:469-481.

Berens P, Keliris GA, Ecker AS, Logothetis NK, Tolias AS (2008) Feature selectivity of the gamma-band of the local field potential in primate primary visual cortex. Front Neurosci 2:199-207.

Brocher S, Artola A, Singer W (1992) Agonists of Cholinergic and Noradrenergic Receptors Facilitate Synergistically the Induction of Long-Term Potentiation in Slices of Rat Visual-Cortex. Brain Research 573:27-36.

Brown DA, Abogadie FC, Allen TG, Buckley NJ, Caulfield MP, Delmas P, Haley JE, Lamas JA, Selyanko AA (1997) Muscarinic mechanisms in nerve cells. Life Sci 60:1137-1144.

Bruce CJ, Goldberg ME (1985) Primate frontal eye fields. I. Single neurons discharging before saccades. J Neurophysiol 53:603-635.

Buehlmann A, Deco G (2008) The neuronal basis of attention: rate versus synchronization modulation. J Neurosci 28:7679-7686.

Buhl EH, Tamas G, Fisahn A (1998) Cholinergic activation and tonic excitation induce persistent gamma oscillations in mouse somatosensory cortex in vitro. J Physiol 513 (Pt 1):117-126.

Bulbring E, Burn JH (1941) Observations bearing on synaptic transmission by acetylcholine in the spinal cord. J Physiol 100:337-368.

Buschman TJ, Miller EK (2007) Top-down versus bottom-up control of attention in the prefrontal and posterior parietal cortices. Science 315:1860-1862.

Bushnell MC, Goldberg ME, Robinson DL (1981) Behavioral enhancement of visual responses in monkey cerebral cortex. I. Modulation in posterior parietal cortex related to selective visual attention. J Neurophysiol 46:755-772.

Casamenti F, Prosperi C, Scali C, Giovannelli L, Pepeu G (1998) Morphological, biochemical and behavioural changes induced by neurotoxic and inflammatory insults to the nucleus basalis. Int J Dev Neurosci 16:705-714.

Chalk M, Herrero JL, Gieselmann MA, Delicato LS, Gotthardt S, Thiele A (2010) Attention reduces stimulus-driven gamma frequency oscillations and spike field coherence in V1. Neuron 66:114-125.

Cockcroft VB, Osguthorpe DJ, Barnard EA, Friday AE, Lunt GG (1990) Ligand-Gated Ion Channels - Homology and Diversity. Mol Neurobiol 4:129-169.

Colby CL, Duhamel JR, Goldberg ME (1996) Visual, presaccadic, and cognitive activation of single neurons in monkey lateral intraparietal area. J Neurophysiol 76:2841-2852.

Colegate RL, Hoffman JE, Eriksen CW (1973) Selective Encoding from Multielement Visual-Displays. Percept Psychophys 14:217-224.

Collingridge GL, Bliss TVP (1987) Nmda Receptors - Their Role in Long-Term Potentiation. Trends in Neurosciences 10:288-293.
Collingridge GL, Singer W (1990) Excitatory amino acid receptors and synaptic plasticity. Trends Pharmacol Sci 11:290-296.
Connor CE (2006) Attention: beyond neural response increases. Nat Neurosci 9:1083-1084.
Connor CE, Gallant JL, Preddie DC, Van Essen DC (1996) Responses in area V4 depend on the spatial relationship between stimulus and attention. J Neurophysiol 75:1306-1308.
Connor CE, Preddie DC, Gallant JL, Van Essen DC (1997) Spatial attention effects in macaque area V4. J Neurosci 17:3201-3214.
Corbetta M, Shulman GL (2002) Control of goal-directed and stimulus-driven attention in the brain. Nat Rev Neurosci 3:201-215.
Cotman CW, Monaghan DT, Ganong AH (1988) Excitatory amino acid neurotransmission: NMDA receptors and Hebb-type synaptic plasticity. Annu Rev Neurosci 11:61-80.
Coull JT, Nobre AC (1998) Where and when to pay attention: The neural systems for directing attention to spatial locations and to time intervals as revealed by both PET and fMRI. Journal of Neuroscience 18:7426-7435.
Crick F (1984) Function of the thalamic reticular complex: the searchlight hypothesis. Proc Natl Acad Sci U S A 81:4586-4590.
Crook JM, Kisvarday ZF, Eysel UT (1997) GABA-induced inactivation of functionally characterized sites in cat striate cortex: effects on orientation tuning and direction selectivity. Vis Neurosci 14:141-158.
Crook JM, Kisvarday ZF, Eysel UT (1998) Evidence for a contribution of lateral inhibition to orientation tuning and direction selectivity in cat visual cortex: reversible inactivation of functionally characterized sites combined with neuroanatomical tracing techniques. Eur J Neurosci 10:2056-2075.
Das A, Gilbert CD (1999) Topography of contextual modulations mediated by short-range interactions in primary visual cortex. Nature 399:655-661.
DeAngelis GC, Freeman RD, Ohzawa I (1994) Length and width tuning of neurons in the cat's primary visual cortex. J Neurophysiol 71:347-374.
Deco G, Thiele A (2009) Attention: oscillations and neuropharmacology. Eur J Neurosci 30:347-354.
Desimone R, Duncan J (1995) Neural mechanisms of selective visual attention. Annu Rev Neurosci 18:193-222.
Disney AA, Aoki C (2008) Muscarinic acetylcholine receptors in macaque V1 are most frequently expressed by parvalbumin-immunoreactive neurons. J Comp Neurol 507:1748-1762.
Disney AA, Domakonda KV, Aoki C (2006a) Differential expression of muscarinic acetylcholine receptors across excitatory and inhibitory cells in visual cortical areas V1 and V2 of the macaque monkey. J Comp Neurol 499:49-63.
Disney AA, Domakonda KV, Aoki C (2006b) Differential expression of muscarinic acetylcholine receptors across excitatory and inhibitory cells in visual cortical areas V1 and V2 of the macaque monkey. J Comp Neurol 499:49-63.
Distler C, Hoffmann KP (2001) Cortical input to the nucleus of the optic tract and dorsal terminal nucleus (NOT-DTN) in macaques: a retrograde tracing study. Cereb Cortex 11:572-580.
Downing PE (2000) Interactions between visual working memory and selective attention. Psychol Sci 11:467-473.
Dragoi V, Sur M (2000) Dynamic properties of recurrent inhibition in primary visual cortex: contrast and orientation dependence of contextual effects. J Neurophysiol 83:1019-1030.
Ego-Stengel V, Shulz DE, Haidarliu S, Sosnik R, Ahissar E (2001) Acetylcholine-dependent induction and expression of functional plasticity in the barrel cortex of the adult rat. J Neurophysiol 86:422-437.
Eriksen CW, Hoffman JE (1973) Extent of Processing of Noise Elements during Selective Encoding from Visual-Displays. Percept Psychophys 14:155-160.

Fisahn A, Pike FG, Buhl EH, Paulsen O (1998) Cholinergic induction of network oscillations at 40 Hz in the hippocampus in vitro. Nature 394:186-189.
Fleidervish IA, Binshtok AM, Gutnick MJ (1998) Functionally distinct NMDA receptors mediate horizontal connectivity within layer 4 of mouse barrel cortex. Neuron 21:1055-1065.
Fournier GN, Semba K, Rasmusson DD (2004) Modality- and region-specific acetylcholine release in the rat neocortex. Neuroscience 126:257-262.
Fox K, Sato H, Daw N (1989) The location and function of NMDA receptors in cat and kitten visual cortex. J Neurosci 9:2443-2454.
Fox K, Sato H, Daw N (1990) The Effect of Varying Stimulus-Intensity on Nmda-Receptor Activity in Cat Visual-Cortex. Journal of Neurophysiology 64:1413-1428.
Fries P, Reynolds JH, Rorie AE, Desimone R (2001) Modulation of oscillatory neuronal synchronization by selective visual attention. Science 291:1560-1563.
Furey ML, Pietrini P, Haxby JV, Drevets WC (2008) Selective effects of cholinergic modulation on task performance during selective attention. Neuropsychopharmacology 33:913-923.
Gieselmann MA, Thiele A (2008) Comparison of spatial integration and surround suppression characteristics in spiking activity and the local field potential in macaque V1. Eur J Neurosci 28:447-459.
Giesselmann UC, Wiegand T, Meyer J, Vogel M, Brandl R (2008) Spatial distribution of communal nests in a colonial breeding bird: benefits without costs? Austral Ecol 33:607-613.
Gil Z, Conners, B.W., and Amitai, Y. (1997) Differential regulation of neocortical synapses by neuromodulators and activity. Neuron 19:679–686.
Gilbert CD, Hirsch JA, Wiesel TN (1990) Lateral interactions in visual cortex. Cold Spring Harb Symp Quant Biol 55:663-677.
Gioanni Y, Rougeot C, Clarke PBS, Lepouse C, Thierry AM, Vidal C (1999) Nicotinic receptors in the rat prefrontal cortex: increase in glutamate release and facilitation of mediodorsal thalamo-cortical transmission. Eur J Neurosci 11:18-30.
Goldman-Rakic PS, Muly EC, 3rd, Williams GV (2000) D(1) receptors in prefrontal cells and circuits. Brain Res Brain Res Rev 31:295-301.
Gray CM, Singer W (1989) Stimulus-specific neuronal oscillations in orientation columns of cat visual cortex. Proc Natl Acad Sci U S A 86:1698-1702.
Gregoriou GG, Gotts SJ, Zhou HH, Desimone R (2009a) High-Frequency, Long-Range Coupling Between Prefrontal and Visual Cortex During Attention. Science 324:1207-1210.
Gregoriou GG, Gotts SJ, Zhou HH, Desimone R (2009b) Long-range neural coupling through synchronization with attention. Prog Brain Res 176:35-45.
Hagihara K, Tsumoto T, Sato H, Hata Y (1988) Actions of excitatory amino acid antagonists on geniculo-cortical transmission in the cat's visual cortex. Exp Brain Res 69:407-416.
Han ZY, Le Novere N, Zoli M, Hill JA, Champtiaux N, Changeux JP (2000) Localization of nAChR subunit mRNAs in the brain of Macaca mulatta. Eur J Neurosci 12:3664-3674.
Hasselmo ME (1995) Neuromodulation and cortical function: modeling the physiological basis of behavior. Behav Brain Res 67:1-27.
Hasselmo ME, Bower JM (1992) Cholinergic suppression specific to intrinsic not afferent fiber synapses in rat piriform (olfactory) cortex. J Neurophysiol 67:1222-1229.
Hasselmo ME, Sarter M (2010) Modes and Models of Forebrain Cholinergic Neuromodulation of Cognition. Neuropsychopharmacology.
Hasselmo ME, Stern CE (2006) Mechanisms underlying working memory for novel information. Trends Cogn Sci 10:487-493.
Herrero JL, Nikolaev AR, Raffone A, van Leeuwen C (2009) Selective attention in visual short-term memory consolidation. Neuroreport 20:652-656.
Herrero JL, Roberts MJ, Delicato LS, Gieselmann MA, Dayan P, Thiele A (2008) Acetylcholine contributes through muscarinic receptors to attentional modulation in V1. Nature 454:1110-1114.

Houser CR, Crawford GD, Salvaterra PM, Vaughn JE (1985) Immunocytochemical localization of choline acetyltransferase in rat cerebral cortex: a study of cholinergic neurons and synapses. J Comp Neurol 234:17-34.
Ichida JM, Schwabe L, Bressloff PC, Angelucci A (2007) Response facilitation from the "suppressive" receptive field surround of macaque V1 neurons. J Neurophysiol 98:2168-2181.
Johnson RR, Burkhalter A (1996) Microcircuitry of forward and feedback connections within rat visual cortex. J Comp Neurol 368:383-398.
Jones KA, Baughman RW (1988) Nmda-Receptor and Non-Nmda-Receptor Components of Excitatory Synaptic Potentials Recorded from Cells in Layer-V of Rat Visual-Cortex. Journal of Neuroscience 8:3522-3534.
Juliano SL, Ma W, Eslin D (1991) Cholinergic depletion prevents expansion of topographic maps in somatosensory cortex. Proc Natl Acad Sci U S A 88:780-784.
Kanai T, Szerb JC (1965) Mesencephalic Reticular Activating System and Cortical Acetylcholine Output. Nature 205:80-82.
Kapadia MK, Ito M, Gilbert CD, Westheimer G (1995) Improvement in visual sensitivity by changes in local context: parallel studies in human observers and in V1 of alert monkeys. Neuron 15:843-856.
Kapadia MK, Westheimer G, Gilbert CD (2000) Spatial distribution of contextual interactions in primary visual cortex and in visual perception. J Neurophysiol 84:2048-2062.
Katz PS, Frost WN (1996) Intrinsic neuromodulation: Altering neuronal circuits from within. Trends in Neurosciences 19:54-61.
Khayat PS, Pooresmaeili A, Roelfsema PR (2009) Time course of attentional modulation in the frontal eye field during curve tracing. J Neurophysiol 101:1813-1822.
Kimura F (2000) Cholinergic modulation of cortical function: a hypothetical role in shifting the dynamics in cortical network. Neurosci Res 38:19-26.
Kimura F, Baughman RW (1997) Distinct muscarinic receptor subtypes suppress excitatory and inhibitory synaptic responses in cortical neurons. J Neurophysiol 77:709-716.
Kimura F, Fukuda M, Tsumoto T (1999) Acetylcholine suppresses the spread of excitation in the visual cortex revealed by optical recording: possible differential effect depending on the source of input. Eur J Neurosci 11:3597-3609.
Koenigs M, Barbey AK, Postle BR, Grafman J (2009) Superior Parietal Cortex Is Critical for the Manipulation of Information in Working Memory. Journal of Neuroscience 29:14980-14986.
Kopell N, Ermentrout GB, Whittington MA, Traub RD (2000) Gamma rhythms and beta rhythms have different synchronization properties. P Natl Acad Sci USA 97:1867-1872.
Kruse W, Eckhorn R (1996) Inhibition of sustained gamma oscillations (35-80 Hz) by fast transient responses in cat visual cortex. Proc Natl Acad Sci U S A 93:6112-6117.
Kwon YH, Nelson SB, Toth LJ, Sur M (1992) Effect of Stimulus Contrast and Size on Nmda Receptor Activity in Cat Lateral Geniculate-Nucleus. Journal of Neurophysiology 68:182-196.
Lambe EK, Picciotto MR, Aghajanian GK (2003) Nicotine induces glutamate release from thalamocortical terminals in prefrontal cortex. Neuropsychopharmacology 28:216-225.
Lamme VA (1995) The neurophysiology of figure-ground segregation in primary visual cortex. J Neurosci 15:1605-1615.
Lamme VA, Roelfsema PR (2000) The distinct modes of vision offered by feedforward and recurrent processing. Trends Neurosci 23:571-579.
Lavine N, Reuben M, Clarke PBS (1997) A population of nicotinic receptors is associated with thalamocortical afferents in the adult rat: Laminal and areal analysis. J Comp Neurol 380:175-190.
LeBeau FE, Towers SK, Traub RD, Whittington MA, Buhl EH (2002) Fast network oscillations induced by potassium transients in the rat hippocampus in vitro. J Physiol 542:167-179.
Lee J, Maunsell JH (2010) The effect of attention on neuronal responses to high and low contrast stimuli. J Neurophysiol 104:960-971.

Levey AI, Wainer BH, Rye DB, Mufson EJ, Mesulam MM (1984) Choline acetyltransferase-immunoreactive neurons intrinsic to rodent cortex and distinction from acetylcholinesterase-positive neurons. Neuroscience 13:341-353.
Levy RB, Reyes AD, Aoki C (2006) Nicotinic and muscarinic reduction of unitary excitatory postsynaptic potentials in sensory cortex; dual intracellular recording in vitro. J Neurophysiol 95:2155-2166.
Li W, Thier P, Wehrhahn C (2000) Contextual influence on orientation discrimination of humans and responses of neurons in V1 of alert monkeys. J Neurophysiol 83:941-954.
Lin SC, Gervasoni D, Nicolelis MA (2006) Fast modulation of prefrontal cortex activity by basal forebrain noncholinergic neuronal ensembles. J Neurophysiol 96:3209-3219.
Lucas-Meunier E, Fossier P, Baux G, Amar M (2003) Cholinergic modulation of the cortical neuronal network. Pflugers Arch 446:17-29.
Lucas-Meunier E, Monier C, Amar M, Baux G, Fregnac Y, Fossier P (2009) Involvement of Nicotinic and Muscarinic Receptors in the Endogenous Cholinergic Modulation of the Balance between Excitation and Inhibition in the Young Rat Visual Cortex. Cerebral Cortex 19:2411-2427.
Luck SJ, Chelazzi L, Hillyard SA, Desimone R (1997a) Neural mechanisms of spatial selective attention in areas V1, V2, and V4 of macaque visual cortex. J Neurophysiol 77:24-42.
Luck SJ, Fan S, Hillyard SA (1993) Attention-Related Modulation of Sensory-Evoked Brain Activity in a Visual-Search Task. J Cognitive Neurosci 5:188-195.
Luck SJ, Girelli M, McDermott MT, Ford MA (1997b) Bridging the gap between monkey neurophysiology and human perception: an ambiguity resolution theory of visual selective attention. Cognit Psychol 33:64-87.
Macknik SL, Haglund MM (1999) Optical images of visible and invisible percepts in the primary visual cortex of primates. Proc Natl Acad Sci U S A 96:15208-15210.
Martinez-Trujillo JC, Treue S (2004a) Feature-based attention increases the selectivity of population responses in primate visual cortex. Current Biology 14:744-751.
Martinez-Trujillo JC, Treue S (2004b) Feature-based attention increases the selectivity of population responses in primate visual cortex. Curr Biol 14:744-751.
Maunsell JH, Gibson JR (1992) Visual response latencies in striate cortex of the macaque monkey. J Neurophysiol 68:1332-1344.
McAlonan K, Cavanaugh J, Wurtz RH (2008) Guarding the gateway to cortex with attention in visual thalamus. Nature 456:391-394.
McGaughy J, Dalley JW, Morrison CH, Everitt BJ, Robbins TW (2002) Selective behavioral and neurochemical effects of cholinergic lesions produced by intrabasalis infusions of 192 IgG-saporin on attentional performance in a five-choice serial reaction time task. Journal of Neuroscience 22:1905-1913.
Meirovithz E, Ayzenshtat I, Bonneh YS, Itzhack R, Werner-Reiss U, Slovin H (2010) Population response to contextual influences in the primary visual cortex. Cereb Cortex 20:1293-1304.
Mesulam MM, Mufson EJ, Levey AI, Wainer BH (1983) Cholinergic innervation of cortex by the basal forebrain: cytochemistry and cortical connections of the septal area, diagonal band nuclei, nucleus basalis (substantia innominata), and hypothalamus in the rhesus monkey. J Comp Neurol 214:170-197.
Metherate R (2004) Nicotinic acetylcholine receptors in sensory cortex. Learn Mem 11:50-59.
Metherate R, Cox CL, Ashe JH (1992) Cellular bases of neocortical activation: modulation of neural oscillations by the nucleus basalis and endogenous acetylcholine. J Neurosci 12:4701-4711.
Miettinen RA, Kalesnykas G, Koivisto EH (2002) Estimation of the total number of cholinergic neurons containing estrogen receptor-alpha in the rat basal forebrain. J Histochem Cytochem 50:891-902.
Miller KD, Chapman B, Stryker MP (1989) Visual responses in adult cat visual cortex depend on N-methyl-D-aspartate receptors. Proc Natl Acad Sci U S A 86:5183-5187.

Mitchell JF (1963) The spontaneous and evoked release of acetylcholine from the cerebral cortex. J Physiol 165:98-116.
Mitchell JF, Sundberg KA, Reynolds JH (2007) Differential attention-dependent response modulation across cell classes in macaque visual area V4. Neuron 55:131-141.
Mitchell JF, Sundberg KA, Reynolds JH (2009) Spatial attention decorrelates intrinsic activity fluctuations in macaque area V4. Neuron 63:879-888.
Moore T, Fallah M (2004) Microstimulation of the frontal eye field and its effects on covert spatial attention. J Neurophysiol 91:152-162.
Moran J, Desimone R (1985) Selective attention gates visual processing in the extrastriate cortex. Science 229:782-784.
Motter BC (1993) Focal attention produces spatially selective processing in visual cortical areas V1, V2, and V4 in the presence of competing stimuli. J Neurophysiol 70:909-919.
Motter BC (1994) Neural correlates of attentive selection for color or luminance in extrastriate area V4. J Neurosci 14:2178-2189.
Movshon JA, Newsome WT (1996) Visual response properties of striate cortical neurons projecting to area MT in macaque monkeys. Journal of Neuroscience 16:7733-7741.
Munk MH, Roelfsema PR, Konig P, Engel AK, Singer W (1996) Role of reticular activation in the modulation of intracortical synchronization. Science 272:271-274.
Murphy PC, Sillito AM (1987) Corticofugal feedback influences the generation of length tuning in the visual pathway. Nature 329:727-729.
Murphy PC, Sillito AM (1991) Cholinergic enhancement of direction selectivity in the visual cortex of the cat. Neuroscience 40:13-20.
Murthy A, Humphrey AL (1999) Inhibitory contributions to spatiotemporal receptive-field structure and direction selectivity in simple cells of cat area 17. J Neurophysiol 81:1212-1224.
Nakamura K, Colby CL (2000) Visual, saccade-related, and cognitive activation of single neurons in monkey extrastriate area V3A. J Neurophysiol 84:677-692.
Nelson CL, Sarter M, Bruno JP (2005) Prefrontal cortical modulation of acetylcholine release in posterior parietal cortex. Neuroscience 132:347-359.
Nowak LG, SanchezVives MV, McCormick DA (1997) Influence of low and high frequency inputs on spike timing in visual cortical neurons. Cerebral Cortex 7:487-501.
Paradiso MA, Blau S, Huang X, MacEvoy SP, Rossi AF, Shalev G (2006) Lightness, filling-in, and the fundamental role of context in visual perception. Prog Brain Res 155:109-123.
Parikh V, Kozak R, Martinez V, Sarter M (2007) Prefrontal acetylcholine release controls cue detection on multiple timescales. Neuron 56:141-154.
Parikh V, Sarter M (2008) Cholinergic mediation of attention: contributions of phasic and tonic increases in prefrontal cholinergic activity. Ann N Y Acad Sci 1129:225-235.
Parkinson D, Kratz KE, Daw NW (1988) Evidence for a Nicotinic Component to the Actions of Acetylcholine in Cat Visual-Cortex. Exp Brain Res 73:553-568.
Pearson RCA, Gatter KC, Brodal P, Powell TPS (1983) The Projection of the Basal Nucleus of Meynert Upon the Neocortex in the Monkey. Brain Research 259:132-136.
Phillis JW (1968) Acetylcholine release from the cerebral cortex: its role in cortical arousal. Brain Res 7:378-389.
Polat U, Mizobe K, Pettet MW, Kasamatsu T, Norcia AM (1998) Collinear stimuli regulate visual responses depending on cell's contrast threshold. Nature 391:580-584.
Polat U, Sagi D (1992) Lateral Interactions between Spatial Channels - Suppression and Facilitation Revealed by Lateral Masking Experiments. Invest Ophth Vis Sci 33:1345-1345.
Polat U, Sagi D (1993) Lateral Interactions between Spatial Channels - Suppression and Facilitation Revealed by Lateral Masking Experiments. Vision Res 33:993-999.
Polat U, Sagi D (1994) The architecture of perceptual spatial interactions. Vision Res 34:73-78.
Pooresmaeili A, Herrero JL, Self MW, Roelfsema PR, Thiele A (2010) Suppressive lateral interactions at parafoveal representations in primary visual cortex. J Neurosci 30:12745-12758.

Posner MI, Inhoff AW, Friedrich FJ, Cohen A (1987) Isolating Attentional Systems - a Cognitive-Anatomical Analysis. Psychobiology 15:107-121.
Posner MI, Snyder CR, Davidson BJ (1980) Attention and the detection of signals. J Exp Psychol 109:160-174.
Press WH, Teukolsky SA (1997) Numerical recipes: Does this paradigm have a future? Comput Phys 11:416-424.
Preuss TM (1995) Do Rats Have Prefrontal Cortex - the Rose-Woolsey-Akert Program Reconsidered. J Cognitive Neurosci 7:1-24.
Prusky GT, Shaw C, Cynader MS (1987a) Nicotine Receptors Are Located on Lateral Geniculate-Nucleus Terminals in Cat Visual-Cortex. Brain Research 412:131-138.
Prusky GT, Shaw C, Cynader MS (1987b) Nicotine receptors are located on lateral geniculate nucleus terminals in cat visual cortex. Brain Res 412:131-138.
Randic M, Padjen A (1967) Effect of calcium ions on the release of acetylcholine from the cerebral cortex. Nature 215:990.
Reynolds JH, Chelazzi L, Desimone R (1999) Competitive mechanisms subserve attention in macaque areas V2 and V4. J Neurosci 19:1736-1753.
Reynolds JH, Heeger DJ (2009) The normalization model of attention. Neuron 61:168-185.
Richmond BJ, Wurtz RH, Sato T (1983) Visual responses of inferior temporal neurons in awake rhesus monkey. J Neurophysiol 50:1415-1432.
Rizzolatti G, Riggio L, Dascola I, Umilta C (1987) Reorienting attention across the horizontal and vertical meridians: evidence in favor of a premotor theory of attention. Neuropsychologia 25:31-40.
Robbins TW (2005) Chemistry of the mind: neurochemical modulation of prefrontal cortical function. J Comp Neurol 493:140-146.
Roberts M, Delicato LS, Herrero J, Gieselmann MA, Thiele A (2007) Attention alters spatial integration in macaque V1 in an eccentricity-dependent manner. Nat Neurosci 10:1483-1491.
Roberts MJ, Zinke W, Guo K, Robertson R, McDonald JS, Thiele A (2005) Acetylcholine dynamically controls spatial integration in marmoset primary visual cortex. J Neurophysiol 93:2062-2072.
Robinson DL, Kertzman C (1995) Covert orienting of attention in macaques. III. Contributions of the superior colliculus. J Neurophysiol 74:713-721.
Rodriguez R, Kallenbach U, Singer W, Munk MHJ (2004) Short- and long-term effects of cholinergic modulation on gamma oscillations and response synchronization in the visual cortex. Journal of Neuroscience 24:10369-10378.
Roelfsema PR (2005) Elemental operations in vision. Trends Cogn Sci 9:226-233.
Roelfsema PR (2006) Cortical algorithms for perceptual grouping. Annu Rev Neurosci 29:203-227.
Roelfsema PR, Lamme VA, Spekreijse H (1998) Object-based attention in the primary visual cortex of the macaque monkey. Nature 395:376-381.
Roerig B, Kao JP (1999) Organization of intracortical circuits in relation to direction preference maps in ferret visual cortex. J Neurosci 19:RC44.
Rokem A, Silver MA (2010) Cholinergic enhancement augments magnitude and specificity of visual perceptual learning in healthy humans. Curr Biol 20:1723-1728.
Russchen FT, Amaral DG, Price JL (1985) The afferent connections of the substantia innominata in the monkey, Macaca fascicularis. J Comp Neurol 242:1-27.
Sahin M, Bowen WD, Donoghue JP (1992) Location of nicotinic and muscarinic cholinergic and mu-opiate receptors in rat cerebral neocortex: evidence from thalamic and cortical lesions. Brain Res 579:135-147.
Salt TE (1986) Mediation of Thalamic Sensory Input by Both Nmda Receptors and Non-Nmda Receptors. Nature 322:263-265.
Sarter M, Hasselmo ME, Bruno JP, Givens B (2005) Unraveling the attentional functions of cortical cholinergic inputs: interactions between signal-driven and cognitive modulation of signal detection. Brain Res Rev 48:98-111.

Sarter M, Parikh V, Howe WM (2009) Phasic acetylcholine release and the volume transmission hypothesis: time to move on. Nat Rev Neurosci 10:383-390.
Sato H, Hata Y, Hagihara K, Tsumoto T (1987a) Effects of cholinergic depletion on neuron activities in the cat visual cortex. J Neurophysiol 58:781-794.
Sato H, Hata Y, Masui H, Tsumoto T (1987b) A functional role of cholinergic innervation to neurons in the cat visual cortex. J Neurophysiol 58:765-780.
Sato H, Katsuyama N, Tamura H, Hata Y, Tsumoto T (1995) Mechanisms underlying direction selectivity of neurons in the primary visual cortex of the macaque. Journal of Neurophysiology 74:1382-1394.
Sato H, Katsuyama N, Tamura H, Hata Y, Tsumoto T (1996) Mechanisms underlying orientation selectivity of neurons in the primary visual cortex of the macaque. J Physiol 494 (Pt 3):757-771.
Serences JT, Boynton GM (2007) Feature-based attentional modulations in the absence of direct visual stimulation. Neuron 55:301-312.
Serences JT, Yantis S (2007) Spatially selective representations of voluntary and stimulus-driven attentional priority in human occipital, parietal, and frontal cortex. Cereb Cortex 17:284-293.
Shao Z, Burkhalter A (1996) Different balance of excitation and inhibition in forward and feedback circuits of rat visual cortex. J Neurosci 16:7353-7365.
Shima K, Tanji J (1993a) Involvement of Nmda and Non-Nmda Receptors in Motor Task-Related Activity in the Primary and Secondary Cortical Motor Areas of the Monkey. Cerebral Cortex 3:330-347.
Shima K, Tanji J (1993b) Involvement of NMDA and non-NMDA receptors in motor task-related activity in the primary and secondary cortical motor areas of the monkey. Cereb Cortex 3:330-347.
Shomstein S, Yantis S (2004) Control of attention shifts between vision and audition in human cortex. Journal of Neuroscience 24:10702-10706.
Shulman GL, Ollinger JM, Akbudak E, Conturo TE, Snyder AZ, Petersen SE, Corbetta M (1999) Areas involved in encoding and applying directional expectations to moving objects. J Neurosci 19:9480-9496.
Sillito AM (1977) Inhibitory processes underlying the directional specificity of simple, complex and hypercomplex cells in the cat's visual cortex. J Physiol 271:699-720.
Sillito AM, Kemp JA (1983) Cholinergic modulation of the functional organization of the cat visual cortex. Brain Res 289:143-155.
Silver MA, Shenhav A, D'Esposito M (2008) Cholinergic Enhancement Reduces Spatial Spread of Visual Responses in Human Early Visual Cortex. Neuron 60:904-914.
Sperling G (1979) Citation Classic - Information Available in Brief Visual Presentations. Cc/Soc Behav Sci 18-18.
Spitzer H, Desimone R, Moran J (1988) Increased Attention Enhances Both Behavioral and Neuronal Performance. Science 240:338-340.
Steriade M (2001) Impact of network activities on neuronal properties in corticothalamic systems. J Neurophysiol 86:1-39.
Sundberg KA, Mitchell JF, Reynolds JH (2009) Spatial attention modulates center-surround interactions in macaque visual area v4. Neuron 61:952-963.
Swets JA (1988) Measuring the accuracy of diagnostic systems. Science 240:1285-1293.
Swindale NV (1998) Orientation tuning curves: empirical description and estimation of parameters. Biol Cybern 78:45-56.
Szerb JC (1967) Cortical acetylcholine release and electroencephalographic arousal. J Physiol 192:329-343.
Thiele A, Delicato LS, Roberts MJ, Gieselmann MA (2006) A novel electrode-pipette design for simultaneous recording of extracellular spikes and iontophoretic drug application in awake behaving monkeys. J Neurosci Methods 158:207-211.

Thiele A, Distler C, Korbmacher H, Hoffmann K-P (2004a) Contribution of inhibitory mechanisms to direction selectivity and response normalization in macaque middle temporal area. PNAS 101:9810-9815.
Thiele A, Distler C, Korbmacher H, Hoffmann KP (2004b) Contribution of inhibitory mechanisms to direction selectivity and response normalization in macaque middle temporal area. Proc Natl Acad Sci U S A 101:9810-9815.
Thiele A, Distler C, Korbmacher H, Hoffmann KP (2004c) Contribution of inhibitory mechanisms to direction selectivity and response normalization in macaque middle temporal area. P Natl Acad Sci USA 101:9810-9815.
Thiele A, Pooresmaeili A, Delicato LS, Herrero JL, Roelfsema PR (2009) Additive effects of attention and stimulus contrast in primary visual cortex. Cereb Cortex 19:2970-2981.
Thompson RF (1986) The Neurobiology of Learning and Memory. Science 233:941-947.
Tiesinga PH, Fellous JM, Salinas E, Jose JV, Sejnowski TJ (2004) Inhibitory synchrony as a mechanism for attentional gain modulation. J Physiol Paris 98:296-314.
Tigges M, Tigges J, Rees H, Rye D, Levey AI (1997) Distribution of muscarinic cholinergic receptor proteins m1 to m4 in area 17 of normal and monocularly deprived rhesus monkeys. J Comp Neurol 388:130-145.
Tolhurst DJ, Movshon JA, Thompson ID (1981) The dependence of response amplitude and variance of cat visual cortical neurones on stimulus contrast. Exp Brain Res 41:414-419.
Traub RD, Pais I, Bibbig A, LeBeau FE, Buhl EH, Hormuzdi SG, Monyer H, Whittington MA (2003) Contrasting roles of axonal (pyramidal cell) and dendritic (interneuron) electrical coupling in the generation of neuronal network oscillations. Proc Natl Acad Sci U S A 100:1370-1374.
Treue S, Martinez Trujillo JC (1999) Feature-based attention influences motion processing gain in macaque visual cortex. Nature 399:575-579.
Treue S, Maunsell JH (1996) Attentional modulation of visual motion processing in cortical areas MT and MST. Nature 382:539-541.
Treue S, Maunsell JH (1999) Effects of attention on the processing of motion in macaque middle temporal and medial superior temporal visual cortical areas. J Neurosci 19:7591-7602.
Turchi J, Sarter M (2001a) Antisense oligodeoxynucleotide-induced suppression of basal forebrain NMDA-NR1 subunits selectively impairs visual attentional performance in rats. Eur J Neurosci 14:103-117.
Turchi J, Sarter M (2001b) Bidirectional modulation of basal forebrain N-methyl-D-aspartate receptor function differentially affects visual attention but not visual discrimination performance. Neuroscience 104:407-417.
Ungerleider LG, Gaffan D, Pelak VS (1989) Projections from inferior temporal cortex to prefrontal cortex via the uncinate fascicle in rhesus monkeys. Exp Brain Res 76:473-484.
Vidal C, Changeux JP (1993) Nicotinic and Muscarinic Modulations of Excitatory Synaptic Transmission in the Rat Prefrontal Cortex in-Vitro. Neuroscience 56:23-32.
von Engelhardt J, Eliava M, Meyer AH, Rozov A, Monyer H (2007) Functional characterization of intrinsic cholinergic interneurons in the cortex. The Journal of neuroscience : the official journal of the Society for Neuroscience 27:5633-5642.
von Stein A, Chiang C, Konig P (2000) Top-down processing mediated by interareal synchronization. Proc Natl Acad Sci U S A 97:14748-14753.
Voytko ML, Olton DS, Richardson RT, Gorman LK, Tobin JR, Price DL (1994) Basal forebrain lesions in monkeys disrupt attention but not learning and memory. J Neurosci 14:167-186.
Wang XJ (2001) Synaptic reverberation underlying mnemonic persistent activity. Trends Neurosci 24:455-463.
Watson AB (1979) Probability summation over time. Vision Res 19:515-522.
Weibull GW (1981) Citation Classic - a Statistical Distribution Function of Wide Applicability. Cc/Eng Tech Appl Sci 18-18.

Williford T, Maunsell JH (2006) Effects of spatial attention on contrast response functions in macaque area V4. J Neurophysiol 96:40-54.
Wise SP, Weinrich M, Mauritz KH (1983) Motor aspects of cue-related neuronal activity in premotor cortex of the rhesus monkey. Brain Res 260:301-305.
Womelsdorf T, Schoffelen JM, Oostenveld R, Singer W, Desimone R, Engel AK, Fries P (2007) Modulation of neuronal interactions through neuronal synchronization. Science 316:1609-1612.
Wonnacott S (1997) Presynaptic nicotinic ACh receptors. Trends Neurosci 20:92-98.
Xing J, Heeger DJ (2001) Measurement and modeling of center-surround suppression and enhancement. Vision Res 41:571-583.
Yu AJ, Dayan P (2002) Acetylcholine in cortical inference. Neural Netw 15:719-730.
Zenger-Landolt B, Koch C (2001) Flanker effects in peripheral contrast discrimination - psychophysics and modeling. Vision Res 41:3663-3675.
Zinke W, Roberts MJ, Guo K, McDonald JS, Robertson R, Thiele A (2006) Cholinergic modulation of response properties and orientation tuning of neurons in primary visual cortex of anaesthetized Marmoset monkeys. Eur J Neurosci 24:314-328.